CHARACTERISATION OF A POXVIRUS ASSOCIATED WITH THE DECLINE OF RED SQUIRRELS IN THE UK

Kathryn Thomas

Thesis submitted for the Degree of Doctor of Philosophy

The University of Edinburgh

October 2003

Research carried out at Moredun Research Institute, Edinburgh

DECLARATION

The work carried out in this thesis is my own original work, except where otherwise stated, and it has not been submitted for any other degree or professional qualification.

ACKNOWLEDGEMENTS

I would like to thank my supervisor Dr Colin McInnes for all of his help and encouragement throughout the project, and for his patient explanations of the usage of "was and were". Thanks also go to my other supervisor Dr Robert Dalziel for his help in producing this thesis, to Dr Peter Nettleton for his enthusiasm for this project, and the Sir James Knott trust for funding this research.

A big thank you goes to Ann Wood for all of her technical advice, for providing the ORFV cDNA clones and generally keeping our lab in line and running smoothly. Thanks to Kay Hall and Janice Gilray for their tissue culture expertise and for providing the ELISA antigens. A thank you also to the lads at the Moredun Functional Genomics Unit for the DNA sequencing and to the staff at CVLA, Lasswade for the electron microscopy.

Thanks must also go to the champions of red squirrels, Anthony Sainsbury and Dr John Gurnell for the collection of SPPV affected squirrels and for allowing me to raid their freezers at London zoo to gather scab samples. Thank you to Dr Malcolm Bennett for providing the wood mice and bank vole sera and to Dr Frank Wright for his phylogenetic expertise. Thanks must also go to Mike McLauchlan for resuscitating my computer at several critical moments.

To the staff and students at Moredun, thank you to you all for making Moredun an enjoyable and unforgettable experience. Last, but not least, a big thank you and a hug goes to my fiancé Paul Bartley and my friend Rubina Sharif, for their cheerfulness, constant support and friendship.

ABSTRACT

Competition between the red and grey squirrels and an epidemic disease caused by a *Squirrel parapoxvirus* (SPPV) both play a crucial role in the replacement of red squirrels by the grey species. Serological evidence suggests that the grey squirrel may act as a reservoir host for SPPV, however no route of transmission between the two species has been identified. The aims of this study were to characterise the SPPV genome and to identify other potential host species. Knowledge gained from this will be invaluable for the future development of a vaccine against SPPV, which could be used in conjunction with red squirrel conservation programmes.

A preliminary investigation to identify rodent species that may act as a reservoir for SPPV was carried out. Sera collected from wood mice and bank voles were screened for antibodies to SPPV using an enzyme-linked immunosorbent assay. No alternative hosts were identified using this approach.

Viral DNA was purified from scab material collected from a red squirrel found dead in the wild during an epidemic of SPPV in Northumbria. The composition of the SPPV genome is G+C-rich at approximately 66%, and the genome is estimated to be 158kb in size. The G+C content is comparable with parapox and molluscipox viruses, but the genome does not correspond in size to viruses belonging to either of these genera. DNA hybridisation studies indicate that the central regions of the SPPV and *Orf virus* (ORFV) genomes are highly related; however the two viruses are divergent towards the genome ends. Twenty-eight previously identified poxvirus genes were identified and mapped on to the SPPV genome, including two genes previously believed to be unique to the molluscipox virus *Molluscum contagiosum* (MOCV). Comparison of the organisation of genes in SPPV with *Vaccinia* (VACV), MOCV and ORFV revealed an overall conservation in the order of genes, but differences in the spatial distribution.

Further characterisation revealed that three known parapoxvirus-specific genes that are associated with virus virulence and immuno-modulation (homologues of interleukin-10 and vascular endothelial growth factor and the granulocyte macrophage colony stimulating factor inhibitory protein) appear to be absent in SPPV. In addition, sequence analysis of a putative SPPV homologue of the conserved poxvirus interferon (IFN) inhibitory gene suggests that

this gene is disrupted in SPPV and not involved in the inhibition of IFN-induced anti-viral pathways.

The genomic inconsistencies between SPPV and the other parapoxviruses suggest that the initial classification of SPPV as a parapoxvirus may be incorrect. Preliminary phylogenetic analysis suggests that SPPV does not belong in any of the previously described poxvirus genera.

SUMMARY OF ABBREVIATIONS

Viruses

BPSV	*Bovine papular stomatitis virus*
CMPV	*Camelpox virus*
CPV	*Cowpox virus*
ECTV	*Ectromelia virus*
FPV	*Fowlpox virus*
LSDV	*Lumpy skin disease virus*
MOCV	*Molluscum contagiosum virus*
MPV	*Monkeypox virus*
MYXV	*Myxoma virus*
ORFV	*Orf virus*
PCPV	*Pseudocowpox virus*
PVNZ	*Parapoxvirus of red deer in New Zealand*
ReindeerPPV	Reindeer parapox virus
RPXV	*Rabbitpox virus*
SealPPV	Seal parapox virus
SFV	*Shope fibroma virus*
SPPV	*Squirrel parapox virus*
SPV	*Sheeppox virus*
SQFV	*Squirrel fibroma virus*
SWPV	*Swinepox virus*
VACV	*Vaccinia virus*
VARV	*Variola virus*
YLDV	*Yaba like disease virus*
YMTV	*Yaba monkey tumour virus*

Standard abbreviation

bp	Base pair
cfu	Colony forming units
CPE	Cytopathic effect
DIG	Digoxigenin-11-deoxyuracil triphosphate
DNA	Deoxyribonucleic acid
EEV	Extracellular enveloped virus

RNA	Ribonucleic acid
dsDNA	Double stranded DNA
dsRNA	Double stranded RNA
dNTP	Deoxynucleotide triphosphate
FBS	Foetal bovine serum
FLMC	Foetal lamb muscle cells
IEV	Intracellular enveloped virus
IFN	Interferon
IL	Interleukin
IMV	Intracellular mature virus
IPTG	Isopropyl-β-D-thio-galactopyranoside
IV	Immature virus
kb	Kilobase pair
LBA	Luria Bertani agar
LB	Luria Bertani broth
MBq	Mega Becquerel
MCS	Multiple cloning site
MHC	Major histocompatibility complex
MOI	Multiplicity of infection
NPH I	Nucleoside triphosphate phosphohydrolase I
OD	Optical density
rpm	Revolutions per minute
PBS	Phosphate buffered saline
RNA	Ribonucleic acid
SDS	Sodium dodecyl sulphate
SSC	Sodium chloride/ Sodium citrate buffer
TBE	Tris-Borate buffer
TE	10mM Tris-HCl pH 8, 1mM EDTA pH 8
TNF	Tumour necrosis factor
U	Units enzyme
VEGF	Vascular endothelial growth factor
VETF	VACV early transcription factor
VITF	VACV intermediate transcription factor
VLTF	VACV late transcription factor
X-gal	5-bromo-4-chloro-3-indolyl-β-D-galactopyranoside

CHAPTER 1.0

INTRODUCTION

1.1 GENERAL INTRODUCTION

In 1981 a virus morphologically similar to the parapox viruses when visualised by electron microscopy was identified in scab material collected from a British red squirrel (Scott *et al.*, 1981). It was proposed that this virus contributed to the rapid decline in red squirrel population numbers in the UK (section 1.8). The squirrel virus was shown to be antigenically distinct from the parapoxvirus species *Orf virus* (ORFV), *Pseudocowpox virus* (PCPV) and *Bovine papular stomatitis virus* (BPSV) by immunodiffusion agar gel tests using polyclonal sera (Sands *et al.*, 1984). Based on this and its morphological similarities to other parapoxvirus species, the squirrel virus was formally classified as a separate species of the parapoxvirus genus and named *Squirrel parapoxvirus* (SPPV) (van Regenmortel *et al.*, 2000).

The *Poxviridae* family contains viruses that are capable of infecting both vertebrate (subfamily *Chordopoxviridae*) and invertebrate (subfamily *Entomopoxviridae*) hosts. The Chordopoxviruses are epitheliotropic and produce a broad spectrum of disease severity, ranging from localised self limiting infection (for example ORFV) to systemic disease with high mortality [for example the smallpox virus *Variola* (VARV)] and a number of poxviruses [for example *Molluscum contagiosum* virus (MOCV)] induce tumour formation (Driven, 2001). Disparity in host range is common in the poxviruses; for example MOCV is restricted to a human host, whereas *Vaccinia virus* (VACV) has a wider host range affecting humans and experimental animals.

Successful vaccination against one species of poxvirus can be obtained using another related species, as illustrated by the protection against VARV provided by vaccination with VACV. This strategy proved so successful that the World Health Organisation (WHO) embarked on a global smallpox eradication programme in 1967. The WHO achieved its goal in 1977, and the world was certified free of smallpox in 1979 (WHO, 1980).

Routine smallpox vaccination has been halted since VARV eradication, but vaccine research has continued because of the risk of VARV re-emergence due to bioterrorism and the degree of protection it provides against emerging poxvirus diseases like that caused by *Monkeypox virus* (MPV) (Heymann *et al.*, 1998; Smith and McFadden, 2002). In addition, there has been a resurgence of interest in VACV due to the ease of creating recombinant virus. Recombinant VACVs are utilised for expression of foreign proteins enabling characterisation of protein structure and function, and as experimental vaccines (Moss, 1996a).

Many poxviruses, like ORFV, *Fowlpoxvirus* (FPV) and the capripoxviruses result in significant economic losses for commercial farmers (Robinson and Balassu, 1981; Fenner, 1996; Afonso *et al.,* 2000). The need for effective vaccines and control methods has resulted in considerable research of these poxviruses. Although not commercially important; SPPV is significant from a welfare and conservation perspective and the development of an effective vaccine may prove to be pivotal for the survival of the red squirrel in the UK (Sainsbury *et al.,* 1997; Gurnell *et al.,* 1999).

As a result of its use as the vaccine against smallpox, VACV is the most characterised member of the poxvirus family and is used as a model for other poxviruses. Much of the literature reviewed here (chapter 1.0) is based on VACV, however differences between VACV and the parapoxviruses undoubtedly exist, and these will be discussed where relevant.

1.2 GENERAL MORPHOLOGY AND CLASSIFICATION OF THE *POXVIRIDAE*

Poxviruses are the largest of all animal viruses and posses a single, covalently closed, double stranded DNA (dsDNA) genome ranging from 130kb to 375kb in length (van Regenmortel *et al.,* 2000). Poxviruses contain RNA-polymerase activity and transcriptional systems that are pre-packaged into the viral core (Kates and McAuslan, 1967b; Munyon *et al.,* 1967) and viral replication and assembly occurs within the host cell cytoplasm.

Sufficient variation exists within the *Chordopoxviridae* to warrant subdivision into eight genera, summarised in table 1.1. Generally genus members share a similar morphology and are genetically and antigenically related (Moss, 1996b). As the names suggest the virus species belonging to the leporipox, avipox and capripox genera also infect similar host species.

Viruses belonging to the parapoxvirus genus were generally considered to affect ruminants, until the inclusion of *Parapoxvirus of red deer in New Zealand* (PVNZ). In addition, phylogenetic evidence suggests that a seal poxvirus (sealPPV) also belongs in the parapox genus (Becher *et al.,* 2002). Other tentative parapoxvirus species have been reported such as auzduk disease virus, reindeer parapoxvirus and chamois contagious disease virus (Mercer *et al.,* 1997a; Tryland *et al.,* 2001).

Genera	Member viruses	Characteristics
Orthopoxvirus	*Vaccinia*[a] *Variola* *Cowpox* *Monkeypox*	Brick-shaped virion, DNA~200 Kb, G+C content~36%, variable host range.
Parapoxvirus	*Orf*[a] *Pseudocowpox* *Bovine papular stomatitis* *Red deer parapox* *Squirrel parapox*	Ovoid-shaped virion, DNA~140 Kb, G+C~64%, hosts mainly ungulates.
Avipoxvirus	*Fowlpox*[a] *Canarypox*	Brick-shaped virion, DNA~150 Kb, G+C ~35%, bird hosts, insect vector.
Capripoxvirus	*Sheeppox*[a] *Lumpy skin disease*	Brick-shaped virion, DNA~150 Kb, hosts ungulates, insect vector.
Leporipoxvirus	*Myxoma*[a] *Shope fibroma* *Squirrel fibroma*	Brick-shaped virion, DNA~160 Kb, G+C ~40%, fibroma, insect vector.
Suipoxvirus	*Swinepox*[a]	Brick-shaped virion, DNA~170 Kb, narrow host range
Molluscipoxvirus	*Molluscum contagiosum*[a]	Brick-shaped virion, DNA~190 Kb, G+C ~60%, tumours, human host.
Yatapoxvirus	*Yaba monkey tumour*[a] *Yaba like disease* *Tanapox*	Brick-shaped virion, DNA~145 Kb, G+C ~33%, host range limited.

Table 1.1 Classification of the subfamily *Chordopoxviridae* summarising the characteristic of each genus and examples of species classified with in each genus (adapted from van Regenmortel *et al.*, 2000). The prototypal species of each genus is indicated by the suffix ([a]).

Poxviruses are generally brick-shaped and range in size from 220 to 450nm in length by 140 to 260nm in width, except for the parapoxviruses which are ovoid in shape and vary between 220 to 300nm in length by 140 to 170nm in width (van Regenmortel *et al.*, 2000). A basket weave surface morphology is a characteristic of all parapoxviruses when visualised using negative contrast electron microscopy (Nagington and Horne, 1962; Nagington *et al.*, 1962; Wilson and Sweeney, 1970; Falk, 1978; Scott *et al.*, 1981; Horner *et al.*, 1987). The regular criss-cross surface details of the parapoxviruses was determined to consist of a single tubular thread that winds around the virus core in a left-hand spiral coil, which crosses at regular intervals (Nagington *et al.*, 1964). Other members of the poxvirus family display short tubular or globular filaments on the surface of the virion and are therefore morphological distinguishable from parapoxviruses (van Regenmortel *et al.*, 2000).

Sectioned negative contrast images have shown that the internal organisation of VACV consists of a nucleoprotein biconcave core and two adjacent structures known as lateral bodies bound by a membrane(s) (Medzon and Bauer, 1970). The surface morphology, the biconcave shape of the core and the lateral bodies may be artefacts produced as a result of the virion collapsing inward due to dehydration in sample preparation (Dubochet *et al.*, 1994). However due to the reproducibility, these artefacts must result from some underlying structure.

1.3 POXVIRUS GENOMES

Vertebrate poxviruses possess large double-stranded DNA genomes. The complete genome sequence for at least one species of each genus, except for the parapoxvirus genus, have been published (Goebel *et al.*, 1990; Johnson *et al.*, 1993; Massung *et al.*, 1994; Senkevich *et al.*, 1997; Cameron *et al.*, 1999; Willer *et al.*, 1999; Afonso *et al.*, 2000; Tulman *et al.*, 2001; Lee *et al.*, 2001; Afonso *et al.*, 2002; Shchelkunov *et al.*, 2002; Gubser and Smith, 2002). The length and the guanine and cytosine (G+C) content of poxvirus genomes varies dramatically between the genera. Chordopoxvirus genomes vary between 131kb and 288kb (van Regenmortel *et al.*, 2000) and G+C content is generally less than 50%, except for the parapox and mollusci poxviruses, which have G+C contents greater than 60% (Wittek *et al.*, 1979; Senkevich *et al.*, 1997). The general structure and organisation of poxvirus genomes are reviewed in the following sections. However, as SPPV has been classified as a parapoxvirus, particular emphasis is given to parapoxvirus genomes.

1.3.1 General Properties of Parapoxvirus Genomes

Parapoxviruses are the smallest poxviruses in terms of genome size. Their genomes range from 131kb to 158kb in length (Gassmann *et al.,* 1985; Robinson *et al.,* 1987; Mercer *et al.,* 1987; Cottone *et al.,* 1998; Mazur *et al.,* 2000; McInnes *et al.,* 2001). Parapox and molluscipox genomes are comparable in terms of G+C content at 64.5% for ORFV, 61.5% for BPSV and 66% for MOCV (Wittek *et al.,* 1979; Senkevich *et al.,* 1997). The high G+C content of the MOCV and the parapoxvirus genomes implies that translation stop codons (TAA, TAG, TGA) will be rare. The paucity of stop codons means that identifying true open reading frames (ORFs) is relatively difficult, as many potential overlapping ORFs exist within the genome (Fraser *et al.,* 1990; Fleming *et al.,* 1993; Senkevich *et al.,* 1997). However, since the high G+C content results in the use of codons which contain a G or a C residue at the third position (Fleming *et al.,* 1993), codon usage provides an excellent tool for predicting ORFs. This was found to be true for MOCV (Senkevich *et al.,* 1997).

1.3.2 Hairpin Loops

Rapid renaturation of FPV and VACV DNA following heat and chemical denaturation indicated the presence of cross-linkage within poxvirus genomes (Szybalski *et al.,* 1963; Berns and Silverman, 1970). The terminal location of the cross-link was first described in VACV virus (Geshelin and Berns, 1974) and further work demonstrated that cross-linked ends are a general feature of the *Poxviridae* (Wittek *et al.,* 1977; Menna *et al.,* 1979; Thomas *et al.,* 1980; Gassmann *et al.,* 1985; Mercer *et al.,* 1987).

DNA sequencing of the terminal fragments in VACV revealed that each terminus consists of a hairpin loop structure, which are complementary and inverted with respect to each other. The VACV terminal loop structure is A+T rich, 104bp in length, and consists of many mismatched bases (Baroudy *et al.,* 1982). Although terminal DNA sequence is not available for ORFV, the terminal loop is estimated to be approximately 100bp and is therefore consistent with VACV in terms of length (Mercer *et al.,* 1987).

During the replication of poxvirus genomes, concatamers are formed of progeny genomes (Willer *et al.,* 2000). Several models of genome replication have been proposed (Baroudy *et al.,* 1982). The terminal hairpin loops are a structural necessity for genomic replication in all

proposed models and concatamer junctions require processing to separate the progeny strands. VACV proteins encoded by the genes H6R and A22L are able to cleave synthetic concatamers (Holliday junctions) *in vitro* (Sekiguchi *et al.*, 2000; Garcia *et al.*, 2000). In addition, *in vivo* characterisation of a VACV A22L deletion mutant demonstrated that A22L is essential for the cleavage of the concatameric forms into genome length units and successful virus replication (Garcia and Moss, 2001).

1.3.3 Inverted Terminal Repetitions

The presence of identical terminal sequences, which are inverted with respect to each other [inverted terminal repeats (ITRs)] were first suspected when restriction endonuclease fragments of equal length were cleaved from both ends of the VACV and *Rabbit poxvirus* (RPXV) genomes (Wittek *et al.*, 1978a). Single stranded VACV DNA was also observed by electron microscopy to circularise presumably by the hybridisation of terminal regions (Garon *et al.*, 1978). Hybridisation of DNA fragments derived from one end of the genome with fragments from the other end also demonstrated the presence of ITRs in parapoxvirus genomes (Menna *et al.*, 1979; Gassmann *et al.*, 1985; Mercer *et al.*, 1987).

The DNA sequence of the ITR regions are not conserved amongst the parapoxvirus genus, as demonstrated by the absence of terminal fragment hybridisation between the different parapox species (Gassmann *et al.*, 1985; Robinson and Mercer, 1995). In addition, cross-hybridisation of the ITR fragments derived from different ORFV isolates produced varying hybridisation intensities suggesting that there is some degree of ITR sequence divergence between isolates of the same species (Robinson *et al.*, 1987).

Sequencing of the terminal regions of VACV revealed that the ITRs consist of blocks of sequence ranging in size from 54 to 125bp which are tandemly repeated up to 18 times (Baroudy *et al.*, 1982). Repetitions of short sequences located within the ITRs appear to be a general feature of poxvirus genomes, with the exception of *Shope fibroma virus* (SFV) (Willer *et al.*, 1999). Sequencing of the left end[+] of ORFV strain NZ2 revealed a 15bp sequence repeated

[+] Fleming *et al.*, (1993) reversed the orientation of the ORFV genome to allow alignment with VACV. All references prior to this paper incorrectly orientate the ORFV genome. This review corrects for this discrepancy when referring to the left or right of the genome.

fourteen times, and sequences of 16 to 36bp repeated two to four times; these repeats were inter-spaced with unique regions (Fraser *et al.,* 1990). The size variation of terminal fragments in the VACV genome was shown to be the result of differences in the number of repeated elements. Variation in ITR size is postulated to arise from unequal recombination events during DNA replication or incorrect processing of the concatamers (Baroudy *et al.,* 1982). It is unknown if blocks of repeated sequence provide a selective advantage in replication or whether they are non-functional. The lack of repeats in SFV supports the latter view (Fraser *et al.,* 1990; Willer *et al.,* 1999).

Fraser *et al.,* (1990) described the ORFV ITRs as being organised into three distinct regions comprising of the hairpin loop structure, a non-coding region consisting of tandem repeats (adjacent to the hairpin) and coding regions (near to or overlapping the ITR/unique sequence junction). DNA sequencing recognised a number of potential ORFs in the ORFV ITR. Whether all of these are transcribed is uncertain, although conserved poxvirus transcription promoter sequences were identified preceding two of the potential ORFs: one overlapping the ITR junction (ORF2) and one present within the ITR (ORF3) (Fraser *et al.,* 1990). To date only ORF3 has been confirmed as being transcriptionally active, encoding for an early protein of unknown function (Fleming *et al.,* 1991; Fleming *et al.,* 1992; Vos *et al.,* 1992).

1.3.4 Conservation and variation of poxvirus genomes

Poxvirus genomes are organised into distinctly conserved and variable regions. Restriction endonuclease mapping of several orthopoxvirus species has revealed a high degree of conservation within the central regions of the genomes (Wittek *et al.,* 1977; Mackett and Archard, 1979; Esposito and Knight, 1985). However, the restriction maps of the terminal regions are only identical or similar between isolates of the same species (Mackett and Archard, 1979; Esposito and Knight, 1985). In contrast, the central regions of the different parapoxvirus species do not exhibit the same level of cross-species restriction site conservation as seen in the orthopoxviruses (Wittek *et al.,* 1980; Robinson *et al.,* 1982; Rafii and Burger, 1985), nor the same level of conservation between isolates of the same species (Wittek *et al.,* 1980; Robinson *et al.,* 1982; Rafii and Burger, 1985; Gassmann *et al.,* 1985; Robinson *et al.,* 1987; Gilray *et al.,* 1998; Mazur *et al.,* 2000). Wittek *et al.,* (1980) proposed that lack of restriction site conservation between the different parapoxvirus species and isolates must result from a greater divergence at the nucleotide level when compared to the situation in orthopoxviruses. Despite restriction site

heterogeneity, central fragments from different parapoxviruses hybridise strongly with each other (Gassmann *et al.,* 1985; Robinson and Mercer, 1995). These fragments mapped to similar genomic locations, revealing the true conserved nature of the central regions of the different parapoxvirus genomes.

DNA hybridisation has been used to investigate the degree of conservation between poxviruses belonging to the different genera. For example, the central region of the capripoxvirus genome was shown to be essentially collinear to VACV (Gershon *et al.,* 1989). The use of DNA hybridisation as a method of investigating the genomic relationship between the parapoxviruses and other genera is however redundant due to the dissimilarity in the G+C content. This situation has been largely resolved with DNA sequencing. Although the complete genome sequence of a parapoxvirus has yet to be determined, non-contiguous sequences amounting to approximately 20% of the total genome of ORFV has been published (Mercer *et al.,* 1997a). Predicted amino acid sequences of putative ORFV genes exhibit a high degree of identity to many essential VACV proteins (Fleming *et al.,* 1993; Mercer *et al.,* 1995). The orientation and location of these conserved genes were similar for ORFV and VACV (Mercer *et al.,* 1989; Naase *et al.,* 1991; Fleming *et al.,* 1993). A genetic map of ORFV demonstrated that of the thirty-seven putative genes identified, thirty-two share homology and are relative in position, orientation and spatial arrangement with VACV genes (Mercer *et al.,* 1995).

The complete genome sequencing of numerous poxviruses has revealed that the central regions of poxvirus genomes are essentially collinear. However, the FPV genome is unusual in that several major rearrangements of the central region have occurred, resulting in a marked reduction in collinearity with other poxviruses (Afonso *et al.,* 2000). Comparison of the complete gene complements of several poxviruses from different genera suggests that the central core of genes required for viral replication extends from the homologue of the VACV gene F9L to A34R (Gubser and Smith, 2002). The divergence of poxviruses into genera and species may have arisen from alterations in gene content, homology and organisation in the variable region (Gershon *et al.,* 1989). Alterations in the genome can occur via a number of mechanisms: deletion, recombination, duplication and translocation of sequences, also insertion of foreign DNA.

Rafii and Burger (1985) were the first to report deletions within the genome of ORFV. Comparison of the restriction maps of numerous ORFV low passage tissue culture strains and wild-type isolates demonstrated that inter-strain variation was at its greatest in the right half of the genome (Robinson *et al.*, 1987). Heterogeneity in restriction profiles within a species is most apparent in viruses that have undergone prolonged passage in tissue culture. For example, serially passaged VACV exhibits genome-length heterogeneity (Wittek *et al.*, 1978b). The disparity in length was attributed to the deletions of terminal sequence (Panicali *et al.*, 1981). Many of the genes located towards the genome ends encode proteins that are not essential for virus replication in tissue culture, and are often associated host range, tissue tropism and modulation of the host immune response (Moss, 1996b).

Mutants arising from prolonged passage in tissue culture of ORFV strains NZ2, D1701 and orf-11 have been studied. Characterisation of ORFV-NZ2 revealed that the right terminal 19.3kb had been duplicated and translocated to the left end of the genome, replacing the left terminal 6.6kb of DNA. The net results were the enlargement of the ITRs to 19.3kb and the deletion of 3.3kb of unique DNA that encodes for at least three non-essential genes designated ORFV E2L, E3L and G1L (Fleming *et al.*, 1995). Similar duplication/deletion events have occurred within the genomes of the ORFV strains, orf-11 and D1701, which have been extensively passaged in tissue culture. In strain orf-11, the ORFV E2L, E3L, G1L and one further non-essential gene designated ORFV G2L (normally found adjacent to G1L) are deleted (McInnes *et al.*, 2001). In strain D1701, only the ORFV E2L is deleted (Cottone *et al.*, 1998). All three of these ORFV stains are highly attenuated *in vivo*, which implies that the deleted genes may be associated with virulence. The ORFV E2L is predicted to encode a 6KDa protein, which is conserved in several orthopoxviruses and has compositional similarity to the African swine fever virus p10 DNA-binding protein (Mercer *et al.*, 1996a). The ORFV E3L was originally believed to be a homologue a retroviral pseudoprotease (Mercer *et al.*, 1989). However later analysis identified it as a deoxyuridine 5'triphosphate nucleotide hydrolase (dUTPase) and a homologue of the VACV gene F2L (Fleming *et al.*, 1995). Exactly how dUTPase contributes to virulence is unknown, although several potential roles have been suggested. dUTPase catalyses the hydrolysis of dUTP to dUMP, thus reducing the incorporation of dUTP into the replicating viral DNA genome (Cottone *et al.*, 2002). dUTPase may also increase the pool dTTP available for viral DNA replication (Fleming *et al.*, 1995). The G1L gene encodes an ankyrin repeat protein of

unknown function (Sullivan *et al.*, 1995b). The ORFV G2L protein is a homologue of the uncharacterised VACV F11L protein (Sullivan *et al.*, 1995a).

1.4 REPLICATION CYCLE AND GENE EXPRESSION OF POXVIRUSES

Several infectious forms of poxviruses exist, representing different stages in the morphogenesis and egress of viral particles. The occurrence of the different forms during the replication cycle of VACV is summarised in figure 1.1. Immature virus (IV) develop into intracellular mature virus (IMV), which are the most abundant form of infectious virus and are released upon destruction of the host cell. A proportion of IMV acquires additional lipid membranes forming intracellular enveloped virus (IEV). IEV is transported to the cell surface where the majority remains cell associated (CEV), whilst a small proportion is released to become extracellular enveloped virus (EEV) (Smith and Vanderplasschen, 1998)

In vitro studies on VACV mutants deficient in EEV production, and comparison of VACV strains that produce differing amounts of EEV, suggest that EEVs are the main effectors of long range virus dissemination whilst CEVs are responsible for localised cell to cell spread (Blasco and Moss, 1991; Blasco and Moss, 1992).

The replication cycle of VACV is reviewed here in section 1.4. However, due to the conserved nature of the virus replication genes that are located in the central regions of different poxvirus genomes (section 1.3.4), it is thought likely that different poxviruses will also have similar replication mechanisms.

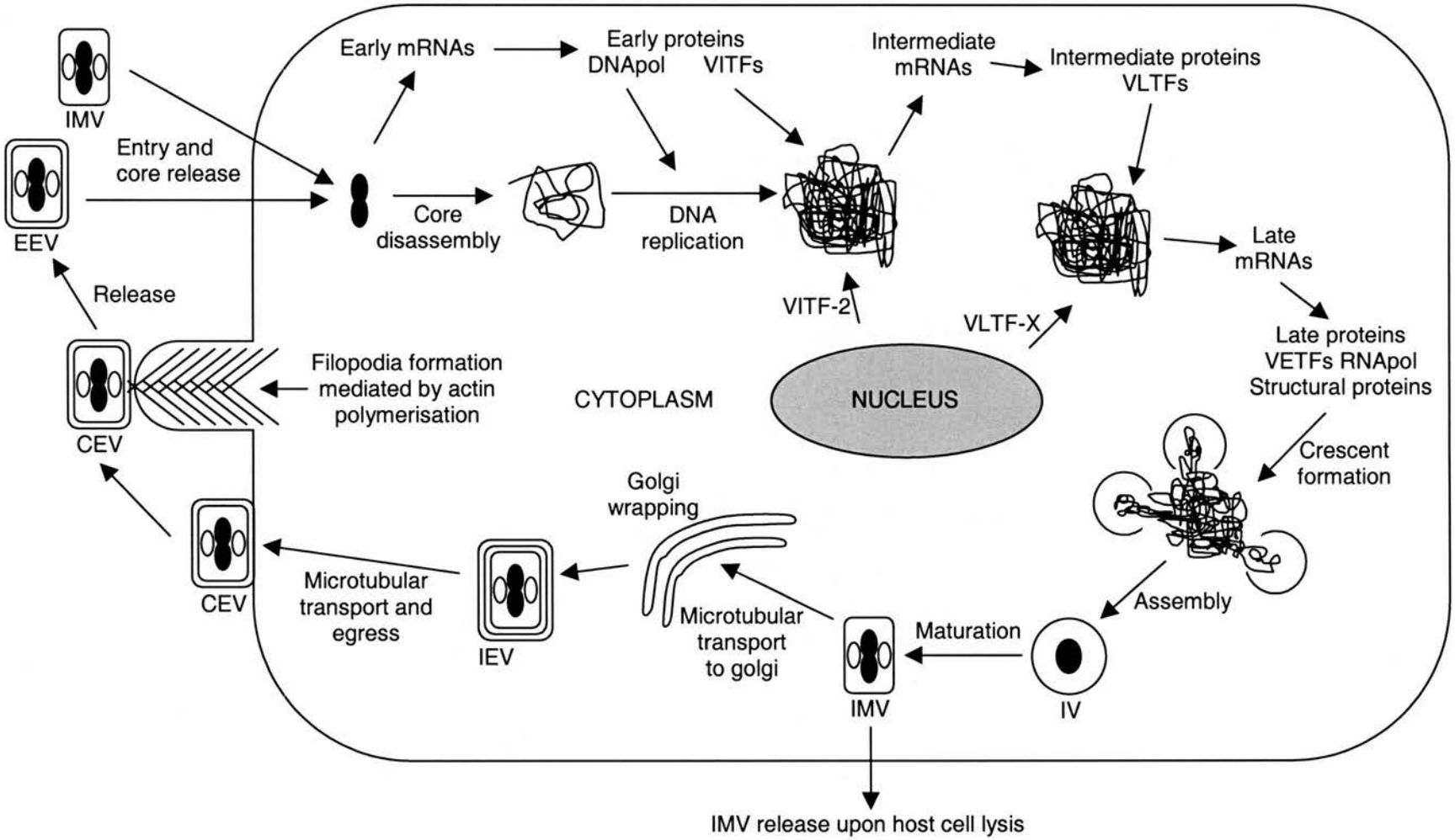

Figure 1.1 Generalised schematic representation of the replication cycle of VACV, which is described in more detail in section 1.3 [adapted from van Regenmortel *et al.,* (2000) and Smith *et al.,* (2002)]. Abbreviations are defined in the summary of abbreviation (located at the beginning of this thesis), except for DNApol and RNApol, which correspond to DNA and RNA polymerase.

1.4.1 Poxvirus attachment, entry and disassembly of protein core

Poxvirus attachment and entry to the host cell is a contentious issue and is complicated by the apparent difference in the mechanism(s) of attachment and entry of IMV and EEV. Several lines of evidence support different attachment/entry mechanisms of IMV and EEV. 1) Different protein compositions of outer membranes of IMV and EEV (Payne, 1978; Jensen *et al.*, 1996). 2) EEV have a higher specific infectivity than IMV (Payne and Norrby, 1978; Vanderplasschen and Smith, 1997; Locker *et al.*, 2000). 3) A monoclonal antibody that blocks attachment of IMV to the cell surface does not affect EEV attachment (Chang *et al.*, 1995b). 4) Treatment of cells with pronase, trypsin and neuraminidase to differentially disrupt cellular surface proteins result in varying binding efficiencies of VACV EEV and IMV particles, conclusively demonstrating that IMV and EEV bind to different cellular receptors (Vanderplasschen and Smith, 1997).

Considerable progress has been made in identifying putative IMV attachment proteins. In VACV, IMV proteins A27L and H3L have been implicated in the attachment of IMV to the cellular receptor for heparin sulphate and VACV D8L to the cellular receptor for chondroitin sulphate (Chung *et al.*, 1998; Hsiao *et al.*, 1999; Lin *et al.*, 2000). In contrast to IMV, little is known about the EEV mechanism(s) of cellular attachment. This is mainly due to technical difficulties in obtaining pure preparations of undamaged EEV particles for study (Smith and Vanderplasschen, 1998). Mutant VACVs lacking genes encoding EEV membrane proteins are being studied. To date, only the EEV membrane protein, A34R has been directly implicated with EEV infectivity (McIntosh and Smith, 1996). Whether A34R is critical for EEV attachment is unclear, as antibody specific for A34R did not inhibit viral infectivity. In addition, monoclonal antibodies against the EEV membrane B5R also resulted in a reduced infectivity, suggesting that B5R may also be involved in cellular attachment or entry (Galmiche *et al.*, 1999); however this is disputed (Vanderplasschen *et al.*, 1997). These data suggest that like IMV, several mechanisms may exist for the attachment of EEV to a cellular receptor(s), mediated by several envelope proteins.

Following viral attachment to the surface of the cell, the viral particle is internalised via an entry mechanism(s), which results in the removal of the EEV and IMV lipid membranes and the release of the "naked" nucleoprotein core into the cytoplasm. Several possible entry mechanisms have been proposed, although much of the supporting data is contradictory.

An EEV entry mechanism involving the direct fusion of the viral envelope with the plasma membrane was proposed (Doms *et al.*, 1990). However direct fusion of virions possessing more than one membrane would not result in the release of naked cores into the cytoplasm (Smith *et al.*, 2002). Alternatively endocytosis was suggested after viral entry was inhibited in the presence of cytochalasin drugs, which disrupt the actin/ezrin filament involved in endocytosis (Payne and Norrby, 1978). However some disagreement exists as to whether entry of just IMV or both IMV and EEV are affected by cytochalsin drugs (Vanderplasschen *et al.*, 1998; Locker *et al.*, 2000). Ichihashi proposed that following endocytosis, the EEV membrane is disrupted in the endosome in a low pH-dependent manner. Subsequent fusion of the remaining membrane with the endosome membrane would release the viral core into the cytoplasm (Ichihashi, 1996). In support, Vanderplasschen and Smith (1998) reported that the detection of naked viral cores within the cytoplasm was reduced following infection of cells with EEV in the presence of lysosomotropic drugs that increase intracellular pH, however this is disputed by Doms *et al.*, 1990. Clearly, endocytosis, membrane fusion and pH may all be involved in virus entry, although more research is required to determine the precise mechanism(s) by which entry occurs.

Core disassembly results in the release of viral DNA into the cytoplasm. This process is considered complete when the viral DNA becomes susceptible to the action of DNAase (Joklik, 1964). Proteins isolated by fractionation of infected cell extracts were assessed *in vitro* for core uncoating properties. A 23KDa trypsin-like protease was shown to disassemble the viral core *in vitro* (Pedley and Cooper, 1987). Cessation of viral transcription and protein synthesis by treatment with actinomycin D and cyclohexamide prevents uncoating, which suggests that the core-disassembly protein is virally encoded and synthesised *de novo*. However the gene encoding this protein remains unidentified.

1.4.2 Sequential Gene Expression

Poxviruses undergo three distinct phases of gene expression in the replication cycle, characterised by early, intermediate and late genes (figure 1.1). Sequential expression of these genes is under the regulation of phase-specific promoters and transcription factors (Moss, 1990). Early gene transcription begins immediately after infection whilst the viral DNA is still coated and is carried out by the core associated early transcription machinery (Kates and McAuslan, 1967b; Kates and McAuslan, 1967a; Munyon *et al.*, 1967; Kates and Beeson, 1970; Gershon and

Moss, 1990; Ahn and Moss, 1992). Prevention of viral DNA uncoating by cyclohexamide treatment results in prolonged early transcription (Baldick and Moss, 1993). This has led to the suggestion that core disassembly and/or DNA replication negatively regulates early transcription (McDonald *et al.,* 1992; Moss, 1996b). Replication of the viral DNA genome is required for the replication cycle to proceed to intermediate phase; interruption of DNA replication with hydroxyurea prevents intermediate transcription (Baldick and Moss, 1993).

Transcription is carried out by two forms of virally encoded DNA-dependent RNA polymerase. Both RNA polymerase forms consist of eight common subunits: RPO147, 132, 35, 30, 22, 19, 18 and 7, which are encoded by the VACV genes J6R, A24R, A29L, E4L, J4R, A5R, D7R and G5.5R respectively (Condit and Niles, 2002). However, the RNA polymerase form that specifically transcribes early genes possesses the additional 94Kda RNA polymerase associated protein, which is encoded by the VACV H4L gene (Ahn and Moss, 1992; Ahn *et al.,* 1994).

Despite overall differences in genome G+C content, poxvirus genes from different genera are preceded by conserved phase-specific A+T-rich promoter elements (Davison and Moss, 1989a; Davison and Moss, 1989b; Fleming *et al.,* 1991; Fleming *et al.,* 1993; Baldick *et al.,* 1992; Senkevich *et al.,* 1997). Transcription is best characterised in VACV and therefore VACV is reviewed here, however all of the co-factors and control sequences appear to be conserved throughout the pox virus family. Known VACV transcription initiation factors and cofactors are summarised in table 1.2 and are described in more detail in the following sections.

Factor/function(s)	Gene(s)	Reference(s)
Early transcription factors		
VETF	A8L (70Kda) D6R (82Kda)	Gershon and Moss, 1990
RAP 94	H4L (94KDa)	Ahn and Moss, 1992
Intermediate transcription factors		
VITF-1	E4L (30KDa)	Rosales *et al.*, 1994a
VITF-2	cellular protein	Rosales *et al.*, 1994b
VITF-3	A8R (34KDa) A23R (45KDa)	Sanz and Moss, 1999
Capping enzyme	D1R (95KDa) D12L (33KDa)	Morgan *et al.*, 1984 Niles *et al.*, 1989
Late transcription factors		
VLTF-1	G8R (30KDa)	Keck *et al.*, 1990
VLTF-2	A1L (17KDa)	Keck *et al.*, 1990
VLTF-3	A2L (26KDa)	Keck *et al.*, 1990
VLTF-4	H5R (36KDa)	Kovacs and Moss, 1996
VLTF-X	cellular protein(s)	Gunasinghe *et al.*, 1998
Transcript modification		
5' capping complex	D1R (95KDa) D12L (33KDa) J3R (39KDa)	Morgan *et al.*, 1984 Niles *et al.*, 1989 Schnierle *et al.*, 1992
Poly(A) polymerase	E1L (55KDa) J3R (39KDa)	Gershon *et al.*, 1991
Transcription regulation		
E/I/L helicase	A18R	Simpson and Condit, 1995
I/L negative elongation factor	A18R	Xiang *et al.*, 1998 Lackner and Condit, 2000
I/L negative elongation factor	J3R	Latner *et al.*, 2000
transcript modification and VITF	J3R	see above
I/L positive transcription	G2R	Black and Condit, 1996
E elongation factor	NPH I	Deng and Shuman, 1998
E transcription termination factor	NPH I	

Table 1.2 Summary of the VACV transcription factors involved in the initiation and regulation of early/intermediate and late (E/I/L) transcription and the modification of transcripts. Abbreviations are defined in the summary of abbreviations (located at the beginning of this thesis).

1.4.2.1 Early gene expression

Studies on VACV have shown that the conserved promoter core acts as cross-linking site for the VACV early transcription factor (VETF) (Cassetti and Moss, 1996). The RAP94 subunit of the early RNA polymerase specifically interacts with the VETF/early promoter complex and mediates the recruitment of the RNA polymerase complex to the DNA template (Ahn *et al.*, 1994; Mohamed *et al.*, 2002).

Termination of VACV early transcription occurs approximately 50bp downstream from a TTTTTNT sequence (Yuen and Moss, 1987). Specific termination results in early transcripts of a discreet length. Termination of transcription is a complex process that is poorly understood. However, several RNA polymerase associated factors including the RAP94, the capping enzyme (section 1.4.2.3) and nucleoside triphosphate phosphohydrolase I (NPH I) (section 1.4.2.4) are involved in transcription termination and transcript release in response to the UUUUUNU sequence in the nascent RNA (Shuman *et al.*, 1987; Shuman and Moss, 1988; Luo *et al.*, 1995; Deng and Shuman, 1998; Mohamed and Niles, 2000; Mohamed and Niles, 2001; Mohamed *et al.*, 2002).

1.4.2.2 Intermediate and late gene expression

Intermediate and late transcription have several features in common that are different from early transcription. Firstly, RAP94 is not required for intermediate or late transcription (Wright and Coroneos, 1995; Condit and Niles, 2002). Secondly, no transcription termination signals have been identified for intermediate or late genes and probably as a result, intermediate and late transcripts are heterogeneous in length at the 3'-termini (Weir and Moss, 1984; Baldick and Moss, 1993). Thirdly, intermediate and late transcripts are polyadenylated at the both ends, 5' polyadenylation is believed to be the result of an RNA polymerase slippage mechanism (Ahn and Moss, 1989). Initiation of intermediate and late gene transcription is poorly understood, but presumably RNA polymerase is recruited to the promoter region via phase-specific transcription factors as with early transcription.

Three intermediate and five late VACV transcription factors have been identified (table 1.2), which are all required in combination with RNA polymerase for the activation of transcription *in vitro* (Keck *et al.*, 1990; Kovacs and Moss, 1996; Sanz and Moss, 1998). In addition, the capping enzyme is required for the initiation of intermediate transcription *in vitro* (Vos *et al.*, 1991).

Surprisingly, VITF-2 and VLTF-X were also purified from uninfected cells, suggesting that these factors are cellular proteins (Rosales *et al.*, 1994b; Wright *et al.*, 1998). It was later established that VLTF-X specifically binds to VACV late promoter DNA (Gunasinghe *et al.*, 1998). However, the precise function of VLTF-X and its interaction with other VLTFs and RNA polymerase is yet to be established. Likewise, the VITF(s) involved in VITF/promoter interaction and the mechanism of RNA polymerase recruitment is also yet to be determined.

1.4.2.3 Transcript modifications

Poxvirus transcripts are capped by methylation of the 5'-purine and are polyadenylated at the 3'-end. The cap structure is essential for the binding of viral mRNAs to ribosomes and hence translation. Polyadenylation at the 3'-end is likely to contribute to stability of the mRNA (Moss, 1990). The mechanisms of transcript modification have mainly been investigated in early transcription; although it is presumed that the same mechanisms function in intermediate and late phases (Condit and Niles, 2002).

The cap structure is formed on the nascent RNA and is catalysed by the capping enzyme complex (table 1.2), which is recruited to the 5'-end of nascent RNA by stable association with the RNA polymerase complex via the RAP94 subunit (Mohamed *et al.*, 2001). Polyadenylation of the 3'-end of RNA is catalysed by the VACV-encoded heterodimeric poly(A) polymerase protein (table 1.2) (Gershon *et al.*, 1991).

1.4.2.4 Transcription cofactors

Several VACV proteins have been identified as positive or negative transcription elongation factors, which prevent premature termination of transcription or extensive read through of genes (table 1.2). Some of these factors play a role in all phases of infection and some have other functions besides transcription regulation.

For example the VACV A18R gene is expressed and functions as a DNA helicase during all phases of infection (Simpson and Condit, 1995). In addition, A18R acts in conjunction with other as yet unidentified proteins as a negative elongation factor, effecting the release of intermediate and late transcripts from the transcription complex, thereby preventing extensive read through of genes (Lackner and Condit, 2000). In contrast, VACV G2R functions as a positive elongation factor for intermediate and late genes, preventing the premature termination

of transcription (Black and Condit, 1996). Interestingly, the deletion of the G2R gene appears to compensate for the deletion of the A18R gene, which suggests that G2R and A18R interact either directly or indirectly with each other in the regulation pathways of intermediate and late transcription (Condit *et al.,* 1996). Likewise, in addition to transcription initiation and transcript modification (sections 1.4.2.2 and 1.4.2.3), the VACV J3R also functions as an intermediate and late transcription positive elongation factor (Latner *et al.,* 2000). To date, only one putative early gene elongation factor (NPH I) has been identified. In addition to its role in early gene termination (section 1.4.2.1), NPH I may also play a non-essential role in RNA elongation by preventing the early termination of transcription in response to T-rich regions in the template DNA (Deng and Shuman, 1998; Condit and Niles, 2002).

1.4.3 Virion Development and Release

1.4.3.1 Membrane formation

Assembly of progeny virus occurs in the dense areas of the cytoplasm referred to as the viroplasm or virus factories. The first stage of virus assembly is characterised by the appearance of crescent-shaped membranes, which develop into spherical immature virus (IV). Several authors have reported that the developing crescent membranes are formed *de novo* (Morgan, 1976; Hollinshead *et al.,* 1999). This is contested by reports that in VACV and ORFV assembly, the viral crescents are derived from the cellular membranes of the smooth endoplasmic reticulum (Sodeik *et al.,* 1993; Onwuka *et al.,* 1995). The generation and study of a range of VACV deletion, temperature sensitive or drug dependent mutants has identified several genes, including A14L, A17L, D13L and F10L, that are essential for the correct formation of the crescent membranes (Sodeik *et al.,* 1994; Sodeik *et al.,* 1994; Rodriguez *et al.,* 1995; Rodriguez *et al.,* 1998; Traktman *et al.,* 1995). Putative roles for these proteins have been suggested, including protein-protein or protein-membrane interactions that alter the cellular derived membrane and provide scaffolding-like support for the developing crescents (Sodeik and Krijnse-Locker, 2002).

1.4.3.2 Packaging of nucleoprotein, DNA and IMV development

The electron dense nucleoprotein core material is seen in close association with the developing crescents, and later becomes encapsulated by the membrane to form IV (Morgan, 1976). Following packaging, the IV core undergoes what is described as the condensation of the nucleoprotein material to form IMV (Morgan, 1976; Sodeik *et al.,* 1993). Evidence suggests that several proteins (A4L, A9L, A30L, A32L, L4R, E10R, J1R and G7R) may be involved in

packaging of the core and subsequent core protein cleavage to form IMV (Wilcock and Smith, 1996; Cassetti *et al.,* 1998; Risco *et al.,* 1999; Yeh *et al.,* 2000; Senkevich *et al.,* 2000; Chiu and Chang, 2002; Szajner *et al.,* 2003). It is unknown how the early gene transcription machinery is packaged into the virus core. It was suggested that the machinery is packaged along with the viral DNA as a complex, via a VETF/early promoter binding mechanism (Li *et al.,* 1994). Conversely, Cassetti determined that the transcriptional machinery is also packaged independently of the DNA (Cassetti *et al.,* 1998).

1.4.3.3 Development of IEV

A proportion of IMV are transported from the viral factories along microtubules to the trans golgi network, where the IMV are wrapped in additional membranes forming IEV (Sodeik *et al.,* 1993; Sanderson *et al.,* 2000) (figure 1.1). The IMV cellular attachment protein A27L (section 1.4.1) is also essential for the microtubular transport of the IMV to the golgi and the wrapping of IMV with the additional golgi-derived membranes (Sanderson *et al.,* 2000; Vazquez and Esteban, 1999). Two EEV membrane proteins F13L and B5R localise to the golgi-derived membranes (Hiller and Weber, 1985; Ward and Moss, 2000) and are essential for the wrapping of IMV with additional membranes (Blasco and Moss, 1991; Engelstad and Smith, 1993; Wolffe *et al.,* 1993). This has lead to the hypothesis that F13L and/or B5R may interact with the IMV surface via A27L facilitating the efficient wrapping of IMV particles (Sanderson *et al.,* 2000; Smith *et al.,* 2002). However a direct interaction between A27L and either B5R or F13L has yet to be demonstrated.

1.4.3.4 Transport of IEV to the cell membrane and release

It was proposed that the movement of IEV to the cell periphery is via propulsion on the tip of a polymerising actin tail, and upon viral egress, actin-containing filopodia form beneath the CEV projecting it from the cell surface (Cudmore *et al.,* 1995). Evidence indicates that the IEV membrane protein A36R is responsible for actin polymerisation in association with the IEV membrane proteins A33R and A34R (Wolffe *et al.,* 1997; Wolffe *et al.,* 1998; Roper *et al.,* 1998; Frischknecht *et al.,* 1999; Rottger *et al.,* 1999). Upon the fusion of IEV with the cell membrane, the A36R protein becomes concentrated in the cytosolic face of the cell membrane immediately beneath the CEV (van Eijl *et al.,* 2000). As a result, it was suggested that actin filaments form at the plasma membrane underneath CEV producing the filopodia structure. In support, VACV mutants deficient in the membrane proteins A33R, A34R and A36R failed to

induce the formation of actin filaments and filopodia, however these mutants still produced virus, although the resulting plaques were smaller (Wolffe *et al.,* 1997; Wolffe *et al.,* 1998; Roper *et al.,* 1998). This suggests that firstly, the formation of actin containing filopodia beneath CEV particles promotes efficient cell to cell spread (Johnson and Huber, 2002) and secondly, that the transport of IEV and the egress to form CEV is not dependent upon A33R, A34R or A36R and hence actin microfilaments. An alternative model of IEV movement was proposed whereby virus is transported to the cell membrane via microtubules (Hollinshead *et al.,* 2001; Geada *et al.,* 2001). The evidence provided by Hollinshead and Geada is compelling. Firstly, actin filaments were observed at the periphery of infected cells but not in the centre. Secondly the movement of IEV to the cell periphery was inhibited with the microtubule disrupting drug nocadazole. Studies using F12L deletion mutants implied that the IEV-specific F12L protein is essential for microtubular movement of IEV to the cell periphery (van Eijl *et al.,* 2002).

1.5 POXVIRUS GENES ASSOCIATED WITH VIRUS VIRULENCE

The genes involved in virus replication (discussed in section 1.4) are generally located towards the centre of the genome and are conserved in all poxviruses. Towards the ends of poxvirus genomes, species or genus-specific genes that are not essential for virus replication in tissue culture are found. Several of these non-essential genes have been characterised and are associated with virus virulence *in vivo*. These virulence genes are in addition to the genes encoding immuno-modulatory proteins, which will be reviewed in context of the immune response to poxviruses in section 1.6. Examples of virulence genes are the virus-encoded growth factors, which are found in poxviruses belonging to most genera (table 1.3).

Homologues of the mammalian vascular endothelial growth factor (VEGF-E) were identified in the ORFV strains NZ2 and NZ7 near to the right ITR junction (Lyttle *et al.,* 1994). The NZ2 and NZ7 VEGF-Es exhibit little homology to each other at the DNA level and only 41.1% identity at the peptide level. It was postulated that these genes were acquired from the host, but that the sequence variation between NZ2 and NZ7 VEGF-Es is the result of separate gene acquisition events or sequence divergence from an ancestral strain (Wise *et al.,* 1999). The variation between the two ORFV strains is reflected in the VEGF-receptor (VEGF-R) affinities. Both ORFV VEGF-Es have a high affinity to VEGF-R2, however ORFV NZ2 VEGF-E also binds to neurophillin (NP-1) (Ogawa *et al.,* 1998; Wise *et al.,* 1999).

Mammalian VEGFs promote mitosis of vascular endothelial cells and angiogenesis, and increase vascular permeability (Risau, 1997). VEGFs from ORFV NZ2, NZ7 and strain D1701 all appear to be biologically functional. Mitotic activity, increased vascular permeability and chemotactic migration of epithelial cells have all been demonstrated *in vitro* with ORFV VEGF-E (Ogawa *et al.,* 1998; Wise *et al.,* 1999; Meyer *et al.,* 1999). In addition, VEGF-E induced angiogenesis has been demonstrated *in vivo* in the cornea of the rabbit (Meyer *et al.,* 1999). Infection of sheep with a recombinant ORFV, in which the VEGF-E gene was disrupted, resulted in lesions that were less severe, less vascularised and resolved more quickly than lesions induced with wild-type virus (Savory *et al.,* 2000). VEGF-E induced vascularisation of ORFV lesions may contribute to virulence by supporting extended dermal regeneration, thereby providing actively proliferating epithelial cells for the virus to infect and replicate within (Savory *et al.,* 2000). In addition extensive infectious scab formation and shedding into the environment may assist in the transmission of ORFV between individuals.

Genes have been identified in VACV, CPV, MYXV and SFV that encode polypeptides with structural similarity to mammalian epithelial growth and transforming growth factor alpha (Twardzik *et al.,* 1985; da Fonseca *et al.,* 1999; Cameron *et al.,* 1999; Willer *et al.,* 1999). VACV mutants deficient in VACV growth factor (VGF) were shown to be attenuated (Buller et al., 1988b). Conversely, wild type VACV with a functional VGF gene were fully virulent and shown to induce cell proliferation *in vivo* (Buller *et al.,* 1988a). The VGF is predicted to increase virus virulence *in vivo* in similar manner to ORFV VEGF-E by simulating epithelial cells to divide thereby providing target cells for VACV to infect (Haig, 2001).

Response targeted	Virus/gene	Mechanism
Apoptosis	MOCV 159L and 160L	Interacts with FADD preventing caspase activation
	CPV *crm*A; VACV B13R	Inhibition of caspase-1 and IL-1β
	MYXV 011L	Inhibits apoptosis by effecting mitochondrial permeability
NK function	MOCV 080R	MHC I homologue, putative role in preventing NK
Complement	VACV C21L	Complement C3b and C4b binding protein
	VACV host	Host derived complement control proteins in EEV
Cytokines	VACV E3L; ORFV 20.0L	Binds dsRNA and inhibits the PKR and RNAase L IFN-induced anti-viral pathways
	VACV K3L	Pseudo-substrate for PKR phosphorylation
	VACV B8R; MYXV 007L/R	Soluble IFNγ receptor homologue
	VACV B18R	Soluble and envelope IFNα/β receptor homologue
	CPV *crm*B; CPV *crm*D	TNFα and TNFβ receptor homologues
	CPV *crm*C&D; VACV A53R	TNFα receptor homologue
	ORFV IL-10; LSDV 005L	Homologue of IL-10, down-regulates Th1 response
	ORFV GIF	Soluble GM-CSF and IL-2 binding protein
	MCV 053L	Soluble IL-18 binding protein, inhibits IL-18 induced IFNγ production
	VACV D7L	Soluble IL-18 binding protein, inhibits IL-18 induced IFNγ production and NK activity
	VACV B15R	Soluble IL-1β binding protein.
Chemokines	SWPV K2R	Soluble IL-8 receptor homologue
	MCV 148R	CC chemokine antagonist
	VACV B29R; MYXV 001LR	Soluble CC binding protein, inhibits inflammatory cell accumulation
	MYXV 007L/R; SFV 007L/R	IFNγ receptor which also binds and inhibits C, CC and CXC chemokines
Growth factors	ORFV VEGF-E	Soluble homologue of VEGF, promotes angiogenesis
	FPV 080	Soluble homologue of transforming growth factor β
	VACV C11R; MYXV 010L; LSDV 016; YLDV 15L	Soluble homologue of epidermal growth factor/transforming growth factor alpha

Table 1.3 Summary of a selection of poxvirus encoded immuno-modulating and virulence factors. Data is adapted from Smith *et al.,* (1997); Moss *et al.,* (2000); Alcami and Koszinowski, (2000) and Haig, (2001). The identity of each virus is indicated by its standard abbreviation (van Regenmortel *et al.,* 2000) or as defined in the summary of abbreviations (located at the beginning of this thesis).

1.6 IMMUNITY TO POXVIRAL INFECTIONS

The mammalian host has evolved many complex mechanisms for dealing with viral infections. A successful immune response results in the clearance of virus and long term immunity, whereas an unsuccessful response results in clinical disease and recurring infections. The immune response to infection is characterised by two phases, the innate response and the adaptive response. Poxviruses have involved many strategies to inhibit or subvert both responses. Immunity and counter immunity is reviewed here (sections 1.6.1 to 1.6.3) with particular emphasis on ORFV, however as the immune response to VACV is the most well characterised it is also included.

1.6.1 Innate response

The innate immune response is antigen non-specific and is characterised by apoptosis, complement activation, macrophage and natural killer cell (NK) activity and the production of interferons (IFN) and inflammatory cytokines. Viral inhibition of these responses is predicted to provide the virus with increased capacity to produce progeny virus early in infection and hinder the hosts ability to mount a successful adaptive response to infection (Haig, 2001).

Type I interferons (IFNα and IFNβ) are produced by virus-infected cells and induce an antiviral state in neighbouring cells by interfering with protein synthesis pathways (see below). Type II interferon (IFNγ) is produced by activated NK and T-cells and also induces an antiviral cell state; in addition IFNγ is a potent mediator of adaptive immune responses (Goodbourn *et al.*, 2000). The study of VACV infection in IFNα/β/γ receptor knock out mice has shown that IFNs I and II are important in reducing VACV viral replication and pathogenesis *in vivo* (van den Broek *et al.*, 1995). VACV possesses two genes, E3L and K3L that inhibit the action of IFNs (Beattie *et al.*, 1991; Watson *et al.*, 1991). The existence of a homologue of the VACV E3L gene in ORFV (OV20.0L) may explain the resistance of ORFV-infected cultured ovine cells to the action of type I and II IFNs (McInnes *et al.*, 1998; Haig *et al.*, 1998).

Two dsRNA-dependent IFN-induced anti-viral pathways have been described in mammalian cells (Goodbourn *et al.*, 2000). The first pathway involves the activation of the enzyme P1/eIF-2 protein kinase (PKR) by a dsRNA-induced autophosphorylation reaction. Activated PKR phosphorylates the α subunit of the protein synthesis initiation factor (eIF-2α), which in its

natural non-phosphorylated form is involved in the initiation step of protein translation. Phosphorylation of the eIF-α subunit by PKR inhibits the eIF-2α function, disrupting protein synthesis and virus replication. The VACV E3L protein has a high binding affinity for dsRNA and has been shown to inhibit the activation of PKR *in vitro* by actively competing with PKR for dsRNA (Davies *et al.,* 1993). Likewise, the ORFV homologue of the VACV E3L inhibits the autophosphorylation of PKR *in vitro* and binds dsRNA in the same manner as the VACV E3L protein (Haig *et al.,* 1998). The second IFN/dsRNA-induced antiviral pathway is mediated by 2',5'-oligoadenylate synthetase (2-5A). This pathway results in the RNAase L mediated cleavage of mRNA and rRNA, thereby inducing an antiviral cell state by disrupting protein synthesis. The VACV E3L also inhibits the 2-5A pathway by competing with 2-5A for dsRNA (Rivas *et al.,* 1998).

The K3L gene encodes the second VACV protein that is involved in the modulation of the PKR anti-viral pathway. The K3L protein shares identity with the eIF-2α subunit, particularly over the serine-51 region, the site of phosphorylation (Beattie *et al.,* 1991). It is hypothesised that K3L acts as a pseudo-substrate for PKR preventing the phosphorylation of eIF-2α (Davies *et al.,* 1992; Davies *et al.,* 1993).

Host cell apoptosis is induced in a variety of ways including: viral entry, cytokines such as tumour necrosis factor (TNF) and IFN, cell cycle dysfunction (via the p53 pathway), release of cytochrome C from mitochondria and the overload of the endoplasmic reticulum (Everett and McFadden, 1999). Activation of PKR and 2-5A has also been linked to apoptosis (Goodbourn *et al.,* 2000), although it remains to be demonstrated directly if poxvirus interference of these results in the inhibition of apoptosis (Haig and McInnes, 2002). Poxviruses have nevertheless evolved numerous other mechanisms to inhibit apoptosis mainly by disrupting the apoptosis signalling pathways (table 1.3 for examples). In addition, many poxviruses encode soluble cytokine receptor homologues or binding proteins for cytokines such as TNF and IFNs (table 1.3). Sequestration of TNF and IFN not only prevents pro-apoptotic signalling but also subverts the induction of the anti-viral cell state and immune signalling involved in the activation of immune cell populations (Haig, 2001).

Natural killer cells (NK) are important contributors to the innate defence against viruses (Biron *et al.,* 1999). NK cells are activated by IFNα and IFNβ and are involved in NK cell-mediated cytotoxicity and production of cytokines that enhance the innate response and up-regulate adaptive immunity. Although little is known about the mechanisms NK cells use to recognise virus-infected cells, an inverse correlation exists between major histocompatability complex I (MHC I) expression and NK cell killing (Biron *et al.,* 1999). MOCV encodes homologues of MHC I (table 1.3). When expressed, the MHC I homologues are predicted to protect virus-infected cells from NK-mediated killing (Senkevich *et al.,* 1996).

Complement proteins play a role in limiting spread of many viruses during the viremic stage, principally by destroying virus-infected cells or by damaging or inhibiting viral particles (Ochsenbein and Zinkernagel, 2000). VACV EEV are resistant to the action of complement and this is predicted to be due to an array of host derived complement control proteins (table 1.3), which are localised on the surface of the EEV envelope (Smith *et al.,* 2002). In addition, the VACV gene C21L encodes a complement binding protein that interferes with the activation of the complement cascades (Isaacs *et al.,* 1992).

1.6.2 Adaptive response

The adaptive response is antigen specific and is "learned" from the interaction of B and T-cells with antigen presented by the antigen presenting cells (APCs) in the lymph node draining the site of infection. Activated B-cells produce antibody that is specific for viral proteins and functions to neutralise virus directly or in conjunction with cytotoxic T-cells (TCs), NK cells, phagocytes and complement. Activated TCs, particularly the T-helper cells (Th), produce cytokines that enhance B-cell function or that stimulate TC-mediated killing of virus-infected cells (Haig, 2001).

1.6.2.1 Antibody response

Ovine antibodies to ORFV can be detected at 48 hours post infection by a variety of methods (Robinson and Balassu, 1981). A number of ORFV immuno-dominant antigens elicit detectable antibody responses, but whether these antibodies are involved in the clearance of virus is unknown (McKeever *et al.,* 1988; Mercer *et al.,* 1994; Haig and Mercer, 1998). Although these antibodies are often detected at very high titres, indicating a seemingly normal humoral response

to ORFV, animals are susceptible to re-infection (McKeever *et al.,* 1988; Yirrell *et al.,* 1989). In addition, passively acquired antibodies do not protect lambs from challenge with ORFV (Buddle and Pulford, 1984; Mercer *et al.,* 1994). Recently however, a positive correlation between antibody titre and the resolution of ORFV lesions has been reported, suggesting that antibodies may play a small role in viral clearance, although they do not confer protection against reinfection (Lloyd *et al.,* 2000).

In contrast, a specific antibody response against the surface proteins of VACV EEV is likely to be important for immunity (Smith *et al.,* 1997). Protection however, does not appear to be the result of antibody mediated virus neutralisation. Instead antibodies specific for the EEV surface protein B5R result in the aggregation of the virus and prevent the release of progeny virus from infected cells (Vanderplasschen *et al.,* 1997). As EEV is the main effector of long range virus spread, antibody mediated reduction of EEV may reduce or eliminate viremia. ORFV is a localised infection and viremia does not occur even when antibody responses are inhibited (Lloyd *et al.,* 2000), which suggests a humoral response does not play an important role in preventing dissemination of the virus. The lack of convincing evidence supporting antibody-mediated protective or passive immunity or a role for antibody in virus containment suggests that immunity is largely, if not solely, the result of a cellular-mediated response.

1.6.2.2 Cellular immunity and subversion

Infection of the epidermis by ORFV induces an inflammatory response characterised by the influx of immune cell populations and the expression of cytokines in and around the lesion. Protective immunity is only partial, as previously infected animals are susceptible to reinfection, however the resulting lesions are less severe. The immune and inflammatory cell populations present in ORFV induced lesions have been characterised by histopathological examination with monoclonal antibody staining. Upon primary infection with ORFV, neutrophil and basophil numbers rapidly increase and infiltrate lesions. In addition MHC class II^+ dendritic cells (DC), B-cells and several populations of T-cells, including γδT-cells, $CD4^+$ and $CD8^+$ T-cells accumulate in the dermis below the developing lesion. Unusually for a response to a viral infection the $CD4^+$cells are more numerous than $CD8^+$ T-cells or B-cells (Jenkinson *et al.,* 1990; Jenkinson *et al.,* 1991; Jenkinson *et al.,* 1992). Re-infection also promotes the same cellular response, although response times are reduced and the lesion resolves more rapidly.

The accumulating MHC class II$^+$ DCs forms a dense network below the damaged epidermis and are hypothesed to act as a barrier preventing the further invasion of the dermis by ORFV. In addition, this network of DCs may also function as an inflammatory centre for the recruitment of other cell types (Jenkinson *et al.,* 1991). Reported functions of DCs also include antigen presentation, activation of T and B cells and stimulation of CD4$^+$ memory cells. They may also play a role in clonal selection of T-cells in the lymph node. Some DCs have also been shown to function as phagocytes *in vitro* (Haig *et al.,* 1999).

The lymphoproliferative response to infection with ORFV was studied in the afferent (draining the site of infection) and efferent (draining the local lymph node) lymph (Yirrell *et al.,* 1991b; Yirrell *et al.,* 1991a). The efferent lymph showed an increase in CD4$^+$ T-cells, indicating that immune cell stimulation in response to ORFV had occurred. Characterisation of afferent lymph in response to ORFV reinfection demonstrated a biphasic increase in CD4$^+$ T-cells, CD8$^+$ T-cells, B-cells and DC populations, and as with the skin analysis the CD4$^+$ T-cells were the most abundant (Haig *et al.,* 1992; Haig *et al.,* 1996a; Lear *et al.,* 1996). In addition there was an increase in the levels of IFNγ and granulocyte macrophage colony stimulating factor (GM-CSF) and the interleukins, IL-2, IL-1β and IL-8 detected in the efferent lymph following ORFV reinfection (Haig *et al.,* 1992; Haig *et al.,* 1996b; Haig and McInnes, 2002). Comparison of cytokine mRNA expression in primary and secondary lesions demonstrated that TNFα was expressed during primary and secondary infection, whereas IFNγ was only detected following secondary infection (Anderson *et al.,* 2001). This is consistent with an early memory Th1 mediated response resulting in the activation of T-cells within the dermis and lymph node and the recruitment of antigen specific cells to the site of infection. The activation and recruitment of CD8$^+$ T-cells to the lesion corresponds with viral replication levels, which suggests that an cytotoxic lymphocyte response is effective in limiting viral replication during reinfection (Haig *et al.,* 1996b). The acquired partial immunity to ORFV can be abrogated by treatment with cyclosporin A, presumably by eliminating IL-2 and IFNγ induced T-cell activation (Haig *et al.,* 1996c).

A novel ORFV protein (GIF) has been shown to bind and inhibit the biological function of both ovine GM-CSF and IL-2 *in vitro*. However no homology was evident to host GM-CSF/IL-2 receptor molecules, suggesting GIF is not a receptor homologue (Deane *et al.,* 2000). GM-CSF

and IL-2 are present in the lymph draining from ORFV lesions (Haig *et al.,* 1996a). IL-2 is a multifunctional cytokine promoting proliferation and activation of a variety of T-cells, B-cells, NK-cells, DCs and monocytes (Roitt *et al.,* 1998). GM-CSF promotes proliferation and differentiation of granulocytes and macrophages and is crucial for the development of DCs (Hamilton, 2002). GM-CSF has specifically been implicated with the recruitment of DCs to ovine skin and the proliferation of afferent lymph DCs *in vitro* (Haig *et al.,* 1995a; Haig *et al.,* 1995b). It is possible that the ORFV GIF protein could inhibit any or all of the IL-2 and GM-CSF functions (Haig, 2001). Deane *et al.,* (2000) proposed that the localised presence of GIF around the ORFV lesion would interfere in the cell-mediated response to ORFV and may hinder the development of protective immunity.

A homologue of the ovine cytokine IL-10 has been identified in ORFV (Fleming *et al.,* 1997). Functional characterisation demonstrated that ORFV IL-10 stimulates ovine and murine thymocyte and mast cell proliferation (Fleming *et al.,* 1997; Fleming *et al.,* 2000; Imlach *et al.,* 2002; Haig *et al.,* 2002). However the production of the cytokines TNFα, IL-1β and IL-8 by activated ovine macrophages, monocytes and keratinocytes, and GM-CSF and IFN-γ by peripheral lymphocytes is reduced in response to IL-10 (Fleming *et al.,* 2000; Haig *et al.,* 2002). Experimental infection of sheep with an ORFV mutant specifically lacking the IL-10 gene resulted in an increased production of IFNγ in and around the lesion site (Fleming *et al.,* 2000). These data indicate that ORFV IL-10 suppresses the production of pro-inflammatory cytokines and IFNγ (Haig *et al.,* 2002). The exertion of all these effects may skew the immune response towards a type-2 humoral response, which is an inappropriate defence against ORFV-infected cells. Recent evidence also indicates that virus-encoded IL-10 inhibits the maturation, migration and antigen presenting function of murine DCs (Lateef *et al.,* 2003). This may explain why an acquired immunity to ORFV is incomplete resulting in repeated infections.

A homologue of a chemokine-binding factor has been recently identified in ORFV (Fleming *et al.,* 2000). Although this binding factor has not yet been characterised, it may function in conjunction with IL-10 to reduce inflammation and may account for the lack of accumulation of $CD8^+$ T-cells. Several chemokine-binding factors have been identified in other poxviruses (table 1.3).

1.7 VACCINES

Poxvirus vaccination strategies often involve the use of one poxvirus species to protect against a related virus, for example the use of VACV for the protection against VARV (section 1.1). In contrast, vaccine strategies for the control of ORFV involves the administration of virulent ORFV (prepared from scab material) to a scarified site, usually on the thigh (Robinson and Balassu, 1981; Reid, 1991). This form of vaccination results in lesion formation at the site of scarification, but not around the mouth as is often the case in natural infections. Vaccination with ORFV does not provide complete protection against challenge, however the resulting lesions are usually much less severe when compared to primary natural infections. Because vaccines propagated in animals risk contamination with other viruses or bacteria, the use of live tissue-culture propagated ORFVs as an alternative to scab derived virus was investigated (Pye, 1990; Nettleton *et al.,* 1996a). Vaccination of sheep with tissue culture propagated ORFV strain Nara was shown to confer partial protection against challenge, however some ORFV strains did not (Pye, 1990). The reduced level of protection provided by some tissue-culture propagated ORFV strains may be due to attenuation occurring during adaptation to tissue culture (McInnes *et al.,* 2001). The use of live ORFV as a vaccine is not satisfactory as infectious virus can be shed into the environment (Haig and Mercer, 1998). To address this problem, an alternative vaccine strategy using recombinant VACV that express immuno-dominant ORFV proteins may have merit (Mercer *et al.,* 1997b). Vaccination with a panel VACV recombinants containing 90% of the ORFV genome provided the same degree of protection as did vaccination with tissue culture grown ORFV, but without the formation of ORFV-like lesions.

Construction of recombinant poxviruses generally involves insertion of the desired foreign gene into the thymidine kinase gene (TK) locus of the virus by homologous recombination (Brown *et al.,* 1986). Experimental vaccination with recombinant VACVs has proved successful in protecting animals from subsequent challenge with many pathogens including hepatitis, malaria, rabies and HIV (Paoletti, 1996). Recombinant poxviruses used to vaccinate their own specific host species can have the added advantage of providing dual protection. For example, vaccination of poultry with an attenuated FPV vaccine strain expressing Newcastle disease virus (NDV) proteins provide dual-protection to subsequent challenge with both FPV and NDV (Paoletti, 1996).

Safety issues concerning the use of recombinant VACV have arisen due to the extensive host range of VACV and side effects of vaccination. This has prompted research into the feasibility of using severely attenuated and non-replicating VACV strains, for example VACV Ankara, as vaccine vectors (Moss, 1996a). Alternatively, poxviruses with a limited host range have been assessed for efficacy as vaccine vector. Expression of rabies, measles and feline leukaemia virus genes in a *Canary poxvirus* vector have proved successful when used to vaccinate non-avian species (Paoletti, 1996). The use of highly attenuated parapoxviruses, such as ORFV strain D1701, as recombinant vaccine vectors are being considered primarily because they have a relatively limited host range, produce localised infection without viremia and can promote a vigorous immune response in natural and non-permissive hosts (Rziha *et al.,* 1999). Due to their non-essential nature, the ORFV VEGF-E and G1L genes were chosen as a possible sites for foreign gene insertion (Rziha *et al.,* 1999; Rziha *et al.,* 2000; McInnes *et al.,* 2001; Marsland *et al.,* 2003). Several foreign proteins have been successfully expressed from recombinant ORFVs, however to date only the humoral response in mice to foreign protein expression has been assessed (Rziha *et al.,* 2000).

1.8 POXVIRUS DISEASE OF RED SQUIRRELS

1.8.1 Decline of the red squirrel

In the 17th and 18th centuries, deforestation coupled with changes in agricultural and industrial practices brought the European red squirrel (*Sciurus vulgaris*) population in some areas of Britain to the verge of extinction. Red squirrels numbers recovered and became abundant in the 19th and early 20th century (Lloyd, 1983). However since the introduction of the American grey squirrel (*Sciurus carolinesis*) in the late 19th century, red squirrel numbers have been decreasing rapidly (Shorten, 1946; Shorten, 1957; Lloyd, 1983; Gurnell and Pepper, 1993; Pepper and Paterson, 1998). The prognosis for the survival of the British red squirrel is poor, with extinction in England possible within ten to twenty years (Kenward and Holm, 1989; Gurnell and Pepper, 1991; Gurnell and Pepper, 1993). The endangered status of the red squirrel has placed it on the protected species list of the Wildlife and Countryside Act 1981. The cause of the rapid decline of red squirrels is not fully understood, although it is clear from the literature that the grey squirrel is implicated, possibly exerting effect by competition and the transmission of disease.

1.8.1 Species replacement, the role of competition and disease

Ecological replacement of the native red squirrel by the greys is dependent upon a number of factors including the deciduous or coniferous nature of the habitat and availability of food resources. Behavioural traits such as direct aggression, interference in red squirrel courtship and red squirrel passive avoidance of the grey squirrel may all play a role in local replacement (Skelcher, 1997). Several authors attribute population decline or extinction on a local level to the presence of SPPV (Middleton, 1930; Edwards, 1962; Scott *et al.*, 1981; Sainsbury and Ward, 1996; Sainsbury *et al.*, 1997; Sainsbury and Gurnell, 1997). Some populations of red and grey squirrels have co-existed for prolonged periods of time in Ireland, this may be due to the diverse local habitat, or the absence of SPPV (Tangney and Montgomery, 1995; Skelcher, 1997; Teangara *et al.*, 1999). Suspected cases of SPPV in Ireland have been reported but not confirmed (Sainsbury *et al.*, 1997). This lead to speculation that the absence of SPPV in Ireland has deprived the grey squirrel of a competitive advantage, thus preventing the efficient replacement of red species, as is so often observed in England (Duff *et al.*, 1996). Coexisting populations are also evident in Scotland (Bryce, 1999), and this situation has also been attributed to the absence of SPPV (Sainsbury *et al.*, 2000).

1.8.2 History of viral epidemic disease in the red squirrel

Several dead squirrels were collected between 1904 and 1926 from squirrel populations that were in decline. Pathological examinations revealed the presence of coccidiosis, which at that time was proposed to be the cause of population decrease. Middleton (1930) reviewed these cases and noted the presence of external symptoms not consistent with coccidiosis. He attributed population reduction to a disease of an unknown nature.

Since Middleton's early work, several outbreaks of epidemic disease in red squirrels resulting in local extinction have been reported as mange, distemper, scab or myxomatosis (Shorten, 1964; Edwards, 1962). In all of these reports, there is a consistency in the description of gross pathology suggesting the same agent is involved. Symptoms usually begin with haemorrhagic ulceration of the eyelids that quickly spreads to the nasal and buccal regions, the resultant swelling causes blindness and difficulty in swallowing. Ear lesions often result in decomposition of the concha. Secondary infection by *Staphylococcus aureus* commonly causes purulent eye and nasal discharge. Exudative dermatitis and haemorrhagic crusts develop, particularly

effecting the thorax, inguinal area, genital region, hands and feet (Edwards, 1962; Sainsbury and Gurnell, 1995). Mortality in the wild is estimated to approach near to one hundred percent (Tompkins *et al.*, 2002).

Post mortem examinations dismissed coccidiosis, mange mites and bacterial disease as the causative agent and a viral candidate was sought (Edwards, 1962). An RNA virus, which demonstrated serological cross-reactivity to encephalomyocarditis viruses, was isolated from an apparently healthy animal captured during an outbreak of disease in Thetford chase (Vizoso *et al.*, 1964). A virus morphologically similar to the paramyxovirus Newcastle virus disease was isolated from lung suspensions obtained from squirrels with severe scabs (Vizoso, 1968). However, the role of these viruses in the aetiology of the scab disease was questioned and fresh attempts were made to identify and isolate a more likely causative agent (Keymer, 1976). No progress was made until electron microscopy of scab material taken from an eyelid of an affected red squirrel revealed SPPV particles present in large numbers (Scott *et al.*, 1981). SPPV was successfully isolated in red squirrel kidney monolayers (Sands *et al.*, 1984).

1.8.3 The role of the grey squirrel in epidemic disease

Middleton (1930) hypothesed that the grey squirrel may act as a carrier for a disease that is non-pathogenic to the grey species but fatal to the red squirrel. To evaluate this proposal the dates of grey squirrel introduction and the onset of disease in the red populations were studied. The first recorded introduction of grey squirrels to England was in 1876 at Henbury Park, Cheshire, but the most important introduction was made at Woburn Park (Bedfordshire) in 1890. Squirrels from the thriving Woburn population were later used to stock sites across the British Isles, including London, Yorkshire, Cheshire, Wales and Ireland. Other stocks of squirrels were also imported from America, independent of the Woburn and Henbury stocks (Middleton, 1930).

A number of authors reported that the onset of disease in local populations coincided with the appearance of grey squirrels and close interaction been the two species (Edwards, 1962; Scott *et al.*, 1981). It was suggested that if grey squirrels introduced the virus, the disease would be observed radiating outwards within the red squirrel population from the points of grey squirrel introductions. This pattern has not been observed at many points of introduction (Shorten, 1964; Keymer, 1983). However Vizoso (1968) argued that it is impossible to know where every

introduction occurred and suggested the expected pattern would be disrupted if the virus were maintained within red squirrels.

In 1994 a grey squirrel from Hampshire was found with lesions on the head resembling those found in red squirrels suffering from SPPV. Electron microscopy of the lesions revealed parapoxvirus-like particles (Duff *et al.,* 1996). It was postulated that this virus was SPPV and that SPPV is maintained in the grey squirrel population but clinical manifestation is rare. Unfortunately this virus was not isolated in culture, nor any scab preserved and therefore it is impossible to confirm whether this grey squirrel virus was indeed SPPV.

Red and grey squirrel sera from all over the United Kingdom have been tested for antibodies to SPPV using a direct enzyme-linked immunosorbent assay (ELISA). The results revealed that grey squirrels have a high sero-prevalence of antibodies to SPPV (discussed further in section 3.1). Furthermore, the geographical distribution of sero-positive grey squirrels correlates well with the reported disease outbreaks in red squirrels. Conversely, no disease has been reported in red squirrels where the grey squirrel population is sero-negative for SPPV. The sero-prevalence in red squirrels was low, which is presumably because of the high mortality caused by the disease and the difficulty in obtaining sera from red squirrels found dead in the wild. These data indicate a high occurrence of endemic SPPV infection of low pathogenicity in grey squirrels, further compounding the role of grey squirrels in the epidemiology of SPPV (Sainsbury *et al.,* 1997; Sainsbury *et al.,* 2000).

The epidemiology of SPPV may involve the transmission of the virus from clinically unaffected grey squirrels to susceptible red squirrel populations (Middleton, 1930; Duff *et al.,* 1996). Alternatively, this disease may be present in both red and grey populations as a sub-clinical infection. The stress resulting from competition (section 1.8.1) at the interface between the two species may exacerbate the infection in red squirrels. The resultant increase in red squirrel mortality rates may enable the grey squirrel to efficiently colonise red territory (Vizoso, 1968; Duff *et al.,* 1996). In summary, the evidence strongly supports the role of the grey squirrel as a reservoir host, but this cannot be endorsed until a mode of transmission is determined.

1.8.4 Present disease status and squirrel conservation strategies

Norfolk has a continuing problem of disease in coexisting squirrel populations and outbreaks in Lancashire resulted in a significant depletion of the red squirrel populations (Sainsbury and Gurnell, 1995; Sainsbury and Ward, 1996). More worrying are reports of SPPV in Cumbria, Northumberland and suspected cases in Scotland, which indicate that the geographic range of SPPV is expanding northwards, into the last stronghold of the red squirrel (Sainsbury *et al.,* 1997; Duff *et al.,* 2001).

Red squirrel conservation strategies are based upon creating an environment that benefits the red squirrel but is sub-optimal for the grey species (Lurz and Garson, 1997). Gurnell and Pepper (1993) suggested that predominately coniferous forests greater than two thousand hectares with an existing red squirrel population should gain red squirrel protection area status. For forests that are at risk of grey squirrel invasion establishing a three-kilometre wide buffer zone consisting of habitat unsuitable for grey squirrels is advisable (Pepper and Patterson, 1998). Red squirrels gain far less nutritional value from food derived from oak woodland than grey squirrels (Kenward and Holm, 1989). Therefore removing oak trees from habitats containing both species of squirrels or creating coniferous habitats for red squirrels may provide a selective advantage to red squirrels. The variety of conifers available should be a mix of species that seed at different times of the year to ensure continuation of food supply for the red squirrels (Gurnell and Pepper, 1991 and 1993; Lurz and Garson, 1997).

Where red squirrel populations are in imminent danger of replacement by grey species, the removal of grey squirrels by trapping or shooting should be considered as a temporary solution (Gurnell and Pepper, 1991; Venning *et al.,* 1997). More humane grey squirrel control methods involving immuno-contraception have been investigated (Moore *et al.,* 1997; Lurz *et al.,* 2002). However trials in the wild have proved inconclusive and research has been temporarily abandoned until more information on grey squirrel reproductive biology and immunology is available (Forestry Commission, 2002).

Fragmentation of red squirrel populations in England and Wales is of concern as it often results in a reduction in genetic diversity, increasing the risk of population extinction (Wauters, 1997). Management of the landscape to create corridors of suitable habitat bridging isolated populations have been shown to substantially increase the genetic diversity by allowing isolated populations

to mix (Hale *et al.,* 2001). However, forest defragmentation schemes underway in Northern England that are connecting prime red squirrel habitat to Southern Scotland may ultimately do more harm than good, by introducing disease to Scotland (Tompkins *et al.,* 2003). Completely isolated populations such as Jersey and Thetford chase in Norfolk are homogeneous in term of genetic diversity (Barratt *et al.,* 1997). The genetic diversity of these populations cannot be managed by linking to other populations using corridors due to geographical distance, however they can be managed by the selective introduction of genetically diverse individuals. Unfortunately this method of population management also increases the risk of introducing disease (Sainsbury and Gurnell, 1995; Hale *et al.,* 2001). Indeed successive attempts to bolster dwindling populations by reintroducing captive bred squirrels or by translocating wild squirrels have met with limited success in North Wales and Norfolk due to SPPV disease (Venning *et al.,* 1997; Jackson, 1999). All of the authors involved in the initial relocation studies agree that the health of the animals to be released and that of the resident red and grey squirrels should be examined closely before attempting to re-stock an area.

Supplemental feeding trials have not conclusively shown long-term benefit to red squirrels (Shuttleworth, 1997), although it is believed to be of benefit in some populations where food is scarce and population density is low (Warren, 1999). However, food hoppers may increase the risk of disease transmission, therefore in areas where SPPV has been reported, all food hoppers should be removed (Warren, 1999; Collins, 1999).

It is estimated that over 2.5 million grey squirrels populate mainland Britain and the coniferous forests of Scotland may prove to be the only region that red squirrels may survive. However these areas are now threatened by the influx of grey squirrels and disease (Sainsbury *et al.,* 1997a; Pepper and Patterson, 1998). Enhancing the survival prospects of the red squirrel by eradicating the grey squirrel from Britain is no longer a feasible option due to the numbers of grey squirrels involved and their wide-spread distribution (Gurnell and Pepper, 1993). The production and application of an effective vaccine may prove to be essential for the successful reintroduction of red squirrels into areas populated by grey squirrels and ultimately for the survival of the red squirrel in the UK (Sainsbury *et al.,* 1997; Gurnell *et al.,* 1999).

1.9 PROJECT AIMS

The formal classification of SPPV as a parapoxvirus suggests that SPPV will have several features in common with ORFV including, similar route(s) of transmission and an analogous complement of non-essential genes encoding proteins involved in virulence and immuno-modulation. However, the classification of SPPV as a parapoxvirus by morphological similarity alone is not sufficient to substantiate its inclusion into the parapoxvirus genus. The general aim of this study is to characterise the molecular relationship of SPPV with the parapoxviruses, thereby providing evidence to support or refute its classification as a parapoxvirus.

The complete genome sequence of ORFV has not yet been determined, despite this the ORFV genome has been well-characterised (section 1.3). Therefore sufficient data is available for ORFV to enable a comparison of the SPPV genome with ORFV. The general structure, G+C content, gene complement and organisation of the two genomes will be compared. Particular emphasis will be given to identifying parapoxvirus genes in the SPPV genome that are associated with virulence and immuno-modulation. In addition the phylogenetic relationships between SPPV and the parapoxviruses will be investigated.

It is envisaged that characterisation of the SPPV genome and its relationship to the parapoxviruses will provide the fundamental data required for a subsequent vaccine feasibility study.

CHAPTER 2.0

MATERIALS AND METHODS

2.1 VIRUSES

2.1.1 Squirrel Parapoxvirus (SPPV)

2.1.1.1 Tissue Culture Grown SPPV

Virus was isolated at Central Veterinary Laboratory Agency (CVLA) at Weybridge from a red squirrel lip lesion by culturing in red squirrel kidney cells, it was then adapted to and passaged six times in sheep choroid plexus cells (Sands *et al.,* 1984). The sample obtained from CVLA Weybridge was contaminated with Aujeszky's disease virus (ADV), which was subsequently absorbed out using anti-ADV antiserum (Warns, 1995). Since then, SPPV was adapted to foetal lamb muscle cells (FLMC) and passaged a further twenty-four times (performed by J.Gilray, Moredun Research Institute).

2.1.1.2 SPPV scab isolate 1296/99

Scab material was collected at *post mortem* from a SPPV seropositive squirrel (originating from the Gateshead SPPV-outbreak, October 1999) which exhibited typical SPPV pathology. The presence of parapoxvirus particles was confirmed by electron microscopy (EM) performed by CVLA, Lasswade.

2.1.2 Orf virus (OV) tissue culture strains and scab isolates

2.1.2.1 Moredun Reference Scab

Moredun Reference Scab (MRI) was originally collected from a clinical case during an outbreak in Scotland (McKeever and Reid, 1986). It has been used to experimentally infect sheep several times, from which further scab material has been collected. MRI has not been passaged in tissue culture.

2.1.2.2 Orf-11

Orf-11 was originally isolated from a clinical case in Scotland. It was passaged twenty-nine times in ovine kidney cell and then subsequently maintained in FLMC (McInnes *et al.,* 2001).

2.2 TISSUE CULTURE

2.2.1 Cells and media

Foetal lamb muscle primary cells (FLMC) were cultured in growth media [199 Medium base supplemented to a final concentration with 10% (v/v) foetal bovine serum (FBS), see section

2.8.2 for preparation]. After inoculation with virus, cells were maintained in maintenance media [199 Medium base supplemented to a final concentration with 2% (v/v) FBS, see section 2.8.2 for preparation]. Cells were utilised from passage 3 to 16.

2.2.2 Production of virus in a tissue culture system

2.2.2.1 Infection of FLMC with virus

FLMC monolayers were cultured in 25cm^2 or 225cm^2 tissue culture flask (Nunc) to a confluence of 50 to 70%. Monolayers were washed twice with warmed phosphate buffer saline (PBS) prior to infection with virus. Each flask was infected at a multiplicity of infection (MOI) of 0.01 to 1 in a suitable volume of maintenance media (2mls to 10mls), or mock infected with maintenance media for the negative control flask. The virus was allowed to adsorb to the cells for 1 hour at 37°C before the addition 8mls or 90mls of maintenance media. Monolayers were incubated at 37°C for three to five days and harvested when approximately 90% cytopathic effect (CPE) was observed.

2.2.2.2 Titration of virus

A serial $\log_{10}$ dilution (10^{-1} to 10^{-6}) of the virus was prepared in maintenance media and 25µl of each virus-dilution was inoculated into 4 wells of a 96 well format tissue-culture plate (Nunc). Four non-infected cell-control wells received 25µl maintenance media. 100µl 2 x 10^5 FLMC/ml suspension prepared in growth media (supplemented with 1mM $MgCl_2$) was then added to each well. Plates were incubated at 37°C for 5 days after which each well was scored for CPE by visualisation using light microscopy. The log 50% tissue culture infective dose per ml (log $TCID_{50}$/ml) was calculated using the Spearman/Karber method (Grist *et al.*, 1979).

2.2.3 Preparation of virus for EM

2.2.3.1 Tissue culture-grown virus

An infected FLMC monolayer from a 25cm^2 tissue culture flask (Nunc) was harvested by scraping cells into medium. The cells were pelleted by centrifugation at 2000xg for 15 minutes at +4°C (CS-6R centrifuge, Beckman instruments). The supernatant was discarded and the cell pellet was suspended in 40µl PBS. The sample was sent directly for negative contrast EM (CVLA, Lasswade).

2.2.3.2 Scab virus

0.4g scab was ground in PBS with sand using a pestle and mortar, and clarified by centrifugation at 2000xg for 30 minutes at 4°C (CS-6R centrifuge, Beckman instruments). The clarified supernatant was layered over a 36% sucrose cushion (w/w in PBS) and the virus pelleted at 71,000xg for 30 minutes at 4°C (SW40ti rotor, Beckman instruments). Virus was suspended in 1ml PBS supplemented with 10mg/ml streptomycin and 10 units/ml penicillin. 100µl of the viral suspension was sent directly for negative contrast EM (CVLA, Lasswade).

2.3 SEROLOGY

2.3.1 Direct enzyme-linked immunosorbent assay (ELISA)

2.3.1.1 Preparation of SPPV and control antigens

SPPV antigen was prepared using the method adapted by Warns (1995). Briefly, eight 225cm^2 flasks of FLMCs were cultured to a confluence of 50% to 70%. Four flasks were infected with SPPV and four flasks were mock infected with maintenance media using the method described in section 2.2.2.1. The infected cells were harvested when the CPE reached approximately 90%; the mock-infected flasks were harvested in parallel and treated in the same way. The media was decanted and clarified by centrifugation at 2000xg at 4°C for 15 minutes (CS-6R centrifuge, Beckman instruments). The cell pellets were washed twice in PBS, resuspended in 3mls cell lysis buffer [1X PBS with 1% (v/v) Nonidet P40 (Sigma)] and then returned to the flasks. The flasks were incubated at 4°C for 2 hours, then the cell lysates decanted into microcentrifuge tubes and clarified by centrifuging at 13,000rpm at room temperature for 5 minutes in a bench top microcentrifuge (Sigma, 1-13). The supernatants derived from the positive and negative flasks were pooled separately and stored at -70°C. A titration was performed and the working concentration of the positive (SPPV infected extract) and negative (mock infected extract) antigens determined to be 1/200 (J. Gilray personal communication).

2.3.1.2 Assessing the suitability of Protein-G

Protein A and Protein G conjugated to Horseradish peroxidase (HRP) have both been shown to recognise red and grey squirrel IgG (Warns, 1995). However protein G was preferentially used in an ELISA to detect anti-SPPV antibodies due its higher sensitivity (Sainsbury *et al.*, 2000). The ability of protein G-HRP to recognise and bind to antibodies present in sera obtained from wood mice and bank voles was assessed using an ELISA and the appropriate dilution of protein

G-HRP determined. Briefly, 1/50 dilutions of sera obtained from red squirrels, BALB/c mice, wood mice and bank voles were made in carbonate-bicarbonate buffer pH 9.6 (section 2.8). 50µl of each diluted serum was added to ten wells of a 96-well microplate (Dynatech, M129B). Twelve wells received 50µl carbonate-bicarbonate buffer pH 9.6. The plate was incubated at 4°C overnight to allow the immunoglobulins to bind. The plates were washed four times with ELISA wash buffer [1X PBS with 0.05% (v/v) Tween 80 (Sigma)]. Non-specific binding sites were blocked with bovine serum albumin (BSA) by the addition of 100µl ELISA dilution buffer [1X PBS with 1% (w/v) BSA (Sigma)] to each well and incubation at 37°C for one hour. The plate was washed four times with ELISA wash buffer. A range of dilutions of Protein G-HRP conjugate (Sigma) in ELISA dilution buffer was added to the plate and allowed to bind at 37°C for one hour. After washing, 100µl of prepared orthophenylene diamine (OPD, Sigma) substrate (section 2.8) was added to each well. The colorimetric reaction was allowed to proceed for approximately eight minutes and then stopped by the addition of 50µl 2.5M Sulphuric acid (H_2SO_4). The optical densities (OD) were read at 492nm in a plate reader (MRX, Dyn-ex Technologies).

2.3.1.3 Direct ELISA conditions

The ELISA was an adaptation of the method used by Sainsbury *et al.,* (2000) to test red and grey squirrel sera for anti-SPPV IgG. Duplicate wells in 96 well microplates (Dynatech, M129B) were coated overnight at 4°C with 50µl of positive and negative antigens (see section 2.3.1.1 for preparation) diluted 1/200 in carbonate-bicarbonate buffer, pH 9.6. Unbound antigen was removed by washing the plate four times in ELISA wash buffer. 100µl of test and control sera, were diluted 1/50 in ELISA dilution buffer and applied in duplicate to wells coated with positive and negative antigen. The plates were incubated at 37°C for one hour. After washing, 100µl of Protein G-HRP conjugate diluted 1/750 in ELISA dilution buffer, was applied to each well and incubated at 37°C for one hour. After washing, 100µl of prepared OPD was added to each well. The colormetric reaction was allowed to proceed for approximately 8 minutes before it was halted by the addition of 50µl 2.5M H_2SO_4 to each well. The OD of each well was read at 492nm with an ELISA plate reader (MRX, Dyn-ex Technologies) and the corrected optical densities for each test and control serum calculated by subtracting the mean OD of the negative antigen wells from the mean OD of the two positive antigen wells.

2.4 MOLECULAR METHODS

2.4.1 Preparation of viral DNA from scab material

The condition of the carcass prior to *post mortem* and the temperature of storage both effect the quality of viral genomic DNA recovered from scab material. DNA recovered from necrotic scabs or scabs that were stored long term at -20°C were heavily contaminated with fragmented host/bacterial DNA which was subsequently co-purified with viral particles. Fragmentation of DNA is a natural process due to apoptosis (Earnshaw, 1995) and the natural decay processes of DNA (Lindahl, 1993).

Viral DNA isolation was performed using a method adapted from Gilray *et al.,* (1998). An additional step was included which involved the pre-treatment of ground scab with Deoxyribonuclease I (DNAase I) prior to the disruption of viral cores, this is reported to reduce the level of contaminating degraded-DNA (Mazur *et al.,* 1991).

Briefly, 1g scab was ground with sand in 10ml PBS using a pestle and mortar, and centrifuged at 2000xg for 30 minutes at 4°C (CS-6R centrifuge, Beckman instruments). The clarified supernatant was layered over a 36% sucrose cushion (w/w in PBS) and the virus pelleted at 71,000xg for 30 minutes at 4°C (SW40ti rotor, Beckman instruments). The pellet was resuspended in 0.5ml DNAase I solution [1μg/ml DNAase I (Sigma) in 2mM $MgCl_2$; 80mM Tris-HCl, pH 7.4] and incubated for 2 hours at 37°C. The virus pellet was washed once in 10ml PBS and repelleted by centrifugation at 71,000g as before. The washed pellet was resuspended in 0.5ml GIT [4M Guanidinium isothiocyanate; 50mM Tris-HCl, pH 7.6; 10mM Ethylenediamine tetraacetic acid disodium salt (EDTA), pH 8; 2% N-lauroylsarcosine; 1% (v/v) β-Mercaptoethanol]. Following agitation at 37°C for 1 hour to disrupt the viral cores, the suspension was overlaid on to a 1.5ml 40% (w/v) Caesium chloride cushion [diluted in TE (10mM Tris-HCl pH 8; 1mM EDTA, pH 8)]. The viral DNA was separated from cellular DNA by centrifugation at 149,000xg for 16 hours at 20°C (SW55ti rotor, Beckman instruments). The viral DNA pellet was suspended in 0.8ml TE buffer with 0.1mg/ml RNAase (Sigma) and incubated for 30 minutes at room temperature to digest the RNA. 10μl of 10mg/ml Proteinase K (Sigma) and 20μl of 20% Sodium dodecyl sulphate (SDS) was added [final concentration 125μg/ml Proteinase K in 0.5% SDS]. This mixture was incubated at 50°C for 4 hours to digest

the protein. Viral DNA was purified using phenol/chloroform extraction and precipitation with absolute ethanol (Sambrook *et al.,* 1989). DNA was resuspended in TE buffer.

2.4.2 Preparation of viral DNA from tissue culture-grown virus

This method is an adaptation of the extraction of cytoplasmic orthopoxvirus-DNA (Meyer *et al.,* 1995). Briefly, five 225cm^2 infected FLMC monolayers were harvested by scraping off the cells into the media and centrifuging at 2000xg for 5 minutes (CS-6R centrifuge, Beckman instruments). The cell pellets were pooled and washed in 30mls isotonic buffer (10mM Tris-HCl pH 8; 150mM NaCl; 5mM EDTA, pH 8) by centrifuging at 2000xg as before. The pellet was suspended in 18mls of hypotonic buffer (10mM Tris-HCl, pH8; 10mM KCl and 5mM EDTA, pH 8) and incubated on ice for 10 minutes. 15µl of 14.3M β-mercaptoethanol (Sigma) and 1ml of 10% (v/v) Triton X-100 were added to the suspension and chilled for a further 10 minutes to solubilize the plasma membrane. Cellular nuclei were removed by centrifuging at 2000xg as before and the pellet discarded. The virus was concentrated by centrifuging the supernatant at 20,000xg for 30 minutes at 4°C (SW40ti rotor, Beckman instruments). The viral pellet was suspended in 0.8ml TE buffer with 0.1mg/ml RNAase and incubated at room temperature for 30 minutes. The viral cores were disrupted by the addition of 15µl of 14.3M β-mercaptoethanol (Sigma), 50µl of 10mg/ml Proteinase K and 0.2ml of 20% N-Laurosyl sarcosinate and incubation at 4°C for 30 minutes. 1.4mls of 54% (w/v) sucrose was added and the extract further incubated at 55°C for 4 hours. 0.4mls 5M NaCl was added and viral DNA extracted by the addition of an equal volume of phenol/chloroform and isolated by precipitation with absolute ethanol (Sambrook *et al.,* 1989). DNA was resuspended in TE buffer.

2.4.1 Spectrophotometric quantification of DNA

DNA was quantified by measuring the light absorbed at the wavelengths 260nm and 280nm (Cecil CE2041 2000 series). An optical density (OD) of 1 at 260nm corresponds to approximately 50µg/ml double-stranded DNA (dsDNA). A calculated ratio value of 1.8 for $OD_{260nm/280nm}$ provides an indication that the DNA is pure. Ratio values below 1.8 suggest contamination with phenol or protein (Sambrook, 1989).

2.4.2 Complete restriction endonuclease digestion

Restriction endonucleases were purchased from Roche or Promega and used in accordance to the manufacturer's instructions. Generally 2 to 4μg of DNA was digested in a total reaction volume of 20μl containing 1X reaction buffer and 10U of enzyme (and 0.1mg/ml acetylated bovine serum albumin as appropriate). Incubation times varied from 1 to 3 hours at the appropriate temperature.

2.4.3 Visualisation of DNA by agarose gel electrophoresis

DNA was visualised using agarose gel electrophoresis and fluorescence under UV. The concentration of the agarose gels varied between 0.3% and 0.8% (w/v dissolved in electrophoresis buffer), depending on the size of the DNA fragments to be resolved. The electrophoresis buffer was 1X Tris-Borate EDTA buffer [TBE (90mM Tris base; 90mM Boric acid; 2mM EDTA, pH 8)] with Ethidium bromide added to a final concentration of 0.5μg/ml. 6X DNA loading buffer was added to the DNA samples to a concentration of 1X, and approximately 1μg to 4μg DNA was loaded into one track. Minigels (dimensions 8x10cm) were electrophoresed at 10 volts/cm for 1 to 3 hours. Maxigels (dimensions 20x20cm) were electrophoresed at 1.5 volts/cm for 24 to 36 hours. Visualisation of the DNA was achieved by illumination under UV light (wavelength 302nm) and the image captured onto heat sensitive paper (Mitsubishi video copy processor, UVP) or digitised and stored (Fujifilm thermal imaging system FT1-500, Amersham Pharmacia Biotech). The fragment sizes were estimated by comparison to known standards in a 1kb ladder (GibcoBRL) and digested λ-phage DNA.

2.4.4 Isolation of DNA from agarose gel

Two commercially available kits were used to isolate DNA from agarose gel: QIAquick gel extraction kit (QIAGEN) and Geneclean II kit (Bio 101). Both rely upon the solubilisation of the agarose to release the DNA followed by DNA-binding to a silica matrix. Both kits can efficiently isolate DNA up to 10kb in size. The kits were used in accordance with the manufacturer's instructions with the buffers supplied in the kits.

2.4.4.1 QIAquick gel extraction kit

The desired DNA band was excised from the gel with a scalpel, weighed and 3 gel volumes of buffer QG was added. The gel slice was incubated at 55°C until the agarose dissolved. 10µl 3M Sodium acetate was added to reduce the pH to less than 7.5, followed by one gel volume of isopropanol. The solution was applied to the QIAquick column and the DNA was bound to the column by centrifuging at 13,000rpm for 1 minute (Sigma, 1-13). The column was washed once with 750µl buffer PE by centrifuging as before. The column flow through was discarded and the column centrifuged again to remove traces of ethanol. 30 to 50µl buffer EB was applied to the column membrane and incubated at room temperature for 1 minute before eluting the DNA into a clean tube by centrifuging as before. If required DNA was concentrated by ethanol precipitation.

2.4.4.2 Geneclean II kit

The desired gel band was excised from the gel and weighed. A 0.5 gel volume of TBE modifier and 4.5 gel volumes of Sodium iodide solutions were added and the gel slice dissolved at 50°C. 5 to 20µl of silica matrix were added and suspension gently mixed for 5 to 15 minutes to allow the DNA to bind to the silica matrix. The suspension was centrifuged at 13,000rpm for 1 minute (Sigma, 1-13) and the silica-bound DNA pellet was washed three times with 200µl of "New Wash" by centrifuging as before. The pellet was air dried for 1 minute to remove residual ethanol, then the DNA was eluted by resuspending the pellet in an equal volume (5 to 20µls) of TE and centrifuging as before. The solublised DNA was transferred to a clean tube.

2.4.5 Hybridisation techniques

Several methods are available for labelling nucleic acid probes and visualising the hybridised nucleic acid. Two labelling methods were employed in this study. DNA probes were labelled with the beta emitter ^{32}Phosphorous (^{32}P) and hybridisation detected by exposure to X-ray film. Alternatively, DNA probes were labelled with Digoxigenin-11-deoxyuracil triphosphate (DIG-11-dUTP) and hybridisation detected via an anti-DIG antibody conjugated to alkaline phosphatase which catalyses a colormetric reaction *in situ.*

The "DIG" system was preferentially used whenever possible because DIG-labelled probes can be stored and used in excess of 1 year, unlike ^{32}P, which has a half-life of 2 weeks. In practice,

hybridisation with ^{32}P-labelled probes generally produces a more intense visual hybridisation signal than DIG-labelled probes. In addition, Southern blots hybridised with ^{32}P-lablled probes can be sequentially washed with increasing stringency conditions. Therefore, in some situations hybridisation with ^{32}P-labelled probes was the preferential technique.

2.4.5.1 Non-radioactive labelling of dsDNA

Two techniques were used to label dsDNA with DIG-11-dUTP in this study.

2.4.5.1.1 Random primed DNA labelling

Labelling of DNA greater than 10kb in size is generally less efficient than labelling smaller DNA fragments. Therefore template DNA greater than 10kb was digested with a restriction endonuclease and purified by phenol/chloroform extraction prior to labelling.

Routinely 1µg of template DNA was labelled using the DIG DNA labelling Kit (Roche). Briefly the template DNA was diluted in distilled water to a total volume of 15µl. The DNA was heat-denatured in a boiling water bath for 10 minutes then immediately placed on ice. The following reagents (supplied by Roche) were added in the following order: 2µl 10X hexanucleotide mixture, 2µl 10X deoxynucleotide triphosphate (dNTP) labelling mixture and 2U of Klenow enzyme. The reaction was mixed and incubated at 37°C for 1 to 20 hours. The reaction was stopped by the addition of 2µl 0.2M EDTA, pH 8. Probes were diluted to a working concentration of 25ng labelled DNA/ml in hybridisation buffer [5XSSC (0.75M NaCl, 75mM Trisodium citrate); 0.1% (w/v) N-laurosylsarcosine; 0.02% (w/v) SDS; 1X blocking reagent (Roche)].

2.4.5.1.2 Nick translation labelling

Template DNA was labelled using DIG-Nick Translation mixture (Roche). 1µg of template DNA was diluted in 16µl distilled water. Then 4µl DIG-Nick translation mixture was added, which contains DNAase I, DNA polymerase I, dNTPs and DIG-dUTP. The reaction was incubated at 15°C for 90 minutes, then terminated by adding 1µl of 0.5M EDTA (pH 8) and incubating at 65°C for 10 minutes to denature the enzymes.

2.4.5.2 Radioactive labelling of DNA

2.4.5.2.1 Random prime labelling of dsDNA using the rediprime II labelling kit

dsDNA templates were labelled in a random-priming reaction with Redivue stabilised [α-^{32}P] dCTP (Amersham Pharmacia Biotech) using the commercially available "*redi*prime II" labelling kit (Amersham Pharmacia Biotech).

25ng of dsDNA diluted in 45µl TE buffer was heat denatured by boiling for 5 minutes, then quenched on ice. The denatured DNA was transferred to a *redi*prime II reaction tube and 5µl of [α-^{32}P] dCTP (1.85MBq) was added. The reaction was gently mixed and incubated at 37°C for 30 minutes. The reaction was stopped by adding 5µl 0.2M EDTA, pH 8 and then stored at -20°C for a maximum of seven days prior to use.

2.4.5.2.2 Polynucleotide kinase mediated labelling of free 5'-hydroxylated termini of oligonucleotides

Polynucleotide kinase (PNK) is used in labelling reactions to catalyse the transfer of the ^{32}P-labelled terminal phosphate group of ATP to the 5'-OH terminus of synthetic oligonucleotides or dephosphorylated nucleic acid.

Oligonucleotides (MWG Biotech) were labelled with the terminal phosphate group derived from redivue [γ-^{32}P] ATP triethylammonium salt (Amersham Pharmacia Biotech) in a PNK catalysed labelling reaction. 4.5pmol of oligonucleotide was mixed with 9pmol [γ-^{32}P] ATP (1.65MBq) in a 15µl reaction containing 1X phosphorylation buffer and 10U of PNK (both supplied by Roche). The reaction was allowed to proceed at 37°C for 1 hour before it was stopped by chilling on ice. The probe was diluted in distilled water to a working concentration of 0.15pmol/µl.

Incorporation of the ^{32}P into the oligonucleotide was determined by chromatography of the oligonucleotide on polyethyleneimine cellulose (PEI) sheets (Machery-Nagel, Dueren) in the solvent: 0.75M potassium phosphate buffer, pH 3.5. A 1:50 dilution of the probe was made in the solvent and 0.5µl was spotted onto the PEI sheet, 2cm from the bottom edge and air-dried. The chromatogram was placed into 1cm depth of solvent and left until the solvent front had migrated at least 8cm. The chromatogram was air dried, wrapped in Saran wrap and exposed to

medical X-ray film (100NIF, Fujifilm) with an intensifier screen for 1 hour. The film was developed using a compact X2 automated film processor (X-Ograph imaging systems). Labelling efficiency was estimated by a visual comparison of incorporated ^{32}P present in the oligonucleotide (situated at the loading site) and the unincorporated soluble ^{32}P, which migrated with the solvent front.

2.4.5.3 Preparation of blots

2.4.5.3.1 Southern blotting

Identical or homologous DNA sequences can be detected using Southern blotting and DNA hybridisation techniques. First the digested DNA is separated by agarose gel electrophoresis. Then after denaturation under alkaline conditions, the DNA is transferred from the gel, to a solid matrix of nylon or nitrocellulose using a technique pioneered by Southern (1975).

An adaptation of Southern's original method was used in this study, involving the use of a dry transfer technique. This dry-blot method, although simpler to perform, results in a decrease in the transfer efficiency of DNA. However, it is adequate for digested plasmid, cosmid and viral DNA, as target sequences are sufficiently concentrated to overcome detection problems associated with transfer inefficiencies (Smith and Summers, 1980).

The DNA was separated by agarose gel electrophoresis and photographed. If fragments exceeded 10kb in length the DNA was depurinated by soaking in 0.25M Hydrochloric acid for 10 minutes. The gel was rinsed in distilled water to remove residual acid. Then dsDNA was denatured and the depurinated sites cleaved by two washes in denaturing buffer (0.5M NaOH; 1.5M NaCl), each for 15 minutes. The pH of the gel was then reduced by washing twice for 15 minute with Southern neutralisation buffer (0.5M Tris-HCl, pH7.5; 3M NaCl). The gel was placed on clingfilm and a sheet of nylon membrane (Hybond-N, Amersham Pharmacia Biotech), pre-wetted in neutralisation buffer was placed on top. This was follow by four pieces of pre-wetted 3MM paper (Whatman), four dry pieces of 3MM paper and a 3cm-thick pile of paper towels. A glass plate with a 500g weight was place on top and the blot was left overnight to allow the DNA to transfer. The blot was disassembled and the membrane air-dried before the DNA was cross-linked to the membrane by UV fixation. The blot was stored in the dark at room temperature until used.

2.4.5.3.2 DNA dot blotting

Commercially available dot-blotting equipment was used to apply DNA samples to a membrane in a 96 well-format, thus enabling the screening of multiple DNA samples simultaneously by hybridisation.

Cloned DNA prepared by the alkaline lysis method was diluted to approximately 10ng/µl in TE. 200µl volumes of the DNA suspensions were placed into the wells of a Thermo-fast 96-well PCR plate (Abgene) and the plate covered with an adhesive sealing foil (Abgene). The plate was placed in a Touchdown thermo cycler (Hybaid) and the DNA heat denatured at 96°C for 10 minutes, then quenched on ice. Using a multi-channel pipette, 50µl of the denatured DNA suspensions were applied to a Hybri-dot manifold (Bethesda Research Laboratories), and drawn through onto a pre-wetted (distilled water) nylon membrane (Hybond-N, Amersham Pharmacia Biotech) by vacuum. The membrane was briefly rinsed in 2X SSC (0.3M NaCl; 3mM Tri-sodium citrate), air-dried and the DNA cross-linked to the membrane by UV fixation.

2.4.5.3.3 Colony lifts, in situ lysis and DNA binding to nylon

Bacterial colonies were transferred from the agar plate to a nylon membrane, lysed and the released DNA bound to the membrane *in situ* using an adaptation of a method developed by Grunstein and Hogness (1975). The membrane, when subsequently hybridised with a labelled probe allowed a large number of transformed colonies to be screened simultaneously.

Bacterial colonies, freshly cultured on Luria-Bertani agar (LBA) plates were chilled at +4°C for 30 minutes. Hybond-N+ membrane (Amersham Pharmacia Biotech) was pre-wetted on a fresh LBA plate and then placed onto the bacterial colonies for one minute to allow adherence. Orientation marks were made by stabbing the membrane and agar with a needle. The membrane was peeled off the agar and directly placed, colony side up, onto a 1ml pool of 10% SDS for 3 minutes. Alternatively, when there was little bacterial adherence, the membrane was cultured colony side up on a fresh LBA plate for a further 4 to 8 hours prior to treatment with 10% SDS. The membrane was transferred to 1ml pools of the following solutions for 5 minutes each, blotting briefly on 3MM paper between each solution: Denaturing solution (0.5M NaOH; 1.5M NaCl), colony neutralising solution (1M Tris-HCl, pH7.5; 1.5M NaCl) and finally 2X SSC. The membrane was air-dried and the bacterial debris removed with a tissue-dampened in 2X SSC.

The membranes were allowed to re-dry and the DNA cross-linked to the membrane by UV fixation.

2.4.5.4 Hybridisation with digoxygenin-labelled DNA probes

2.4.5.4.1 Hybridisation conditions

Membranes were placed into cylindrical hybridisation tubes (Hybaid) with 20ml of standard hybridisation buffer [5X SSC; 0.1% N-laurosylsarcosine; 0.02% SDS; 1X blocking reagent (Roche)] and incubated in a hybridisation oven (Hybaid) at 65°C for at least 2 hours. DIG-labelled probes were diluted in standard hybridisation buffer to a concentration of 25ng/ml, then heat-denatured in a boiling water bath for 10 minutes. The pre-hybridisation solution was replaced with 10ml of the diluted-denatured probe, and the membrane incubated at 65°C. After approximately 16 hours, the probe was decanted and retained for re-use.

2.4.5.4.2 Development of digoxygenin blots

Membranes were washed twice for 5 minutes in 2X wash solution (2X SSC; 0.1% SDS) at room temperature, then twice for 15 minutes in 0.5X wash solution (0.5X SSC, 0.1% SDS) at 65°C to remove non-specifically bound probe. To reduce background, the non-hybridised region of the membrane was blocked by incubating for 1 hour in blocking buffer [1X blocking reagent (Roche) in 1X Maleic acid buffer (0.1M Maleic acid; 0.15M NaCl; pH 7.5)]. The blocking buffer was replaced with 30ml antibody solution [150mU/ml Anti-Digoxigenin-AP (Roche) in blocking buffer], which was allowed to bind for 30 minutes. Excess antibody was removed by two washes in 1X Maleic acid buffer for 15 minutes each. Membranes were equilibrated for 2 minutes in detection buffer (0.1M Tris-HCl, pH9.5; 0.1M NaCl), then flooded with colour substrate [45µl of 75mg/ml nitroblue tetrazolium salt (NBT) in 70% (v/v) dimethylformamide (Roche) and 35µl of 50mg/ml 5-Bromo-4-chloro-3-indolyl phosphate (BCIP) toluidinium salt in dimethylformamide (Roche), diluted in 10ml of detection buffer] and left to develop in the dark. The membrane was washed in distilled water to stop the colour development reaction.

2.4.5.5 Hybridisation with ^{32}P-labelled DNA probes and development of autoradiographs

Membranes were pre-hybridised at 60°C for 2 hours with 10ml Rapid-hyb buffer (Amersham Pharmacia Biotech). ^{32}P-labelled DNA probes (see section 2.4.5.2.1 for labelling procedure) were denatured by boiling for 5 minutes and then quenched on ice for 5 minutes. 25ng of the

denatured probes were then added to 10ml pre-hybridisation solution and the membranes incubated at 60°C for approximately 16 hours.

The membranes were then washed twice for 30 minutes each at room temperature with 2X wash solution (2X SSC/0.1% SDS). The damp membranes were then wrapped in Saran wrap and exposed to medical X-ray film (100NIF, Fujifilm) with an intensifier screen for 30 minutes. The autoradiograph film was developed using a compact X2 automated film processor (X-Ograph imaging systems). If excessive background was visible on the autoradiograph, the damp nylon membrane was then repeatedly washed at higher stringency, exposed to film and developed. Higher stringency washes were performed with 2X wash solution (2X SSC/0.1% SDS) at 60°C and 0.2X wash solution (0.2X SSC/0.1% SDS) at 60°C.

2.4.6 Polymerase chain reaction

A polymerase chain reaction (PCR) was employed to selectively amplify short regions of the viral DNA genome. The technique developed by Saiki *et al.*, (1988) utilises the thermo-stable properties of the DNA polymerase isolated from the bacteria *Thermus aquaticus* (Taq DNA polymerase) to catalyse the polymerisation of DNA that is flanked by regions of known sequence. Briefly, the dsDNA template is denatured by heating to 94°C, then two synthetic oligonucleotide primers that are complementary to the sequence flanking the desired region are annealed to the ssDNA template by reducing the temperature of the reaction to approximately 5°C below the melting temperature (Tm value) of the primers. Replication of DNA is in a 5' to 3' direction and is initiated at the site of primer binding. Taq DNA polymerase catalyses the polymerisation of complementary DNA strands across the desired region when the temperature is raised to 72°C, which is the optimal temperature for Taq DNA polymerase to function.

2.4.6.1 PCR reaction components and conditions

Taq DNA polymerase and the 10X PCR reaction buffer (containing 15mM $MgCl_2$) was supplied by Roche and used in accordance with the manufacturer's instructions. Deoxynucleotides (dNTPs) were supplied by Promega and were diluted to a 10X working concentration consisting of 2mM of each individual dNTP in distilled water. Oligonucleotide primer pairs were designed from known SPPV and ORFV sequence and were generally 18 to 24 bases in length with

comparable Tm values. All oligonucleotides were supplied by MWG biotech and diluted in distilled water to a concentration of 10μM.

All PCR reactions were prepared in 0.5ml microcentrifuge tube (Alpha laboratory supplies) on ice, in 50μl volumes, containing the following solutions.

10X PCR reaction buffer	5μl
10X dNTP mixture (2mM of each base)	5μl
Primer 1 (10μM)	5μl
Primer 2 (10μM)	5μl
Taq DNA polymerase (5units/μl)	0.4μl
DNA template	100ng to 1μg
Distilled water	to final volume of 50μl

The reactions were gently mixed then overlaid with 50μl of mineral oil (Sigma) to prevent evaporation of the samples. The reaction tubes were transferred to the heating block of the OmniGene thermal cycler (Hybaid) and the PCR reactions performed using the following cycle parameters:

Cycle	Denaturation	Primer annealing	DNA polymerisation
1	94°C for 5 minutes	Tm value minus 5°C for 1 minute	72°C for 1 minute
2 to 25	94°C for 1 minute	Tm value minus 5°C for 1 minute	72°C for 1 minute
26	94°C for 1 minute	Tm value minus 5°C for 1 minute	72°C for 10 minute

The completed PCR reactions were cooled to room temperature and the PCR products visualised by agarose gel electrophoresis (section 2.4.3).

2.4.7 DNA sequencing

Two methods of DNA sequencing were developed simultaneously in the 1970's (Sanger *et al.*, 1977; Maxam and Gilbert, 1977). The chain termination method (Sanger *et al.*, 1977) involves the polymerisation of a DNA strand that is complementary to the target region using a procedure similar to PCR. The sequencing reaction mixture contains a DNA polymerase and all four

dNTPs, one of which is radiolabelled, plus one modified dNTP. The modified dNTP is a dideoxynucleotide (dideoxyNTPs) and is incorporated into the growing DNA strand but results in the early termination of strand synthesis. Four separate sequencing reactions are performed, each incorporating a different dideoxyNTP. When the products are electrophoresed on a single DNA-denaturing polyacylamide gel and exposed to medical X-ray film, the DNA sequence can be determined from the resulting DNA bands.

The chain termination method has largely been replaced by more efficient automated sequencing methods, which utilises fluorescent-labelled dNTPs as the DNA strand terminator. The advantages of this method over Sanger's chain termination method include: dsDNA templates may be used, only a single PCR reaction is required as opposed to four, no radioactive isotope is needed and the reading of the sequencing gel is automated and therefore less time consuming. DNA sequencing was carried out at The Functional Genomic Unit (Moredun Research Institute) using the ABI Prism Big Dye Terminator system (Applied Biosystems).

2.4.7.1 DNA sequencing protocol.

In a 0.2ml microcentrifuge tube, 250 to 500ng template DNA was mixed with 4µl Terminator ready reaction mix (Applied Biosystems) and 1µl of primer (3.2pmol concentration), distilled water was added to give a total PCR reaction volume of 10µl. The PCR reaction was amplified on the Applied Biosystems 9700 thermal cycler using the following cycle parameters: DNA denaturation at 96°C for 10 seconds, primer annealing at 50°C for 15 seconds and DNA polymerisation at 60°C for 4 minutes; for twenty-five cycles. The reactions were cooled to 4°C and the DNA precipitated by the addition of 1µl of 3M Sodium acetate and 25µl of 95% (v/v) ethanol. After incubation at room temperature for 20 minutes the DNA was pelleted by centrifugation at 13,000rpm for 20 minutes. The DNA pellet was washed in 125µl of 70% (v/v) ethanol and the DNA resuspended in 2 or 3µl of Sequence loading dye (Applied Biosystems).

The amplified DNA was heat denatured for 2 minutes at 95°C and then loaded onto a 50ml vertical sequencing gel [5% polyacrylamide (Applied Biosystems Long Ranger XL gel solution); 6M Urea and 1X TBE]. The sequencing gel was electrophoresed in the 377 DNA Sequencer (Applied Biosystems) at 51°C in 1X TBE for 9 hours. The DNA sequence was

detected automatically during electrophoresis by a laser and the sequence deciphered using Sequencher software (Applied Biosystems).

2.4.8 Sequence analysis

2.4.8.1 DNA sequence homology searching

DNA sequences were manually checked for errors and edited using Chromas v1.45 graphical software (Technelysium Pty Ltd). Vector sequences were removed and the DNA sequence compared to those deposited in the EMBL nucleotide sequence database (Stoesser *et al.*, 2002) using the FastA 3 algorithm (Pearson and Lipman, 1988). The FastA algorithm was preferentially used to search the databases for homologous sequences due the greater sensitivity FastA offers over the alternative algorithms such as BLAST at detecting distant homologies (Shpaer *et al.*, 1996).

2.4.8.2 Predicted amino acid sequence homology searching

Putative open reading frames (ORFs) were identified using DNASTAR MapDraw v5.00 and translated using DNASTAR EditSeq v5.00 software (DNASTAR Inc.). Translations of each putative ORF were compared to protein sequences deposited in the SWALL library [comprising of SWISSPROT, SPTREMBL and TREMBLNEW databases (Bairoch and Apweiler, 2000) using the FastA3 algorithm (Pearson and Lipman, 1988) in order to identify homologous proteins.

2.4.8.3 Multiple DNA sequence alignments

Sequences were aligned with one another using the ClustalW alignment algorithm function within the DNA MegAlign v5.0 package (Thompson *et al.*, 1994) (DNASTAR Inc.). The sequences were trimmed at both ends to remove non-overlapping sequence. Individual sequence alignments were visualised, annotated and shaded using GeneDoc v2.6.001 software (Nicholas *et al.*, 1997).

2.4.8.4 Phylogenetic analysis

2.4.8.4.1 Multiple amino acid sequence alignment

A preliminary alignment of predicted amino acid sequences was performed using the ClustalW algorithm function within the DNASTAR MegAlign program and the end of the sequences trimmed (section 2.4.8.3). Individual trimmed sequences were converted to a FastA (Pearson)

format using the format conversion program Readseq v2.1.10 (D.G Gilbert) and a compilation file containing all of the trimmed sequences in a FastA format created. A multiple sequence alignment was performed with the data contained in the sequence compilation file using the ClustalW algorithm tool in the UK Human genome mapping resource centre (HGMP) web-based platform. The interleaved multiple sequence alignment was visualised and the physiochemical properties of the amino acid shaded using GeneDoc v2.6.001 software (Nicholas *et al.,* 1997). The percentage of residues that match exactly (percentage identity) between two aligned sequences were obtained from the statistics report function in GeneDoc.

2.4.8.1.2 Preliminary tree construction

Preliminary analysis was performed on the interleaved multiple sequence alignment with the TREE-PUZZEL v5.0 maximum likelihood phylogenetic analysis algorithm program (Schmidt *et al.,* 2002). The TREE-PUZZEL default settings were used for tree creation, except the out-group sequence was changed to FPV and the model rate of heterogeneity was changed to gamma distribution and the invariant rate of heterogeneity. The calculated gamma and invariant rate of change values were used in the tree construction (section 2.4.8.1.3).

2.4.8.1.3 Maximum likelihood tree construction

A maximum likelihood tree was created from the interleaved multiple sequence alignment with the PHYLIP ProML program (Felsenstein, 1993) using the Jones-Taylor-Thornton model (Jones *et al.,* 1992). Analysis was performed with FPV as the out-group and the gamma and invariant rates of heterogeneity values that were calculated by analysis with the TREE-PUZZEL program (section 2.4.8.1.2). To ensure that the input order of the amino acid sequences did not influence the inferred phylogenies, the sequence order was randomised (jumbled) ten times. The likelihood that the tree branching inferred by the ProML program was the most probable was assessed by global rearrangement. The tree was visualised using the graphical software TreeView v1.6.2.1 (Page, 1996). The tree branch lengths correspond to the genetic distance between sequences.

2.4.8.1.4 Tree evaluation

The repeatability or the accuracy of the inferred tree produced by the ProML program was assessed using bootstrap analysis (Felsenstein, 1985). The multiple sequence alignment was re-sampled one hundred times using PHYLIP SEQBOOT program. The SEQBOOT program randomises the data by shuffling the amino acids within the columns of the multiple sequence

alignment. The re-sampled data (consisting of 100 multiple sequence alignments) was then analysed with the PHYLIP ProML program using the same parameters described in section 2.4.8.1.3, except the "analyse multiple sequence data sets" option was activated. The resulting 100 trees were analysed by the PHYLIP CONSENSE program to determine the tree consensus, which was visualised using the graphical software TreeView v1.6.2.1 and compared with the tree produced by the single data set (section 2.1.8.1.3). The bootstrap value calculated for each individual consensus tree branch is a measure how many of the 100 resampled trees supports that particular branch. The branch lengths in the consensus tree correspond to the bootstrap value and not the genetic distance. Therefore the bootstrap values were manually added to the tree produced by the single data set (section 2.1.8.1.3).

2.5 GENERAL MICROBIAL METHODS

2.5.1 Bacterial strains, their genotype and growth media

Strain	Growth media
JM109	Luria-Bertani agar (LBA) and broth (LB) supplemented with 50μg/ml ampicillin when appropriate.
XL1-Blue MR	LBA supplemented with 50μg/ml ampicillin when appropriate. LB supplemented with 10mM Magnesium sulphate, 0.2% (w/v) maltose and with 50μg/ml ampicillin when required.

Table 2.1 Two *E.coli* strains were used in this study. Their growth media requirements are summarised here.

2.5.2 Preparation of JM109 competent cells

Bacterial cells were treated with Calcium chloride ($CaCl_2$) to make them competent for the uptake up exogenous DNA using an adaptation of Cohen's procedure (Cohen *et al.*, 1972).

A glycerol stock of JM109 cells (Stratagene) was streaked out to a single colony on LBA plates and a single colony was used to inoculate 10ml of LB, which was grown overnight at 37°C with vigorous shaking. 2.5ml of the cultured broth was used to inoculate 500ml LB in a 2 litre baffled Erlenmeyer flask. This was grown at 37°C with shaking to an OD of 0.9 at 600nm. The bacteria

were pelleted at 4000xg (JA-14 rotor, Beckman instruments) and the supernatant discarded. The pellet was resuspended in 250ml ice-cold 0.1M $CaCl_2$ and incubated on ice for 20 minutes. The bacteria were pelleted at 4000xg (as before) and the pellet resuspended in 5 to 20ml of ice-cold 0.1M $CaCl_2$. Glycerol was added to a final concentration of 10% (v/v), and aliquots were stored at -70°C.

2.5.3 Preparation of competent XL-1 Blue MR cells

XL-1 Blue MR glycerol stock (Stratagene) was streaked onto a LBA plate to a single colony. A single colony was used to inoculate 10ml of LB supplemented with 10mM Magnesium sulphate and 0.2% (w/v) Maltose. The broth was incubated at 37°C with agitation for 4 to 6 hours. The cells were harvested at 1200xg for 10 minutes (Mistral 2000, MSE Scientific Instruments) and resuspended in 10mM Magnesium sulphate to an OD of 0.5 at 600nm. The cells were used immediately after dilution.

2.5.4 Preparation of glycerol stocks

Transformed cells were prepared for long term storage at -70°C in 1.5ml screw top tubes by the addition of glycerol to a final concentration of 20% (v/v) with the cultured broth.

2.5.5 Preparation of plasmid and cosmid DNA

A number of methods were employed in this study to separate plasmid/cosmid DNA from bacterial chromosomal DNA and cell debris. All methods are based on the conformation of different DNA structures under varying pH conditions. Under alkaline conditions of pH 12 to 12.5 the linear bacterial DNA is denatured, whereas the supercoiled plasmid DNA remains intact. Decreasing the pH by the addition of acid results in the aggregation of the denatured bacterial DNA, protein and RNA. This aggregated mass is then centrifuged to form a pellet, leaving a clear supernatant containing the solublised supercoiled plasmid/cosmid DNA. The plasmid/cosmid DNA can then be purified using phenol/chloroform extraction (Sambrook, 1989). However when DNA preparations free from contaminants were required, for sensitive techniques such as sequencing, a commercially available anion exchange column was used [QIAprep miniprep and maxiprep kits (QIAGEN)].

2.5.5.1 Small scale preparation of plasmid/cosmid DNA by alkali lysis (miniprep)

10ml broth cultures were harvested by centrifugation at 1187xg for 10 minutes (Mistral 2000, MSE Scientific Instruments). The bacterial pellet was resuspended in 100µl glucose buffer (50mM glucose; 10mM EDTA, pH 8; 25mM Tris-HCl, pH 8). 200µl lysis buffer (0.2M NaOH; 1% SDS) was added and the suspension mixed until the bacteria lysed. The majority of protein, RNA and bacterial DNA were precipitated by the addition of 150µl 3M Sodium acetate (pH 4.8) and pelleted by centrifugation at 13,000rpm for 5 minutes (Sigma, 1-13). The cleared lysate was decanted in to a fresh tube and vigorously mixed with an equal volume of phenol/chloroform and clarified by centrifugation at 13,000rpm for 5 minutes as before. The top aqueous layer was decanted to a fresh tube and the plasmid/cosmid DNA precipitated with 2.5 volumes of ice-cold ethanol at -20°C for 1 hour. The DNA was pelleted by centrifugation at 13,000rpm for 10 minutes (Sigma, 1-13) and washed in 70% (v/v) ethanol, then resuspended in 50µl TE buffer containing 0.1mg/ml RNAase A (Sigma).

2.5.5.2 Large scale preparation of plasmid DNA (maxiprep)

Up to 500µg of plasmid DNA was prepared using the QIAprep maxiprep kit (QIAGEN). The procedure was carried out in accordance with the manufacturer's instructions with minor adaptations. All buffers used were provided with the kit except isopropanol, 70% (v/v) ethanol and TE buffer.

Transformed bacterial cells from a 100ml culture were harvested by centrifugation at 4000rpm (JA-14 rotor, Beckman Instruments) for 15 minutes at 4°C. The pellet was resuspended in 10ml of buffer P1 and then 10ml of buffer P2 was added. The sample was mixed and left at room temperature for 5 minutes to lyse the cells. Bacterial debris was precipitated by the addition of 10ml of chilled buffer P3 and incubation on ice for 20 minutes. The mixture was aliquotted into 1.5ml microcentrifuge tubes and centrifuged at 13,000rpm for 10 minutes (Sigma, 1-13). The supernatant was promptly decanted and applied to the column (QIAGEN-tip 500 pre-equilibrated with 10ml of buffer QBT) and allowed to run through. The column was washed twice with 30ml buffer QC and the DNA eluted in 15ml buffer QF. DNA was recovered by precipitation with 10.5ml isopropanol and centrifuging at 13,000rpm for 10 minutes (in microcentrifuge tubes as before). The pellets were pooled in 1ml 70% (v/v) ethanol and

centrifuged as before. The DNA pellet was washed for a second time in 1ml 70% (v/v) ethanol prior to being air-dried and suspended in 1ml TE buffer.

2.5.5.3 Small scale preparation of plasmid/cosmid DNA (QIAprep miniprep)

The QIAprep spin miniprep kit (QIAGEN) can isolate up to 10μg cosmid DNA and 20μg plasmid DNA. The procedure was carried out in accordance with the manufacturer's instructions with the buffers provided with the kit.

Transformed bacterial cells were recovered by centrifugation at 1187xg for 10 minutes (Mistral 2000, MSE Scientific Instruments). The pellet was resuspended in 250μl buffer P1 and then 250μl buffer P2 was added to lyse the cells. Protein and bacterial DNA was precipitated by the addition of 350μl buffer N3 and the precipitate pelleted by centrifugation at 13,000rpm for 10 minutes (Sigma, 1-13). The supernatant was applied to the QIAprep spin column and the column centrifuged for 1 minute at 13,000rpm (Sigma, 1-13). The column was washed with 500μl buffer PB, and then with 750μl buffer PE by centrifuging for 1 minute as before. Residual wash buffer was removed by a further centrifugation for 1 minute. DNA was eluted in 50μl buffer EB (pre-warmed to 70°C for plasmids and cosmids greater then 10kb in size) which was applied directly to the column membrane and incubated at room temperature for 1 minute before eluting by centrifugation.

2.6 VECTORS AND CLONING

2.6.1 Cloning vectors

2.6.1.1 pBluescript SK⁻ phagemid

pBluescript SK- phagemid vector (Stratagene, figure 2.1) is derived from the pUC19 plasmid (Short *et al.*, 1988). The vector has a multiple cloning site (MCS) which consists of twenty-one unique restriction endonuclease sites. The vector can theoretically accommodate DNA fragments up to 18kb in length. The vector contains an ampicillin resistance gene enabling selection of transformed colonies by the addition of ampicillin to the agar. In addition, recombinant vector clones can be selected by blue/white colony screening. The MCS is situated within the plasmid *lacZ* gene. Expression of the *lacZ* gene is repressed in *lacI* bacterial strains, however expression can be induced with isopropyl-β-D-thio-galactopyranoside (IPTG). Addition of the lactose analogue 5-bromo-4-chloro-3-indolyl-β-D-galactopyranoside (X-gal), which is metabolised by

the *lacZ* product (β-galactosidase), results in the formation of a blue product. If the *lacZ* gene is disrupted by insertion of DNA into the MCS, X-gal will not be metabolised and therefore the colonies will remain white

2.6.1.2 SuperCos I vector

Cosmid vectors are useful in mapping sizeable regions of DNA because they can accommodate large fragments of contiguous DNA. Historically, cosmids were engineered for studying mammalian genomes, however they have been utilised extensively in characterising and manipulating large viral DNA genomes.

The SuperCos I vector (Stratagene, see figure 2.2) was used in this study due to the advantages this double *cos* site vector offers over traditional single *cos* site vectors. The method of preparing the SuperCos I vector for cloning (see figure 2.3) eliminated the need to dephosphorylate the vector's cloning site to prevent the formation of cosmid vector concatamers. This allows the insert DNA to be dephosphorylated, preventing the multiple insertion of fragments into the cloning site, thus removing the need to size fractionate the insert DNA. As size fractionation results in a large loss of DNA, this vector is particularly useful when the insert DNA is in short supply.

Ampicillin and neomycin resistance markers allow for positive selection of transformed cells on selective agar. The *Bam* HI cloning site is flanked by the bacteriophage T3 and T7 promoters, which allow the transcription of end-specific RNA probes.

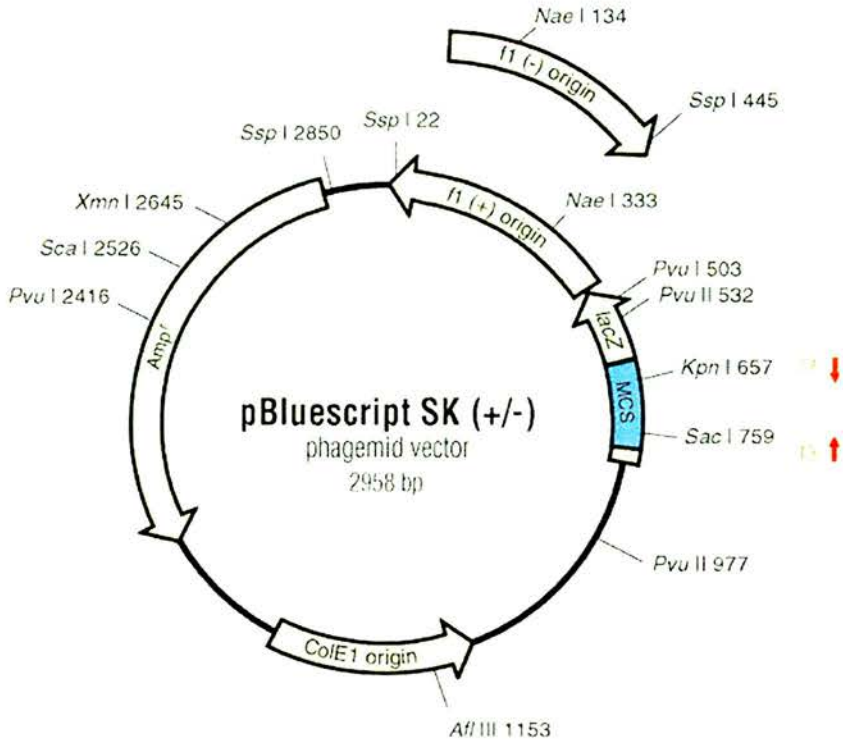

Figure 2.1 Circular map of pBluescript SK$^{-/+}$ phagemid vector. The vector is 2958bp in length and contains a multiple cloning site (MCS) consisting of twenty-one unique restriction endonuclease sites.

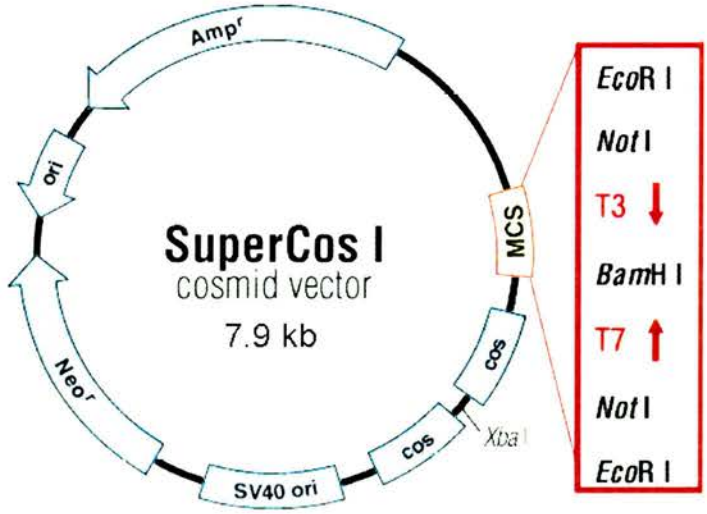

Figure 2.2 Circular map of SuperCos I vector. The cosmid vector is 7.9kb in size and contains two 12bp recognition cos sites and a MCS with a *Bam* HI restriction endonuclease cloning site.

2.6.2 Random cloning of SPPV restriction fragments into pBluescript SK$^-$

2.6.2.1 Preparation of pBluescript SK$^-$ plasmid DNA

JM 109 cells transformed with the pBluescript SK$^-$ plasmid vector (Stratagene) were streaked out to single colonies onto a LBA plate containing 50μg/ml ampicillin. A single colony was used to inoculate 10ml LB supplemented with 50μg/ml ampicillin and grown for 16 to 18 hours. 2.5ml of the culture was used to seed 100ml LB supplemented with 50μg/ml ampicillin and grown for 16 to 18 hours. Vector DNA was isolated using the QIAprep maxiprep kit (section 2.5.2.2).

2.6.2.2 Restriction endonuclease digestion of plasmid and insert DNA

1μg total viral genomic DNA and 1 μg pBluescript SK$^-$ DNA were completely digested with 10 units of *Bam* HI (Roche), *Not* I (Roche) or *Kpn* I (Promega) restriction endonucleases in accordance with the manufacturers instructions (section 2.4.2). Reactions were incubated at 37°C for 1 hour then stopped by heat denaturation of the enzyme at 65°C for 15 minutes.

2.6.2.3 Ligation of DNA

The compatible ends produced by restriction endonuclease digestion of insert and plasmid DNA were ligated together to form a covalent bond in a reaction catalysed by T4 DNA ligase (Roche). Briefly, 50ng of digested vector DNA was ligated with digested genomic DNA in ratios of 1:3 to 1:7 in a total volume of 20μl containing 1X ligation buffer and 1 unit T4 DNA ligase. Reactions were carried out at 22°C for 4 hours or at 4°C overnight.

2.6.2.4 Transformation of competent JM109 *E.coli* cells

50ng of ligated vector/insert DNA was mixed with 50μl of competent *E.coli* (strain JM109) and incubated on ice for 30 minutes, followed by heat shock treatment for 2 minutes at 42°C. Transformations were spread onto LBA supplemented with 50μg/ml ampicillin, 10μl 2% (w/v) IPTG and 10μl 10% (w/v) X-gal per plate. Plates were inverted and incubated overnight at 37°C.

2.6.2.5 Isolation and amplification of a single colony

10ml LB supplemented with 50μg/ml ampicillin was inoculated with a single, white, transformed bacterial colony. Following 16 to 18 hours of incubation at 37°C with agitation, 1ml

glycerol stocks were prepared (section 2.5.4) and the plasmid DNA isolated using the alkaline lysis method (section 2.5.5.1).

Alternately, when a large number of clones were generated, 1ml glycerol stocks were prepared from the 10ml broth cultures and stored at -70°C. Prior to freezing, 200µl was removed and placed into the wells of a 96-well tissue culture plate (Nunc), the plate was then sealed with an adhesive cover and stored at -70°C. When required, LBA plates were inoculated in grid format by transferring the glycerol stocks to an agar plate using a multichannel pipette.

2.6.3 Cloning the genome into SuperCos I vector

Preparation of the cosmid arms, the ligation of insert DNA and packaging of the cosmid into λ phage capsids are represented schematically in figure 2.3.

2.6.3.1 Preparation of the cosmid arms

10µg of circular SuperCos I vector was digested with 90U of *Xba* I restriction endonuclease (Roche) at 37°C for 1 hour. A small aliquot of the digest was electrophoresed on a 0.8% (w/v) agarose gel to check for complete digestion. The linearised *Xba* I-vector was extracted once with phenol/chloroform and precipitated in ethanol. The DNA was washed in 70% (v/v) ethanol and suspended in 10µl distilled water.

To prevent the vector *Xba* I sites from re-annealing during the subsequent ligation reaction, the *Xba* I sites were dephosphorylated. Briefly, 10µg of the *Xba* I-digested vector (8pmol termini) was dephosphorylated with 0.8U of calf intestinal alkaline phosphatase (CIAP, Stratagene) in 20µl reaction containing 1XCIAP buffer (50mM Tris-HCl, pH 8; 100mM EDTA, pH 8). The reaction was stopped after 30 minutes at 37°C by raising the EDTA concentration to 15mM and heating at 68°C for 10 minutes. The DNA was purified by phenol/chloroform extraction and ethanol precipitation as before.

The *Xba* I-CIAP-vector DNA was then digested with 40U *Bam* HI for 1 hour at 37°C. A small aliquot was electrophoresed on a 0.8% (w/v) agarose gel to check for complete digestion. DNA was purified by phenol/chloroform extraction, then ethanol precipitated and suspended in distilled water.

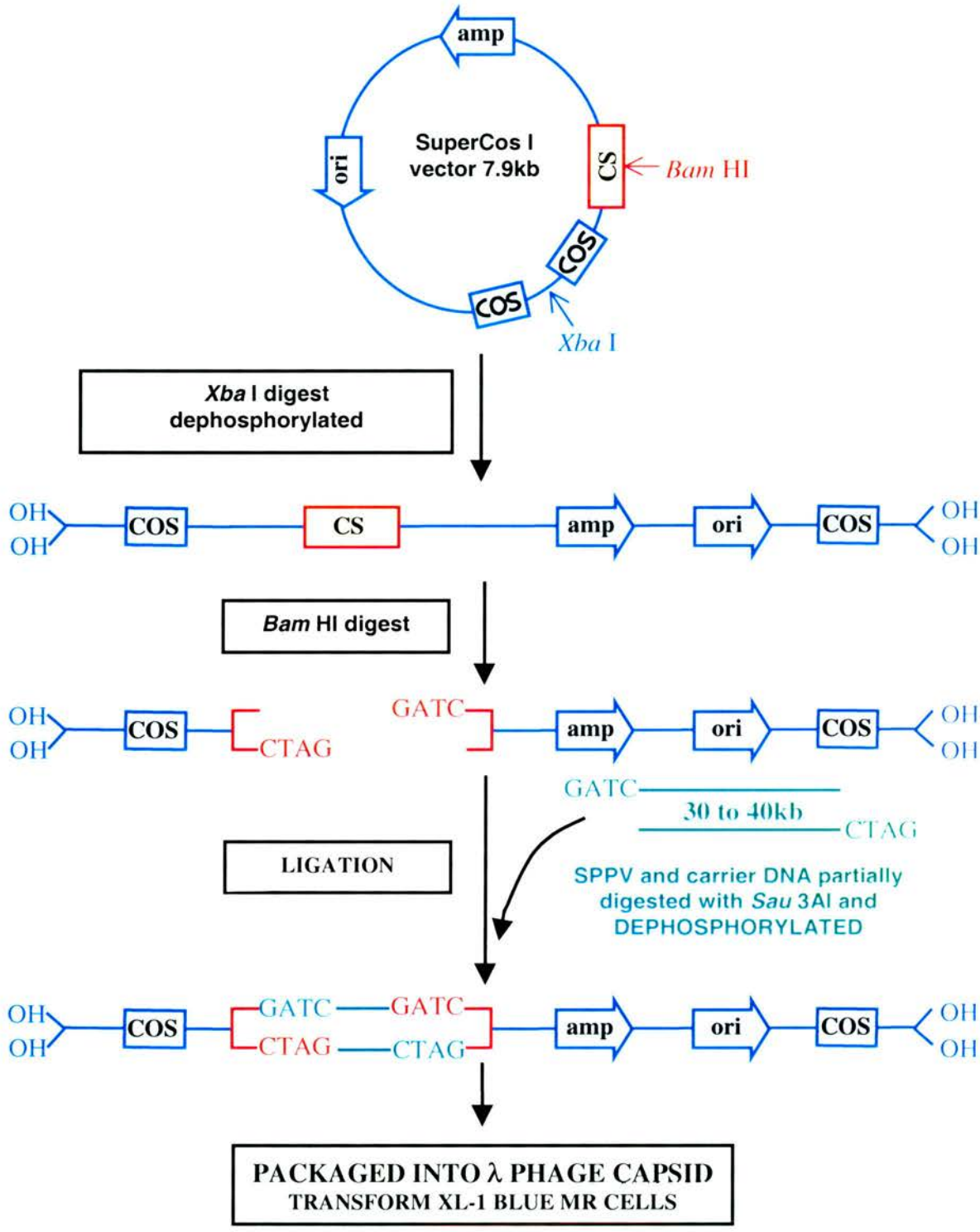

Figure 2.3 Schematic representation of the preparation of SuperCos I arms and ligation with the partially digested and dephosphorylated SPPV/carrier DNA.

2.6.3.2 Preparation of insert DNA

Due to the limited quantity of SPPV DNA, a carrier DNA was used. The carrier DNA source was rainbow trout (*Oncorhynchus mykiss*). This was selected due to the low G+C content, which is generally 40 to 50% G+C (R. Sharif personal communication) and the abundance of fish tissue in the laboratory where this study was performed.

2.6.3.2.1 Isolation of SPPV DNA

DNA from SPPV scab isolate 1296/99 was prepared using the protocol detailed in section 2.4.1.

2.6.3.2.2 Isolation of salmonid carrier DNA

Approximately 2g of trout kidney was ground in liquid nitrogen using a pestle and mortar and suspended in 15ml of lysis solution (10mM NaCl; 20mM Tris-HCl, pH 8; 1mM EDTA, pH 8; 0.5% SDS; 100µg/ml proteinase K). The suspension was incubated at 50°C for 12 hours without agitation. An equal volume of phenol/chloroform was added and the mixture was gently inverted for 10 minutes and then centrifuged at 1187xg (Mistral 2000, MSE Scientific Instruments). The aqueous layer was decanted to a fresh tube and 3M Sodium acetate was added to a final concentration of 0.3M. Two volumes of ethanol were layered over the aqueous layer and the DNA gently spooled from the interface with a fine glass rod. The precipitated DNA was gently washed in 70% (v/v) ethanol, drained without centrifugation and air-dried. The DNA was allowed to suspend in TE buffer with 0.1mg/ml RNAase at 4°C for 2 days without agitation.

2.6.3.2.3 Partial digest of insert DNA with Sau3A I and dephosphorylation

Bam HI has a 6bp recognition sequence and *Sau*3A I has a 4bp recognition sequence. Both enzymes produce a 4bp 5'-extension of the sequence GATC, therefore *Sau*3A I digested insert DNA can be ligated into the *Bam* HI site of the cloning vector. *Sau*3A I partial digest conditions were optimised for both SPPV and carrier DNA to obtain fragments in the region of 30 to 42kb in size.

SPPV and carrier DNA were diluted to 0.1µg/µl in 1X reaction buffer and digested with 0.05U *Sau* 3A I/µg DNA at 37°C. Aliquots of the SPPV reaction were stopped after 15, 30 and 45 seconds incubation by the addition of 1µl 0.5M EDTA (pH 8) and heating to 68°C for 10 minutes. The carrier DNA reaction was stopped at 30, 45 seconds and 1 minute. The partial

digests were pooled together in a ratio of 1:4 μg SPPV to carrier DNA. The DNA was phenol/chloroform extracted once, ethanol precipitated and resuspended in TE buffer.

20μg of partially digested SPPV/carrier DNA was dephosphorylated in a 20μl reaction containing 20U CIAP in 1X CIAP buffer. The reaction was incubated at 37°C for 1 hour before it was stopped by raising the EDTA concentration to 15mM and heating at 68°C for 10 minutes. The partially digested and dephosphorylated DNA was phenol/chloroform extracted once, ethanol precipitated and resuspended in TE buffer ready for use.

2.6.3.3 Ligation and packaging of DNA

2.5μg of the partially digested and dephosphorylated insert DNA was ligated into 1μg prepared SuperCos I vector in a 20μl reaction containing 1X ligation buffer and 1U T4 DNA ligase (Roche). The reaction was performed at 4°C for 24 hours.

Ligated DNA was packaged into λ phage capsids contained in the Gigapack III Gold packaging extract (Stratagene). Briefly 0.7μg ligated DNA was gently mixed with one thawed packaging extract. The packaging reaction was incubated at 22°C for 2 hours. Then 500μl SM buffer (100mM NaCl; 50mM Tris-HCl, pH 7.5; 8mM Magnesium sulphate heptahydrate; 0.01% (w/v) gelatine) and 20μl chloroform were added. The solution was gently mixed and pulsed in a microcentrifuge to sediment the debris.

2.6.3.4 Titration of the packaging reaction

The packaging reaction was titrated prior to library amplification (section 2.6.3.5). The packaging reaction was used at three concentrations: undiluted, 1:10 and 1:50 (diluted in SM buffer). 25μl of each concentration was mixed with an equal volume of XL-1 Blue MR competent cells (see section 2.5.3 for preparation). The transduction mix was incubated at 22°C for 30 minutes to allow the phage to attach to the bacterial cell membrane. 200μl of LB was added, and the broth incubated at 37°C for 1 hour to allow the pre-expression of ampicillin resistance. Using a glass spreader each broth was plated onto a LBA plate supplemented with 50μg/ml ampicillin and grown overnight at 37°C. The colonies were counted and the titre of the packaging reaction was calculated as colony forming units per ml (cfu/ml).

2.6.3.5 Amplification and titering the cosmid library

Transducing the packaging reaction and amplifying the library enables the library to be stored long term as glycerol stocks and subsequently to be screened many times.

A volume of the packaging reaction containing 40,000cfu was mixed with an equal volume of XL-1 Blue MR competent cells (see section 2.5.3 for preparation) and incubated at 22°C for 30 minutes. Four volumes of LB were added and the transducing mix incubated at 37°C for 1 hour with agitation. The cells were harvested by centrifugation at 1187xg for 10 minutes (Mistral 2000, MSE Scientific Instruments) and the pellet suspended in 1.5ml of LB. Using a glass cell spreader, the bacterial cells were spread onto a 225mm x 225mm LBA plate supplemented with 50μg/ml ampicillin. The plate was incubated overnight at 37°C. The library was harvested by washing and scraping the colonies off the agar into two 3ml volumes of LB supplemented with 50μg/ml ampicillin. The agar washes were pooled and glycerol was added to a final concentration of 20% (v/v). The library was aliquotted and stored at -70°C.

The library titre was established by plating out 50 μl of 10^{-2}, 10^{-4} and 10^{-6} serial dilutions of the library onto LBA plates supplemented with 50μg/ml ampicillin. After incubation at 37°C overnight, a colony count was performed and the cfu/ml was calculated.

2.7 COSMID RESTRICTION ENZYME MAPPING WITH ^{32}P-LABELLED PROBES

2.7.1 Linearisation of the cosmids with lambda-terminase

Cosmid DNA isolated using QIAprep spin miniprep kit (QIAGEN) was linearised with a commercially available λ-terminase (Amersham Pharmacia Biotech) in the following 10μl reaction performed at 30°C for 1 hour.

Cosmid DNA	0.6μg
5X basal buffer	2μl
λ-terminase (4U/μl)	2μl
Distilled water	to 10μl reaction volume

2.7.2 Partial digest of linearised cosmids with restriction endonucleases

Linearised cosmid DNAs were partially digested separately with the restriction enzymes, *Bam* HI, *Hind* III, *Eco* RI and *Kpn* I. Generally 0.3μg of cosmid DNA was partially digested with 0.15U of restriction enzyme in a total reaction volume of 10μl, containing a 1X concentration of the appropriate reaction buffer. Reactions were pre-warmed at 37°C before the addition of the enzyme, then allowed to proceed for approximately 2 minutes. The addition of 0.5μl of 0.5M EDTA (pH 8) and heat denaturation of the enzyme at 68°C for 10 minutes stopped the reaction.

2.7.3 Preparation of digested λ-phage DNA standards

DNA standards were created by digestion of genomic λ-phage DNA with restriction endonucleases to produce *cos*-end fragments of known sizes.

Non-methylated linear λ-phage DNA (Sigma) was completely digested in separate reactions with *Bam* HI, *Cla* I, *Hind* III, *Kpn* I, *Stu* I and *Xho* I. The enzymes were inactivated and 0.5μg of each digest was pooled together with 0.25μg uncut λ-phage DNA. The mix contained twelve DNA end fragments ranging in size from 2kb to 33.4kb and the whole genome of 48.5kb.

2.7.4 Liquid hybridisation of linearised partially-digested cosmids and λ-phage standards with ^{32}P-labelled oligonucleotides

Linearised-partially digested cosmid DNAs were hybridised separately with two ^{32}P-labelled oligonucleotides (ON-L and ON-R, see section 2.4.5.2.2 for labelling procedure) in the following liquid reaction:

λ-terminase-partially digested cosmid DNA	0.15ug
1M Sodium chloride	0.8μl
ON-L/ON-R (0.15pmol/μl)	1μl
Distilled water	to 8μl reaction volume

The reaction was heated to 75°C for 5 minutes to disassociate the *cos* ends then incubated at 45°C for 30 minutes to allow the oligonucleotides to hybridise.

Hybridisation of the labelled oligonucleotides to the λ-phage DNA standards was performed using the same conditions as the cosmids, except that both ON-L and ON-R were hybridised simultaneously in the following reaction:

λ-phage digested DNA	0.2ug
1M Sodium chloride	0.8µl
ON-L (0.15pmol/µl)	0.5µl
ON-R (0.15pmol/µl)	0.5µl
Distilled water	to 8µl reaction volume

2.7.5 Visualisation of the hybridised cosmid fragments

6X DNA loading buffer (section 2.8.1) was added to all samples and standards to a final concentration of 1X. 0.15µg hybridised cosmid DNA and 10ng standards were loaded into the wells of a 0.45% (w/v) agarose gel (for ON-R hybridised samples) and a 0.6% (w/v) agarose gel (for ON-L hybridised samples) and electrophoresed at 2 volts/cm for 16 to 30 hours in 1X TBE buffer.

Gels were briefly rinsed in 1X TBE then dried onto DE-81 chromatography paper (Whatman). The dried gel was wrapped in Saran wrap and exposed to medical X-ray film (100NIF, Fujifilm) with an intensifier screen for 24 to 48 hours. The autoradiograph was developed using a compact X2 automated film processor (X-Ograph imaging systems).

2.7.6 Construction of cosmid restriction endonuclease maps

Autoradiographs were scanned and digitised using an Image Scanner and ImageMaster Labscan v3.00 software (Amersham Pharmacia Biotech). Images were imported into the 1D image analysis program in ImageMaster TotalLab v1.00 package (Amersham Pharmacia Biotech). Molecular size calibration was performed between the λ-phage standards and a curve was plotted. Cosmid band sizes were estimated from the curve and the size difference between the bands calculated. Cleavage maps were constructed for each cosmid from the data created from labelling the linnearised cosmid from the left end with ON-L and the right end with ON-R.

2.8 REAGENTS

2.8.1 Commonly used reagents

6X DNA loading buffer

Bromophenol blue sodium salt, M.wt. 691.9 (BDH)	0.025g
Xylene cyanol FF, M.wt. 538.6 (Sigma)	0.025g
Glycerol, M.wt. 92.09 (Sigma)	3ml
Distilled water	7ml

1M Ethylene diamine tetraaacetic acid (EDTA), pH 8

EDTA disodium salt, M.wt. 372.2 (Sigma)	186.1g
Distilled water	400ml

Mix and pH to 8 with 10M NaOH. Make up the volume to 500ml with distilled water. Autoclave to sterilise.

70% (v/v) ethanol

Ethanol	70ml
Distilled water	30ml

20% (w/v) N-Lauroyl sarcosine

N-Lauroyl sarcosine sodium salt, M.wt. 293.4 (Sigma)		10g
Distilled water	up to	50ml

Phenol/Chloroform

Phenol saturated with TE buffer, pH 7.4 (GibcoBRL)	200ml
Chloroform (Fisher chemicals)	198ml
Isoamyl alcohol (Sigma)	2ml

5M Sodium chloride (NaCl)

Sodium chloride, M.wt. 58.44 (Fisher Chemicals)		29.22g
Distilled water	up to	500ml

Autoclave to sterilise.

1M Sodium hydroxide (NaOH)

Sodium hydroxide, M.wt. 40.0 (Fisher Chemicals)		20g
Distilled water	up to	500ml

Autoclave to sterilise.

20% (w/v) Sodium dodecyl sulphate (SDS)

Sodium dodecyl sulphate (sodium salt), M.wt. 288.4 (Promega)		40g
Distilled water	up to	200ml

10X TBE buffer (0.9M Tris-borate/2mM EDTA)

Tris base, M.wt. 121.1 (Promega)		108g
Boric acid, M.wt. 61.83 (Sigma)		55g
0.5M EDTA, pH 8		40ml
Distilled water	up to	1000ml

Autoclave to sterilise.

TE buffer (10mM Tris-HCl/1mM EDTA)

1M Tris-HCl, pH 8.0	5ml
0.5M EDTA, pH 8.0	1ml
Distilled water	494ml

Autoclave to sterilise.

1M Tris-HCl, pH variable.

Tris base, M.wt. 121.1 (Promega)	121.1g
Distilled water	800ml

Mix and pH to the desired value with concentrated Hydrochloric acid (HCl). Make up to 1000ml volume with distilled water. Autoclave to sterilise.

2.8.2 Tissue culture reagents

199 media base

10X Medium 199 (Gibco BRL)	50ml
29.5g/litre Tryptose phosphate broth (Moredun Scientific Services)	50ml
80g/litre Sodium bicarbonate (Moredun Scientific Services)	3ml
0.1M Glutamine (Moredun Scientific Services)	5ml
250µg/ml Amphotericin B (Sigma)	1.5ml
10,000U/ml Penicillin, 10mg/ml Streptomycin solution	2.5ml
100U/ml Polymixin B Sulphate	1.5ml
Distilled sterile water	337ml

Growth 199 media

199 media base	450ml
Foetal bovine sera* (GibcoBRL)	50ml

* Heat inactivated at 56°C for 30 minutes

Maintenance 199 media

199 media base	450ml
Foetal bovine sera* (GibcoBRL)	10ml
Distilled sterile water	40ml

10X Phosphate buffered saline (PBS)

1.4M Sodium chloride, M.wt. 58.44 (Fisher Chemicals)		80g
2.7mM Potassium chloride, M.wt. 74.55 (Sigma)		2g
0.1M Di-Sodium hydrogen orthophosphate, M.wt.141.96 (Sigma)		11.5g
1.9mM Potassium phosphate monobasic, M.wt. 136.1 (Sigma)		2g
Distilled water	up to	1000ml

Autoclave to sterilise.

2.8.3 Bacteriology reagents

50mg/ml Ampicillin

Ampicillin (Sigma)	500mg
Distilled water	10ml

Filter through a 0.45μm filter (Millipore) to sterilise.

2% (w/v) Isopropyl-β-D-thio-galactopyranoside (IPTG)

IPTG (Bioline)	200mg
Distilled water	10ml

Filter through a 0.45μm filter (Millipore) to sterilise.

Luria-Bertani broth (LB) (Moredun Scientific Services)

Bacto tryptone (DIFCO)	10g
Bacto yeast extract (DIFCO)	5g
Sodium chloride (Fisher Chemicals)	10g
Distilled water	1000ml

Mix and pH to 7.0, then autoclave to sterilise.

Luria-Bertani agar (LBA) (Moredun Scientific Services)

Luria-Bertani broth (Moredun Scientific Services)	500ml
Bacto agar (DIFCO)	15g

Autoclave to sterilise.

10% (w/v) 5-bromo-4-chloro-3-indolyl-β-D-galactoside (X-gal)

X-gal (Bioline)	100mg
N,N-dimethylformamide, (Sigma)	1ml

Filter through a 0.45μm filter (Millipore) to sterilise.

2.8.4 Enzyme-linked immunosobent assay (ELISA) reagents

Carbonate-bicarbonate buffer

0.2M Sodium carbonate (Sigma)	7.9ml
0.2M Sodium hydrogen carbonate (Sigam)	17.1ml
Distilled water	75ml

Correct pH the solution to 9.6 by the addition of 0.2M Sodium carbonate or 0.2M Sodium hydrogen carbonate.

ELISA diluent buffer

ELISA Wash buffer	100ml
Bovine serum albumin (Sigma)	1g

ELISA wash buffer

10X Phosphate buffered saline	1000ml
Tween 80 (Sigma)	5ml
Distilled water	9000ml

Orthophenylene diamine (OPD substrate)

0.1M Citric acid (Sigma)	121.5ml
0.2M Di-Sodium hydrogen orthophosphate (Sigma)	128.5ml
Distilled water	250ml

Adjust the pH of the solution to 5.0 using either of the above solutions as required, then to 100ml of the solution add:

Orthophenylene diamine 80mg tablet (Sigma)	1X 80mg tablet
30% Hydrogen peroxide (Sigma)	80µl

2.8.5 DNA hybridisation reagents

Denaturing buffer (0.5M NaOH/1.5M NaCl)

Sodium hydroxide, M.wt. 40.0 (Fisher chemicals)		20g
Sodium chloride, M.wt. 58.44 (Fisher chemicals)		87.66g
Distilled water	up to	1000ml

Colony neutralisation buffer (1M Tris-HCl, pH 7.5/1.5M NaCl)

Sodium chloride, M.wt. 58.44 (Fisher chemicals)	87.66g
1M Tris-HCl, pH 7.5	1000ml

DIG colour substrate

75mg/ml NBT in 70% (v/v) dimethylformamide (Roche)	45µl
50mg/ml BCIP toluidinium salt in dimethylformamide (Roche)	35µl
Detection buffer	10ml

Detection buffer (0.1M Tris-HCl, pH 9.5/0.1M NaCl)

1M Tris-HCl, pH 9.5		100ml
Sodium chloride, M.wt. 58.44 (Fisher chemicals)		5.84g
Distilled water	up to	1000ml

10X DIG blocking reagent

Blocking reagent (Roche)	10g
5X Maleic acid buffer	20ml
Distilled water	80ml

Mix and gently heat in a microwave until the blocking reagent dissolves. Autoclave to sterilise.

5X Maleic acid buffer (0.1M Maleic acid/0.15M NaCl)

Maleic acid, M.wt. 116.08 (Fisher chemicals)		58.04g
Sodium chloride, M.wt. 58.44 (Fisher chemicals)		43.83g
Distilled water	up to	1000ml

Mix and pH the solution to 7.5 with concentrated Sodium hydroxide and autoclave

Southern neutralisation buffer (0.5M Tris-HCl, pH 7.5/3M NaCl)

1M Tris-HCl, pH 7.5		500ml
Sodium chloride M.wt. 58.44 (Fisher chemicals)		175.32g
Distilled water	up to	1000ml

20X SSC buffer (3M NaCl/0.3M Sodium citrate)

Sodium chloride, M.wt. 58.44 (Fisher chemicals)		175.32g
Tri-Sodium citrate, M.wt. 294.10 (Fisher chemicals)		88.2g
Distilled water	up to	1000ml

Correct pH to 7.0 with concentrated Sodium hydroxide.

Standard hybridisation buffer

20X SSC	250ml
10% (w/v) N-lauroylsarcosine	10ml
20% (w/v) SDS	1ml
10X DIG blocking reagent	100ml
Distilled water	739ml

Wash solutions

Wash solution	20X SSC	20% (w/v) SDS	Distilled water
2X	100ml	5ml	895ml
0.5X	25ml	5ml	970ml
0.2X	10ml	5ml	985ml

CHAPTER 3.0

CHARACTERISATION OF THE TISSUE CULTURE ADAPTATED STRAIN OF SPPV AND EPIDEMIOLOGICAL STUDIES

3.1 INTRODUCTION

The causative agent of the epidemic scab disease that causes high mortality in red squirrels was tentatively identified by electron microscopy as a parapoxvirus by Scott *et al.,* (1981). Experimental infections subsequently confirmed that the *Squirrel parapoxvirus* (SPPV) was the agent responsible for the scab disease in red squirrels (Tompkins *et al.,* 2002). Virus from a single animal was isolated in cell culture in the early 1980's (Sands *et al.,* 1984) and to this day it remains the only isolated strain of SPPV as subsequent isolation attempts have failed.

The availability of a tissue culture system for the production of virus would offer numerous advantages for the characterisation of SPPV over virus derived from scab material. For example, large quantities of virus can be produced in tissue culture and several methods for the extraction of poxviral DNA from tissue culture exist. In contrast, only small amounts of scab material can be recovered from an individual animal and the passage of SPPV in red squirrels to produce more virus for study is rarely allowed due to ethical considerations and the protected status of red squirrels in the UK. The availability of a tissue culture system would also enable viral gene expression, viral development and the function of individual genes to be characterised. Therefore, due to the limited quantities of scab material recovered from infected wild red squirrels, characterisation of SPPV was attempted in the first instance, using virus purified from tissue culture.

Sainsbury *et al.,* (2000) successfully developed an enzyme-linked immunosorbent assay (ELISA) for the detection of anti-SPPV antibodies in red and grey squirrels sera using Nonidet P40 (Sigma) extracts of the tissue culture grown SPPV virus isolate as antigen (section 2.3.1.1). The origin of SPPV is not clear, however grey squirrels are suspected to be the source as no clinical disease was recorded until the introduction of grey squirrels to Britain in the late 19th century (Sainsbury and Gurnell, 1995). Using the ELISA, Sainsbury reported that 61% of 223 apparently healthy grey squirrels sampled from across the UK had antibodies to SPPV (Sainsbury *et al.,* 2000). The high sero-prevalence suggests that the grey squirrel may act as a reservoir for SPPV, providing that the virus is maintained in the grey squirrel and can be transmitted to the red species. It was postulated that transmission of SPPV might be via a similar route to the parapoxviruses (Sainsbury and Gurnell, 1997). To date there has only been one confirmed report of SPPV induced disease in a wild grey squirrel (Duff *et al.,* 1996) and experimental infections of captive grey squirrels failed to induce clinical disease (Tompkins *et*

al., 2002). The apparent absence of SPPV-induced scab lesions in grey squirrels raises several questions regarding the transmission of the virus from the grey to red squirrels. Grey to red squirrel transmission is unlikely to be via direct contact with infectious scab material shed into the environment, which is considered to be the main route of transmission for other parapoxviruses (Robinson and Balassu, 1981; Nettleton *et al.*, 1996b). However the epidemiology of parapoxviruses is poorly understood, and the transmission potential of individuals with subclinical ORFV infections has not been discounted (Yirrell *et al.*, 1994; Nettleton *et al.*, 1996b). Further studies are required to assess the transmission potential of subclinically infected grey squirrels. In addition other routes of transmission cannot be ruled out, such as the involvement of other host species. To address this question, sera was collected from other rodent species (wood mice and bank voles) from a geographical location where persistent SPPV infection is a problem. The sera was analysed using the ELISA (Sainsbury *et al.*, 2000) for antibodies to SPPV and the possible role of other rodent species in the epidemiology of SPPV is discussed (section 3.3).

3.2 MORPHOLOGY OF SPPV

Virus was prepared from FLMC monolayers infected with virus previously passaged 25 times in FLMCs (sections 2.2.2.1 and 2.2.3.1) and from scab material (isolate 1296/99) (section 2.2.3.2). The prepared samples were stained with 2% phosphotungstic acid and visualised using negative contrast electron microscopy (performed by CVLA, Lasswade). SPPV (tissue-culture strain) viral particles were observed at a concentration in excess of $1x10^6$ particles per ml. The estimated size of tissue culture strain SPPV particles was 270nm in length by 206nm in width, which is somewhat different when compared to other parapoxviruses (refer to table 3.1). SPPV had a similar length to ORFV, BPSV and PVNZ, but was much shorter than PCPV and much longer than PVNZ. However SPPV was wider than all of the accepted members of the parapoxvirus genus by approximately 35nm to 45nm giving the appearance of a slightly more rounded or barrel-shaped particle when compared to ORFV particles (figures 3.1A and C). In contrast, the dimensions of SPPV viral particles prepared from scab material (isolate 1296/99) were similar to other parapoxviruses and the overall shape was ovoid (figure 3.1B).

SPPV resembled the parapoxviruses in term of general surface morphology of. The virus possessed a regular basket-weave surface pattern, however a difference was noted in the appearance of the basket-weave pattern when compared to other parapoxviruses (figure 3.1),

which supports previous observations described by Scott (Scott *et al.*, 1981). In SPPV scab and tissue culture preparations the surface striations appear to cross at approximately 120°, whereas in other parapoxviruses this angle is more acute.

Virus species	Estimated length (nm)	Estimated width (nm)	References
SPPV tissue culture strain	270	205	This thesis
SPPV wild type isolate 1296/99	275	175	This thesis
ORFV	263	157	(Nagington and Horne, 1962)
BPSV	277	169.5	(Nagington *et al.*, 1962)
PCPV	300	150	(Cohen *et al.*, 1964)
PVNZ	250	160	(Horner *et al.*, 1987)
Sealpoxvirus[a]	316	192	(Simpson *et al.*, 1994)
VACV	303	240	(Nagington and Horne, 1962)
Western grey squirrelpox	308	247	(Regnery, 1975)

Table 3.1 The dimensions and axis ratios of the accepted and tentative ([a]) species of parapoxvirus genus with the Western grey squirrelpox and VACV for comparison. Sizes were estimated from negatively stained virus preparations examined by electron microscopy. Two forms of sealpoxvirus were described by Simpson *et al.*, (1994), only the sizes of parapox-like virus are both presented here.

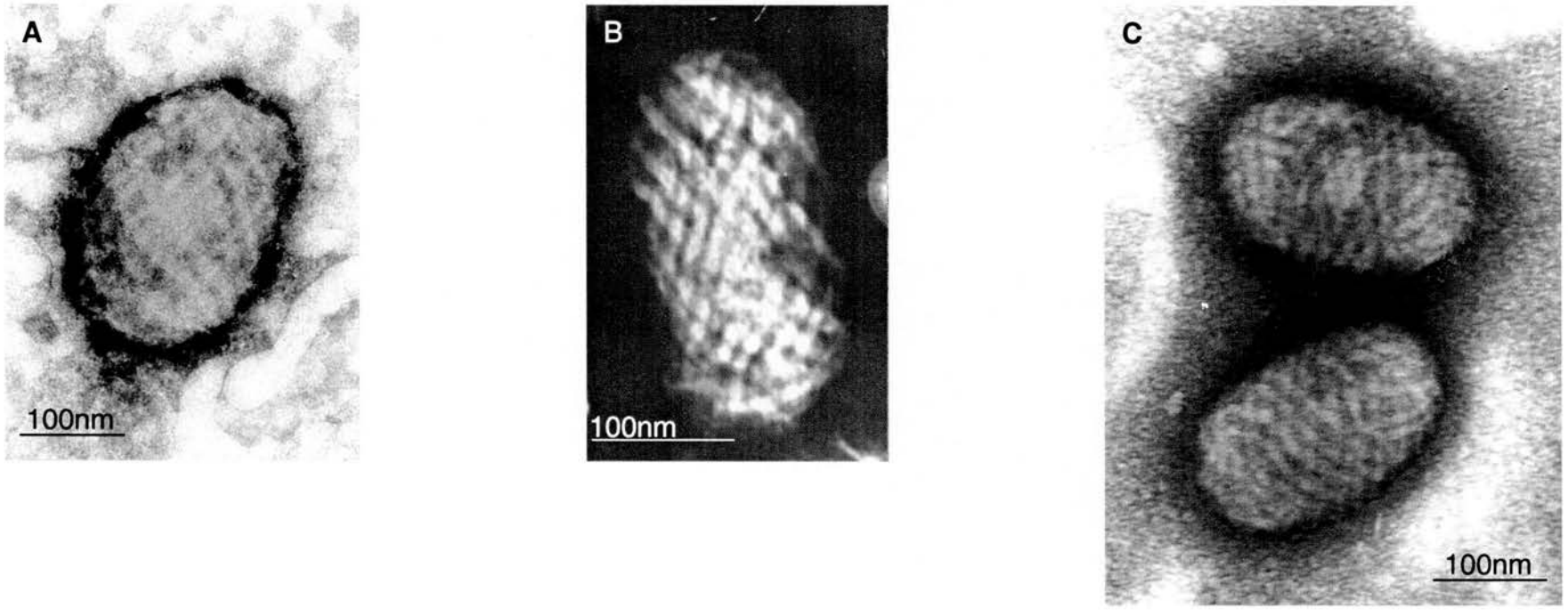

Figure 3.1 Negative contrast electron micrographs of poxvirus particles stained with phosphotungstic acid . (**A**) SPPV tissue culture stain (passage 26 in FLMC), (**B**) SPPV wild type isolate 1296/99 and (**C**) ORFV strain orf-11 (courtesy of Dr Peter Nettleton).

3.3 Epidemiology of SPPV

Protein A and G conjugated to horseradish peroxidase (Protein G/A-HRP) were shown to recognise and bind red and grey squirrel IgG in an ELISA system (Warns, 1995). The ELISA was further developed by incorporating an antigen binding step to produce an assay capable of detecting anti-SPPV IgG antibodies in sera obtained from red and grey squirrels (Sainsbury *et al.*, 2000). Protein G-HRP was the conjugate of choice in the squirrel ELISA because it exhibited a greater sensitivity when compared to Protein A. The squirrel ELISA was used to test wood mice and bank vole sera collected in July and August 2000 and 2001 from Manor Woods (Wirral, Merseyside) for anti-SPPV antibodies.

3.3.1 ELISA development

Before the squirrel ELISA system could be used to screen rodent sera obtained from wood mice and bank voles, the ability of Protein G-HRP to bind to sera from these rodent species was assessed. Sera obtained from a red squirrel (pooled from three animals), a BALB/c mouse, two wood mice (B821 and B826) and two bank voles (B017 and B825) were coated onto a microplate at a 1/50 dilution (section 2.3.1.2). Reciprocal dilutions of Protein G-HRP were added to the plates and allowed to bind to the coating antibodies. The optical density (OD) of each well following the addition of the HRP substrate orthophenlyene diamine (OPD) were measured and the resulting data used to assess the sensitivity of protein G-HRP in detecting serum antibodies derived from the different rodent species.

The mean OD value of each duplicate was calculated and the results are presented in table 3.2. Protein G-HRP reacted with the sera from all the different rodent species, but differences between different rodent species were noted. The OD values with protein G-HRP at a concentration of 1/500 ranged from 0.221 to 1.941, with bank vole and red squirrel sera producing the highest OD values and BALB/c mouse the lowest.

The OD values decreased proportionately with decreasing concentrations of Protein G-HRP until a point was reached were the concentration of Protein G-HRP was too low to detect the rodent antibodies. This pattern is most obvious with the strongly reacting sera. For example with bank vole B017 the OD values decreased from 2.805 to 1.082 with the Protein G-HRP dilution range 1/250 to 1/750. A similar pattern was also observed with the red squirrel and wood mice sera,

	1	2	3	4	5	6	7	8	9	10	11	12	Protein G-HRP dilution
A	1.866		0.370		0.617		0.397		2.805		0.773		1/250
B	1.424		0.221		0.363		0.307		1.941		0.576		1/500
C	1.062		0.162		0.229		0.222		1.182		0.359		1/750
D	0.234		0.072		0.097		0.096		0.144		0.109		1/1000
E	0.143		0.068		0.083		0.070		0.163		0.073		1/1500
F	0.052		0.051		0.052		0.053		0.052		0.055		CONTROL
Sera 1/50	red squirrel pool		BALB/c mouse		wood mouse B821		wood mouse B826		bank vole B017		bank vole B825		

Table 3.2 Summary of the OD values produced by the sera from different rodent species with varying concentration of Protein G-HRP using the method described in section 2.3.1.2. The OD_{492nm} values presented are the mean values of the duplicate wells. The rows A to E of a 96-well plate were coated overnight with sera obtained from the different rodent species (indicated in the bottom row of the table). Different concentrations of Protein G-HRP added to each row (concentrations are indicted in the right end column). Control row F is a OPD control, row F was coated overnight with carbonate-bicarbonate buffer (pH 9.6) and did not received protein G-HRP. Strongly positive OD values are shaded in grey.

despite overall lower OD values than bank vole sera. All of the wood mouse and bank vole sera produced OD values in excess of 0.2 with a protein G-HRP dilution of 1/750, however with protein G-HRP diluted to 1/1000 OD values were less than or approximately 0.2. Therefore it was determined that the lowest dilution of protein G-HRP that produced a strongly positive reaction for wood mice and bank vole sera was 1/750. Hence a dilution of 1/750 of protein G-HRP was used in the ELISA to detect anti-SPPV antibodies in wood mice and bank vole sera; and a nominal OD value of 0.2 was decided upon as a cut off value to discriminate between positive and negative antibody detection.

3.3.2 Bank vole and wood mice assay results

A total of 43 wood mouse and 130 bank vole sera were screened for anti-SPPV antibodies using the ELISA protocol described in section 2.3.1.3. The mean corrected OD values were calculated by subtracting the negative antigen mean OD values from the mean positive OD values. The positive control samples (seropositive grey squirrel serum) were consistently positive (corrected OD values ranged from 1.223 to 1.482) and the negatively controls (seronegative grey squirrel and BALB/c mouse) all had corrected OD values less than 0.1. Likewise, all the corrected OD values for the wood mice and bank vole sera were less than 0.1 and therefore seronegative for SPPV.

The173 rodent sera were previously screened using an immuno-fluorescence assay and 43 sera were seropositive for antibodies specific for *Cowpox virus* (CPV) (performed by K. Tolliday, University of Liverpool). No cross-reaction between anti-SPPV and anti-CPV antibodies was detected.

Red and grey squirrel sera collected from 1994 to 2003 from several locations in the counties of Merseyside and Lancashire were also tested as part of the ongoing, UK-wide survey of red and grey squirrel sero-prevalence to SPPV. The ELISAs were performed using the same assay conditions as Sainsbury (Sainsbury *et al.*, 2000). 29 grey squirrels from a sample size of 42 individuals tested positive for SPPV antibodies, which indicates that approximately 69.0% of grey squirrels in the Northwest of England are seropositive for SPPV antibodies. In direct contrast, only 4 red squirrels tested positive for SPPV from a sample size of 23 animals, which corresponds to a 18% seroprevalence in red squirrel populations (results courtesy of P. Nettleton).

3.4 MOLECULAR CHARACTERISATION OF TISSUE CULTURE GROWN SPPV

3.4.1 SPPV-DNA extraction from infected foetal-lamb muscle cells (FLMCs)

Several attempts were made to extract high-quality viral DNA from SPPV-infected FLMC monolayers using an adaptation of the method described by Meyer (section 2.4.2)(Meyer *et al.*, 1995). Confluent FLMCs monlayers contained in five 225cm^2 tissue-culture flasks were infected with the tissue-cultured strain of SPPV at a MOI of 1 (sections 2.1.1.1 and 2.2.2.1). Viral DNA was harvested from infected FLMCs that were approaching 80% cytopathic effect (CPE). Consistently, very little DNA was recovered, with an average of only 8µg of DNA in total from five flasks. In addition, when the viral DNA was digested with the restriction endonuclease *Eco* RI and electrophoresed on an agarose gel, no defined viral DNA bands were visible and the sample appeared to be heavily contaminated with ovine genomic DNA and ribosomal RNA (figure 3.2). Digestion with the restriction endonucleases *Hin*d III and *Kpn* I also did not produced defined viral DNA bands (results not shown). In contrast, viral DNA recovered from ORFV (orf-11) infected FLMCs (performed in parallel with SPPV extractions) produced defined viral DNA bands with very little contamination (figure 3.2). Furthermore, ORFV DNA extracted solely from viral particles isolated from the cell supernatant appeared to have a greater purity than cytoplasmic DNA extracts. Therefore SPPV DNA was extracted from cell supernatant in an attempt to produce a purer preparation of viral DNA. However, only 1.8µg of DNA was recovered from the media decanted from five 225cm^2 flasks and the purity of the viral DNA was still poor when compared to the ORFV DNA extracts (results not shown).

3.4.2 Random cloning of SPPV DNA extracted from infected FLMCs

Despite the poor purity and low concentration of viral DNA extracted from tissue culture grown virus, the random cloning of SPPV *Kpn* I restriction endonuclease fragments was attempted (section 2.6.2). When transformed cells were spread onto agar plates containing IPTG and X-gal, the resulting bacterial colonies were predominantly blue in coloration. Very few white bacterial colonies were observed, which suggests that the ligation of the plasmid vector with viral DNA was inefficient. The few white colonies were isolated in culture and plasmid DNA extracted and digested with *Kpn* I to cut the cloned viral DNA out of the vector. When electrophoresed on an agarose gel, only one clone (designated K1-TC) appeared to possess a cloned restriction fragment, which was approximately 4.65kb in length. DNA sequence was obtained from both

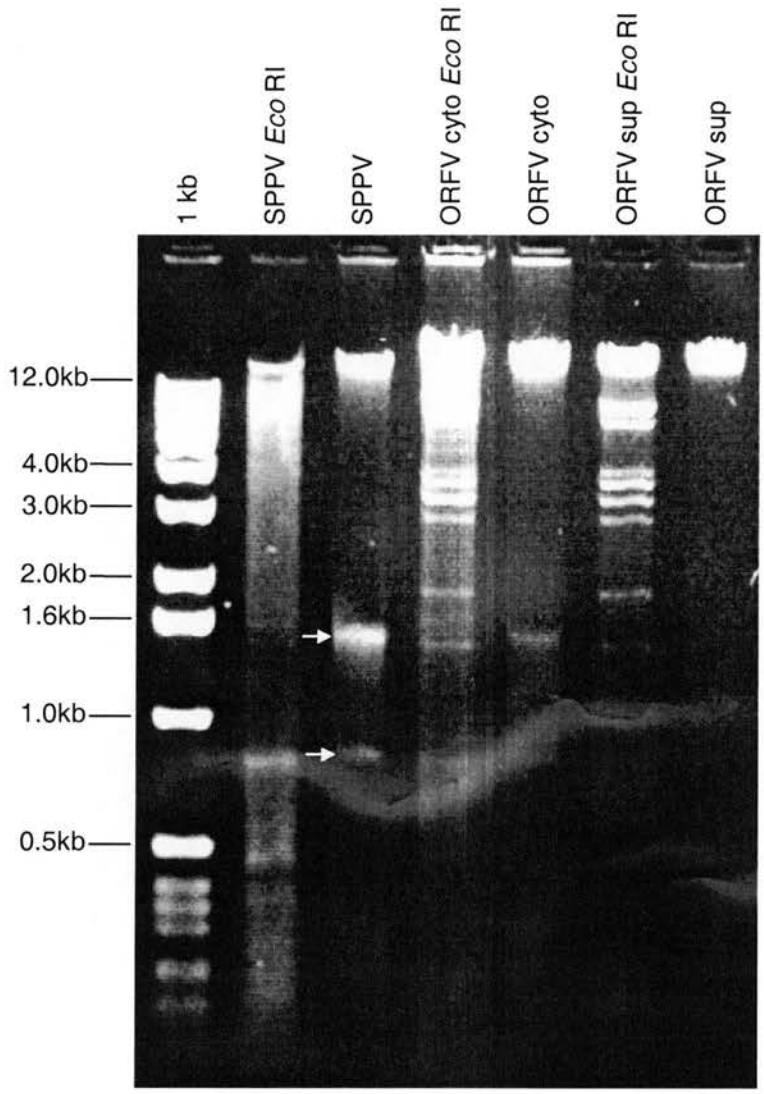

Figure 3.2 Agarose gel electrophoresis of SPPV and ORFV (orf-11) viral DNA extracted from FLMCs. ORFV DNA was purified from the cytoplasmic extract of FLMCs (ORFV cyto) and from cell supernatant (ORFV sup). Viral DNA was digested with *Eco* RI and digest products electrophoresed on a 0.8% (w/v) agarose gel along with undigested viral DNA and DNA size markers (1kb ladder supplied by Gibco BRL). The two bands indicated by the arrows on the gel are likely to be ribosomal RNA.

ends of K1-TC by sequencing with oligonucleotide primers (T7 and T3) specific for the vector sequence that flanks the cloning site (section 2.4.7). The average G+C content of the two sequences was extremely high at 71%, which suggests that the clone is not mammalian in origin. The nucleotide sequences were compared to those deposited in the EMBL databases using the FastA algorithm to search for homologous sequence (section 2.4.8.1). The most significant match for both sequences was with the G+C-rich genome sequence of MOCV (GenBank accession number U60315), indicating that K1-TC is likely to be poxviral in origin. The percentage nucleotide homology of the left and right ends of K1-TC with MOCV was 65.5% and 69.3% respectively.

3.5 DISCUSSION

The dimensions and barrel shape of the SPPV particles isolated from tissue culture corresponded with those reported by Scott (Scott *et al.*, 1981). However the viral particle derived from scab material (isolate 1296/99) appeared to be more elongated than the tissue culture grown virus and was characteristically parapoxvirus-like in shape. The barrel shape of the tissue-culture grown strain of SPPV is not due to adaptation of the virus to tissue culture, as all wild type SPPV isolates examined by electron microscopy to date are barrel shaped (Scott *et al.*, 1981; J. Stewart personal communication). This suggests that the ovoid shape of the scab isolate 1296/99 particle may be an aberration. However, as only one virus particle from this isolate was clearly photographed this cannot be confirmed. Despite the apparent variation in overall virion shape, the appearance of the surface striations of SPPV prepared from both scab and tissue-culture were comparable, suggesting that they are the same species of virus. Differences in the surface morphology of SPPV when compared to the other parapoxvirus species, enables SPPV to be distinguished from other parapoxviruses (Nagington and Horne, 1962; Nagington *et al.*, 1962; Cohen *et al.*, 1964; Wilson and Sweeney, 1970; Falk, 1978; Horner *et al.*, 1987; Tryland *et al.*, 2001). Regular surface striations have also been reported for several unclassified poxviruses including a Western grey squirrel virus of North America and crocodile and caiman poxviruses (Regnery, 1975; Gerdes, 1991). The Western grey squirrel virus resembles SPPV in shape, although the surface striations are much narrower and more closely packed than seen in SPPV. The surface morphology of SPPV is indistinguishable from the caiman poxvirus.

Productive use of the tissue culture strain has enabled antigen to be prepared for ELISA. The high incidence of squirrels that tested positive for SPPV antibodies by ELISA and the reports of

clinical disease in the red squirrel populations of Ormskirk, Rufford, Southport and Formby (Sainsbury and Ward, 1996; P. Nettleton personal communication) suggests that SPPV is endemic in squirrel populations in the Northwest of England. All of the wood mouse and bank vole sera tested proved to be negative for SPPV antibodies which indicates that these rodent species do not play a role in the maintenance and transmission of SPPV. However this result may not be conclusive as the geographical region the samples were collected from was limited. It is possible that other rodent species may play a role in the transmission of SPPV, but remains to be demonstrated.

Extraction of high quality viral DNA from tissue culture grown SPPV using methods previously described for orthopox and parapox virus DNA purification proved unsuccessful. The amount of DNA recovered from SPPV was consistently less and of poorer quality when compared with ORFV DNA extracts. The growth of SPPV and ORFV in FLMCs was shown to be comparable by immuno-fluorescent test (IFT) using the parapoxvirus and SPPV cross-reacting IC7 monoclonal antibody (Housawi, 1997) (results not shown). Therefore the low recovery of viral DNA from SPPV infected cells is not the result of poor growth in tissue culture. A method must be established to extract concentrated, pure viral DNA from infected cell monolayers if work is to continue on tissue culture adapted SPPV. It is possible that some fundamental difference in the development and egress of SPPV *in vitro* may hinder the purification of viral cores from the cytoplasm of infected cells and hence result in the poor recovery of viral DNA. Closer examination of the extraction method may reveal a step where virus is inadvertently discarded.

Cloning of the *Kpn* I fragments produced by digestion of viral DNA prepared from cytoplasmic cell extracts was unproductive and only one clone (K1-TC) was isolated. Disproportionate numbers of clones consisting of just plasmid vector DNA were produced, suggesting that the ligation of the plasmid vector with the *Kpn* I digested viral DNA was inefficient. Sequence analysis of the clone K1-TC revealed a G+C content of approximately 71% and homology at the DNA level with MOCV in excess of 65%. Taken together, these data indicate that the genome of SPPV is likely to be comparable in G+C content and share sequence homology with the G+C rich viruses belonging to the molluscipox and parapox virus genera (Wittek *et al.*, 1979; Senkevich *et al.*, 1997). This is discussed further in chapter 4.0.

Tissue-culture work was abandoned in favour of working with the wild type virus for several reasons. 1) Sufficient high quality viral DNA could not be recovered from tissue culture to enable the SPPV genome to be cloned into a plasmid vector. 2) Adaptation of parapoxviruses to tissue culture often initiates genomic rearrangement including duplication, translocation and deletion events particularly in the terminal regions of the genome (Senkevich and Moss, 1998; Fleming *et al.,* 1995; Cottone *et al.,* 1998; McInnes *et al.,* 2001). Genomic rearrangement is often accompanied by a decrease in virulence and pathogenesis. As one aim of this study is to identify possible genes associated with virulence *in vivo*, it was therefore considered appropriated to study the fully virulent wild type virus. Isolation of viral DNA and the construction of restriction endonuclease maps of the wild type isolate 1296/99 genome are discussed in chapter 4.0.

CHAPTER 4.0

RESTRICTION ENDONUCLEASE MAPPING OF THE SPPV GENOME

4.1 INTRODUCTION

Restriction endonuclease maps have been published for the parapoxvirus species ORFV, PCPV and BPSV (Menna *et al.,* 1979; Gassmann *et al.,* 1985; Mercer *et al.,* 1987; Robinson *et al.,* 1987; Cottone *et al.,* 1998; McInnes *et al.,* 2001). Restriction endonucleases employed in the mapping of parapoxvirus genomes include, *Eco* RI, *Hin*d III, *Hpa* I, *Bam* HI and *Kpn* I.

Due to the shortage of highly purified viral DNA, as explained in section 4.2.1, restriction endonuclease maps of SPPV could not be determined from single, double or partial restriction digests of genomic DNA. Therefore SPPV *Not* I, *Bam* HI and *Kpn* I restriction fragments were randomly cloned into a plasmid vector and the maps constructed using the cloned fragments. The restriction endonucleases, *Not* I, *Bam* HI and *Kpn* I were selected for the following reasons.

Sequence analysis of the *Kpn* I clone (K1-TC) produced from tissue-culture grown SPPV suggested a G+C content of approximately 71% (section 3.4.2). The recognition sites of *Not* I, *Bam* HI and *Kpn* I restriction endonucleases are G+C rich, hence these enzymes were predicted to cleave the G+C rich SPPV genome frequently to produce fragments of a size that could be easily cloned into a plasmid vector.

The genomes of 12 ORFV strains and isolates were shown to each comprise of between 20 and 24 *Kpn* I fragments (Robinson *et al.,* 1987; McInnes *et al.,* 2001). Analysis of the SPPV *Kpn* I restriction profile (figure 4.1) indicated the SPPV genome is comprised of 14 or more *Kpn* I fragments, of which the largest was estimated to be 17kb by comparison to known fragment sizes in digested Orf-11 DNA (figure 4.1). This data indicated that it would be theoretically possible to clone all the SPPV *Kpn* I fragments into the pBluescript plasmid, with the exception of the two terminal fragments which were assumed to contain a terminal hairpin loop at one end rather than a *Kpn* I site.

The genomes of 12 ORFV strains and isolates were shown to each comprise of only 9 to 11 *Bam* HI fragments of which two or three fragments were of a size difficult to clone into a plasmid vector. However, *Bam* HI sites appear to be more abundant in SPPV than ORFV. Analysis of the *Bam* HI restriction profile (figure 4.1) suggest that 13 or more *Bam* HI fragments exist, with the largest being approximately 15kb in size. Therefore it was assumed the majority of the genome could be cloned into pBluescript SK$^-$ again with the exception of the terminal fragments.

Not I restriction maps have not been published for any parapoxvirus species. Nevertheless *Not* I was selected for use in cloning the SPPV genome because the recognition site consists solely of G and C bases. It was hypothesised and later confirmed from the agarose gel depicted in figure 4.1 that *Not* I would cleave the SPPV genome with a greater frequency than *Bam* HI and *Kpn* I. Strategic cloning and mapping of the smaller fragments produced by *Not* I was carried out to effectively increase the number of locations available for DNA sequencing, without the need to subclone the larger *Bam* HI or *Kpn* I clones.

For the reason discussed in section 4.7.1, the restriction endonuclease maps of SPPV could not be completed solely with the restriction fragments cloned into a plasmid vector. Therefore, a second cloning and mapping strategy was employed to complete the *Bam* HI and *Kpn* I maps. The use of a cosmid vector allowed larger contiguous lengths of the genome to be cloned, with individual cosmid clones being mapped with ease using an end-labelling and partial digest method outlined in section 4.4.4. The use of cosmid clones enabled further characterisation of the SPPV genome by mapping the restriction endonuclease sites *Hin*d III and *Eco* RI without the need to clone individual restriction fragments.

4.2 RESTRICTION ENDONUCLEASE MAPPING THE SPPV GENOME USING CLONED RESTRICTION FRAGMENTS

4.2.1 Preparation of viral genomic DNA and the cloning strategy

Wild type SPPV genomic DNA was prepared from the scab isolate 1296/99 using the method described in section 2.4.1. 1g of scab (trimmed to remove surrounding healthy tissue) yielded a total of 45µg of viral DNA. Single digests of 2µg of viral DNA were performed with *Not* I, *Bam* HI and *Kpn* I and the digested DNA visualised by agarose gel electrophoresis (figure 4.1). The SPPV restriction profile was difficult to interpret due to the low amount of SPPV DNA present and extensive contamination by squirrel genomic DNA, which completely obscured viral DNA fragments less than 6kb in size. In an attempted to enhance the restriction profiles of SPPV a Southern blot was prepared and hybridised with a DIG-labelled probe prepared from the extracted viral SPPV DNA. Although hybridisation with the genomic probe intensified the viral DNA bands, it was not sufficient to clearly visualise the profiles (figure 4.2). Therefore the SPPV DNA was deemed too poor in both quality and quantity to enable successful mapping of the genome using single, double or partial restriction digests.

4.2.2 Cloned restriction fragments

Three genomic libraries were produced consisting of 238 *Kpn* I, 235 *Bam* HI and 182 *Not* I cloned fragments. Each cloned DNA fragment was given an identification number that was preceded by the letter K for *Kpn* I, B for *Bam* HI or N for *Not* I (e.g. K21-1). For clarity in the text that follows, plasmid clones have been given the additional "p" prefix in order to distinguish between the entire plasmid (e.g. pK21-1) and the cloned SPPV DNA fragment.

It was predicted that not all of the clones would contain genomic SPPV DNA, a proportion was likely to be derived from contaminating squirrel DNA. In total 16 *Kpn* I, 23 *Bam* HI and 34 *Not* I clones were identified as being derived from the SPPV genome during subsequent mapping procedure.

Clones containing SPPV DNA were digested with the appropriate restriction endonuclease to excise the insert and the DNA bands resolved by agarose gel electrophoresis. The size of each cloned restriction fragment was estimated by comparison to λ phage DNA singularly digested with various restriction endonucleases and a commercially available 1kb DNA ladder (figure 4.3). Table 4.1 provides a summary of the cloned SPPV-derived restriction fragments and their approximate sizes.

The approximate sizes of the cloned *Kpn* I fragments totalled 79.55kb. As parapoxvirus genomes vary in length between 130kb to 150kb (van Regenmortel *et al.*, 2000), it was predicted that only approximately half of the genome was represented by the *Kpn* I clones. As expected many small *Not* I restriction fragments were cloned. These ranged from 0.25kb to 10.1kb in length and had a combined size of 105.84kb. The combined size of the twenty-three cloned *Bam* HI restriction fragments was 121.95kb. Therefore the cloned *Bam* HI restriction fragments represented a greater proportion of the genome than either the *Kpn* I or *Not* I cloned fragments.

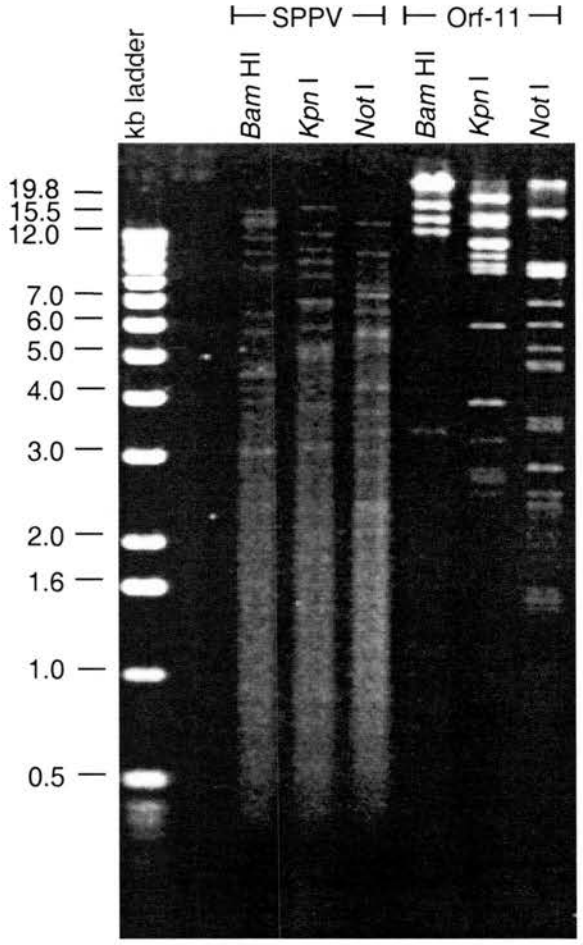

Figure 4.1 *Not* I, *Bam* HI and *Kpn* I digested SPPV (isolate 1296/99) and ORFV (strain Orf-11) DNA electrophoresed on a 0.6%(w/v) agarose gel and stained with Ethidium bromide and visualised under UV light.

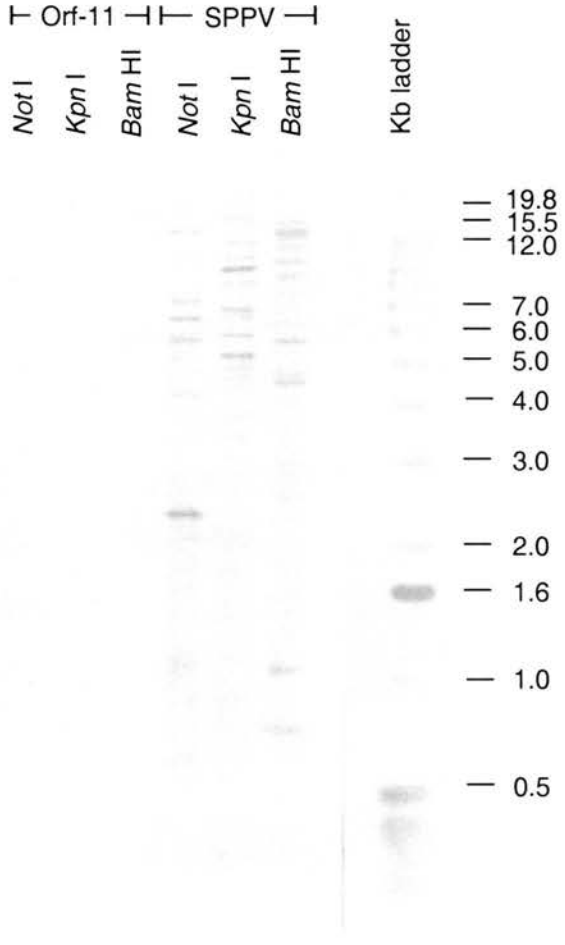

Figure 4.2 Southern blot of the gel depicted in figure 4.1. The Southern blot was probed with DIG-labelled genomic SPPV DNA (isolate 1296/99). 1kb DNA markers (Gibco BRL) were stained separately with a DIG-labelled 1kb DNA.

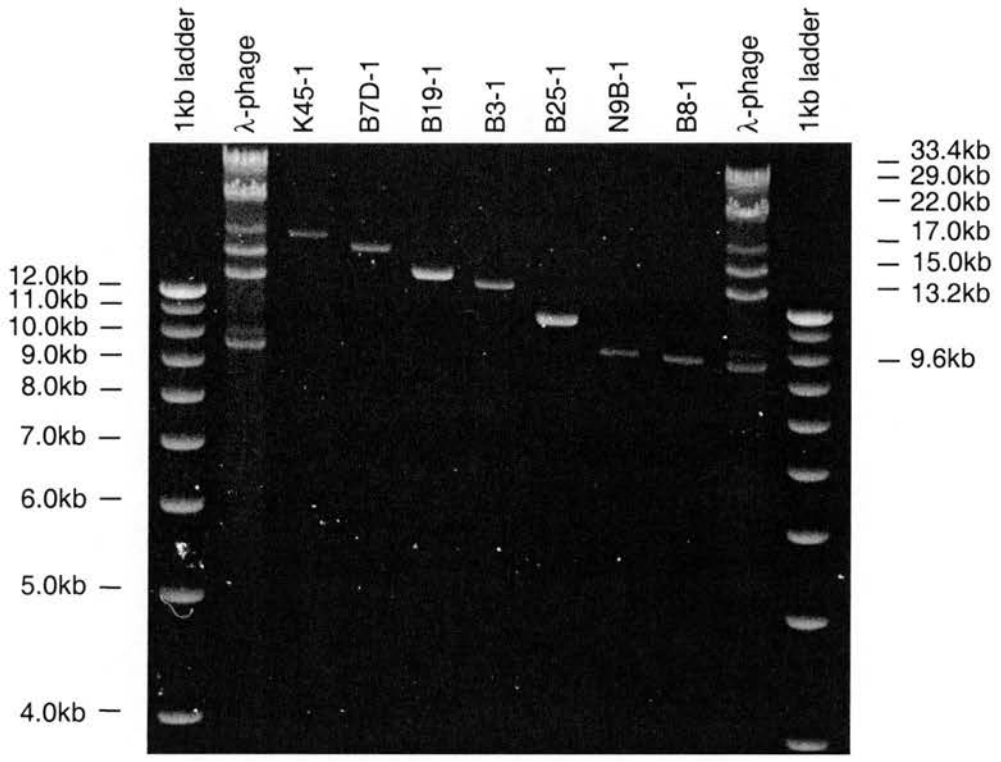

Figure 4.3 A selection of unique clones, digested with the appropriate restriction endonuclease to excise the cloned DNA fragment and electrophorised on a 0.6% agorose gel. Estimation of the sizes of cloned DNA fragments were made by comparison to known DNA standards present in a 1kb ladder and λ-phage DNA digested with Xho I, *Kpn* I and Bgl II. Note the 2.96kb vector band is not visible on this gel as it is smaller than the lowest marker.

***Kpn* I Fragments**		***Bam* HI Fragments**		***Not* I Fragments**	
Clone	Size (kb)	Clone	Size (kb)	Clone	Size (kb)
K45-1	17.5	B7D-1	15.8	N9B-1	10.1
K18-1	7.1	B19-1	13.8	N42-2	7.75
K31-1	6.8	B3-1	13.3	N7-1	7.25
K46-1	6.55	B25-1	11.35	N5-1	6.6
K21-1	5.9	B8-1	9.9	N22A-1	5.75
K47-1	5.25	B11-1	6.3	N10B-1	5.45
K13-1	4.9	B51-2	5.7	N4-1	5.3
K43-1	4.8	B16C-1	4.75	N13-1	5.15
K1-TC	4.65	B5-2	4.65	N26A-1	4.7
K32-1	3.9	B98-2	4.6	N16-1	4.3
K1-1	3.25	B164-2	4.1	N65-2	4.15
K4-1	2.8	B6A-1	3.9	N12-1	3.75
K11-2	2.05	B13-1	3.15	N14D-1	3.3
K19-1	1.8	B1A-1	3.15	N15D-1	3.1
K11-1	1.6	B26-1	3.05	N3-1	2.8
K24-1	0.55	B20B-1	2.95	N5-2	2.4
		B20A-1	2.65	N55-2	2.4
Total	**79.55kb**	B7C-1	2.6	N24-1	2.35
		B30-2	2.55	N9A-1	2.3
		B70-2	1.15	N30-1	2.3
		B12-1	1.1	N1-1	2.15
		B2-1	0.8	N11A-1	1.55
		B24-1	0.65	N6-1	1.5
				N15H-1	1.35
		Total	**121.95kb**	N14A-1	1.3
				N11H	1.25
				N2-1	1.2
				N15A-1	1.05
				N34-1	1.04
				N14C-1	0.9
				N33-1	0.8
				N22B-1	0.35
				N31-1	0.3
				Total	**105.84kb**

Table 4.1 Summary of the unique *Bam* HI, *Not* I and *Kpn* I SPPV fragments cloned into pBluescript SK$^-$ plasmid vector and their approximate sizes.

4.2.3 Mapping Strategy

Partial restriction endonuclease maps of the SPPV genome were determined using a strategy, which is explained schematically in figure 4.4, to identify and align overlapping cloned restriction fragments. Details of the methods used are presented in sections 4.2.3.1 to 4.2.3.3 and an example of map construction of a small region of the SPPV genome is described in detail in section 4.2.3.4.

4.2.3.1 Selection of map anchors

Several *Not* I and *Bam* HI clones were randomly selected from the genomic libraries and the DNA sequenced derived from both ends of the clone analysed (sections 2.4.7 and 2.4.8.1). 8 *Not* I fragments were selected for use as map anchors on the basis of DNA homology with other poxviruses. All eight *Not* I anchor fragments exhibited at least 58% sequence homology to MOCV or ORFV DNA at one or both ends (table 4.2) and alignment to the MOCV subtype 1 genome (accession number U60315) indicated that the *Not* I anchor fragments were likely to span the SPPV genome (figure 4.5). One *Bam* HI fragment, B7C-1, was used as an anchor fragment. B7C-1 did not however exhibit DNA homology with any poxvirus sequence and its use as an anchor fragment is explained in section 4.3.2.1.2.1.

The cloned DNA fragments were excised from the plasmids by digestion with *Not* I and purified from agarose gels. These were labelled with DIG using the random priming or nick translation methods (section 2.4.5.1).

4.2.3.2 Hybridisation to identify overlapping cloned fragments

The DNA of a selection of *Not* I, *Kpn* I and *Bam* HI clones were spotted onto nylon membrane (section 2.4.5.3.2) and screened with DIG-labelled restriction fragments. In the event of the probe failing to hybridise with any of the clones, a greater number of clones were screened. This was achieved by the screening transformed bacterial colonies prepared by the methods detailed in sections 2.6.2.5 and 2.4.5.3.3. All of the hybridisation data used in the construction of SPPV restriction maps is presented in appendix I (located at the end of this thesis), tables A1.1 to A1.6. The tables summarise hybridisation data derived from dot blots, Southern blots and colony screening. However, it should be noted that some cloned fragments were not utilised as probes as they would not have extended the mapped regions.

STEP 1 – Identify overlapping *Bam* HI clones:

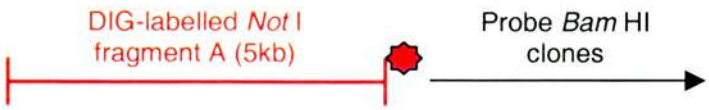

Two *Bam* HI clones identified: 1 (2.5kb) and 2 (3.75kb).

STEP 2 – Align the Bam HI fragments to the Not I fragment:

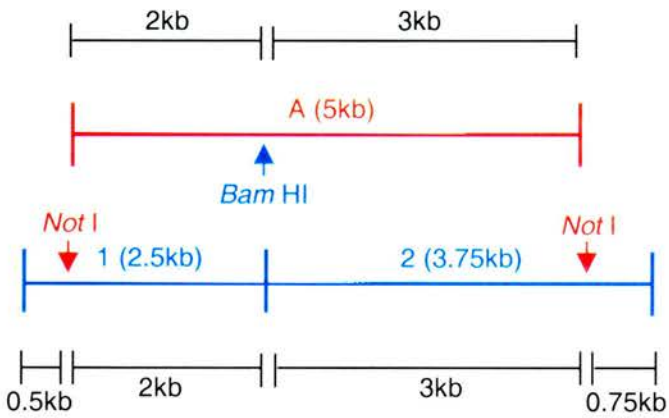

A *Bam* HI restriction digest of the *Not* I clone A and *Not* I digestion of the *Bam* HI clones 1 and 2 performed. Confirmed the location of the *Not* I (▼) and *Bam* HI (▲) sites. Determined the overlap sizes of the *Not* I and *Bam* HI clones and aligned the fragments.

STEP 3 – Identify the overlapping *Not* I fragment:

Not I fragment A hybridised by *Bam* HI probe 2 and fragment B

STEP 4 – Align the *Not* I fragment B to the *Bam* HI fragment 2:

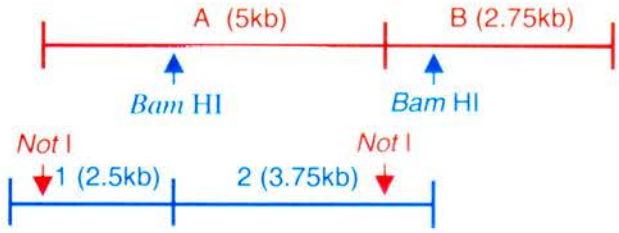

Not I (▼) and *Bam* HI (▲) sites confirmed with restriction digests and the fragments aligned as in step 2.

Figure 4.4 Schematic representation of the technique used to identify overlapping clones and their alignment to produce a restriction endonuclease map of SPPV.

Step 1) A cloned *Not* I fragment (anchor fragment) predicted to be viral in origin by sequence analysis was labelled with digoxygenin (DIG) and used to identify overlapping cloned *Bam* HI fragments by hybridisation. **Step 2)** The overlapping fragments were then accurately aligned to the map anchor by a series of restriction endonuclease digestions to calculate the size of the overlaps. **Step 3)** The overlapping fragments were labelled with DIG and used to identify, by hybridisation, the overlapping *Not* I fragments, **Step 4)** which were subsequently aligned using data from restriction endonuclease digests. This technique enabled the small mapped sections of the SPPV genome to be gradually extended by identifying adjacent and overlapping fragments.

Clone	Primer	Sequence Homologies	% Homology
N1-1	T3	MOCV (region 142.4kb – 143.2kb)	72.2%/762 nucleotides
	T7	MOCV (region 144.6kb – 144.9kb)	60.9%/324 nucleotides
N6-1	T3	MOCV (region 142.0kb – 142.4kb)	66.7%/409 nucleotides
	T7	MOCV (region 141.0kb – 141.5kb)	58.5%/535 nucleotides
N7-1	T3	none	none
	T7	MOCV (region 157.9kb – 158.3kb)	66.2%/370 nucleotides
N12-1	T3	MOCV (region 55.kb – 56.1kb)	73.9%/762 nucleotides
		MOCV (region 52.7kb – 53.2kb)	65.9%/518 nucleotides
	T7		
N13-1	T3	MOCV (region 52.1kb – 52.7kb)	71.6%/564 nucleotides
	T7	MOCV (region 40.8kb – 41.3kb)	71.0%/518 nucleotides
N16-1	T3	MOCV (region 30.3kb – 30.5kb)	69.5%/220 nucleotides
	T7	MOCV (region 24.1kb – 24.3kb)	58.8%/255 nucleotides
N22A-1	T3	MOCV (region 93.0kb – 93.6kb)	82.4%/550 nucleotides
	T7	MOCV (region 99.1kb – 99.4kb)	67.7%/279 nucleotides
N24-1	T3	MOCV (region 30.5kb – 30.9kb)	61.3%/424 nucleotides
	T7	none	none
B7C-1	T3	none	none
	T7	none	none

Table 4.2 Summary of the sequence data from the selected cloned map anchor fragments. In column 3, data in the brackets ( ) represents the region of the MOCV genome that is homologous with SPPV. Column 4 provides the percentage DNA homology of SPPV with MOCV, calculated from the alignment of sequences by the FastA algorithm (section2.4.8.1).

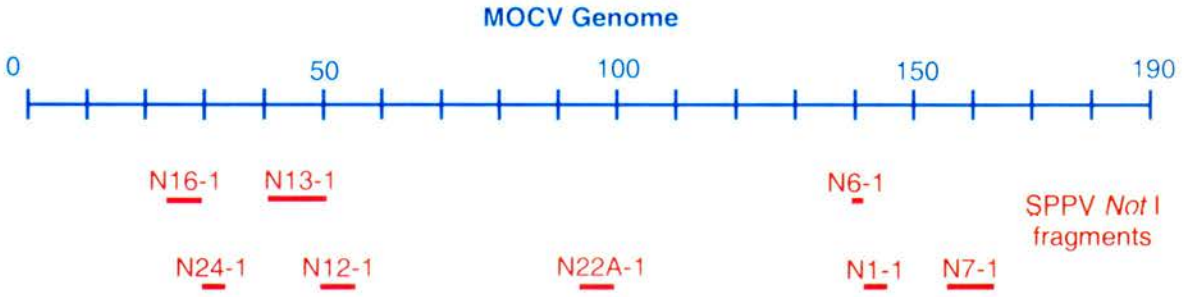

Figure 4.5 Preliminary alignment of SPPV *Not* I anchor fragments to MOCV subtype 1 genome, based upon the sequence homology of the SPPV *Not* I fragments with MOCV (table 4.2).

4.2.3.3 Alignment of overlapping fragments

Hybridising fragments were accurately aligned using restriction endonuclease digests to determine the extent of overlap. This was achieved by comparing their restriction profiles to identify fragments that are common in size (figure 4.8 for an example). The sizes of the fragments produced by single digestion of each *Kpn* I clone with *Not* I and *Bam* HI were determined, and the data is summarised in appendix I, table A1.7. The data from the digestion of the *Bam* HI clones with *Kpn* I and *Not* I are summarised in table A1.8. Likewise, the data from the digestion of the *Not* I clones with *Bam* HI and *Kpn* I is presented in table A1.9.

4.2.3.4 Example of restriction endonuclease map construction

The progressive steps involved in the construction of restriction endonuclease maps are explained here in the form of a detailed explanation of the mapping of a small region of the SPPV genome.

The DIG-labelled *Not* I fragment 5-1 (N5-1) hybridised with pK21-1, pB7D-1 and the duplicates pB51-2 and pB22-2 (figures 4.6 B, G and I). In figures 4.6 A and D, DIG-labelled B51-2 hybridised with pK21-1and pN5-1. In figures 4.6 C and F DIG-labelled B7D-1 hybridised with pK21-1 and pN5-1. In figures 4.6 E and H, DIG-labelled K21-1 hybridised with pN5-1 and pB7D-1; the hybridisation of K21-1 with pB51-1 was not tested. These results indicate that N5-1 and K21-1 overlap each other and both overlap B7D-1 and B51-2, in the arrangement depicted in figure 4.7.

Establishing the size of the overlap between the fragments by comparing restriction profiles of the clones enabled the fragments to be accurately aligned. pN5-1 was singularly digested with *Bam* HI or *Kpn* I, likewise pB7D-1 and pB51-2 were singularly digested with *Not* I and *Kpn* I; and finally pK21-1 singularly digested with *Not* I and *Bam* HI (figure 4.8).

Bam HI digestion of pN5-1 produced two bands of approximately 7.0kb and 2.55kb. As a unique *Not* I, *Bam* HI and *Kpn* I vector restriction sites are located within the multiple clone site of pBluescript SK$^-$; when pN5-1 is digested with *Bam* HI the DNA is cleaved at the vector site and once within N5-1 producing two fragments. However, the vector DNA remains attached to one end of the cleaved N5-1 DNA. The 7.0kb fragment must include the plasmid vector because the 2.55kb band is too small to contain the 2.96kb vector. Hence, when the size of the vector was

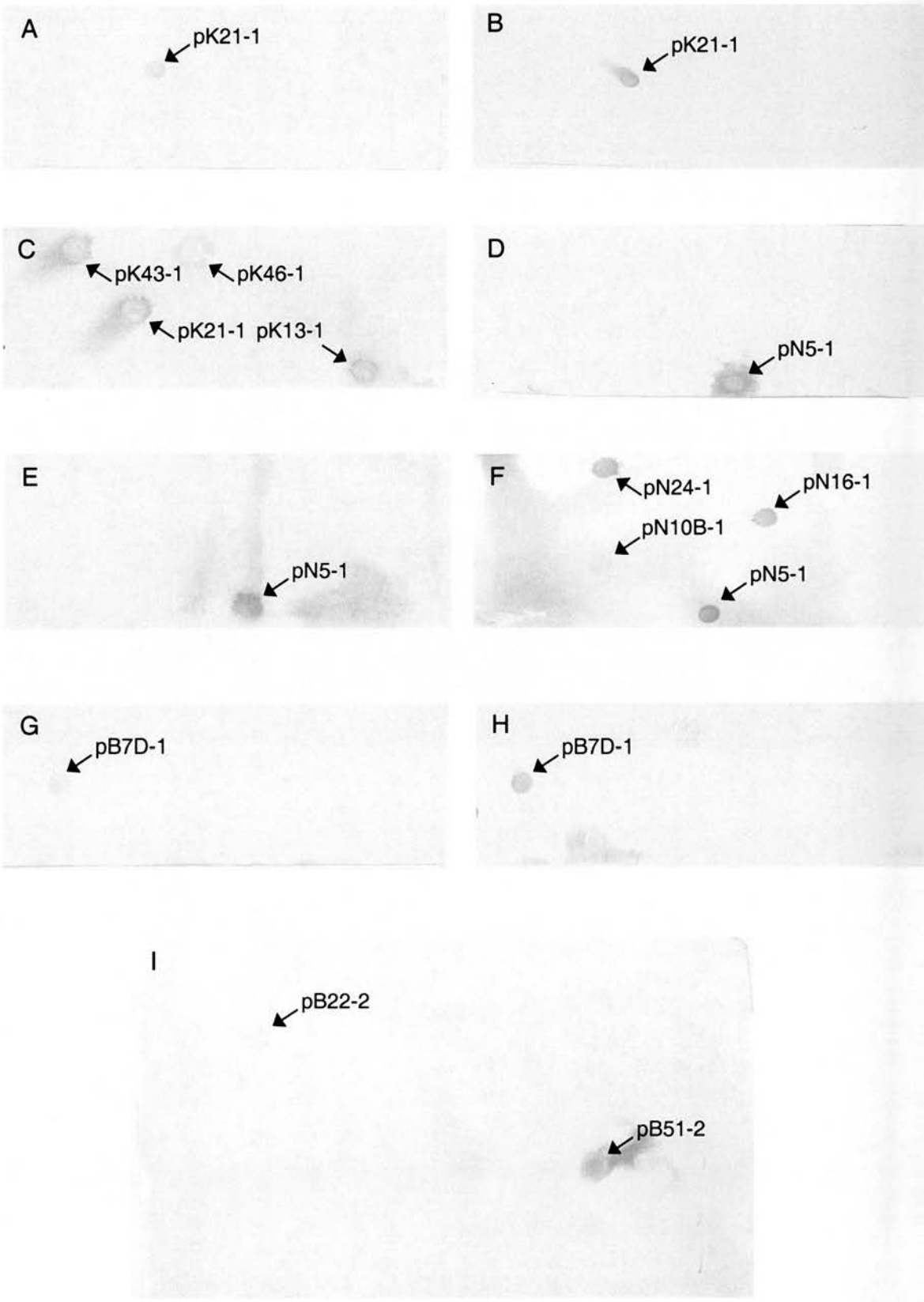
A
pK21-1
B
pK21-1
C
pK43-1
pK46-1
pK21-1
pK13-1
D
pN5-1
E
pN5-1
F
pN24-1
pN16-1
pN10B-1
pN5-1
G
pB7D-1
H
pB7D-1
I
pB22-2
pB51-2

Figure 4.6 Hybridisation examples of overlapping fragments. Blots A to H are of plasmid DNAs spotted onto nylon membranes and screened with DIG labelled probes. A, B and C are duplicate blots of a selection of *Kpn* I clones screened with DIG-labelled B51-2 (blot A), N5-1 (blot B) and B7D-1 (blot C), all three probes hybridised with pK21-1. Blots D, E and F are duplicate blots of a selection of a selection of *Not* I clones screened with DIG-labelled B51-2 (blot D) and K21-1 (blot E) and B7D-1 (blot F), all three probes hybridised with pN5-1. G and H are duplicate blots of a selection of *Bam* HI clones screened with DIG-labelled N5-1 (blot G) and K21-1 (blot H), both probes hybridised with pB7D-1. Blot I shows the immobilised transformed colonies B1-2 to B81-2, screened with DIG-labelled N5-1, which hybridised with the duplicates: pB51-2 and pB22-2.

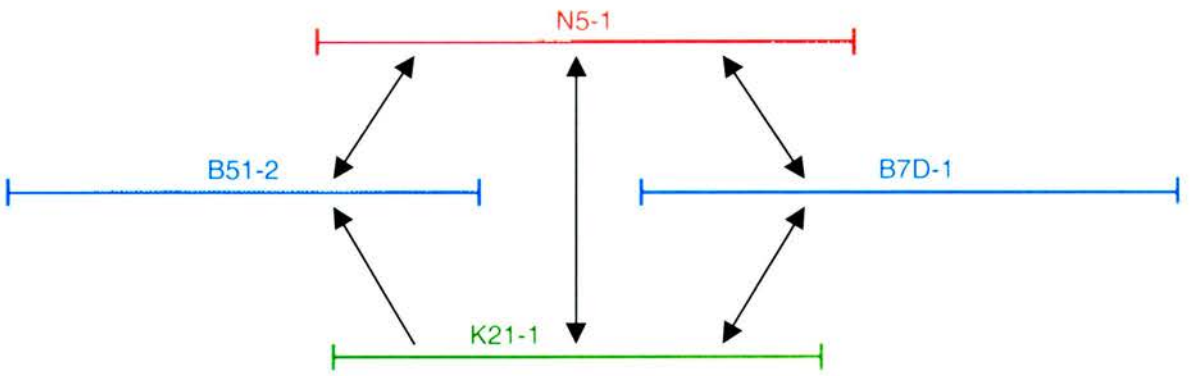

Figure 4.7 Schematic representation (not drawn to scale) of the initial alignment of N5-1, B7D-1, B51-2 and K21-1 based upon dot blot and colony screening hybridisation data. The double black arrows (↕) represent hybridisation analysis that was positive both ways. The single black arrow (↑) indicates DIG-labelled K21-1 hybridised to B51-2 but DIG-labelled B51-2 was not tested against K21-1.

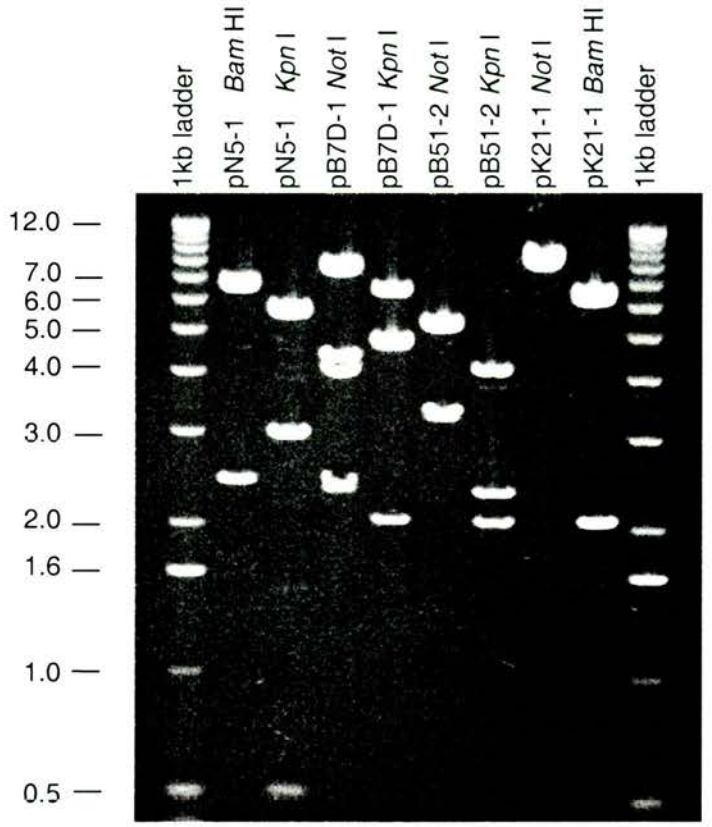

Figure 4.8 pN5-1, pB7D-1, pB51-2 and pK21-1 singularly digested with *Bam* HI, *Not* I or *Kpn* I and electrophoresed on a 0.6% (w/v) agarose. The fragment sizes were estimated by comparison to known standards present in the 1kb ladder (Gibco BRL). In order to estimate the size of the larger fragments, the gel was electrophoresed further to resolve the high molecular weight fragments (gel not shown).

subtracted from the 7.0kb band, the remaining N5-1 fragment was estimated to be approximately 4.05kb. N5-1 hybridises with two *Bam* HI fragments identified as B51-2 and B7D-1; therefore N5-1 must overlap with one *Bam* HI fragment by 4.05kb and with the other *Bam* HI fragment by 2.55kb. It then it follows that single digestions of pB51-2 and pB7D-1 with *Not* I must each produce a fragment corresponding in size to 4.05kb or 2.55kb. *Not* I digestion of pB51-2 produces two fragments of approximately 3.25kb and a 5.5kb. When the size of the vector is subtracted from the 5.5kb band it corresponds to the 2.55kb overlap with N5-1, indicating that the overlap between N5-1 and B51-2 is 2.55kb (figure 4.9).

As N5-1 only possessed one *Bam* HI site it can be predicted that N5-1 will overlap B7D-1 by 4.05kb. In support digestion of pB7D-1 with *Not* I produced a number of bands of the approximate sizes: 8.0kb, 4.4kb, 4.05kb and 2.35kb. The 4.05kb pB7D-1 *Not* I band corresponds in size to the predicted overlap of N5-1 to B7D-1, confirming the alignment of restriction fragments depicted in figure 4.9.

The arrangement is supported by the alignment of a third fragment, K21-1. DIG-labelled N5-1, B51-2 and B7D-1 all hybridised with pK21-1 confirming that like N5-1, K21-1 also overlapped B51-2 and B7D-1. Digestion of pK21-1 with *Not* I produced a single band of approximately 8.8kb. Thus it can be concluded that K21-1 does not possess any *Not* I sites and therefore must be situated completely within the N5-1 fragment. Furthermore, digestion of pN5-1 with *Kpn* I produced three fragments, the 5.9kb fragment corresponds in size to K21-1, which is situated internally within N5-1. The remaining fragments 0.5kb and 0.15kb (the 3.1kb fragment minus the vector) in size must therefore represent the ends of N5-1, which flank K21-1. Digestion of pK21-1 with *Bam* HI produced two fragments, 2.1kb and 6.7kb in size. The 6.7kb fragment must contain the vector. Therefore K21-1 must overlap one *Bam* HI fragment by 2.1kb and the other *Bam* HI fragment by approximately 3.75kb. *Kpn* I digestion of pB51-2 produced three bands, one of which corresponds to the predicted 2.1kb overlap with a *Bam* HI fragment. Hence if K21-1 overlaps B51-2 by 2.1kb, K21-1 must overlap B7D-1 by 3.75kb. The size of the K21-1 and B7D-1 overlap was confirmed by digestion of pB7D-1 with *Kpn* I. Five bands were produced, of which one was approximately 6.7kb, or 3.75kb when the size of the vector was subtracted. Hence the accurate alignment of N5-1, B51-2, B7D-1 and K21-1 could be determined (figure 4.10).

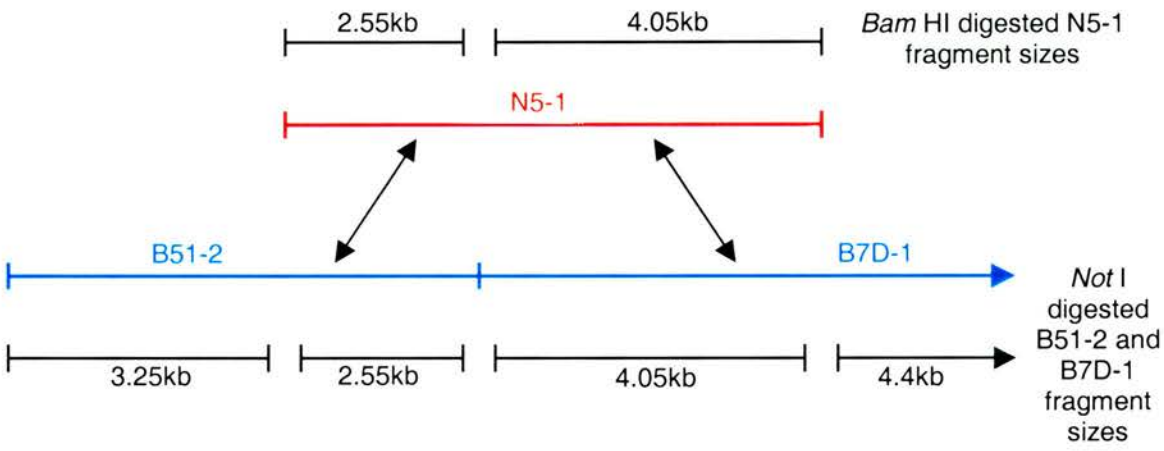

Figure 4.9 Schematic representation of the fine alignment of N5-1, B7D-1, B51-2 based upon restriction digest and hybridisation data (drawn approximately to scale). The black arrows indicate fragments which hybridise with each other and the black bars (⊢——⊣) represent the DNA fragments produced when N5-1 is digested with *Bam* HI and when B51-2 and B7D-1 are digested with *Not* I. Fragment B7D-1 extends beyond the depicted region, which is indicated by the arrow.

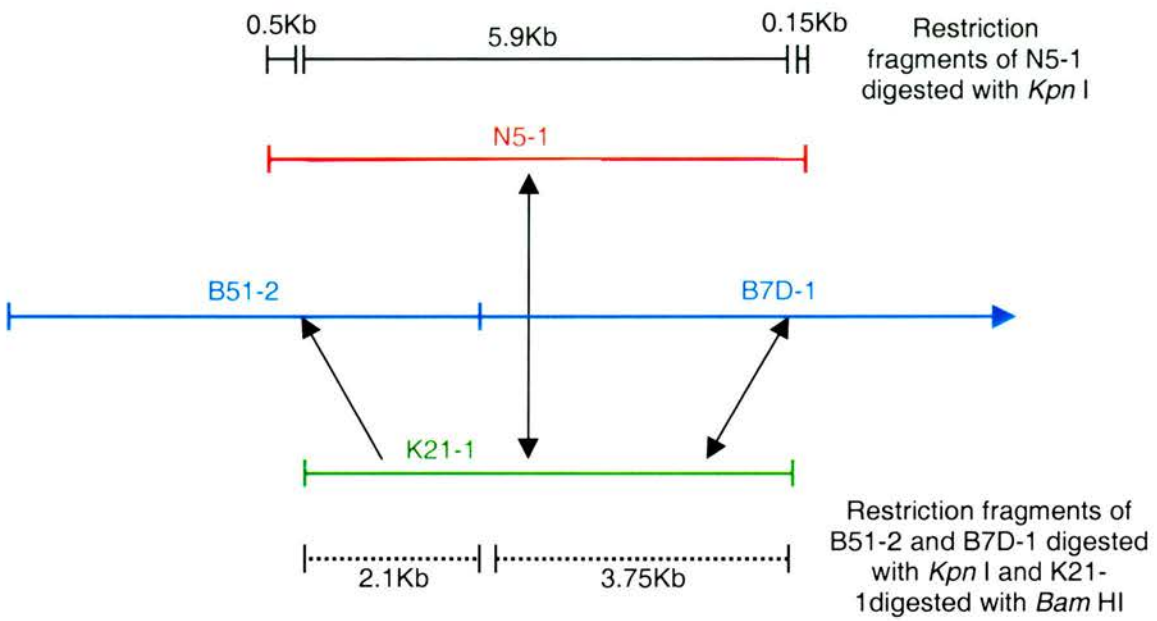

Figure 4.10 Schematic representation of the fine alignment of N5-1, B7D-1, B51-2 and K21-1 based upon hybridisation and restriction digest data (drawn approximately to scale). Fragment B7D-1 extends right, beyond the region depicted in this figure. The broken black bars (|·····|) represent DNA fragments produced when K21-1 is digested with *Bam* HI and when B51-2 and B7D-1 are digested with *Kpn* I. The solid black bars (|——|) represent the fragments produced by digestion of N5-1 with *Kpn* I, the alignment of N5-1 to the *Bam* HI fragments is depicted previously in figure 4.9.

The majority of mapping was completed successfully using DNA hybridisation and restriction profile data, however situations did arise where just these two techniques alone were inadequate to resolve the map. Sequencing was often employed to confirm the presence of a restriction site near to the end of a cloned fragment, where the overlap between 2 fragments was too small to be detected by hybridisation. Southern blotting was often used to resolve difficult areas of the map where the size of the overlap was difficult to determine from the restriction profile data alone.

Bam HI, *Not* I and *Kpn* I restriction maps were determined for the SPPV genome. However, they were incomplete and consisted of four clusters (termed clusters 1, 2, 3A and 3B), each composed of adjacent and overlapping restriction fragments. Clusters 1 and 2 are presented in sections 4.2.4 and 4.2.5 respectively. Clusters 3A and 3B are presented together in section 4.3.

4.2.4 Cluster 1

A schematic representation of the cluster 1 map is presented in figure 4.11. Cluster 1 has a total length of 79kb. A number of restriction fragments have been mapped that are designated as "missing", because no representative clone containing that fragment had been obtained. For clarity in the text that follows, each "missing" fragment has been designated a code consisting of the first letter of the restriction enzyme, M for missing and an identification number, for example; *KM1*. In addition each area that proved difficult to map and requires explanation has been designated a region number; these are annotated on the map diagram and correspond to the following explanations.

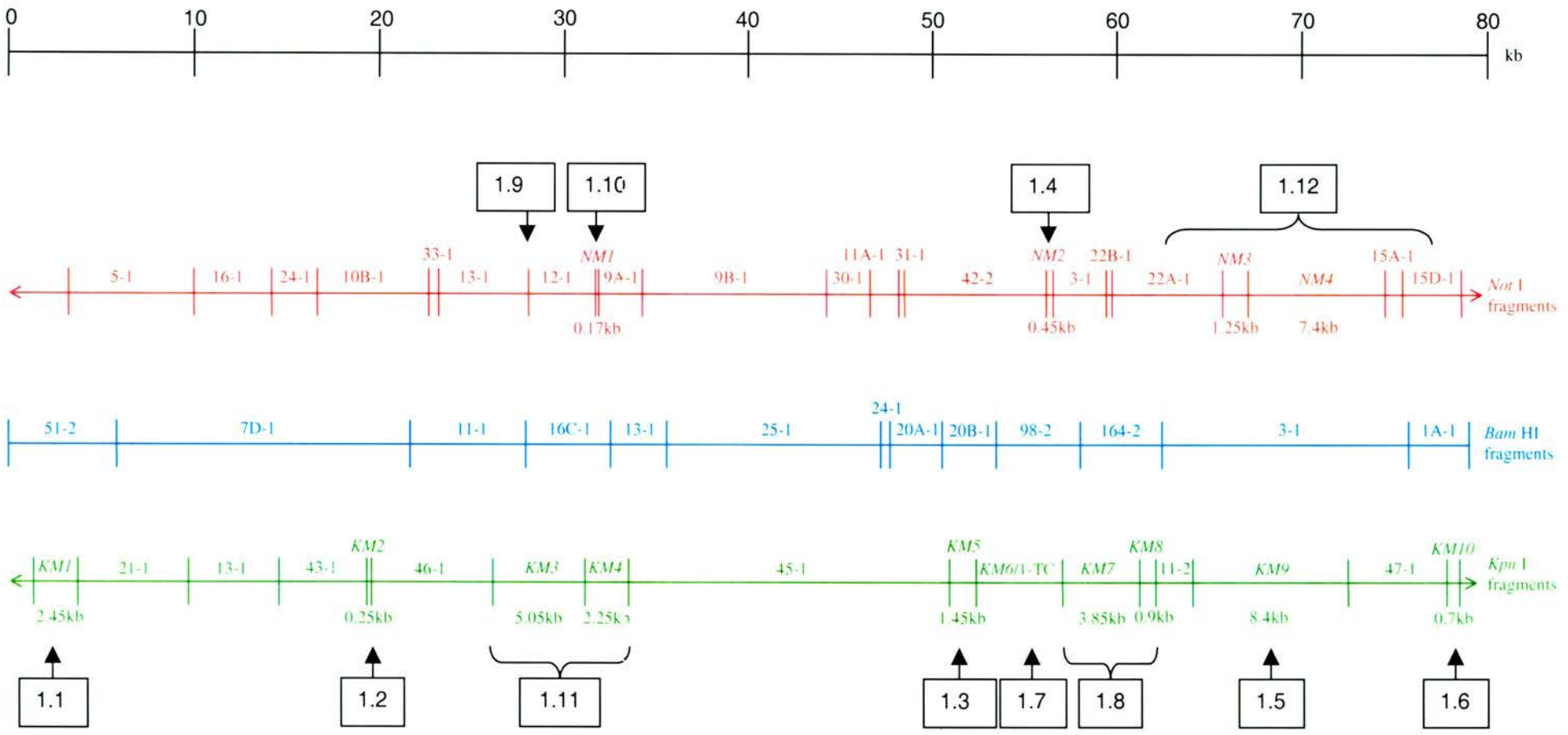

Figure 4.11 Schematic representations of cluster 1 *Not* I, *Bam* HI and *Kpn* I restriction endonuclease maps (drawn to scale). Uncloned fragments that have been mapped are designated a number, in italics, eg) *KM1* with their estimated size shown below the fragment. Regions that were mapped using techniques other than cross hybridisation and restriction endonuclease profiles or require further explanation are designated a region number eg) 1.1 , these numbers correspond to detailed explanations in the text.

Regions 1.1 to 1.6

The annotated regions 1.1 to 1.6 refers to the "missing" restriction endonuclease fragments; *KM1, 2, 5, 9, 10* and *NM2* that have all been mapped to locations that are situated completely internal within a larger cloned fragment. The size and location of the missing fragments were determined with relative ease by restriction mapping the larger clone.

For example, in region 1.1, an uncloned *Kpn* I fragment (designated *KM1*) was mapped to a location internally within B51-2 and adjacent to K21-1. This was established from restriction profile data obtained from pB51-2 digested with *Kpn* I. Three pB51-2/*Kpn* I fragments were produced of the sizes: 2.45kb, 2.1kb and 4.15kb. Only the 4.15kb DNA fragment is the only one large enough to accommodate the vector. Hence, the size of the vector was subtracted from 4.15kb leaving approximately 1.2kb of B51-2 DNA, which extended from the left end of B51-2 (as depicted in figure 4.12) to the first internal *Kpn* I site. As previously explained (section 4.2.3.4), the 2.1kb *Bam* HI fragment overlapped the left end of K21-1, the corresponding 2.1kb fragment being produced by *Kpn* I cleaving pB51-2 at the internal *Kpn* I site and the vector *Kpn* I site. Therefore the terminal *Kpn* I fragments of B51-2 corresponded to the 1.2kb and 2.1kb DNA fragments. It then follows that the 2.45kb DNA band must correspond to fragment *KM1*, which is located internally within B51-2.

The location of the *Kpn* I sites in region 1.3 was determined in a similar manner, however it required the analysis of the two overlapping fragments: B20B-1 and N42-2 (figure 4.13 for a schematic representation). Digestion of pB20B-1 with *Kpn* I produced DNA bands: 3.5kb, 1.45kb and 1.0kb. The 3.5kb band comprised of the vector and a 0.55kb terminal *Kpn* I fragment which corresponded in size to a *Bam* HI digest product of pK45-1; this suggests that the right-end of K45-1 overlaps the left-hand end of B20B-1 by 0.55kb. The order of the remaining pB20B-1 *Kpn* I fragments and the size of the *Kpn* I fragment (*KM5*) located internally within B20B-1 could not be determined from pB20B-1 restriction data alone. As N42-2 spans B20B-1, a *Kpn* I fragment situated internally within B20B-1 must also be situated internally within N42-2. Consequently singular digestions of pN42-2 and pB20B-1 with *Kpn* I produced a common fragment 1.45kb in size, identifying it as the uncloned *Kpn* I fragment, *KM5,* located internally within B20B-1 and N42-2. It then follows that the remaining 1.0kb fragment from the *Kpn* I digestion of B20B-1 must represent the size of the right terminal *Kpn* I fragment.

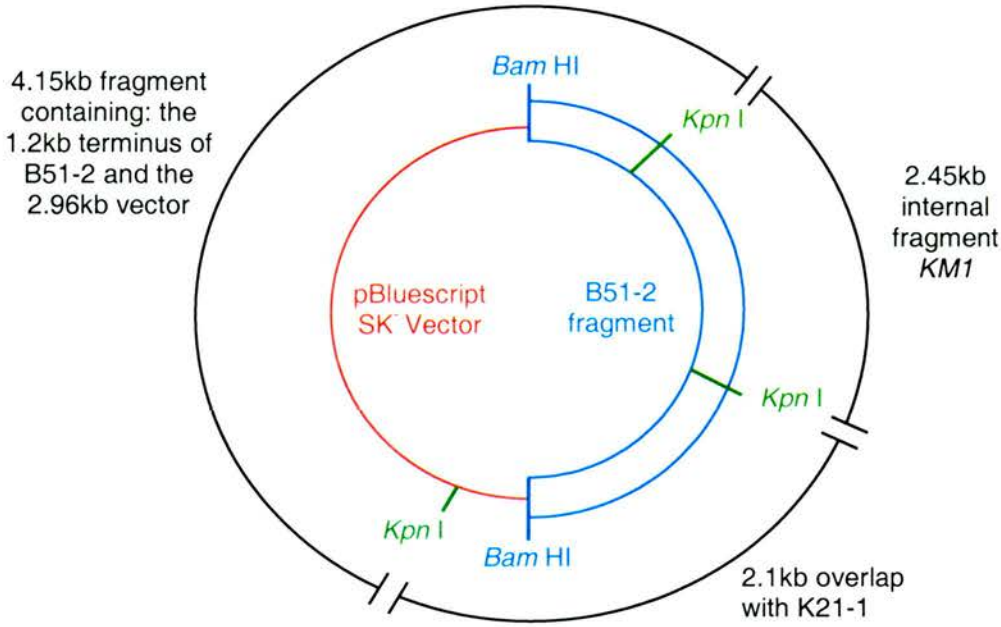

Figure 4.12 *Kpn* I and *Bam* HI restriction endonuclease map of pB51-2 (not drawn to scale) constructed to determine the size of *KM1* (region 1.1). The outer bars represent the fragments produced upon digestion with *Kpn* I.

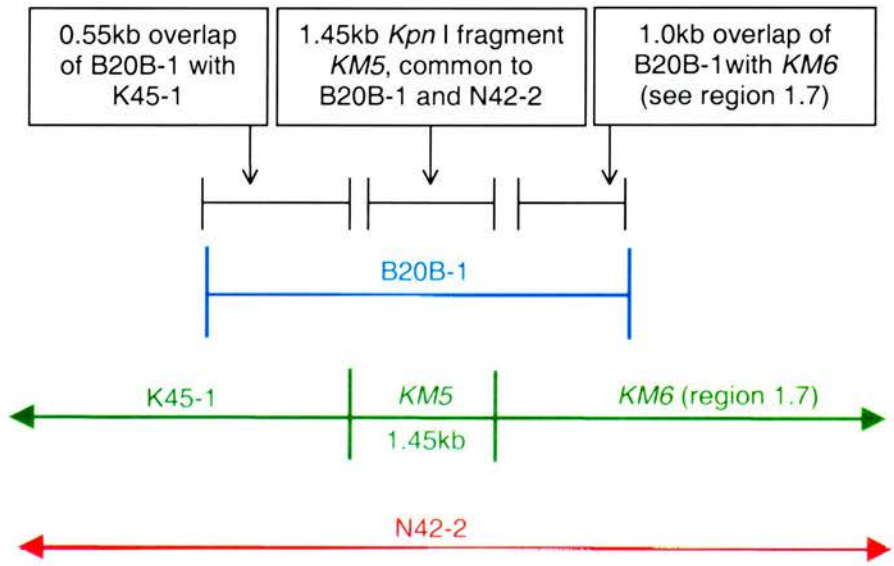

Figure 4.13 Schematic representation of region 1.3, demonstrating how the missing 1.45kb *Kpn* I fragment (*KM5*) was mapped using restriction digest data from the overlapping fragments: N42-2 and B20B-1. The horizontal black bars (├──┤) represent the fragments produced when the overlapping clones were digested with *Kpn* I, the details in the box above each bar gives the fragment size and overlap information.

Region 1.7

Region 1.7 refers to an uncloned *Kpn* I fragment (*KM6*) predicted to overlap the two adjacent *Bam* HI fragments: B20B-1 and B98-2. The approximate size of *KM6* was determined by first establishing the *Kpn* I maps of B20B-1 and B98-2 and then determining the distance between the right *Kpn* I site in B20B-1 and the left *Kpn* I site within B98-2 as depicted in figure 4.14. As previously established (region 1.3) the right terminal *Kpn* I fragment of B20B-1 was 1.0kb. The position of the single *Kpn* I site located within B98-2 was determined by *Kpn* I restriction digestion of pB98-2. The two fragments produced were of the approximate sizes: 3.65kb (with the vector subtracted) and 0.9kb. Therefore there were two possible locations of the single *Kpn* I site in B98-2, either 0.9kb or 3.65kb from the left end. The *Kpn* I site was confirmed to be 3.65kb from the left end of B98-2 by the absence of a third *Kpn* I site situated internally within N42-2 and the presence of an internal *Kpn* I site within N3-1. The addition of the 1.0kb right terminal *Kpn* I fragment of B20B-1 and the 3.65kb left terminal *Kpn* I fragment of B98-2 equalled 4.65Kb, the size of the uncloned *Kpn* I fragment.

The tissue culture-adapted SPPV DNA derived clone, pK1-TC, hybridised to B20B-1, B98-1, N42-2 and N3-1 indicating that K1-TC may be representative of *KM6* wild type fragment. The size of K1-TC was approximately 4.65kb, which correlated with the calculated size of *KM6*. In addition, the *Bam* HI and *Not* I restriction profiles of pK1-TC matched those predicted for *KM6*. Taken together these indicate that fragment K1-TC may be highly conserved in both the tissue culture-adapted strain and the wild-type isolate 1296/99. However, a divergence in the DNA sequence between the wild type and tissue culture-adapted virus within this region may exist.

Region 1.8

Region 1.8 refers to the order of *Kpn* I sites within the two adjacent *Bam* HI fragments: B98-1 and B164-2. Like region 1.7, the *Kpn* I map was deduced by examining *Kpn* I restriction profiles of the two overlapping *Bam* HI clones.

Firstly an "missing" *Kpn* I fragment, (*KM8*) 0.9kb in size, was shown to lie adjacent to K11-2 and internally within B164-2 by mapping the *Kpn* I sites in pB164-2 using the method outlined in regions 1.1 to 1.6 (figure 4.14). It was deduced from the B164-2 *Kpn* I restriction map that the 2.95kb of DNA to the left of *KM8* would overlap the right terminus of a "missing" *Kpn* I fragment (*KM7*). As B98-2 was shown to possess only one *Kpn* I site (region 1.7) and that the

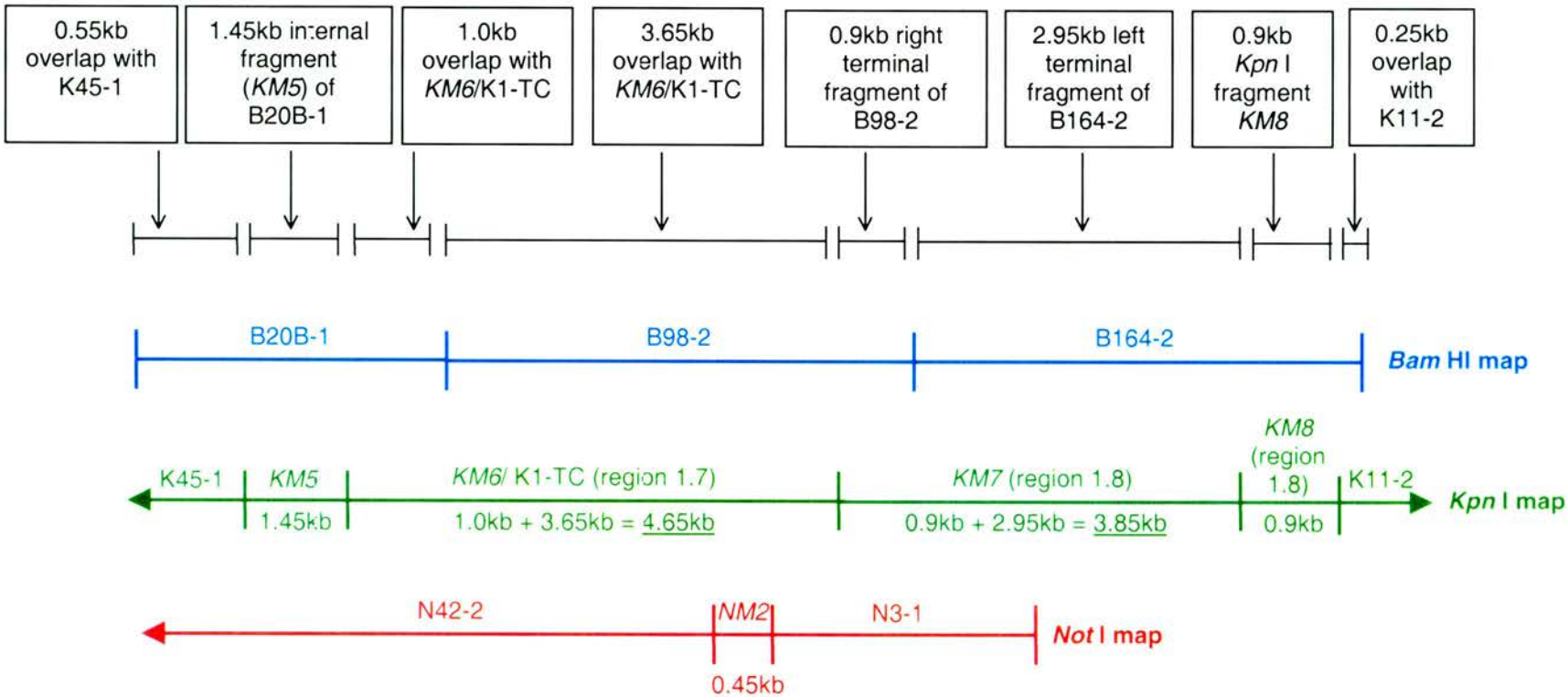

Figure 4.14 Schematic representation demonstrating how the uncloned *Kpn* I fragments: *KM6*, *KM7* and *KM8* (regions 1.7 and 1.8) were mapped using restriction fragment data from the overlapping fragments: N42-2, N3-1, B20B-1, B98-2 and B164-2. The horizontal black bars (|——|) represent the fragments produced when the *Bam* HI clones were digested with *Kpn* I and the details in the box above each bar gives the fragment sizes and overlap informat on.

3.65kb region to the left of the B98-2 *Kpn* I site overlapped *KM6*, then the 0.9kb region to the right of the *Kpn* I site must overlap the left end of *KM7*. Therefore the size of the right terminal *Kpn* I fragment of B98-2 (0.9kb) and the left terminal *Kpn* I fragment of B164-2 (2.95kb), when combined, equals 3.85kb which represents the size of *KM7*.

Region 1.9

Fragments N12-1 and N13-1 were suspected to be adjacent by the alignment of sequence obtained from the right end of N13-1 and from the left end of N12-1 to the MOCV genome. The sequences were made contiguous at the *Not* I site and then compared with those deposited in the EMBL database using the FastA search algorithm (section 2.4.8.1). The contiguous SPPV sequence aligned with the MOCV subtype 1 complete genome (EMBL accession number U60315) over its full 308nt length and demonstrated a 68.8% homology with MOCV (figure 4.15).

N12-1 and N13-1 did not hybridise to any common *Bam* HI or *Kpn* I fragments, and therefore no fragments that overlap both N12-1 and N13-1 were identified in this manner. However N12-1 hybridised with pB16C and N13-1 hybridised with pB11-1. N13-1 was shown to possess one *Bam* HI site situated near to the right end of N13-1 by restriction digestion and DNA sequencing (figure 4.15). Based on the strength of the hybridisation signal and restriction analysis, B11-1 was predicted to overlap the majority of N13-1. In contrast N12-1, which hybridised with B16C-1, lacked a *Bam* HI site. Therefore N12-1 must be situated internally within B16C-1. B16C-1 hybridised with pN12-1 and pN9A-1. N9A-1 contained one *Bam* HI site and must therefore overlap one end of B16C-1. Since N12-1 and N13-1 are predicted to be adjacent, N13-1 must overlap the opposite terminus of B16C-1 to N9A-1, however no hybridisation between B16C-1 and N13-1 was detected to confirm this. Nevertheless the presence of a *Bam* HI site just 29bp in from the right terminus of N13-1 suggested an overlap did exist between B16C-1 and N13-1, but that it was too small to produce a visible signal with hybridisation. The predicted overlap between N13-1 and B16C-1 and the adjacent position of N12-1 and N13-1 was confirmed by the alignment of the end DNA sequences of N12-1, N13-1 with B16C-1 (figure 4.16).

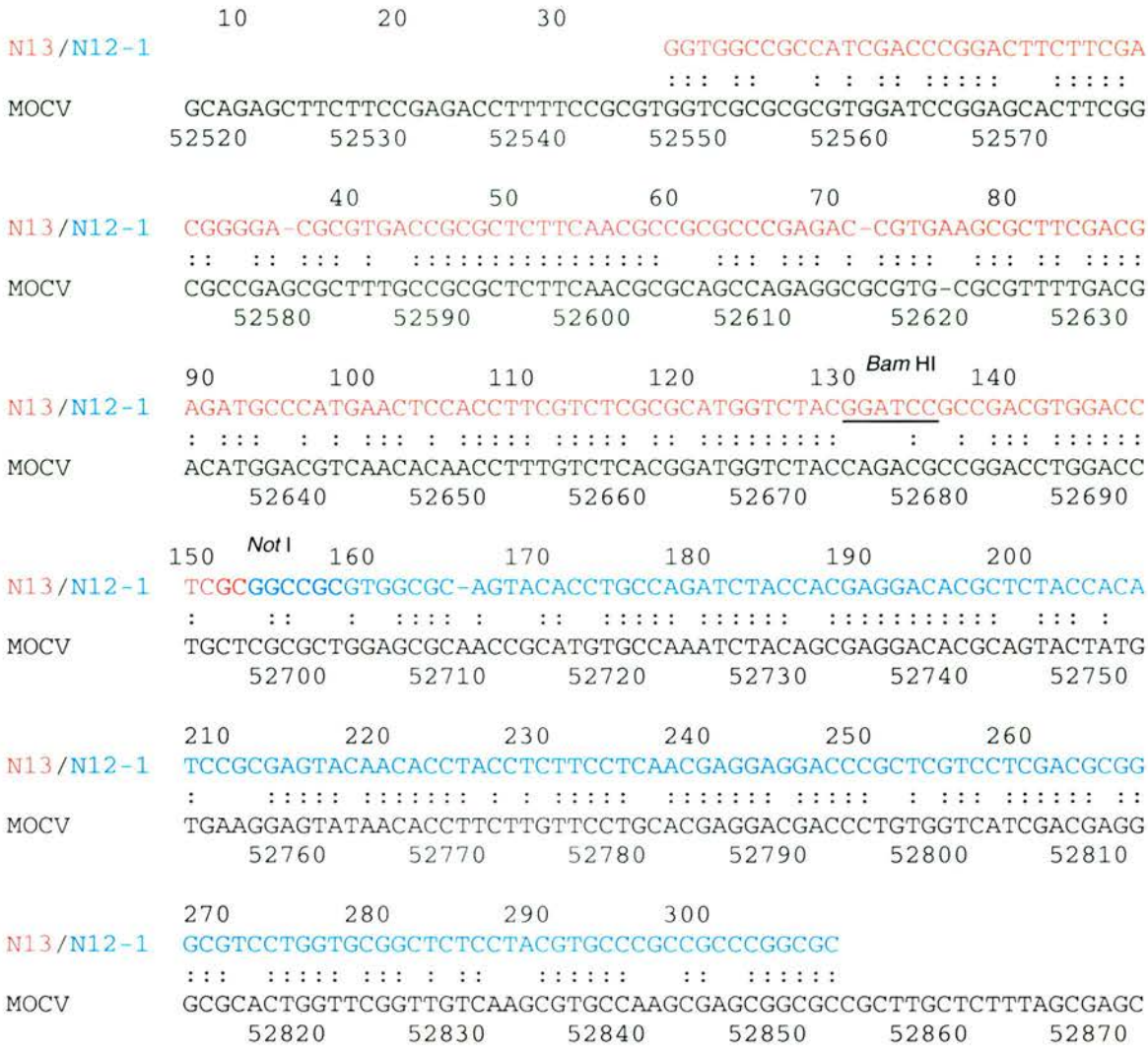

Figure 4.15 FastA alignment of N13-1 (red font) and N12-1 (blue font) nucleotide sequence, made contiguous at the *Not* I site (highlighted in grey), to MOCV subtype 1 complete genome (EMBL accession number U60315). The sequence exhibited 68.8% identity to MOCV subtype 1 over 308 nucleotides.

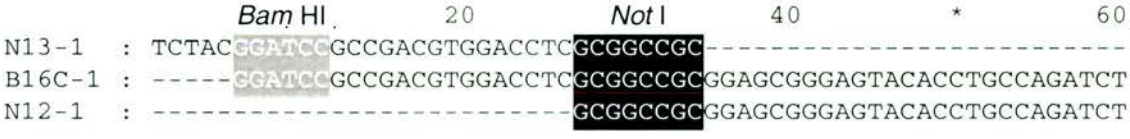

Figure 4.16 Sequence alignment of the clones N13-1, N12-1 and B16C-1. The adjacent clones N13-1 and N12-1 are both overlapped by B16C-1. The common *Not* I and *Bam* HI sites are highlighted in black and grey respectively.

Region 1.10

Once the alignment of B16C-1 to N12-1 and N13-1 had been established, the *Not* I map to the immediate right of N12-1 could be determined. As previously mentioned, N9A-1 was predicted to overlap the right terminus of B16C-1 (region 1.9). The size of this overlap was calculated to be 0.85kb by the comparison of pN9A-1 digested with *Bam* HI and pB16C-1 digested with *Not* I to identify the common sized fragment. This arrangement does not account for a 0.17kb fragment produced by pB16C-1 digested with *Not* I. No *Not* I clone of that size had been obtained during the library screening, so it was assumed that this represents an uncloned fragment (*NM1*). The location of *NM1* was deduced by a process of elimination using a *Not* I restriction map constructed for pB16C-1 (figure 4.17). Briefly, N13-1 overlaps the left terminus of B16C-1, N12-1 is situated immediately to the right of N13-1 and N9A-1 overlaps the right terminus of B16C-1, so the only remaining place *NM1* could be situated was between N12-1 and N9A-1.

Region 1.11

Once the order and alignment of the *Not* I and *Bam* HI fragments had been established for regions 1.9 and 1.10, the *Kpn* I map (region 1.11) could be determined.

B11-1, B16C-1 and B13-1 each possessed one *Kpn I* site, indicating that there were two "missing" *Kpn* I fragments (*KM3* and *KM4*) overlapping B16C-1. Using restriction profile analysis, the location of the *Kpn* I site in B11-1 was easily determined by establishing that the overlap with K46-1 was 4.6kb. Likewise, the location of the *Kpn* I site in B13-1 was determined by establishing that the overlap with K45-1 was 2.35kb. However, the position of the *Kpn* I site in B16C-1 was more difficult to map and required the use of the previously constructed *Not* I map of pB16C-1 (figure 4.17) to establish the orientation of the B16C-1 fragment within the vector. Digestion of pB16C-1 with *Kpn* I produced two fragments, 1.4kb and 6.3kb in size. As the 6.3kb fragment must contain the vector, the *Kpn* I site must be located approximately 1.4kb from the vector *Kpn* I site, which corresponds to 1.4kb in from right terminus of B16C-1.

The sizes of the uncloned *Kpn* I fragments, *KM3* and *KM4*, were estimated by calculating the distance between the *Kpn* I sites mapped within B11-1, N16C-1 and B13-1 (figure 4.18). The sizes of the *KM3* and *KM4* were calculated to be 5.05kb and 2.25kb respectively.

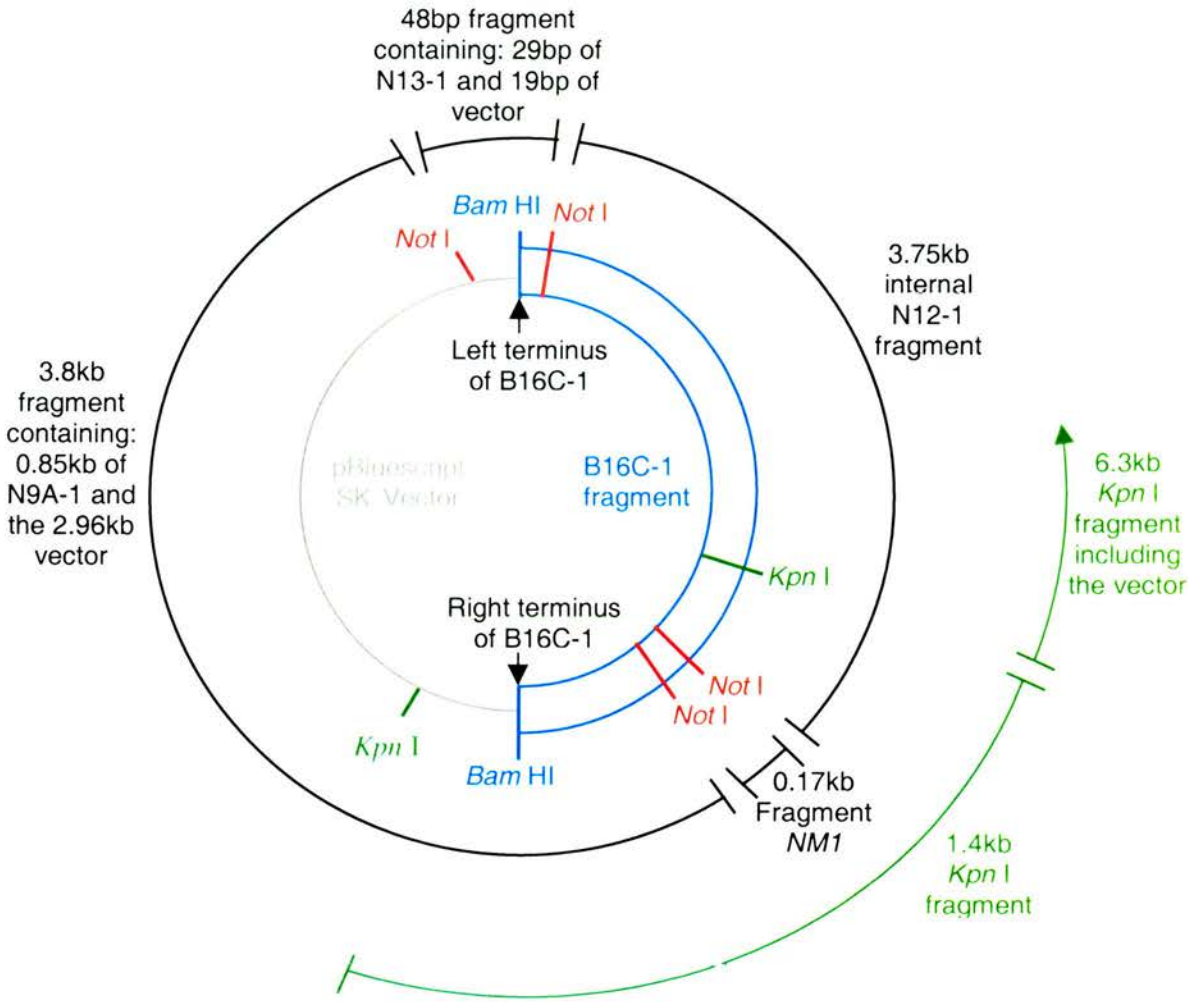

Figure 4.17 *Kpn* I and *Not* I restriction endonuclease map of pB16C-1 (not drawn to scale) constructed in order to deduce the position of the *Not* I and *Kpn* I sites in regions 1.10 and 1.11. The outer black bars represent the fragments produced upon digestion with *Not* I and the outer green bar represents the *Kpn* I fragment.

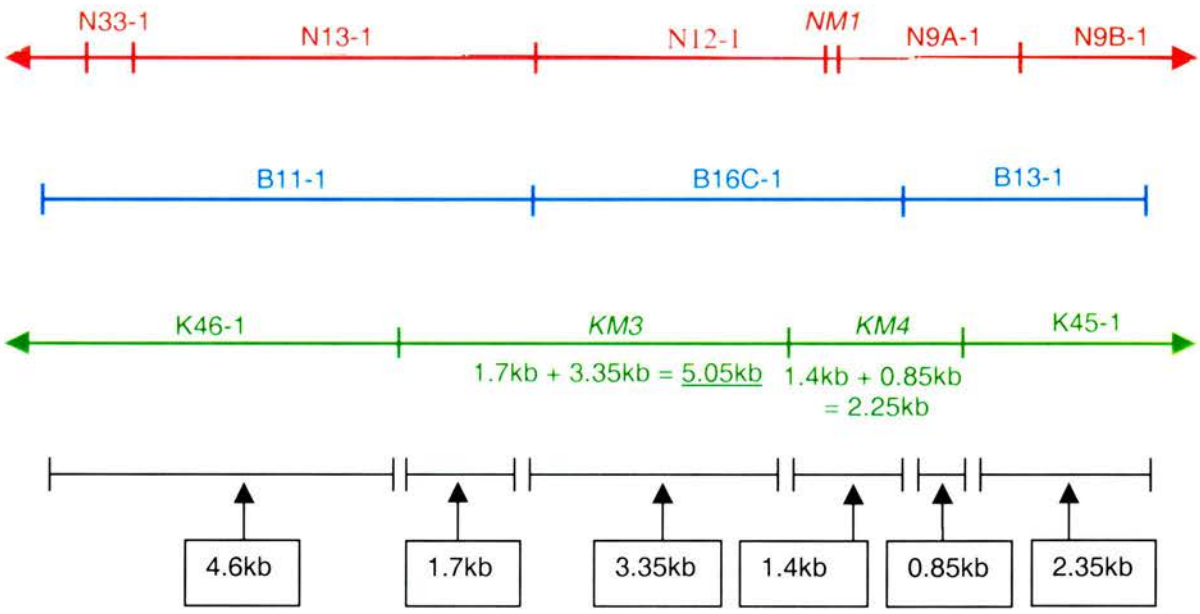

Figure 4.18 Schematic representation region 1.11 (drawn approximately to scale), constructed from data obtained from the restriction profiles of pB11-1, pB13-1 and pB16C-1 digested singly with *Kpn* I. The solid black bars (├──┤) represent the fragments produced when the *Bam* HI fragments are digested with *Kpn* I and the vector is subtracted from the fragment sizes.

Region 1.12

The order of the *Not* I and *Kpn* I fragments within region 1.12 was determined by hybridisation between fragments, restriction profile analysis and Southern blotting. Region 1.12 is represented schematically in figure 4.19 and is described in the text that follows.

B3-1 hybridised with the *Kpn* I clones pK11-2 and pK47-1. By comparing the restriction profiles of pK47-1 and pK11-2 digested with *Bam* HI to that of pB3-1 digested with *Kpn* I, it was deduced that K47-1 and K11-2 overlapped the ends of B3-1 by 3.2kb and 1.8kb respectively. Using the methods explained in regions 1.1 to 1.6, a "missing" *Kpn* I fragment (*KM9*) internal to B3-1 was shown to separate K47-1 and K11-2 by approximately 8.4kb.

B3-1 also hybridised with the *Not* I clones: pN22A-1, pN15D-1 and pN15A-1. N22A-1 and N15D-1 both possessed a *Bam* HI site indicating that they overlapped the ends of B3-1. pN22A-1 when digested with *Bam* HI produced two fragments approximately 3.2kb and 5.7kb in size, one of which contains the vector. The 3.2kb fragment corresponds in size to a fragment obtained from pB3-1 digested with *Not* I, suggesting that N22A-1 overlaps B3-1 by 3.2kb. The predicted overlap was confirmed by probing a Southern blot of pB3-1 that was digested with *Not* I with DIG-labelled N22A-1. As expected N22A-1 hybridised with the 3.2kb band (figure 4.20), confirming the overlap between B3-1 and N22A-1 is 3.2kb.

pB3-1 when digested with *Not* I produced 5 fragments; 7.4kb, 3.4kb, 3.2kb, 1.25kb and 1.05kb in size. As previously established, the 3.2kb overlap with N22A-1 constitutes the left terminal *Not* I fragment of B3-1. As the 3.2kb-left terminal fragment did not contain the vector, it was assumed that the vector would be attached to the *Not* I fragment that is situated at the right end of pB3-1, which constitutes the overlap with N15D-1. Only the 7.4kb and 3.4kb pB3-1 *Not* I fragments were large enough to include the vector, however the 7.4kb fragment was larger than the combined size of N15D-1 and the vector. Therefore N15D-1 must overlap B3-1 by 0.45kb (3.4kb minus the size of the vector). In support, the predicted 0.45kb overlap approximately corresponds in size with a 0.47kb band produced by the digestion of pN15D-1 with *Bam* HI.

The remaining fragments from pB3-1 digestion with *Not* I were 1.25kb, 1.05kb and 7.4kb, as none of these overlap the ends of B3-1 they must represent *Not* I fragments that are situated internally within B3-1. As K47-1 overlapped the right terminus of B3-1 by 3.2kb, DIG-labelled K47-1 was used to probe a Southern blot of pB3-1 digested with *Not* I in order to determine the order of the *Not* I fragments situated internally within B3-1. K47-1 hybridised with the 7.4kb, 3.4kb and one further fragment, which was impossible to determine if it was 1.05kb or 1.25kb in

size from the Southern blot (figure 4.20). The 3.4kb fragment (including the vector) was assumed to correspond to the 0.45kb overlap of B3-1 with N15D-1. N15A-1 has a size of approximately 1.05kb and hybridised with K47-1, but as N15A-1 does not possess a *Kpn* I site, it was predicted to be located internally within K47-1 and hence adjacent to N15D-1. In support, digestion of pK47-1 with *Not* I also produced a 1.05kb band corresponding in size to N15A-1. The final pB3-1 *Not* I band hybridised by K47-1 was 7.4kb in size, this *Not* I fragment (*NM4*) must therefore be located adjacent to N15A-1 and overlap the left terminus of K47-1. The only possible location for remaining 1.25kb *Not* I fragment (*NM3*) is between N22A-1 and *NM4* fragments.

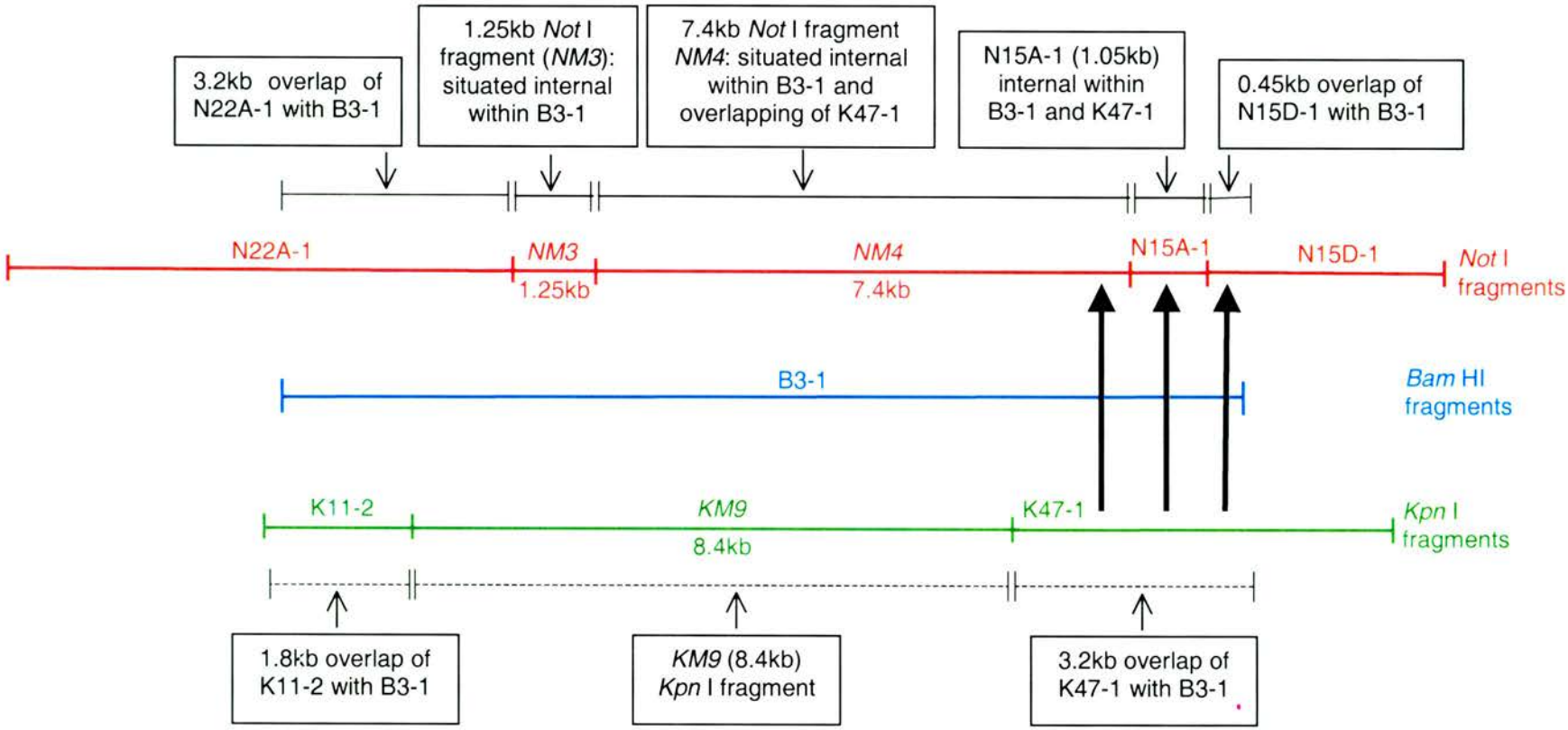

Figure 4.19 Schematic representation region 1.12, constructed from data obtained from hybridisation data and restriction profiles of pB3-1, pN22A-1, pK11-2, K47-1, N15A-1 and pN15D-1; and from Southern blot presented in figure 4.20. The broken black bars (|-----|) represent fragment produced by digestion of B3-1 with *Kpn* I or the *Kpn* I fragments digested with *Bam* HI. Likewise, the solid black bars (|——|) represent fragments produced by digestion of pB3-1 with *Not* I. The large black arrows (↑) denote hybridisation of DIG-labelled K47-1 with Southern blotted pB3-1 *Not* I fragments that correspond to N15A-1, N15D-1 and *NM4*.

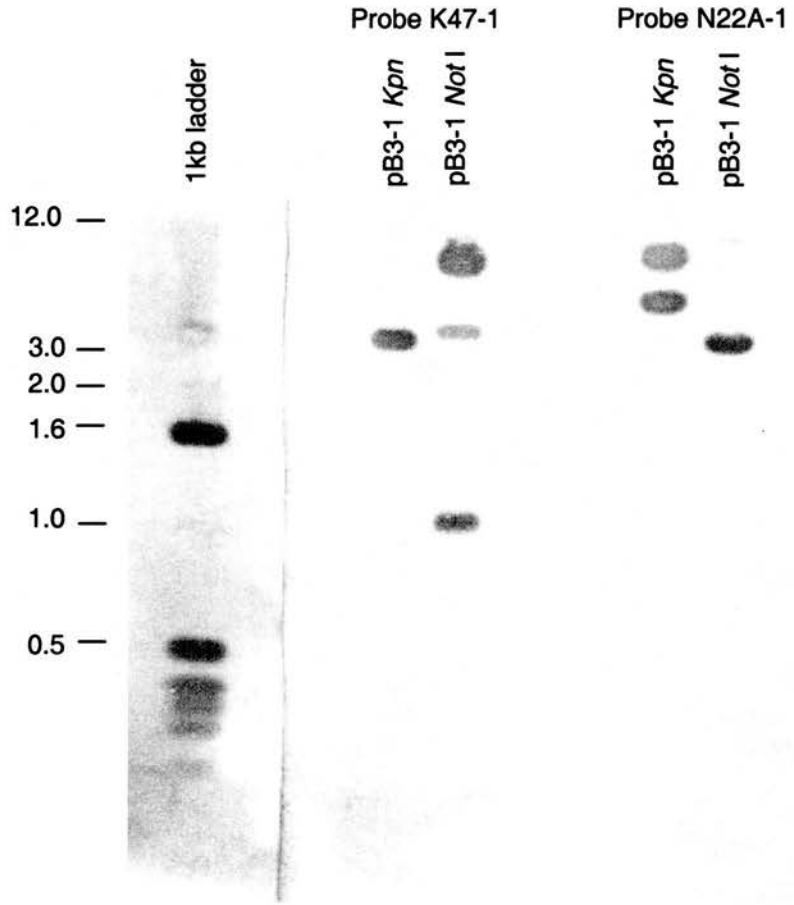

Figure 4.20 DNA fragments of pB3-1 DNA that was singly digested with *Kpn* I and *Not* I were resolved on a 0.8%(w/v) agarose gel and Southern blotted onto nylon membrane. Each digest was probed separately with DIG-labelled K47-1 and N22A-1.

4.2.5 Cluster 2

A second cluster of approximately 40kb was mapped using the techniques described in section 4.2.3. The complete map of cluster 2 is presented in figure 4.21. The regions that were difficult to determine and require further explanation are numerically annotated on figure 4.21, these numbers corresponds with the following descriptions.

Region 2.1

Region 2.1 refers to the order, arrangement and size of five *Not* I fragments that are situated internally within, or overlapping the ends of K32-1 (figure 4.22).

DIG-labelled N6-1 hybridised with pK32-1 and K4-1. As K32-1 and K4-1 possessed two or more *Not* I site they were predicted to overlap the ends of N6-1. As digestion of N6-1 with *Kpn* I and digestion of K32-1 with *Not* I both produced fragments approximately 1.45kb in size, it was predicted that N6-1 and K32-1 overlap by 1.45kb. As the 1.45kb fragment produced by digestion of pK32-1 with *Not* I did not include the vector, it was assumed that the opposite terminal *Not* I fragment of pK32-1 would. Digestion of pK32-1 with *Not* I produced five fragments of the sizes: 3.2kb, 1.45kb, 1.1kb, 0.65kb and 0.45kb, of which only the 3.2kb fragment was large enough to contain the vector. After the size of the vector was subtracted from the 3.2kb fragment, the remaining 0.25kb represented the extent of the overlap with the uncloned *Not* I fragment (*NM5*). The remaining fragments of pK32-1 digested with *Not* I are: 1.1kb, 0.65kb and 0.45kb; these represent three uncloned *Not* I fragments situated internally with K32-1 (annotated as *NM6*, *NM7* and *NM8*). Unfortunately, due to the absence of *Bam* HI or *Kpn* I fragments that partially overlap these *Not* I fragments, their order could not be determined using the methods of hybridisation and restriction profiling.

Region 2.2

Two *Kpn* I sites were identified in the DNA sequence derived from the right end of N6-1, which are situated 117nt and 146nt from the right terminus of N6-1 (figure 4.23). Based on the sequence data, it was predicted that a 33bp *Kpn* I fragment (*KM11*) is situated between K32-1 and K4-1 (figure 4.22).

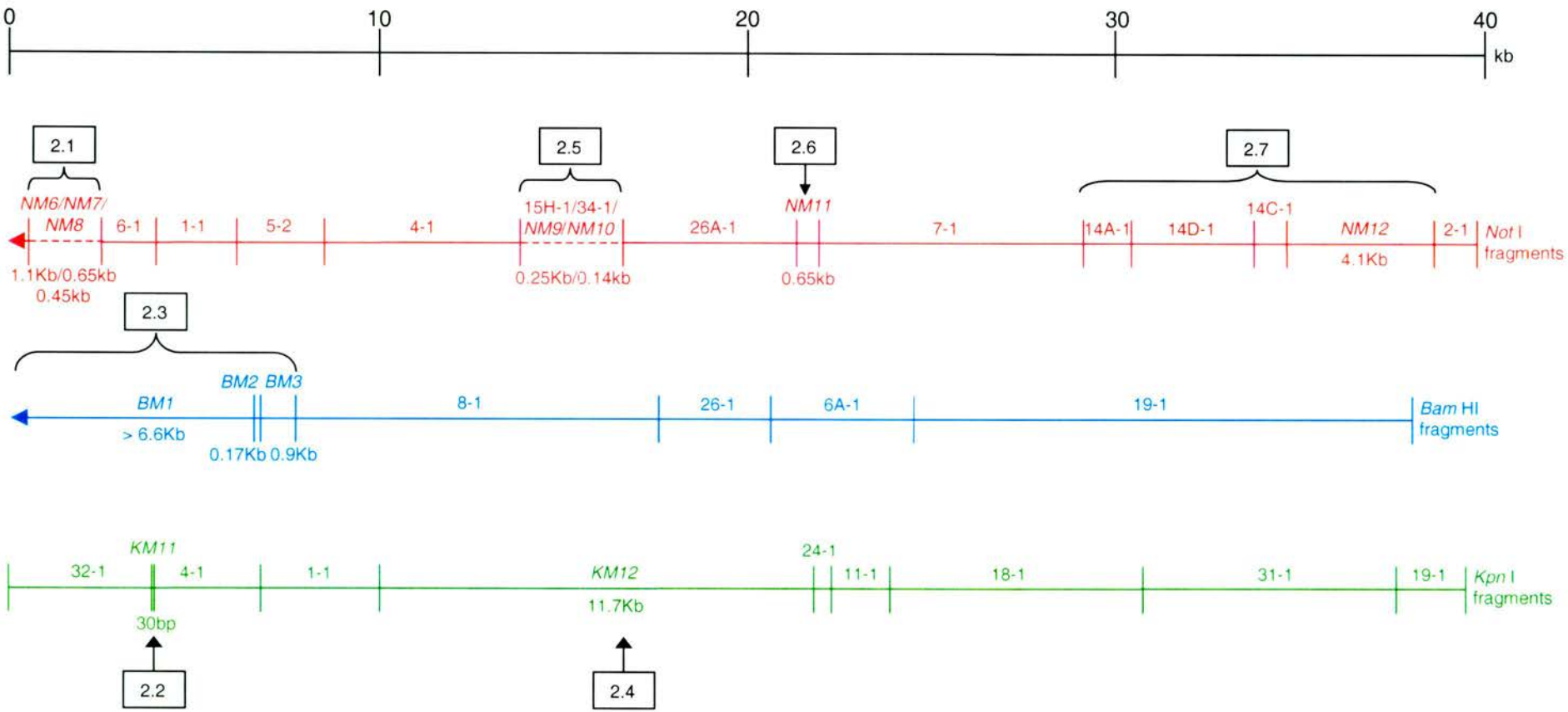

Figure 4.21 Schematic representations of cluster 2 *Not* I, *Bam* HI and *Kpn* I restriction endonuclease maps. Uncloned fragments that were mapped are designated numbers, in italics, eg) *KM11,* with their estimated sizes shown below each fragment. Regions that were mapped using techniques other than cross hybridisation and restriction endonuclease profiles or require further explanation are designated a region number eg) 2.1 , these numbers correspond to detailed explanations in the text.

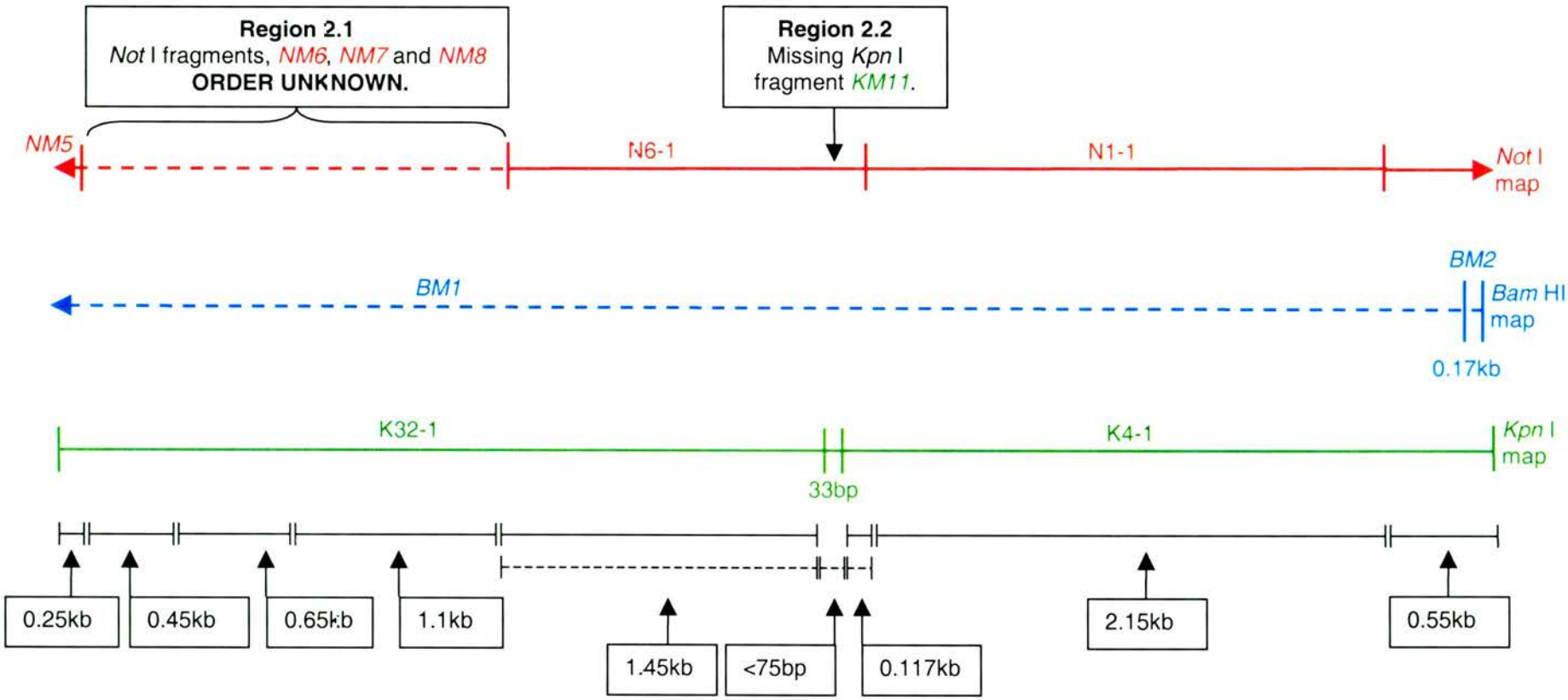

Figure 4.22 Schematic representation of regions 2.1 and 2.2. The solid black bars (├──────┤) correspond to fragments produced when K4-1 and K32-1 are digested with *Not* I. Likewise, the broken black bars (├- - - - - - -┤) correspond to fragments produced when N6-1 is digested with *Kpn* I. The approximate size of each fragment is indicated in the box below the each individual bar.

Figure 4.23 The nucleotide sequence derived from the right end of N6-1 (presented in the 5' to 3' direction of the genome). Two *Kpn* I sites (highlighted and underlined) are present, starting at nucleotide positions 117 and 146.

Region 2.3

The order and size of the "missing" *Bam* HI fragments (*BM1*, *BM2* and *BM3*) in region 2.3 were established by analysing the *Bam* HI restriction profiles of the cloned *Not* I and *Kpn* I fragments which span this region. Region 2.3 is illustrated schematically in figure 4.24 and is explained in more detail in the text that follows.

Firstly, the sizes of the overlap of B8-1 with N5-2 and K1-1 were determined to be 2.4kb and 0.85kb respectively, by the comparison of the *Kpn* I, *Bam* HI and *Not* I restriction profiles of pB8-1, pN5-1 and pK1-1 to identify fragments that are common in size. Digestion of pN5-2 with *Bam* HI produced fragments of 3.35kb, 0.95kb, 0.85kb and 0.17kb in size. As previously established, the 0.85kb fragment corresponds to the right end of N5-2 and the overlap with B8-1. The 3.35kb fragment must contain the vector and a 0.4kb left terminal *Bam* HI fragment of N5-2. The remaining pN5-2 *Bam* HI fragments, 0.17kb and 0.95kb must represent two "missing" *Bam* HI fragments (*BM2* and *BM3)* which are situated internally within N5-2.

The order of the *BM2* and *BM3* fragments was determined by examining the restriction profile of pK1-1. When digested with *Bam* HI, pK1-1 produced two fragments, 3.8kb and 2.4kb in size. As previously established the 2.4kb band represents the overlap with B8-1. Therefore the 3.8kb band must include the vector and overlap with *BM3.* The arrangement was confirmed by examining the *Bam* HI restriction profile of K4-1. When digested with *Bam* HI, pK4-1 produced three fragments of the sizes 2.97kb, 2.7kb and 0.17kb. The 0.17kb fragment corresponded to the predicted size of *BM2*, which is situated within N5-2 and K4-1 (see above). The location of the *BM2* fragment within K4-1, rather than K1-1, confirmed that its location was to the left of the *BM3* fragment. As N1-1 and N6-1 did not possess any *Bam* HI sites, the 2.7kb pK4-1 *Bam* HI fragment must overlap these *Not* I fragments. Furthermore, the 2.97kb fragment produced by *Bam* HI digestion of pK4-1 was the only fragment large enough to include the vector. When the size of the vector was subtracted from 2.97kb the 80bp remaining must represent the overlap of K4-1 with *BM3.*

As there are no *Bam* HI sites present in any of the overlapping *Not* I and *Kpn* I fragments situated to the left of *BM2*, it can be concluded that a large *Bam* HI fragment (*BM1*) greater than 6.6kb extends left from *BM2* to beyond the mapped region. As a consequence, the size of *BM1* could not be determined.

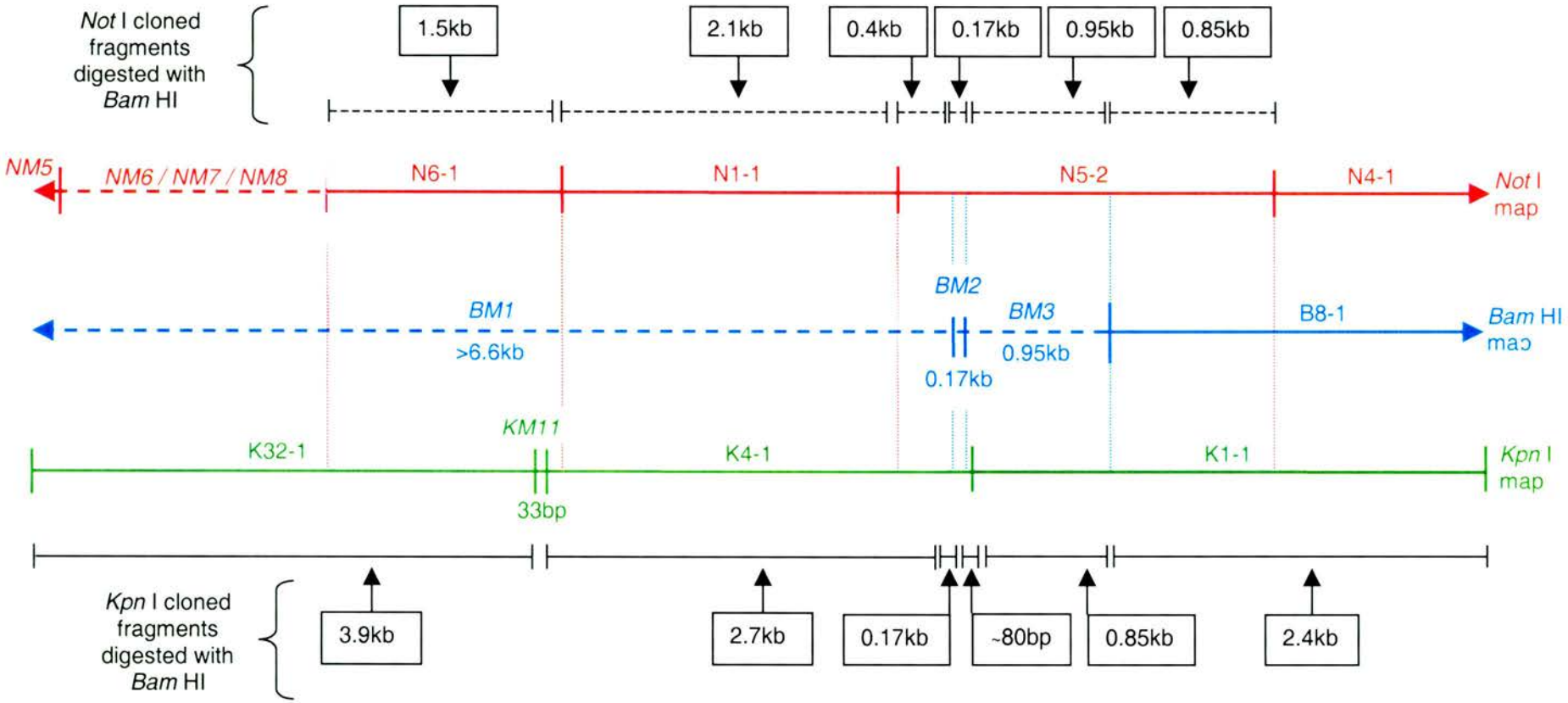

Figure 4.24 Schematic representation of region 2.3, illustrating the order and size of the uncloned *Bam* HI fragments, *BM1*, *BM2* and *BM3*. The vertical broken lines denote restriction sites: *Bam* HI (in blue) and *Not* I (in red). The solid horizontal black bars (├──┤) correspond to fragments produced when pK1-1, pK4-1 and pK32-1 are digested with *Bam* HI, the approximate size of each fragment is indicated in the box below each individual bar. Likewise, the broken horizontal black bars (├-----┤) correspond to fragments produced when pN1-1, pN4-1, pN5-2 and pN6-1 are digested with *Bam* HI, the approximate size of each fragment is indicated in the box above each individual bar.

Region 2.4

Region 2.4 (figure 4.21) refers to a large uncloned *Kpn* I fragment (*KM12*) situated between K1-1 and K24-1 that spans B26-1 and overlaps B8-1 and B6A-1. The size of *KM12* was estimated to be 11.7kb by mapping the *Kpn* I sites within the overlapping fragments, B8-1, B26-1 and B6A-1, and then determining the distance between the *Kpn* I site located in B8-1 and the left *Kpn* I site located in B6A-1.

Region 2.5

Region 2.5 refers to the order of the *Not* I fragments within and overlapping B8-1 (figure 4.21). DIG-labelled B8-1 hybridised with pN4-1, pN5-2, pN15H-1, pN26A-1, N34-1 and K1-1. Digestion of pB8-1 with *Not* I produces a number of fragments; 5.3kb, 4.0kb, 1.35kb, 1.05kb, 0.85kb, 0.25kb and 0.14kb in size. As previously established, N5-2 overlaps the left terminus of B8-1 by approximately 0.85kb (region 2.3), which corresponds to the 0.85kb pB8-1 *Not* I fragment. The 5.3kb pB8-1 *Not* I fragment corresponds in size to N4-1. As K1-1 hybridised with pN5-2 and pN4-1, N4-1 was placed adjacent to the right of N5-2. N26A-1 contained two *Bam* HI sites and hybridised with pB8-1, pB26-1 and pB6A-1 and was therefore predicted to overlap the right terminus of B8-1. The 4.0kb fragment from the digestion of pB8-1 with *Not* I corresponds with a 4.0kb fragment produced by digestion of pN26A-1 with *Bam* HI, when the vector size was subtracted from both fragments it indicated the overlap between these two fragments was 1.0kb. Of the remaining fragments from the digestion of pB8-1 with *Not* I the 1.35kb and 1.05kb fragments correspond in size with the hybridised fragments N15H-1 and N34-1. These two fragments were predicted to be situated internally within B8-1 along with two "missing" *Not* I fragments 0.25kb (*NM9*) and 0.14kb (*NM10*) in size. Because the *Not* I fragments *NM9, NM10,* N15H-1 and N34-1 are all situated internally within B8-1 and *KM12*, it was not possible to order the fragments using hybridisation and restriction profiles.

Region 2.6

Digestion of pB6A-1 with *Not* I produced three bands corresponding to the fragment sizes; 5.6kb (2.65kb with the vector subtracted) and two 0.65kb fragments. It was determined by comparison of restriction profiles that N7-1 overlapped the right terminus of B6A-1 by 2.65kb and that N26A-1 overlapped the left terminus by 0.65kb. Therefore, the remaining 0.65kb *Not* I fragment (*NM11*) must be situated internally within B6A-1 between N26A-1 and N7-1 (figure 4.21).

Region 2.7

Region 2.7 refers to the order of *Not* I and *Kpn* I fragments along the length of B19-1 and the size of the "missing" fragment, *NM12*. The details used to order the fragments along B19-1 are schematically represented in figure 4.25 and are explained in the text that follows.

B19-1 hybridised with pK18-1, pK31-1 and pK19-1. It was predicted that K18-1 and K19-1 overlap the ends of B19-1, as they both possess an internal *Bam* HI site, whereas K31-1 does not. Comparison of the fragment sizes produced when pK18-1 and pK19-1 were digested with *Bam* HI, with that of pB19-1 digested with *Kpn* I confirmed that K18-1 and K19-1 overlap the ends of B19-1 by 6.4kb and 0.65kb respectively. As K31-1 did not possess a *Bam* HI site and corresponded in size to a fragment produced by digestion of pB19-1 with *Kpn* I, K31-1 was predicted to be located internally with B19-2 between K18-1 and K19-1.

The order of the *Not* I fragments along B19-1 was more difficult to determine. B19-1 hybridised with pN7-1, pN14A-1, pN14C-1 and pN14D-1, which identified them as internal to, or overlapping with B19-1. Digestion of pB19-1 with *Not* I produced five bands; 6.65kb, 4.6kb, 3.3kb, 1.3kb and 0.9kb. The 3.3kb, 1.3kb and the 0.9kb bands correspond in size to the fragments, N14D-1, N14A-1 and N14C-1, which were all subsequently shown to lack a *Bam* HI site. Therefore it was predicted that these *Not* I fragments are located internally within B19-1. In contrast, pN7-1 contained one *Bam* HI site and hybridised with pB6A-1 and pB19-1. Comparison of pN7-1 digested with *Bam* HI, with pB19-1 and pB6A-1 digested with *Not* I confirmed that N7-1 overlapped the left terminus of B19-1 by 4.6kb and the right terminus of B6A-1 by 2.65kb.

The order of the internal *Not* I fragments was determined by hybridisation between overlapping fragments and comparison of restriction profiles. Briefly, K18-1 hybridised with pN7-1, pN14A-1 and pN14D-1. Therefore either N14A-1 or N14D-1 is situated adjacent to N7-1. As N14D-1 also hybridised with K31-1 and possesses an internal *Kpn* I site it was determined that N14D-1 overlaps both K18-1 and K31-1 by 0.6kb and 2.7kb respectively. Hence N14A-1 must be situated internally within K18-1 between N7-1 and N14D-1. The size of N14C-1 corresponds in size to the 0.9kb fragment produced by digestion of pB19-1 with *Not* I and as previously established is situated internally within B19-1. Therefore N14C-1 must be located adjacent and to the right of N14D-1. The remaining 6.65kb band (3.7kb with the vector subtracted) must therefore represent the 3.7kb right terminal *Not* I fragment of B19-1, which constitutes the overlap between B19-1 and *NM12*.

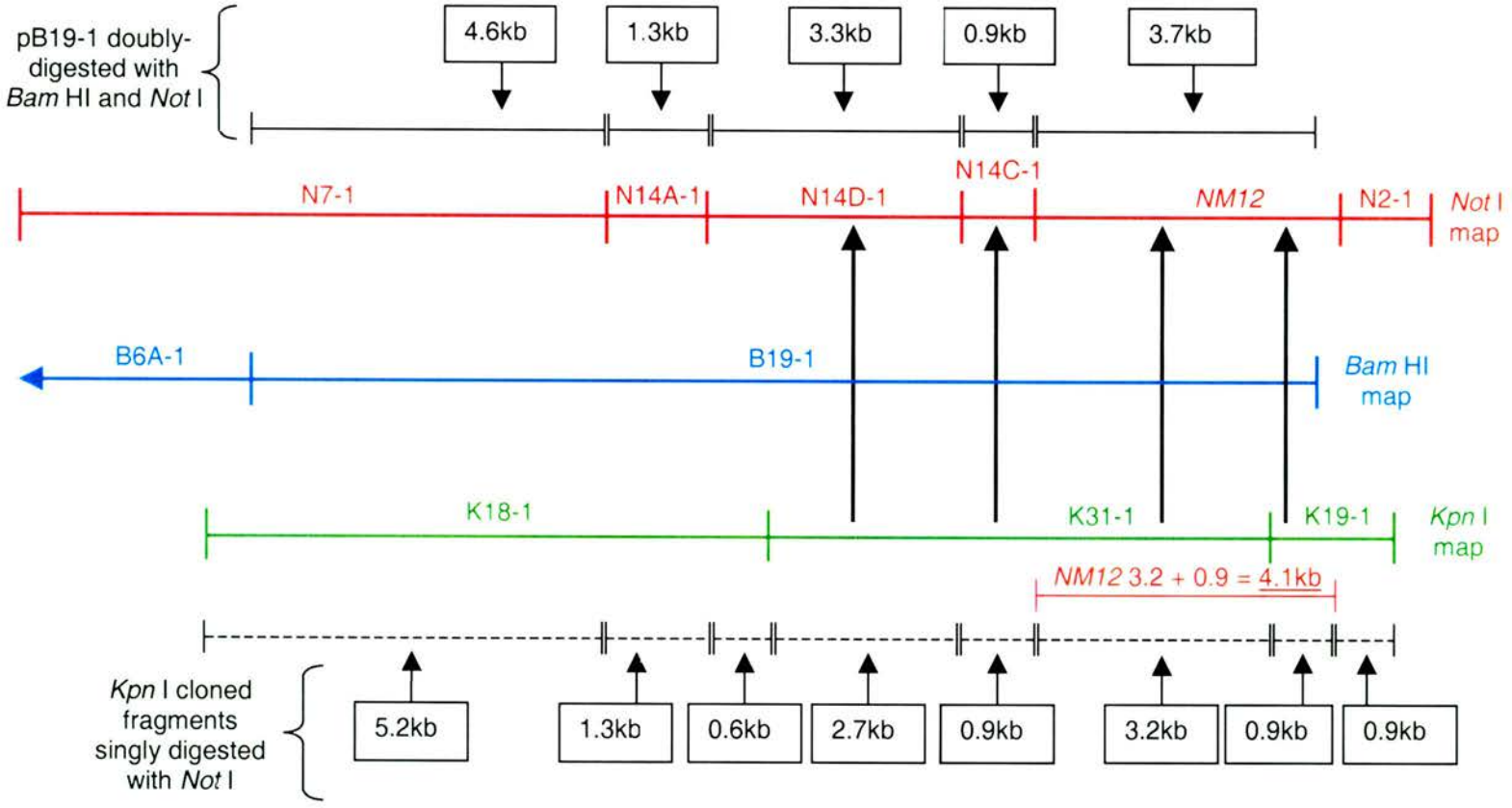

Figure 4.25 Schematic representation of region 2.7, illustrating the order of the *Not* I and *Kpn* I fragments within B19-1. The solid black bars (├——┤) correspond to fragments produced when pB19-1 is digested with both *Not* I and *Bam* HI, the approximate size of each fragment being indicated in the boxes above each individual bar. Likewise, the broken black bars (├------┤) correspond to fragments produced when the *Kpn* I fragments are singly digested with *Not* I, the approximate size of each fragment is indicated in the box below each bar. The large black arrows depict hybridisation of DIG-labelled *Kpn* I fragments with fragments produced by double-digestion of pB19-1 with *Not* I and *Bam* HI (deduced by Southern blotting, for example see figure 4.26).

This arrangement of the *Not* I fragments was supported by the result of a Southern blot shown in figure 4.26. As K19-1 overlapped the right terminus of B19-1 by 0.9kb, a Southern blot of pB19-1 doubly digested with *Not* I and *Bam* HI was hybridised with DIG-labelled K19-1. K19-1 hybridised with a 3.7kb band confirming it as the right-hand *Not* I fragment of B19-1, which represents the 3.7kb overlap with *NM12*. A duplicate Southern blot was probed with DIG-labelled K31-1, which hybridised with three bands, 3.7kb, 3.3kb and 0.9kb. The 3.7kb band represents the overlap of B19-1 with *NM12,* the 0.9kb was the internal N14C-1 fragment and the 3.3kb band represents N14D-1.

The size of NM12 was determined to be 4.1kb by mapping the *Not* I sites within K31-1 and K19-1, then calculating the distance between the *Not* I site within K19-1 and the right-hand *Not* I site within K31-1.

4.2.6 Ordering Clusters 1 and 2 by alignment to MOCV

The positions of the SPPV clusters 1 and 2 within the SPPV genome were estimated by their alignment to the MOCV genome. Sequences derived from the ends of 20 cloned restriction fragments were compared to those deposited in the EMBL database (section 2.4.8.1). Thirteen of the twenty fragments exhibited greater than 60% homology to MOCV subtype 1 complete sequence at one or both termini (table 4.3). The SPPV clusters 1 and 2 were aligned to MOCV using by mapping the locations of homologous sequence (figure 4.27). Cluster 1 approximately corresponds with the MOCV genome between 33kb to 112kb and cluster 2 between 130kb to 170kb.

Due to the collinear nature of poxvirus central regions the preliminary position of clusters 1 and 2 was considered indicative of their actual position within the SPPV genome. Hence, the size of unmapped region situated between clusters 1 and 2 was estimated to be approximately 18kb with the distance between the left-hand end of cluster 1 to the right-hand end of cluster 2 was estimated to be 137kb. Parapoxviruses genomes are generally between 130kb to 150kb in size (van Regenmortel *et al.*, 2000). Therefore it would suggest that the ITR regions were likely to be situated within or close to the left-hand and right-hand ends of clusters 1 and 2 respectively.

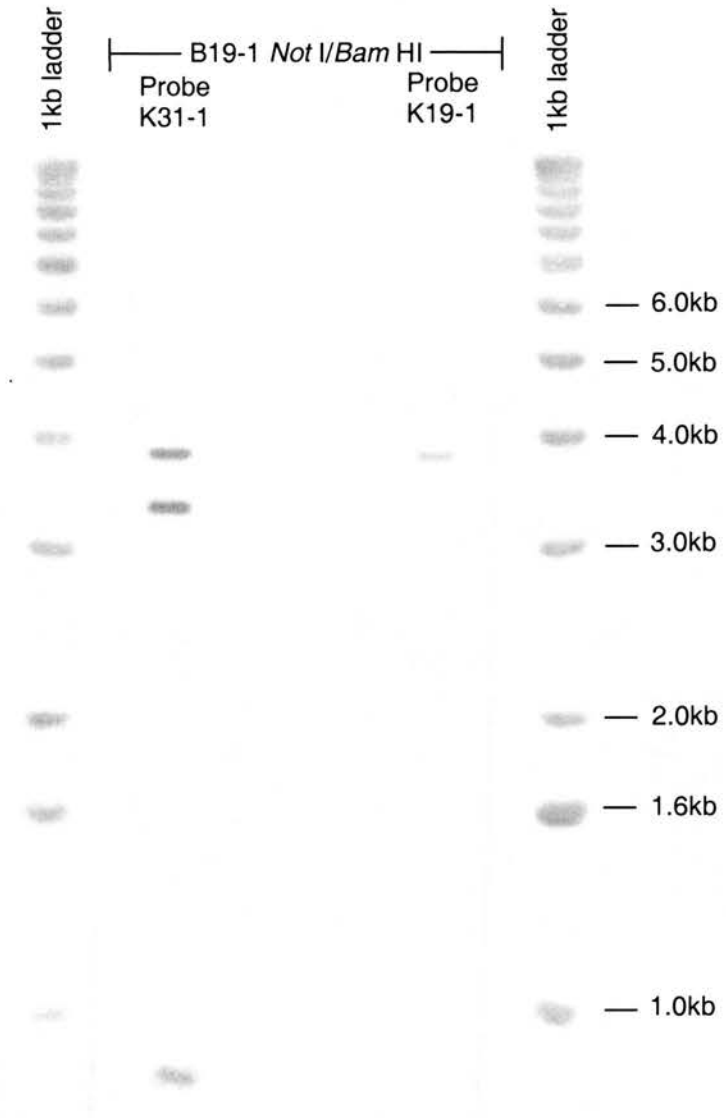

Figure 4.26 pB19-1DNA doubly-digested with *Not* I and *Bam* HI was electrophoresed on a 0.6% agarose gel and the DNA transferred, in duplicate, to nylon membrane. One Southern blot was probed with DIG-labelled K31-1, which hybridised with three bands of the approximate sizes 3.7kb, 3.3kb, and 0.9kb. The second Southern blot was probed with DIG-labelled K19-1, which hybridised with one band estimated to be 3.7kb in size. The sizes of the bands were determined by comparison to known standards in a 1kb ladder (Gibco).

Clone	Primer	G+C %	Homology to MOCV nucleotide sequence	% Homology
N1-1	**T3**	68.5	**MOCV region 142.4kb – 143.2kb**	72.2%/762 nt
	T7	71.4	**MOCV region 144.6kb – 144.9kb**	60.9%/324 nt
N2-1	T3	65.7	No MOCV homology	
	T7	65.5	No MOCV homology	
N3-1	**T3**	69.6	**MOCV region 92.46kb – 92.85kb**	68.6%/404nt
	T7	69.2	**MOCV region 89.90kb – 90.18kb**	61.8%/304nt
N4-1	T3	68.0	No MOCV homology	
	T7	66.6	**MOCV region 147.6kb – 147.9kb**	71.4%/357nt
N5-1	T3	72.6	No MOCV homology	
	T7	59.6	No MOCV homology	
N6-1	**T3**	63.3	**MOCV region 142.0kb – 142.4kb**	66.7%/409 nt
	T7	69.4	**MOCV region 141.0kb – 141.5kb**	58.5%/535 nt
N7-1	T3	69.2	No MOCV homology	
	T7	70.7	**MOCV region 157.9kb – 158.3kb**	66.2%/370 nt
N12-1	**T3**	65.4	**MOCV region 55.4kb – 56.1kb**	73.9%/762 nt
	T7	61.7	**MOCV region 52.7kb – 53.2kb**	65.9%/518 nt
N13-1	**T3**	66.4	**MOCV region 52.1kb – 52.7kb**	71.6%/564 nt
	T7	65.0	**MOCV region 40.8kb – 41.3kb**	71.0%/518 nt
N14C-1	T3	71.1	No MOCV homology	
	T7	65.5	No MOCV homology	
N16-1	**T3**	64.4	**MOCV region 30.3kb – 30.5kb**	69.5%/220 nt
	T7	63.8	**MOCV region 24.1kb – 24.3kb**	58.8%/255 nt
N22A-1	**T3**	63.5	**MOCV region 93.0kb – 93.6kb**	82.4%/550 nt
	T7	65.8	**MOCV region 99.1kb – 99.4kb**	67.7%/279 nt
N24-1	**T3**	63.3	**MOCV region 30.5kb – 30.9kb**	61.3%/424 nt
	T7	63.8	No MOCV homology	
N26A-1	T3	70.3	No MOCV homology	
	T7	65.9	No MOCV homology	
N33-1	T3	65.9	No MOCV homology	
	T7	63.2	No MOCV homology	
B1A	**T3**	66.7	**MOCV region 113.0kb – 113.5kb**	72.6%/449 nt
B11-1	T3	69.2	No MOCV homology	
B16C-1	**T3**	65.2	**MOCV region 52.7kb – 53.2kb**	64.2%/506nt
	T7	63.9	**MOCV region 56.4kb – 56.9kb**	71.1%/543nt
K19-1	T3	65.0	No MOCV homology	
K45-1	**T3**	67.3	**MOCV region 82.1kb – 82.3kb**	71.1%/149 nt

Table 4.3 Summary of sequence homology data of 20 cloned restriction fragments to MOCV. Thirteen of the 20 fragments analysed using the FastA algorithm exhibited greater than 60% nucleotide homology with the complete genome MOCV subtype 1 (EMBL accession number U60315) at one or both termini. The homologous regions present in MOCV that were used to align SPPV clusters 1 and 2 to the MOCV genome (see figure 4.27) are indicated in column 4. The calculated G+C % of each sequence is presented in column 3. The average percentage G+C content of all 36 sequences is 66.4%.

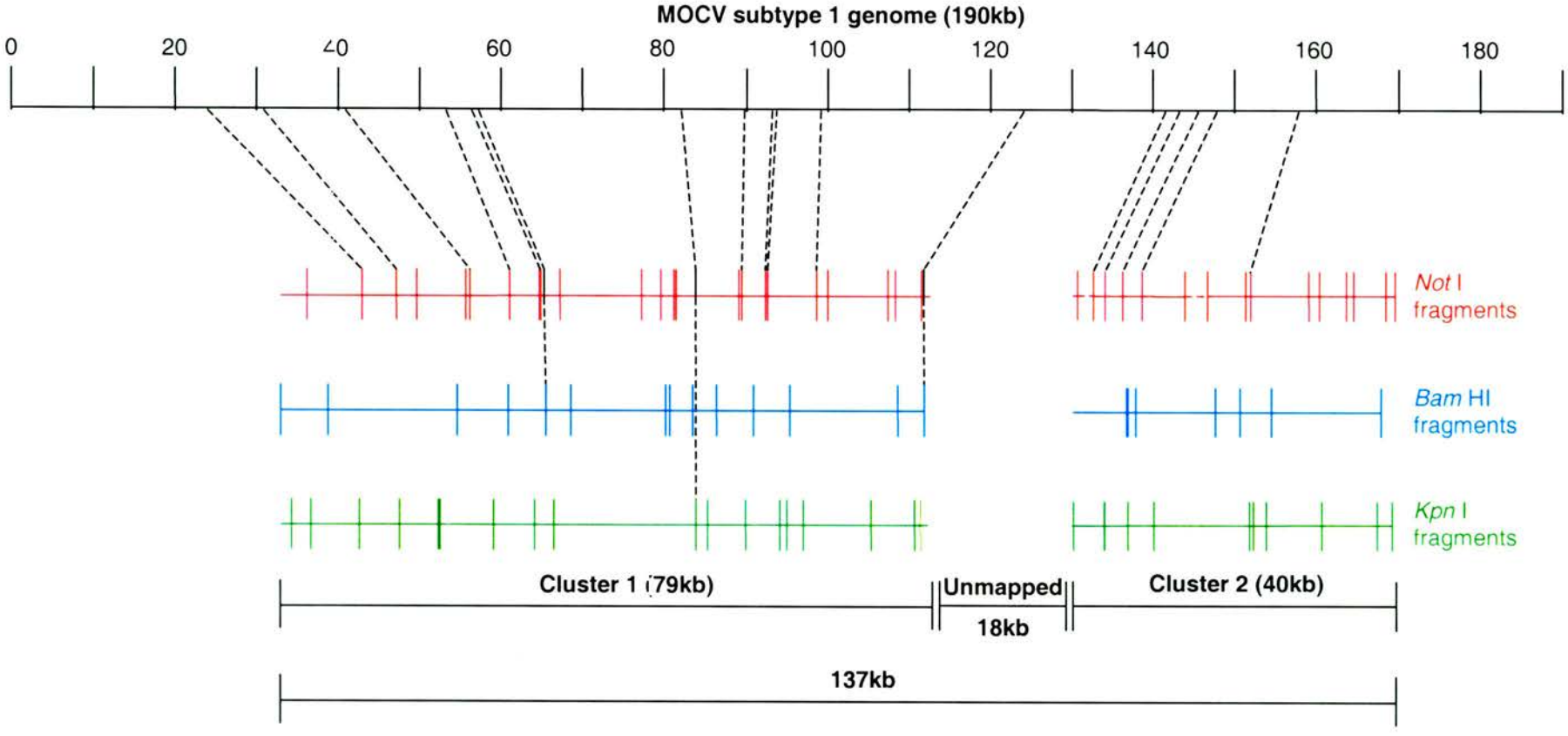

Figure 4.27 Alignment of SPPV clusters 1 and 2 to the MOCV subtype 1 genome (EMBL accession number U60315). The genomic locations of homologous SPPV and MOCV DNA sequences (table 4.3) was used to align SPPV clusters 1 and 2 to the complete genome of MOCV subtype 1. The broken black lines indicate the locations of homologous sequence present in the SPPV and MOCV genomes.

4.3 MAPPING THE ITR REGIONS OF SPPV

4.3.1 Examination of clusters 1 and 2 for the presence of ITR sequence.

The left-hand region of cluster 1 and the right-hand region of cluster 2 lacked obvious restriction site symmetry, which suggested that the putative ITR was absent from one or both clusters. Furthermore, there was no evidence of cross-hybridisation between the terminal fragments. Hence it was concluded that ITR sequence is absent from one or both clusters.

4.3.2 Construction of partial restriction maps of the putative ITR regions

4.3.2.1 Selection of an anchor fragment

A selection of previously uncharacterised and unmapped *Bam* HI DNA fragments were used to screen the genomic libraries in order to identify *Not* I and *Kpn* I fragments located out with clusters 1 and 2. Only one fragment, B7C-1, hybridised with previously unidentified *Not* I fragments. Sequence obtained from both ends of B7C-1 revealed the base pair composition was G+C rich at approximately 63%, suggesting that it is likely to be viral in origin. However no homology with other poxviruses could be detected at the nucleotide level, suggesting that B7C-1 could be located out with the conserved central core.

4.3.2.2 Clusters 3A and 3B

B7C-1 was used as an anchor fragment, enabling the restriction maps of two clusters (3A and 3B) to be constructed. Clusters 3A and 3B exhibit a degree of restriction site symmetry and are therefore predicted to partially span the ITR regions and extend into heterogeneous unique regions. Construction of the two clusters was achieved using hybridisation and restriction profiles of overlapping fragments and is explained schematically in figures 4.28 to 4.31 and in the text that follows.

B7C-1 hybridised with the *Not* I fragments; N11H-1, N55-2 and N65-2, but did not hybridise to any cloned *Kpn* I fragments. Alignment of the three *Not* I fragments with B7C-1 was achieved using restriction profile analysis of the cloned fragments (as described for clusters 1 and 2), which is summarised in figure 4.28. However, as the fragments N11H-1 and *NM13* are both situated internally with B7C-1, their order could not be determined.

The DIG-labelled fragments N11H-1, N55-2 and N65-2 were used as probes to screen *Bam* HI and *Kpn* I genomic libraries. A number of *Bam* HI fragments hybridised with the *Not* I fragments, however no hybridising *Kpn* I fragments were found (summarised in figure 4.29). Alignment of B2-1 and B70-2 to N55-2 (summarised in figure 4.30) was achieved by comparing the *Bam* HI restriction profile of N55-2 with the *Not* I restriction profiles of B2-1 and B70-2 using methods previously described for the construction of cluster 1 and 2. Likewise, B12-1 and B30-2 were mapped as located internally within N65-2, however their order could not be determined from restriction digest data.

B7C-1 and B5-2 are differently sized individual *Bam* HI fragments, however they produce identical hybridisation patterns with the *Not* I fragments. In addition, comparison of the *Not* I restriction profiles of pB7C-1 and pB5-2 revealed that three of the four fragments produced by each clone are identical in size: 1.2kb, 0.45kb and 0.55kb (after the size of the vector was subtracted). The three commonly sized *Not* I digest products correlate in size to N11H-1, *NM13* and the overlap with N55-2 (figure 4.30). These data are highly suggestive of a number of conserved *Not* I sites and indicate that both B7C-1 and B5-2 overlap N55-2 and span NM13 and N11H-1. Despite hybridising with both B7C-1 and B5-2, N65-2 only contained a *Bam* HI site which corresponded to the left-hand end of B7C-1 but not with left hand end of B5-2 (depicted in figure 4.30). Therefore N65-2 cannot overlap B5-2. It was therefore considered likely that B7C-1 and B5-2 are located at opposite ends of the genome and overlap the putative ITR fragments (N11H-1, NM13 and N55-2), the ITR junctions and extend into the unique regions. The ITR junctions must therefore be located between the right-hand end of N65-2 and the left-hand end of B7C-1 and within the corresponding region of B5-2 (figure 4.30). Hence two separate clusters could be deduced representing the regions containing the ITR junctions at either end of the genome (figure 4.31). At this stage clusters 3A and 3B could not be positioned further in terms of which corresponded to which end of the SPPV genome.

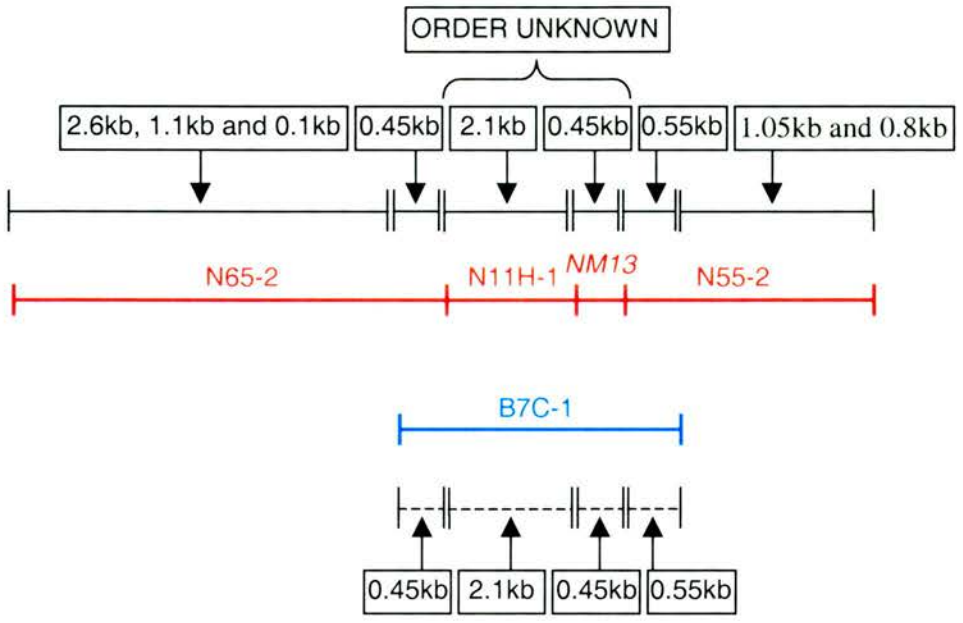

Figure 4.28 Alignment of B7C-1 with the uncloned *Not* I fragment *NM13* and the *Not* I fragments: N11H-1, N55-2 and N65-2. The solid black horizontal bars (├——┤) represent the size of the restriction fragments produced by *Bam* HI digestion of the *Not* I fragments. Likewise, the broken black horizontal bars (├------┤) represent the size of the restriction fragments produced when B7C-1 is digested with *Not* I. The size of each DNA fragment is indicated in the black box above or below each bar.

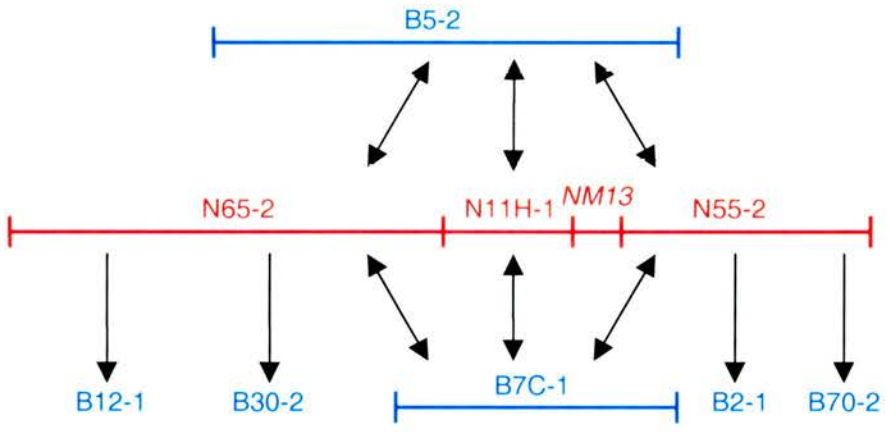

Figure 4.29 The hybridisation pattern of DIG-labelled N11H-1, N55-2 and N65-2 with the cloned *Bam* HI fragments: pB2-1, pB5-2, pB7C-1, pB12-1, pB30-2 and pB70-2. Likewise, hybridisation of the cloned *Not* I fragments: pN11H-1, pN55-2 and pN65-2 with DIG-labelled B7C-1 and B5-2. Hybridisation is indicat\ed by the solid black arrows.

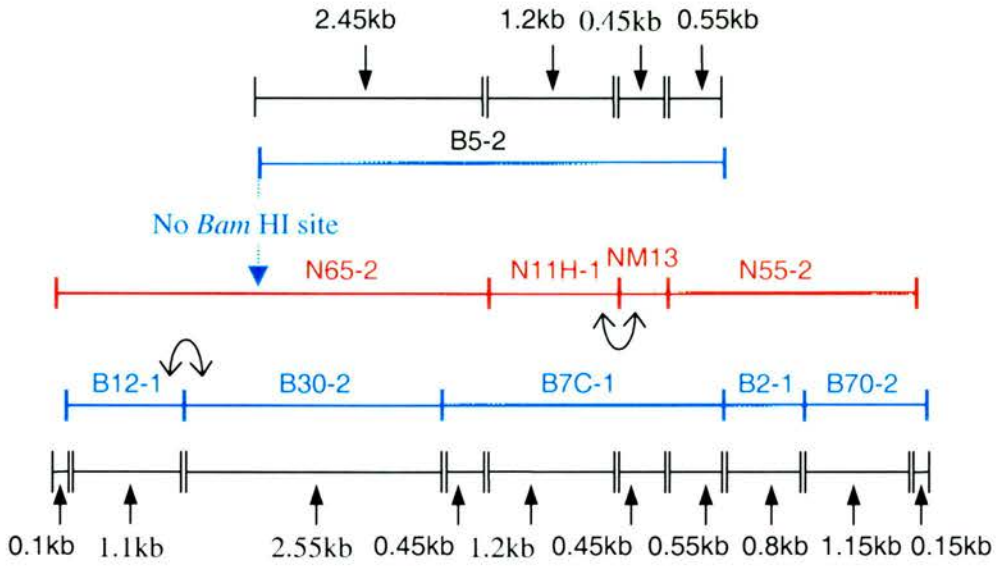

Figure 4.30 Schematic representation of the alignment of the *Bam* HI fragments: B2-1, B7C-1, B12-1, B30-2 and B70-2 aligned with the *Not* I fragments N11H-1, N55-2 and N65-2. The horizontal black bars (|—|) represent the fragments produced by *Not* I digestion of the *Bam* HI fragments and likewise *Bam* HI digestion of the *Not* I fragments. The order of the fragments indicated with the arched arrows (↷) may be situated in an opposite order. B5-2 and B7C-1 cross-hybridisation with the same *Not* I fragments (figure 4.29). However, according to restriction digest data B5-2 does not align with N65-2. The ITR junction (shaded in grey) is predicted to be situated somewhere between the right-hand end of N65-2 and the left end of B7C-1.

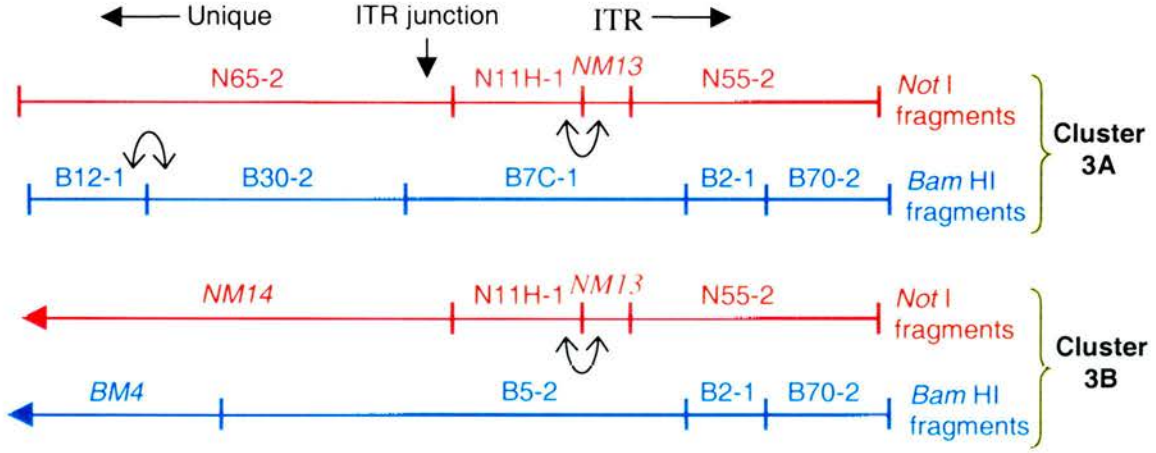

Figure 4.31 Schematic representation of clusters 3A and 3B. The regions predicted to contain the ITR junction is shaded in grey. The order of the fragments indicated by arched arrows (↷) may be in an order opposite to that which is shown on the diagram.

4.4 RESTRICTION ENDONUCLEASE MAPPING OF THE SPPV GENOME USING COSMID CLONES

For the reasons discussed in section 4.7.1, the restriction endonuclease maps of the SPPV genome could not be completed with the plasmid clones. Therefore a second strategy was employed, were larger contiguous DNA fragments were cloned into a cosmid vector. The restriction endonuclease maps were completed by individually mapping overlapping cosmid clones that contained SPPV genomic DNA that spanned the entire length of the genome.

4.4.1 Cosmid library construction

SPPV genomic DNA (isolate 1296/99) was cloned into SuperCos I vector (Stratagene) using the method detailed in section 2.6.3. Briefly, 2.5μg of SPPV/carrier DNA (in a ratio of 1:4) partially digested with *Sau* 3AI was ligated with 1μg of cosmid arms. The whole ligation reaction was packaged into lambda phage and then used to transduce *E.coli* to produce the primary cosmid library. The titre of the primary library was determined to be 80,000 colony forming units per ml (cfu/ml). The primary library was amplified and glycerol stocks of the amplified library prepared. The titre of the amplified library was determined to be 1.38×10^{10} cfu/ml.

4.4.2 Screening the cosmid library

The SuperCos I library was plated onto 90mm Luria-Bertani agar (LBA) plates supplemented with 50μg/ml ampicillin at a density of 150 colonies per plate. Colonies were transferred to nylon membranes and prepared for hybridisation with DIG-labelled DNA probes (section 2.4.5.3.3).

Seven cloned restriction fragments were selected to screen the cosmid library on the basis of their location within clusters 1, 2, 3A and 3B (summarised in table 4.4). The five fragments located within clusters 1 and 2 were chosen because they evenly distributed (figure 4.32) and it was thought likely that screening the cosmid library with these fragments would identify overlapping cosmid clones that span the genome.

A further two fragments, B2-1 and B12-1, previously mapped within clusters 3A and 3B were used to screen for cosmids containing the ends of the SPPV genome. Fragment B2-1 is located within the putative ITRs (section 4.3.2.2.2.2). Therefore it was expected that each cosmid clone

hybridising with B2-1 would contain DNA from the left or right ITR. B12-1, a unique fragment of cluster 3A, was used to distinguish between clones overlapping clusters 3A or 3B.

Eighty-seven hybridised colonies were selected, grown in culture and cosmid DNA prepared using the alkaline lysis method (section 2.5.5.1). The cosmid DNAs were singularly digested with *Not* I, *Bam* HI or *Kpn* I and the products electrophoresed on an agarose gel. Southern blots were prepared and hybridised with the same DIG-labelled restriction fragments used to screen the cosmid library in order to confirm the positive hybridisation status of each cosmid clone. A total of seventy-four clones were confirmed as containing SPPV genomic DNA (summarised in table 4.4).

4.4.3 Selection of overlapping cosmid clones

The approximate position of each clone within the SPPV genome could be deduced from the location of the hybridising restriction fragment in the previously mapped regions: clusters 1, 2, 3A and 3B. However, the clone may extend up to 42kb left or right of the hybridising restriction fragment (figure 4.32).

Ten cosmid clones were selected on the basis that they were predicted to overlap each other and span the whole genome with the exception of the terminal hairpin loop structures. Selection was based upon restriction profiles of the clones when singularly digested with *Not* I, *Bam* HI and *Kpn* I in order to identify fragments of common size and by comparison to the restriction maps of clusters 1, 2, 3A and 3B. The gel depicted in figure 4.33 shows the 10 selected clones digested with *Bam* HI; the fragment sizes are summarised in table 4.5.

To further characterise the location of each clone within the SPPV genome and confirm overlap between the cosmid clones, several previously mapped cloned restriction fragments were individually hybridised with each cosmid clone (figure 4.34). The restriction profile and hybridisation data enabled the position of each clone within the SPPV genome to be clarified (figure 4.35). This is described in more detail in the text that follows.

Restriction fragment	Approximate position within the SPPV genome	Number of positive cosmid clones hybridised
B 51-2	unique LHS	9
K46-1	unique LHS	2
K 32-1	unique Central	13
B1A-1	unique Central	9
N 2-1	unique RHS	15
B12-1	unique RHS or LHS	14
B2-1	ITR	12

Table 4.4 Summary of the SPPV restriction fragments used to screen the cosmid library, their approximated location with the SPPV genome and the number of cosmid clones hybridised (subsequently confirmed by southern blotting).

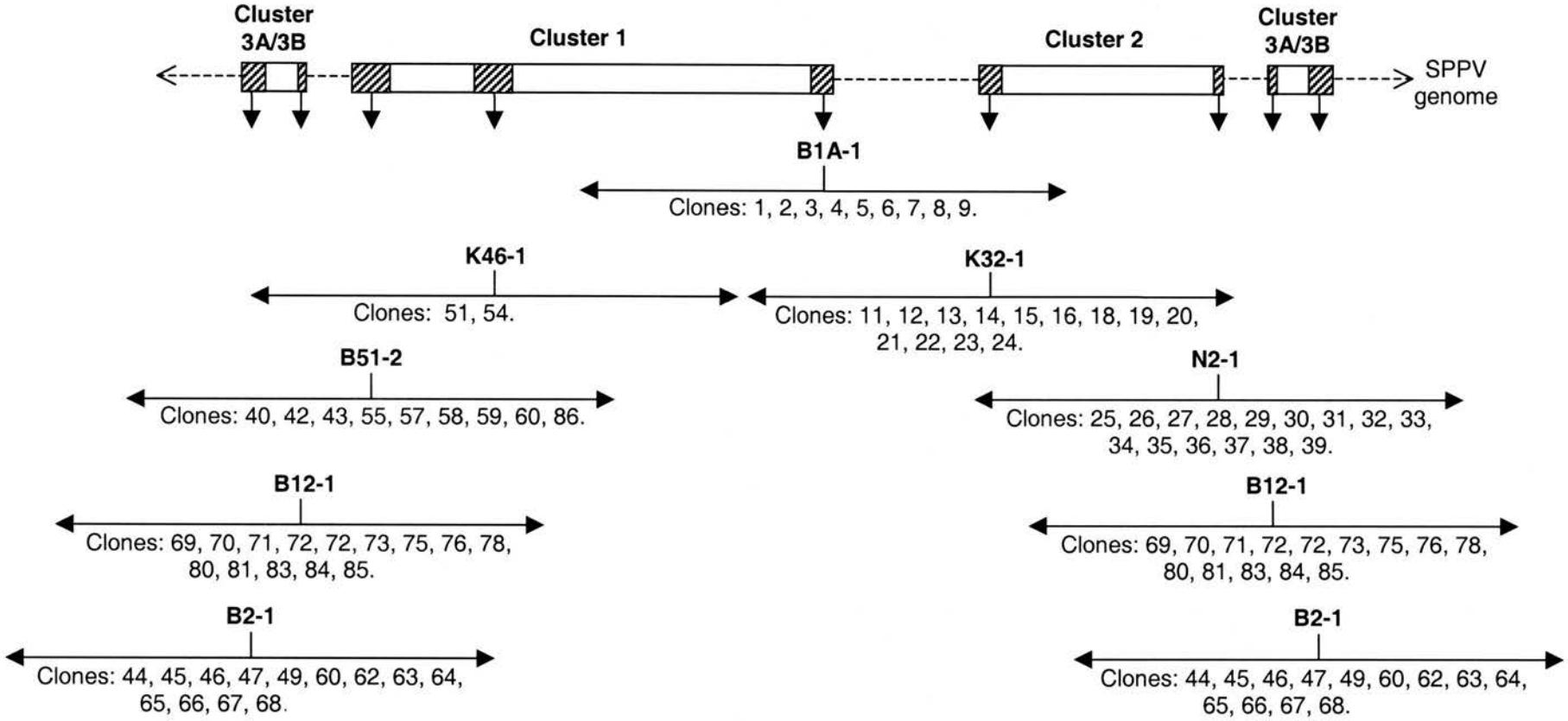

Figure 4.32 The approximate position and possible range of each cosmid clone within the SPPV genome, as determined from the location of the hybridising restriction fragments. The position and the possible range spanned by each hybridising clone is represented by solid horizontal arrows with clone identification numbers stated underneath the arrows. The diagonally shaded regions of the schematic representation of clusters 1, 2 and 3A /3B indicate the location of the hybridising fragments: B1A-1, K46-1, K32-1, B51-2, N2-1, B12-1 and B2-1 within the SPPV genome. The broken horizontal line represents the unmapped regions of the genome. Note the order of clusters 3A and 3B have not been determined at this point, therefore cosmid clones hybridising with B12-1 and B2-1 maybe located at either end of the SPPV genome.

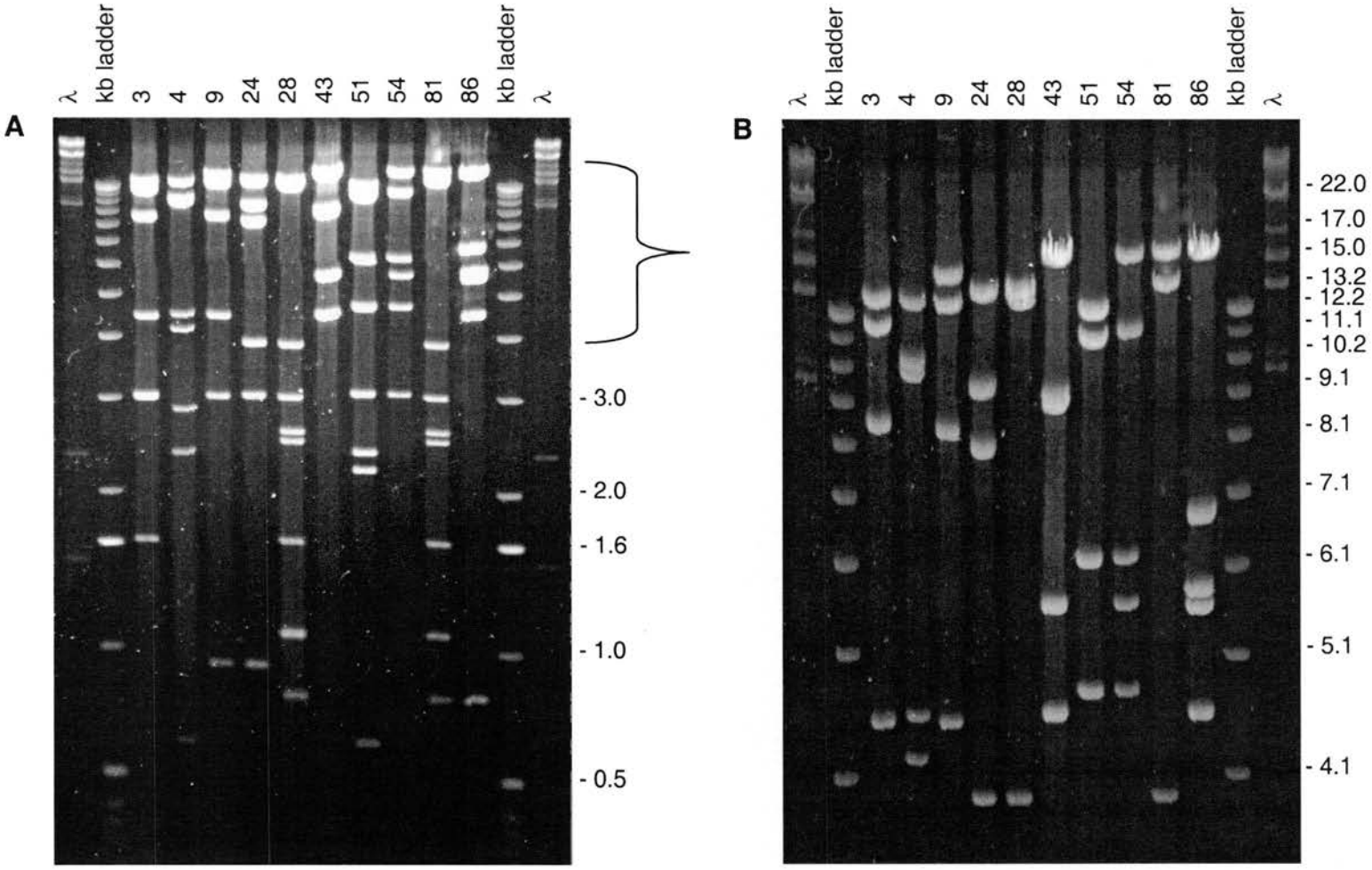

Figure 4.33 A) Selection of cosmid clones digested with *Bam* HI and electrophoresed on a 0.6% (w/v) agarose gel. B) Gel depicted in figure A, electrophoresed further to resolve the larger fragments. The size of each band was estimated by comparison to known standards present in a 1kb ladder (Gibco) and λ-phage DNA, which was individually digested with *Xho* I, *Kpn* I and *Bgl* II than mixed. See table 4.5 for a summary of estimated fragment sizes.

Cosmid clone	*Bam* HI fragment sizes (kb)
3	1.6, 3.1, 3.05, 4.5, 8.5, 11.8, 13.3
5	0.65, 2.65, 2.95, 4.2, 4.6, 9.9, 10.5, 13.3
9	0.17*, 0.9, 3.05, 4.5, 8.5, 12.5, 14.0
24	0.17*, 0.9, 3.05, 3.9, 8.1, 9.5, 13.0
28	0.8, 1.1, 1.15, 1.6, 2.55, 2.6, 3.05, 3.9, 12.5, 13.8
43	4.65, 5.7, 9.0, 15.8
51	0.65, 2.65, 3.15, 4.75, 6.3, 11.35, 12.0
54	4.65, 5.7, 6.3, 11.5, 15.8
81	0.8, 1.1, 1.15, 1.6, 2.55, 2.6, 3.05, 3.9, 13.8, 16.0
86	0.8, 4.65, 5.7, 5.85, 6.85, 15.8

Table 4.5 Summary of the estimated fragment sizes produced by the cosmid clones digested with *Bam* HI. The asterisk (*) refers to fragments too small to be visualised in the gel depicted in figure 4.33.

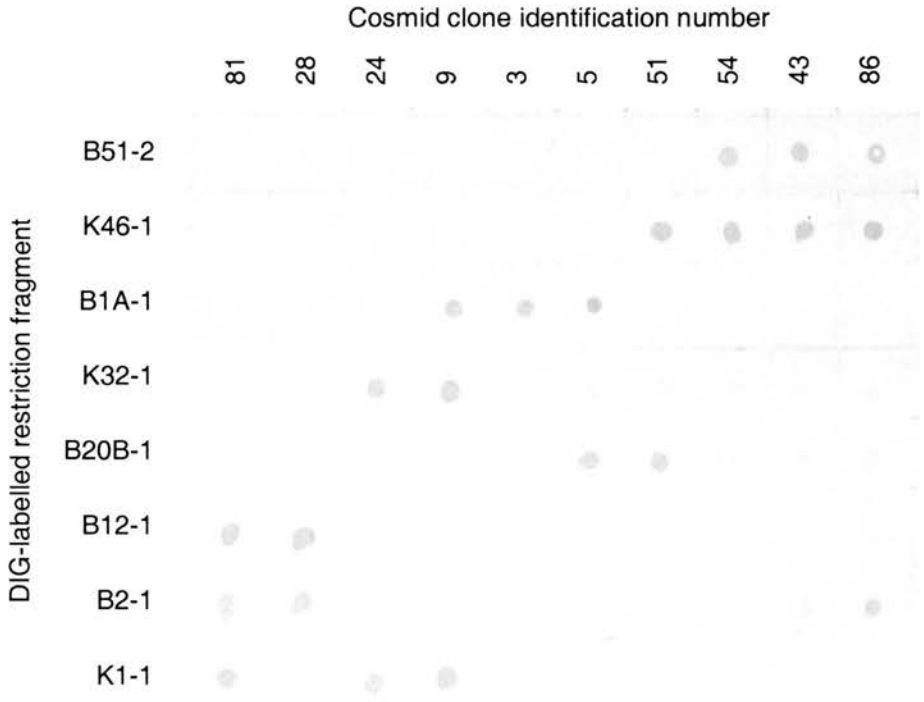

Figure 4.34 0.3μg of DNA from each cosmid clone (prepared by QIAprep spin miniprep kit, QIAGEN) immobilised onto nylon membrane and hybridised with a selection of DIG-labelled SPPV restriction fragments.

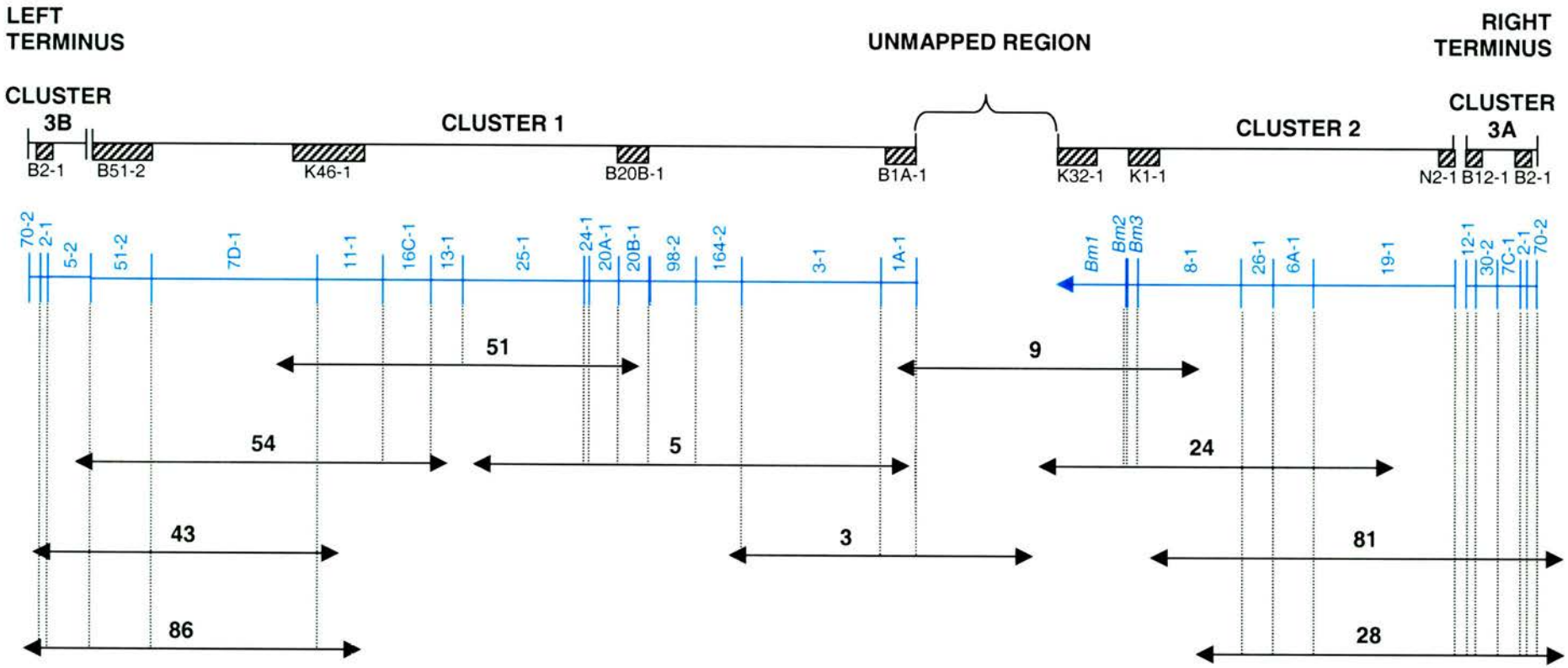

Figure 4.35 Schematic representation of the alignment of the ten selected cosmid clones to clusters 1, 2, 3A and 3B. The approximate location of each clone was determined from hybridisation of the clones with previously mapped restriction fragments (see ▨). Alignment of the cosmid clones (represented by double arrows) to the SPPV genome was achieved by identifying *Bam* HI fragments common in size to both the cosmid clone and the SPPV genome (represented by the vertical broken lines).

Clones 51 and 5 span a region contained completely within cluster 1. Clone 51 hybridised with K46-1 and B20B-1 (figure 4.34) and must therefore span the region between these two fragments. In support, digestion of clone 51 with *Bam* HI produced fragments of 6.3kb, 4.75kb, 3.15kb, 11.35, 0.65kb and 2.65kb (table 4.5), which correspond in size to the contiguous fragments B11-1, B16C-1, B13-1, B25-1, B24-1 and B20A-1. No fragments were produced that corresponded in size to B7D-1 or B20B-1, which flank the contiguous stretch. As clone 51 hybridised with B20B-1, clone 51 must therefore partially overlap B20B-1, but not extend passed the right-terminal *Bam* HI site. Therefore the remaining 12.0kb fragment produced by digestion of clone 51 with *Bam* HI must include the vector and the terminal regions of clone 51, which overlap B20B-1 and B7D-1.

Likewise clone 5 hybridised with B20B-1 and B1A-1. Digestion of clone 5 with *Bam* HI produced eight fragments, of which six corresponded in size to the contiguous fragments: B24-1, B20A-1, B20B-1, B98-1, B164-2 and B3-1. The remaining two fragment are 9.9kb and 10.5kb, as neither fragment correspond in size to B25-1 or B1A-1 (which flank the contiguous fragments), therefore clone 5 must extend into these fragment but not span them. One of the remaining fragments must contain the cosmid vector and one terminus of clone 5. If the size of the vector is subtracted from the 9.9kb fragment, the remaining 3.05kb fragment is small enough to overlap B1A-1 but not beyond the right *Bam* HI site. The remaining 10.5kb, which is too large to overlap with B1A-1 without spanning both *Bam* HI sites must therefore overlap with B25-1. In the case of clone 5 it appears that the left *Sau*3A I recognition site (GATC) was converted to a *Bam* HI site (GGATCC) during the cloning procedure. Conversion to a *Bam* HI site can happen when a cytosine base (C) is located to the right to the *Sau*3A I site (GATCC) or a guanine base (G) is located to the left of a S*au*3A I site (GGATC). Hence when ligated into the *Bam* HI site of the vector a functional *Bam* HI site is formed. In the case of the terminal sequence of clone 5 the left terminal *Sau*3A I site was transformed into *Bam* HI site and upon digestion with *Bam* HI the terminal 10.5kb fragment was cleaved from the vector.

Clones 24, 28, 54, 43, 81 and 86 were all aligned to clusters 1 and 2 using the procedure explained for clones 5 and 51. Clones 43 and 86 are located towards the left of the genome and restriction profile analysis indicated that both clones overlap B51-2 and B7D-1 and extended left, beyond cluster 1 toward the left end of the genome. Likewise, clones 28 and 81 are located at the right of the genome overlapping B26-1, B6A-1 and B19-1 and extend beyond the right

terminal region of cluster 2. Clones 28, 43, 81 and 86 were all predicted to extend into the putative ITR by hybridising with the putative ITR fragment B2-1. Clones 28 and 81 produced almost identical *Bam* HI restriction profiles, five fragments corresponded in size to B12-1, B30-2, B7C-1, B2-1 and B70-2, which had been previously mapped within cluster 3A. Hence cluster 3A is located at the right end of the genome. In support, clones 28 and 81 also hybridised with the cluster 3A fragment B12-1, whilst clones 43 and 86 located at the left of the genome did not. It then follows that cluster 3B must be located at the left of the genome. Digestion of clone 86 with *Bam* HI produced two fragments, 0.8kb and 4.65kb in size, which correspond in size with the cluster 3B fragment B2-1 and B5-2. Clone 43 did not produce a *Bam* HI fragment corresponding in size to B2-1, however a hybridisation signal was visible between clone 43 and B2-1. A possible explanation for this may be that clone 43 terminates within B2-1 or that clone 43 does not overlap B2-1 but repeated sequence may be present within the ITR resulting in hybridisation.

Clone 9 hybridised with B1A-1, K32-1 and K1-1 and was therefore predicted to span the unmapped region situated between clusters 1 and 2. Clones 3 and 24 were predicted to overlap clone 9 and extend into the unmapped region situated between clusters 1 and 2.

4.4.4 Restriction Endonuclease Mapping of the Cosmid Clones

4.4.4.1 *Bam* HI, *Kpn* I and *Eco* RI restriction endonuclease maps of the cosmid clones

Restriction endonuclease maps of the SPPV genomic DNA cloned into the SuperCos I vector were determined using a method originally devised for mapping DNA cloned into λ phage vectors (Rackwitz *et al.*, 1984), which was later adapted for mapping cosmid clones (Rackwitz *et al.*, 1985). The method (section 2.7) relies upon the action of λ-phage-derived terminase, which cleaves the vector at the cos site, producing 12bp 5'-cohesive extensions. The linearised cosmid clone is then partially digested with the desired restriction endonuclease to produce fragments of varying lengths. The fragments are then labelled at one end, by hybridisation with a ^{32}P-labelled oligonucleotide (ON-L or ON-R), which is complementary in sequence to one of the 12bp cos 5'-extensions:

ON-L 5'- AGGTCGCCGCCC - 3'
ON-R 5'- GGGCGGCGACCT - 3'

When the labelled products are electrophoresed and the dried agarose gel exposed to medical X-ray film a laddered banding pattern is visible (figure 4.36 for an example). The image was analysed using TotalLab 1D (v1.00) image analysis software (Pharmacia biotech) to determine the approximate size of each labelled fragment. The restriction map of each cosmid clone could then be determined from the partially digested fragment sizes.

For example, when clone 9 is partially digested with *Bam* HI and labelled with ON-L the smallest visible band is 4.94kb (figure 4.36). The size of this fragment represents the distance between the ON-L labelled vector *cos* site and the nearest *Bam* HI site situated at the left end of the cloned DNA. When the size of the adjoining vector DNA (0.27kb) is subtracted from the total size of the band, the remaining 4.7kb represents the size of the left end of clone 9, up to the first internal *Bam* HI site. The next band in size is approximately 5.83kb. The difference between the sizes 5.83kb and 4.94kb is 0.89kb, which correspond in size to the 0.9kb fragment produced by complete digestion of clone 9 with *Bam* HI (table 4.5); this represents the size of the first complete *Bam* HI restriction fragment adjacent to the 4.7kb terminal fragment. The next band size is 5.99kb and when the 5.83 is subtracted the remaining 0.16kb is the size of the next adjacent *Bam* HI fragment. This analysis was repeated with all the partial digest fragments of clone 9 hybridised with ON-L and ON-R, and when compared to the fragment sizes produced by complete restriction digestion with *Bam* HI a complete *Bam* HI map of clone 9 was deduced. Using this technique the ten selected clones were mapped with *Kpn* I, *Bam* HI, and *Eco* RI. Where possible the *Kpn* I and *Bam* HI restriction endonuclease maps of the cosmid clones were confirmed by comparison to previously mapped regions in clusters 1, 2, 3A and 3B. Likewise, the locations of the *Eco* RI sites were confirmed by digestion of the previously cloned *Bam* HI and *Kpn* I fragments with *Eco* RI (results not shown).

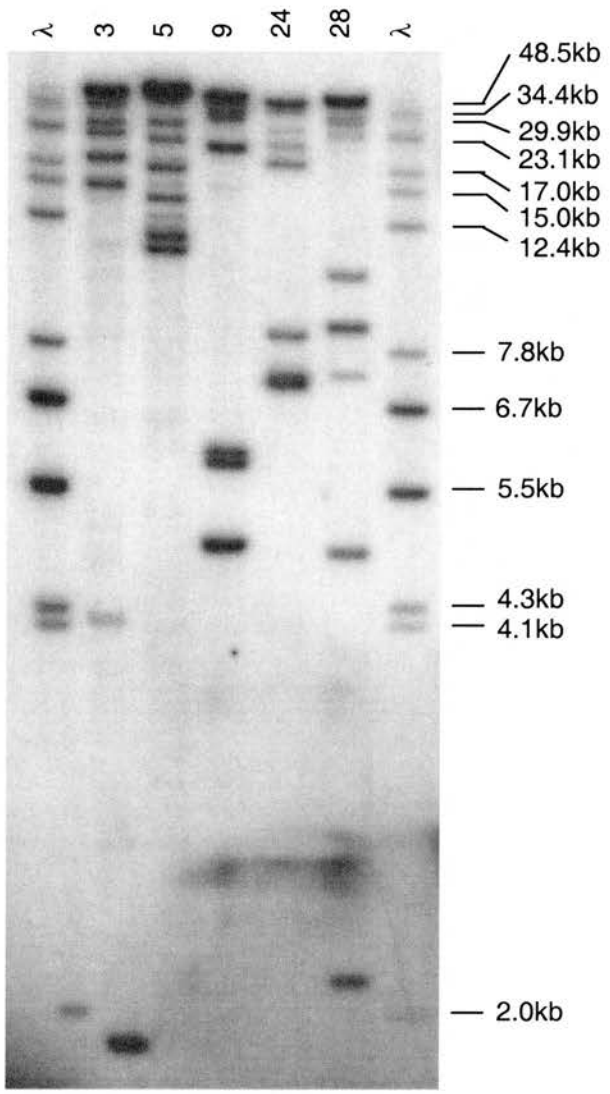

Figure 4.36 Cosmid clones 3, 5, 9, 24 and 28 linearized with λ-terminase and partially digested with *Bam* HI. DNA fragments were then hybridised with the end-labelled oligonucleotide ON-L and electrophoresed on a 0.6% agarose gel. The gel was dried onto DE-81 chromotography paper (Whattman), exposed to medical X-ray film for 48 hours with an intensifier screen and then developed. The size of each fragment was estimated using TotalLab 1D image analysis software (Pharmcia biotech) by comparison to known standard present in λ-phage DNA digested with *Bam* HI, *Cla* I, *Hin*d III, *Kpn* I, *Stu* I, *Xho* I and uncut λ-phage DNA (all end-labelled with ON-L and ON-R).

4.4.4.2 *Hind* III restriction endonuclease maps of the cosmid clones

Hind III restriction sites were shown to be present in clones 3, 5, 28 and 81 by restriction endonuclease digestion of all the selected cosmid clones with *Hind* III (figure 4.37). Clones 3, 5, 28 and 81 produced two bands when digested with *Hind* III, therefore each clone possessed one *Hind* III site within the cloned insert and one site within the vector. As only one *Hind* III site is located within each of the four clones, a different approach to mapping the *Hind* III sites was used. The cloned *Kpn* I and *Bam* HI restriction fragments that are contained within the four cosmid clones were digested with *Hind* III in order to identify which restriction fragments contained *Hind* III sites. Clones 3 and 5 overlap with each other by approximately 18kb and the *Hind* III site is located in the region of overlap within fragment B3-1. Likewise, clones 28 and 81 overlap extensively with each other and the single *Hind* III site is located in the region of overlap within fragments B19-1 and K31-1.

The precise locations of the *Hind* III sites within B3-1, K31-1 and B19-1 were determined by single and double restriction endonuclease digests of the plasmid clones (figure 4.38). Digestion of pB19-1 with *Hind* III produced two fragments; the smallest being approximately 2.1kb and is produced by the enzyme cutting at the vector site and the site internal within fragment B19-1. *Hind* III also cleaves K31-1, which situated internally within B19-1 at the right hand end, therefore the *Hind* III site must be located 2.1kb in from the right terminus of B19-1. In support the 1.5kb fragment produced by double digestion of pK31-1 with *Hind* III and *Kpn* I correspond with the distance between the right *Kpn* I site of K31-1 and the predicted position of the *Hind* III site (figure 4.39A).

The *Hind* III site within B3-1 was mapped in a similar manner. Single digestion of pB3-1 with *Hind* III and double digestion of pB3-1 with *Bam* HI and *Hind* III both produced fragments 5.5kb in size (figure 4.38). This 5.5kb fragment is produced by *Hind* III cleavage of the vector site and the site internally within B3-1, therefore the *Hind* III site must be situated 5.5kb from the left or right terminus of B3-1. The precise location was clarified by comparison of restriction profiles produced by pB3-1 singularly digested with *Kpn* I and doubly digested with *Kpn* I and *Hind* III (figures 4.38 and 4.39B).

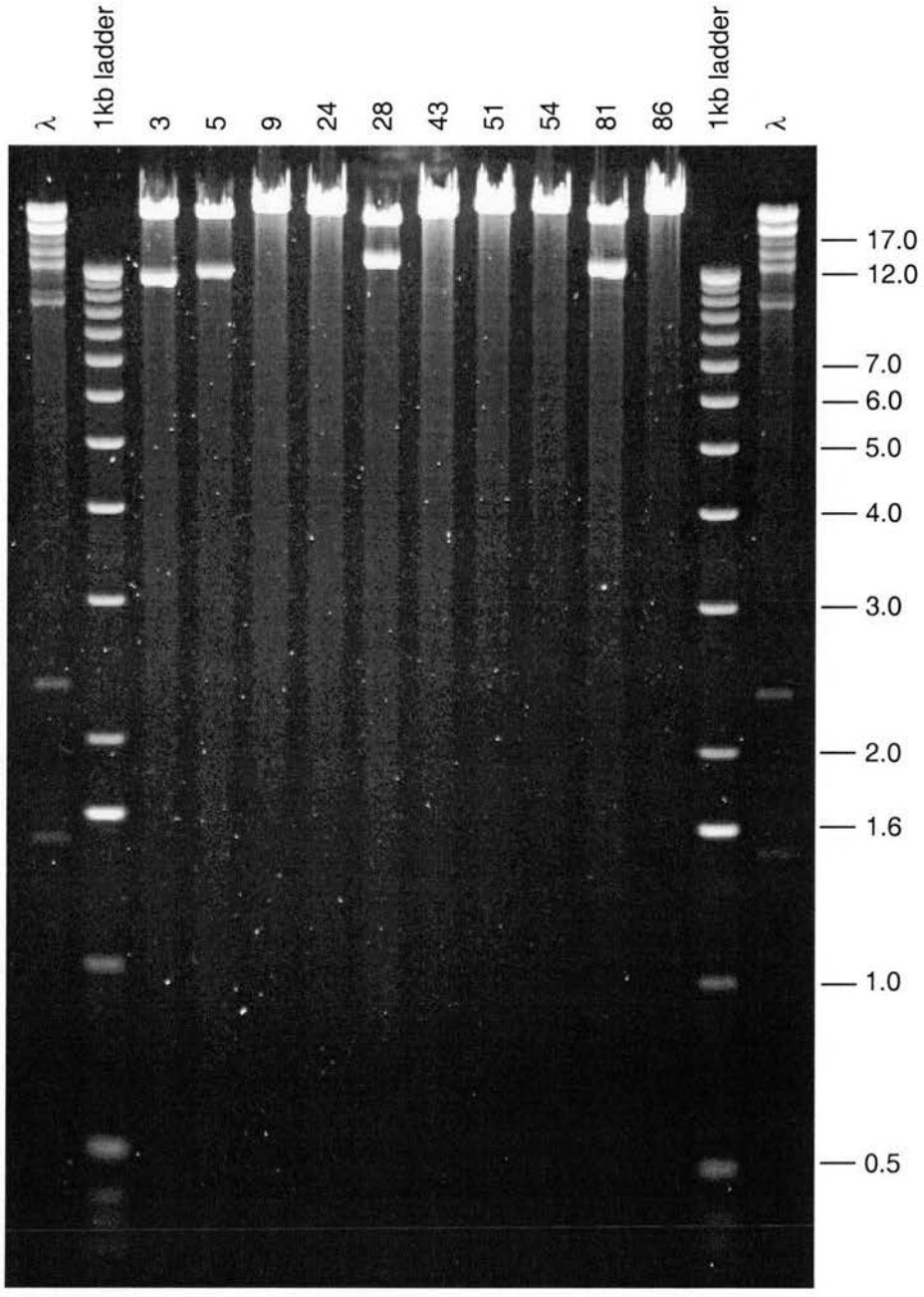

Figure 4.37 Cosmid clones digested with *Hin*d III electrophoresed on a 0.6% agarose gel. Only clones 3, 5, 28 and 81 possess a *Hin*d III site located internally within the cloned insert.

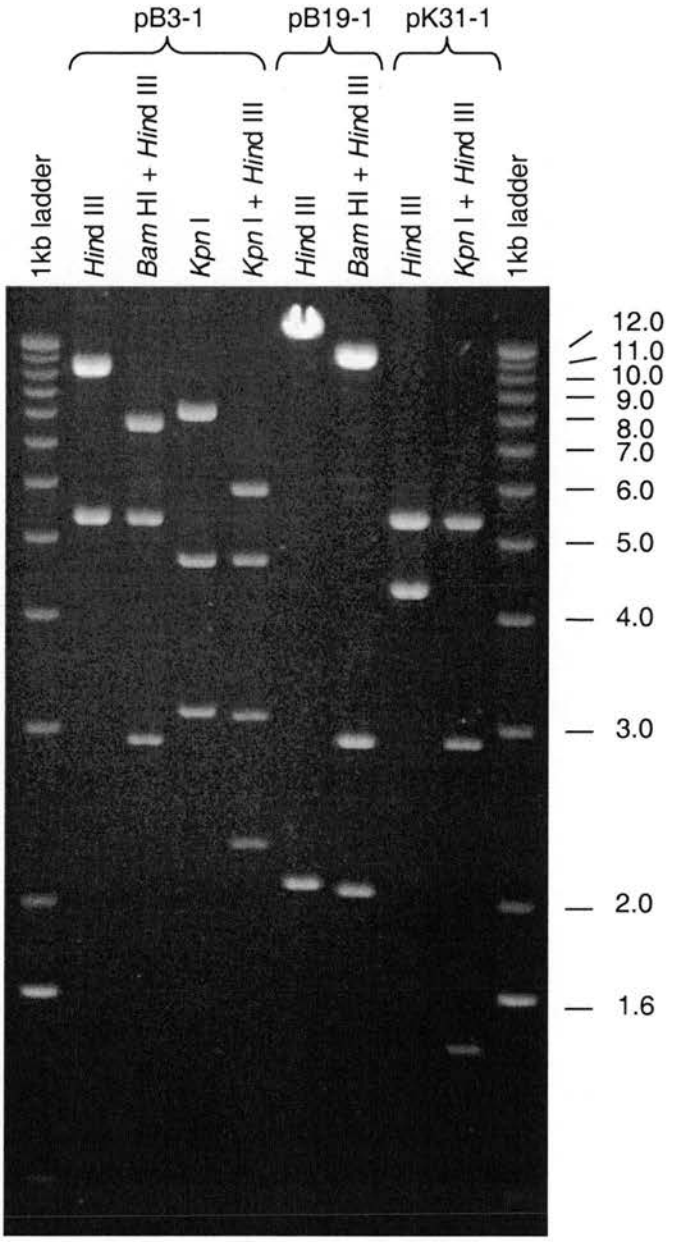

Figure 4.38 Single and double restriction endonuclease digests of restriction fragments pB3-1, pK31-1 and pB19-1 (cloned into pBluescript SK$^-$) electrophoresed on a 0.6% agarose gel.

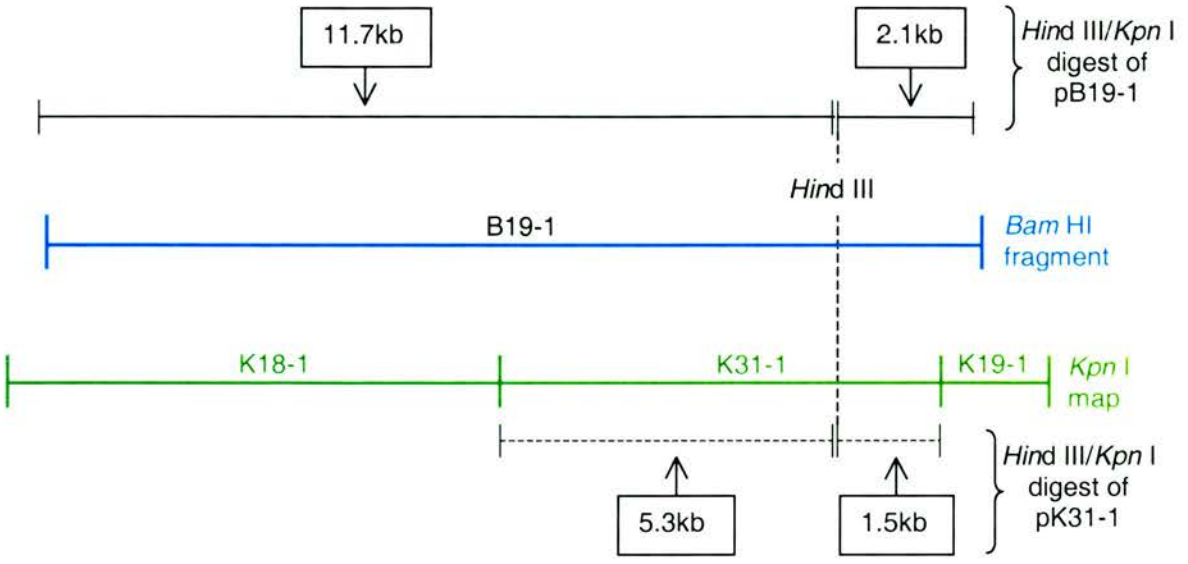

Figure 4.39A Schematic representation demonstrating the location of the *Hind* III site within B19-1 and K31-1, constructed from fragments produced by single and double restriction digests of pB19-1 and pK31-1 (see figure 4.39). The solid black bars (├──┤) represent fragment produced by double digestion of pB19-1 with *Hind* III and *Kpn* I . Likewise, the broken black bars (├----┤) represent fragments produced by of double digestion of pK31-1 with *Kpn* I and *Hind* III.

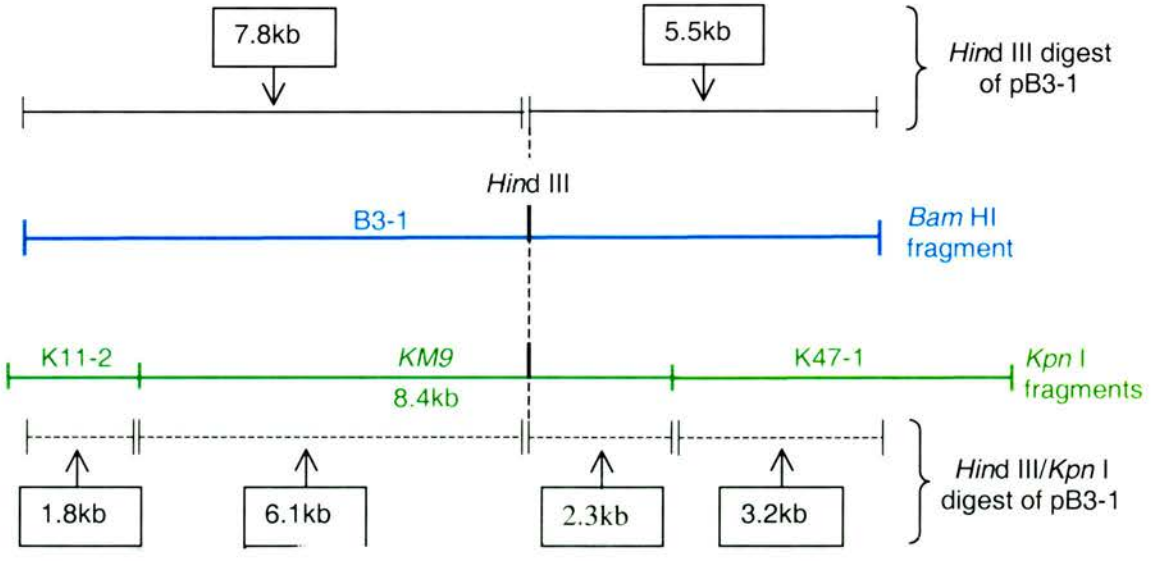

Figure 4.39B Schematic representation demonstrating the location of the *Hind* III site within B3-1 and *KM9*, constructed from fragments produced by single and double restriction digests of pB3-1 (see figure 4.39). The solid black bars (├──┤) represent fragment produced by digestion of pB3-1 with *Hind* III. Likewise, the broken black bars (├----┤) represent fragments produced by of double digestion of pB3-1 with *Kpn* I and *Hind* III.

4.5 STRUCTURE OF THE TERMINAL REGIONS

4.5.1 Establishing the location of the genome ends

The very ends of the genome could not be cloned presumably due to hairpin loop structures that form the termini of all poxvirus genomes. In the absence of a clear restriction profile, the end fragments could not be identified nor their sizes estimated. Therefore the end fragments were identified and their sizes estimated using DNA hybridisation. Digestion of the cloned restriction fragments that are predicted to be located near to the genome ends indicated that no *Kpn* I sites are located in the ITRs. Therefore genomic DNA digested with *Kpn* I was Southern blotted and hybridised with DIG-labelled ITR fragment B2-1 (figure 4.40). Two *Kpn* I fragments, which hybridised with B2-1 were estimated to be 5.3kb and 9.0kb in size. The sizes of these fragments were plotted onto the restriction maps of the terminal regions (figure 4.41). The terminal *Kpn* I fragments were predicted to extend from the *Kpn* I sites nearest the genome ends to 0.35kb and 0.5kb beyond the furthermost mapped *Bam* HI sites. To confirm that these locations did correspond to the ends of the genome rather than a *Kpn* I site situated within the ITR the procedure was repeated using *Dra* I sites. *Dra* I sites nearest to the termini were mapped by restriction profile analysis of cloned terminal restriction fragments. Genomic DNA digested with *Dra* I was Southern blotted and probed DIG-labelled B2-1. Again two fragments that hybridised with B2-1 were identified and were estimated to be approximately 11.2kb and 12.2kb in size. The sizes of these *Dra* I fragments were plotted onto the restriction map of the terminal regions (figure 4.41). The *Dra* I fragments were predicted to extend from the *Dra* I sites nearest the termini to 0.4kb beyond the mapped *Bam* HI sites. Thereby confirming the location of the genome termini as being between 0.35 and 0.5kb (average 0.41kb) beyond the previously mapped *Bam* HI sites.

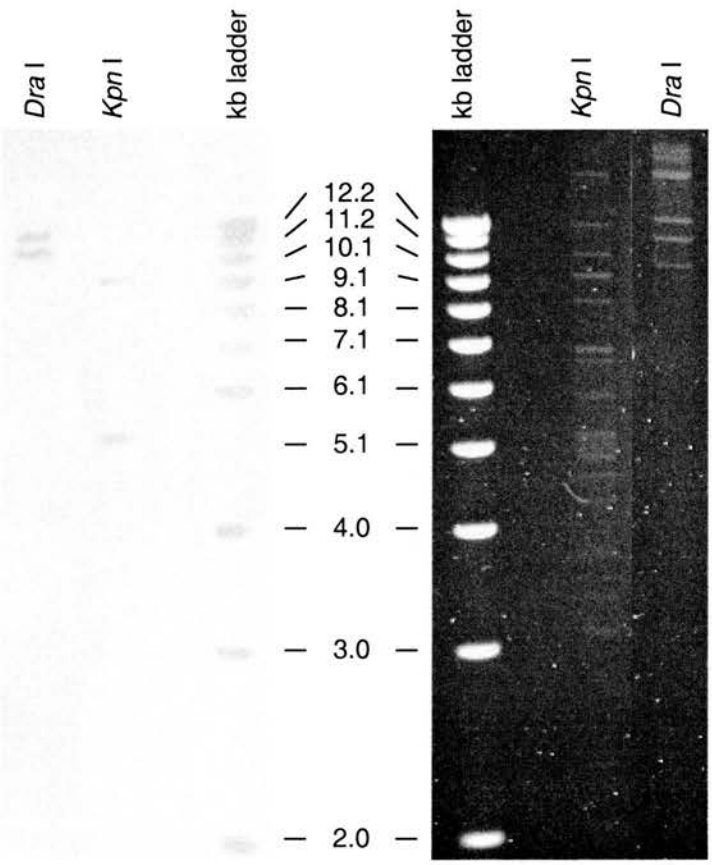

Figure 4.40 Southern blot analysis of genomic SPPV DNA (isolate 1296/99) singly digested with *Kpn* I and *Dra* I, hybridised with DIG-labelled B2-1 (figure 4.41 for probe location). The hybridising *Kpn* I fragments were estimated to be 9.0kb and 5.3kb and the *Dra* I fragments to be 12.2kb and 11.2kb.

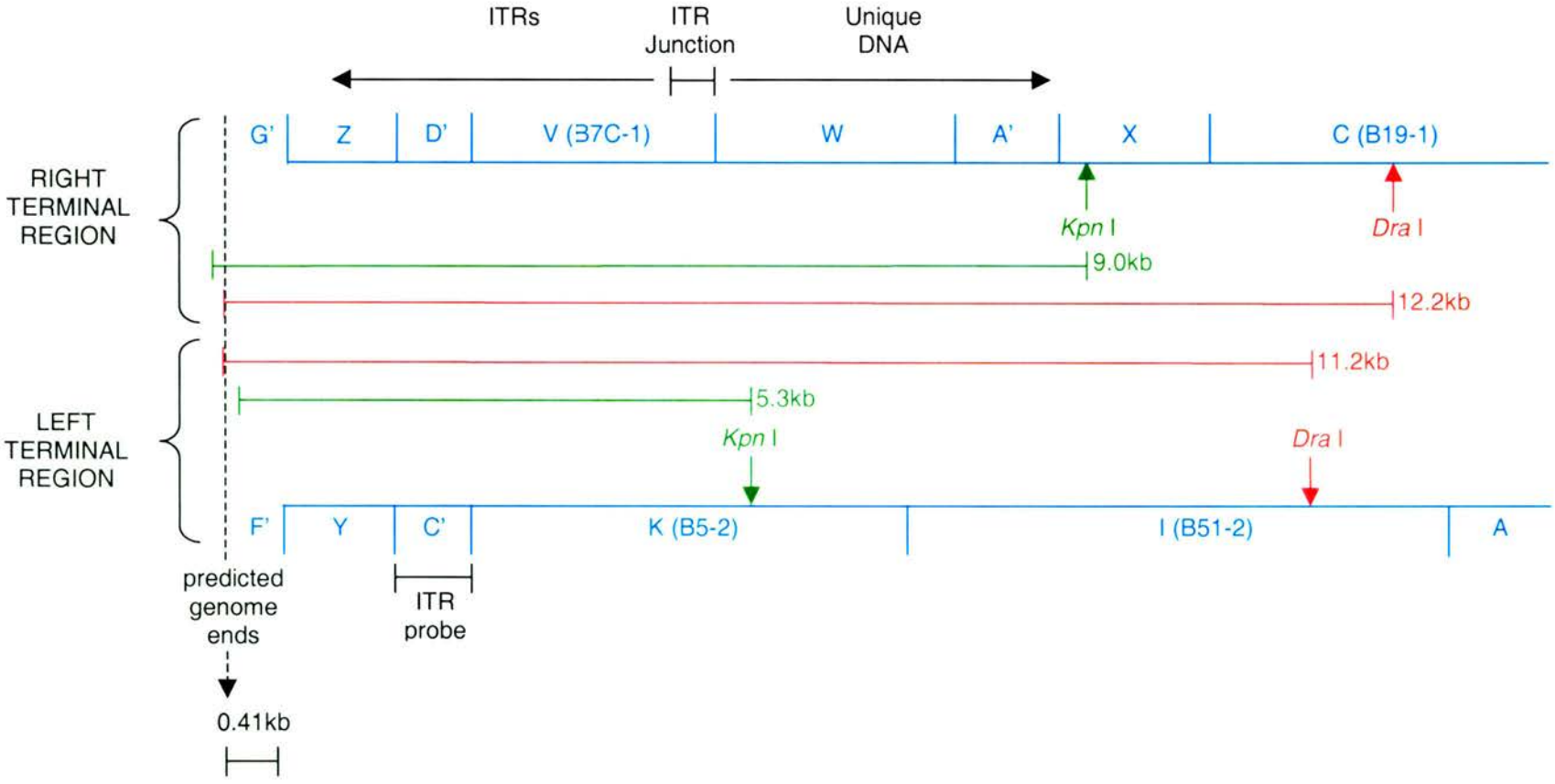

Figure 4.41 Schematic representation of the terminal regions of SPPV. The blue lines depict the *Bam* HI restriction endonuclease maps of the left and right ends of the genome, the annotated *Bam* HI fragments correspond to those in figure 4.45 and table 4.6. The green and red horizontal bars represent the SPPV genomic DNA *Kpn* I and *Dra* I fragments that hybridised with the ITR probe (figure 4.40). The hybridised fragments, when mapped from the terminal *Kpn* I and *Dra* I sites, on average extend approximately 0.41kb beyond the *Bam* HI fragments Y and Z. Therefore the ends of the genomes were predicted to be located 0.41kb left of *Bam* HI fragment Y and 0.41kb right of *Bam* HI fragment Z.

4.5.2 Inverted Terminal Repeats of SPPV

The cloned *Bam* HI fragments B7C-1 and B5-2 (corresponding to fragments designated V and K in figure 4.45 and table 4.6) were predicted to be located at opposite ends of the genome. Both fragments were predicted to span the ITR junction and therefore contain ITR sequence at one end and unique sequence at the other end (section 4.3.2.2.2.2). To confirm the presence of ITRs within fragments B7C-1 (V) and B5-2 (K), sequence was obtained from left end of B5-2 and the right end of B7C-1, with respect to their orientation within the SPPV genome, and both sequences aligned with each other using the ClustalW (section 2.4.8.3). The two sequences were identical confirming that SPPV possess ITRs (figure 4.42A). As poxvirus ITRs are inverted and complementary with respect to each other (Baroudy *et al.*, 1982), the sequence derived from B7C-1 is essentially the complement and reverse of sequence obtained from B5-2.

4.5.2.1 Location of the ITR junctions and ITR size

The position of the ITR junctions were predicted to lie within a 0.45kb region located between area of restriction site conservation and restriction site divergence within the fragments B7C-1 (V) and B5-2 (K) (refer to figure 4.31). To determine the actual location of the ITR junctions, DNA sequences were obtained from the 0.45kb region of B7C-1 (V) and B5-2 (K) and were aligned with each other using ClustalW (section 2.4.8.3). The sequence alignment (figure 4.42B) demonstrates the two sequences are identical over 439bp and diverge at the ITR junction, which is located 22bp from the unique *Bam* HI site of B7C-1.

The sizes of the ITRs were estimated to be 4.96kb by calculating the distance between the ITR junctions and the predicted ends of the genome (figure 4.43).

```
                 *         20         *         40         *
B5-2  : GGATCCGTGGCCTCGTCCCCTCTTCCCTCTCCGAGGAGGGAGCGAGGAGGACATCGACT : K
B7C-1 : GGATCCGTGGCCTCGTCCCCTCTTCCCTCTCCGAGGAGGGAGCGAGGAGGACATCGACT : V

       60         *         80         *        100         *
B5-2  : CGGGATGGATGCACCCGCTCCCTCATGGACGGAGTGGAGCGAGTAGGACATCGACTCGG : K
B7C-1 : CGGGATGGATGCACCCGCTCCCTCATGGACGGAGTGGAGCGAGTAGGACATCGACTCGG : V
```

Figure 4.42A Sequence derived from the left end of cloned fragment B5-2 (fragment K) and the right end of cloned fragment B7C-1 (fragment V) aligned using the ClustalW algorithm (section 2.4.8.3). The *Bam* HI sites, common to both ends of the SPPV genome, are shaded in grey. Because poxvirus ITRs are the complement and reverse of each other, the B7C-1 sequence in this figure would effectively the complement and reverse within the SPPV genome.

```
        Not I    *         20         *         40         *
B5-2  : GCGGCCGCCGGAGCCGAGAGGGCCGCCGGGGCCCGGCGCGGCCAGCGCCGCCCGGGGC : V
B7C-1 : GCGGCCGCCGGAGCCGAGAGGGCCGCCGGGGCCCGGCGCGGCCAGCGCCGCCCGGGGC : K

        60         *         80         *        100         *
B5-2  : ACCATCGCCGCCAGGAGCAGGCACAGGAGGCGGCGCATCTCCGTCGGTCGGTCGGAGG : V
B7C-1 : ACCATCGCCGCCAGGAGCAGGCACAGGAGGCGGCGCATCTCCGTCGGTCGGTCGGAGG : K

       120         *        140         *        160         *
B5-2  : AGCTGGCTCTCGTCTGTCGTCCGCGGTCGAGCGCGAGCTGTCGTCTGTCGTCGAGCGC : V
B7C-1 : AGCTGGCTCTCGTCTGTCGTCCGCGGTCGAGCGCGAGCTGTCGTCTGTCGTCGAGCGC : K

       180         *        200         *        220         *
B5-2  : GAGCTGTCGTCTGTCGTCGAGCGCGAGCTGTCGTCCGTCGTCGAGCGTCCGAGGTCGG : V
B7C-1 : GAGCTGTCGTCTGTCGTCGAGCGCGAGCTGTCGTCCGTCGTCGAGCGTCCGAGGTCGG : K

       240         *        260         *        280         *
B5-2  : TCGCGCGGCGCTCCCTCGCTCGGGGCCTTTGGGGGCGGGCGCTCCTTTTTCGCTTTGG : V
B7C-1 : TCGCGCGGCGCTCCCTCGCTCGGGGCCTTTGGGGGCGGGCGCTCCTTTTTCGCTTTGG : K

       300         *        320         *        340
B5-2  : GGGAACGGGCGGGATCGGGGGAGTGAGGGCGGACCGGGGAGGGCGGACGGCGGATCGG : V
B7C-1 : GGGAACGGGCGGGATCGGGGGAGTGAGGGCGGACCGGGGAGGGCGGACGGCGGATCGG : K

       360         *        380         *        400
B5-2  : GGACGGCGGACCCGGGAGGGCGGAGAAAGACGGCGGCTCAACCGAGGCCGTGCGCGAG : V
B7C-1 : GGACGGCGGACCCGGGAGGGCGGAGAAAGACGGCGGCTCAACCGAGGCCGTGCGCGAG : K

       420         *        440         *        460
B5-2  : GCGCGCGACCCGCGGGACGAGCTGGCGGAGGCCGAGGGGGGCGAGGGCGACGGAG : V
B7C-1 : GCGCGCGACCCGCGGGACGAGCTGGCGGAGGCCTGGTGTGGGAATTAAGGGATCC : K
                                        ITR junction   Bam HI
```

Figure 4.42B Sequences derived from within the cloned fragment B5-2 (K) and the end of B7C-1 (V), which are predicted to span the ITR junctions of SPPV (figure 4.43). The ITR sequence is shaded in black and the unique *Bam* HI site situated at the right end of B7C-1 and the common Not I sites are shaded in grey. The sequence diverges 22bp from the left terminal Bam HI site of B7C-1 at nucleotide position 439, demonstrating the actual location of the ITR junction.

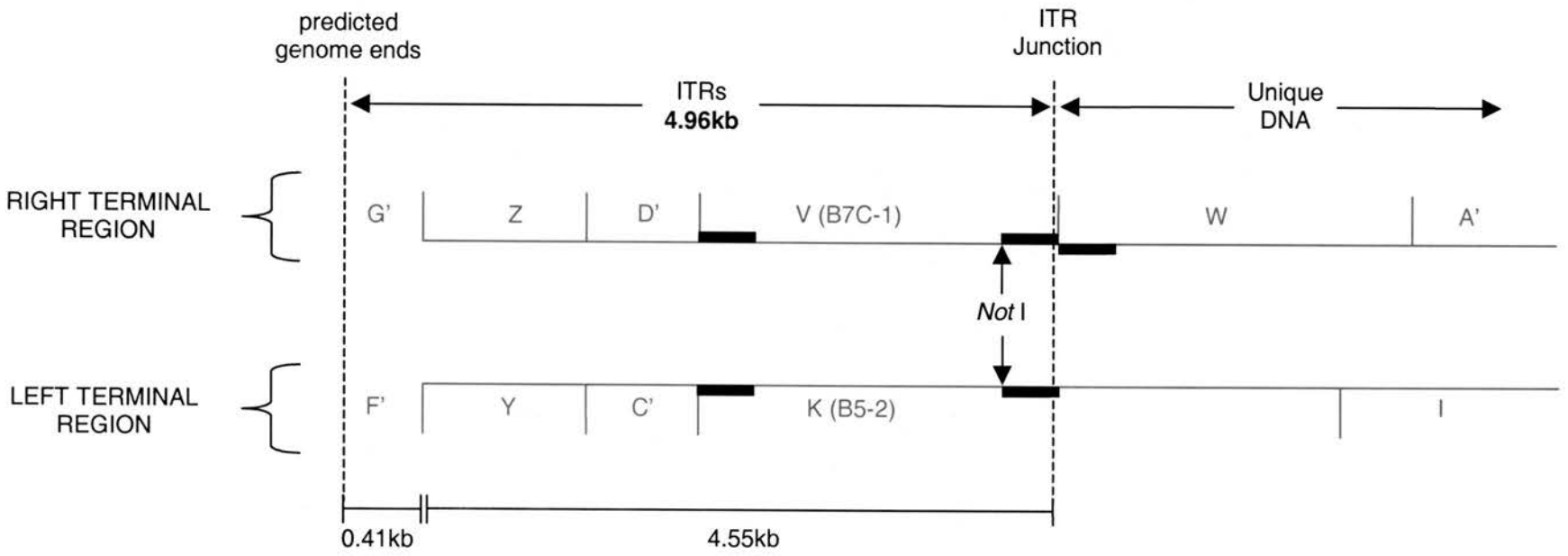

Figure 4.43 Schematic representation of the ITRs of SPPV. The blue lines depict the *Bam* HI restriction endonuclease maps of the left and right ends of the genome, the annotated *Bam* HI fragments correspond to those in figure 4.45 and table 4.6. The genome ends were predicted to be located 0.41kb beyond the *Bam* HI fragments Y and Z. The thick black bars (▬) represent regions of the genome sequenced to confirm the presence of repeated ITRs sequence, the location of the ITR junction (see figures 4.42A and B) and the G+C content around the right ITR junction. The sizes of the ITRs were predicted to be 4.96kb.

4.6 COMPLETE RESTRICTION ENDONUCLEASE MAPS OF SPPV

In order to determine the complete restriction endonuclease maps of SPPV, the ten extensively overlapping cosmid clones were aligned with each other via the *Bam* HI, *Kpn* I, *Eco* RI and *Hin*d III sites present within the overlapping regions (figure 4.44). The positions of restriction sites correlated extensively between overlapping clones. Furthermore, the locations of the *Bam* HI and *Kpn* I sites also correlate with previously mapped regions designated as clusters 1, 2, 3A and 3B (sections 4.2.4, 4.2.5 and 4.2.7), which indicates the accuracy of the restriction maps constructed using the cosmid clones.

The complete restriction endonuclease maps for the *Bam* HI, *Kpn* I, *Eco* RI, and *Hin*d III sites and a partial map of the *Not* I sites are presented in figure 4.45. As previously established (section 4.5.1), the terminal *Kpn* I fragments (designated as J and D in figure 4.45) are approximately 5.3 and 9.0kb in size. Therefore the genome ends were predicted to be located 5.3kb left of the *Kpn* I fragment V and 9.0kb right of *Kpn* I fragment B'. This corresponds to the genome ends being situated 0.41kb beyond the cloned and mapped *Bam* HI fragments of clusters 3A and 3B, hence the terminal *Bam* HI fragments, F' and G' were estimated to be approximately 0.41kb in size.

The size of the *Bam* HI and *Kpn* I fragments were estimated from agarose gels of cosmid clone DNA completely digested with *Bam* HI or *Kpn* I and where possible, compared with the size of individually cloned *Bam* HI and *Kpn* I fragments. However, the majority of *Eco* RI and *Hin*d III fragments often spanned more than one cosmid clone and were too large to be estimated from agarose gels. Therefore the sizes of the *Eco* RI and *Hin*d III fragments were estimated by calculating the distances between adjacent *Eco* RI and adjacent *Hin*d III sites on a diagram drawn to scale. Summation of the approximate sizes of the restriction fragments (table 4.6) indicated that the SPPV genome is approximately 158kb in size.

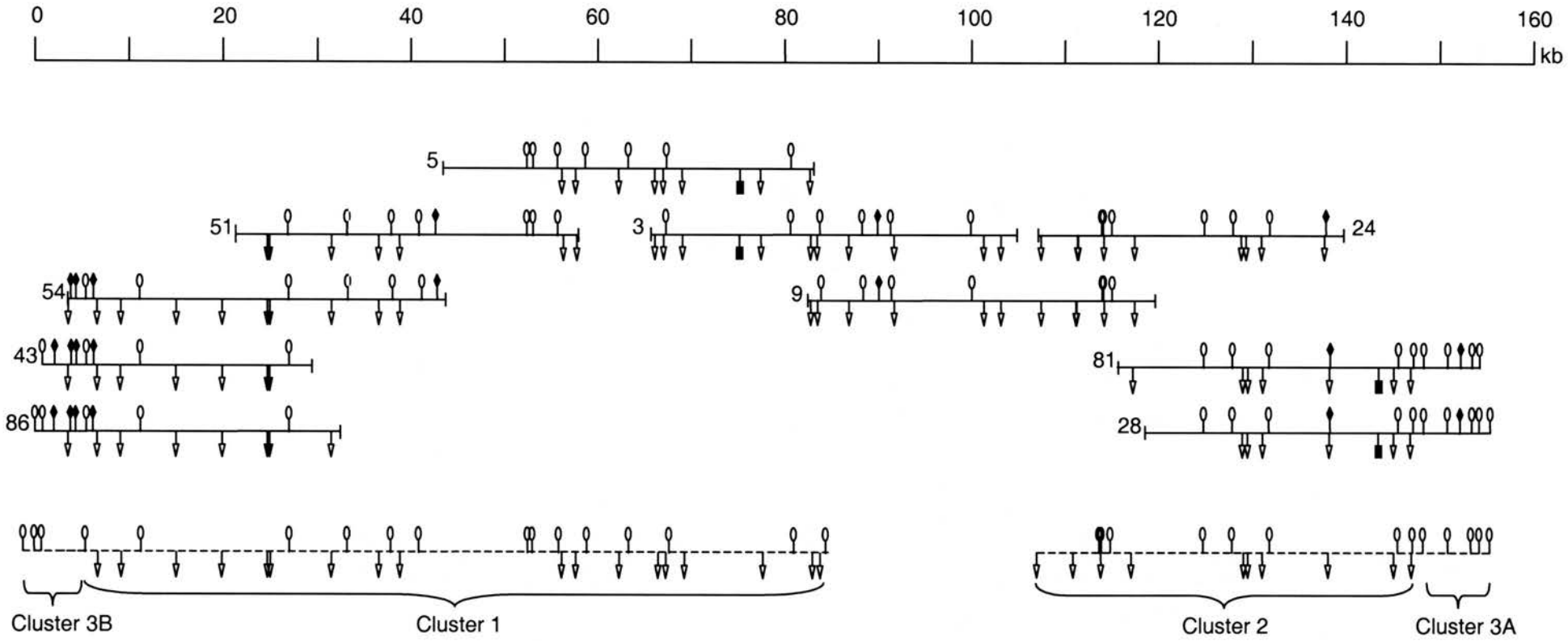

Figure 4.44 Schematic representation of the cosmid clones aligned with each other via *Bam* HI ( ), *Kpn* I ( ), *Hin*d III ( ) and *Eco* RI ( ) restriction endonuclease sites located within the overlapping regions (drawn to scale). Likewise the previously mapped regions; clusters 1, 2, 3A and 3B (see broken lines) aligned with the overlapping cosmid clones via *Bam* HI and *Kpn* I sites.

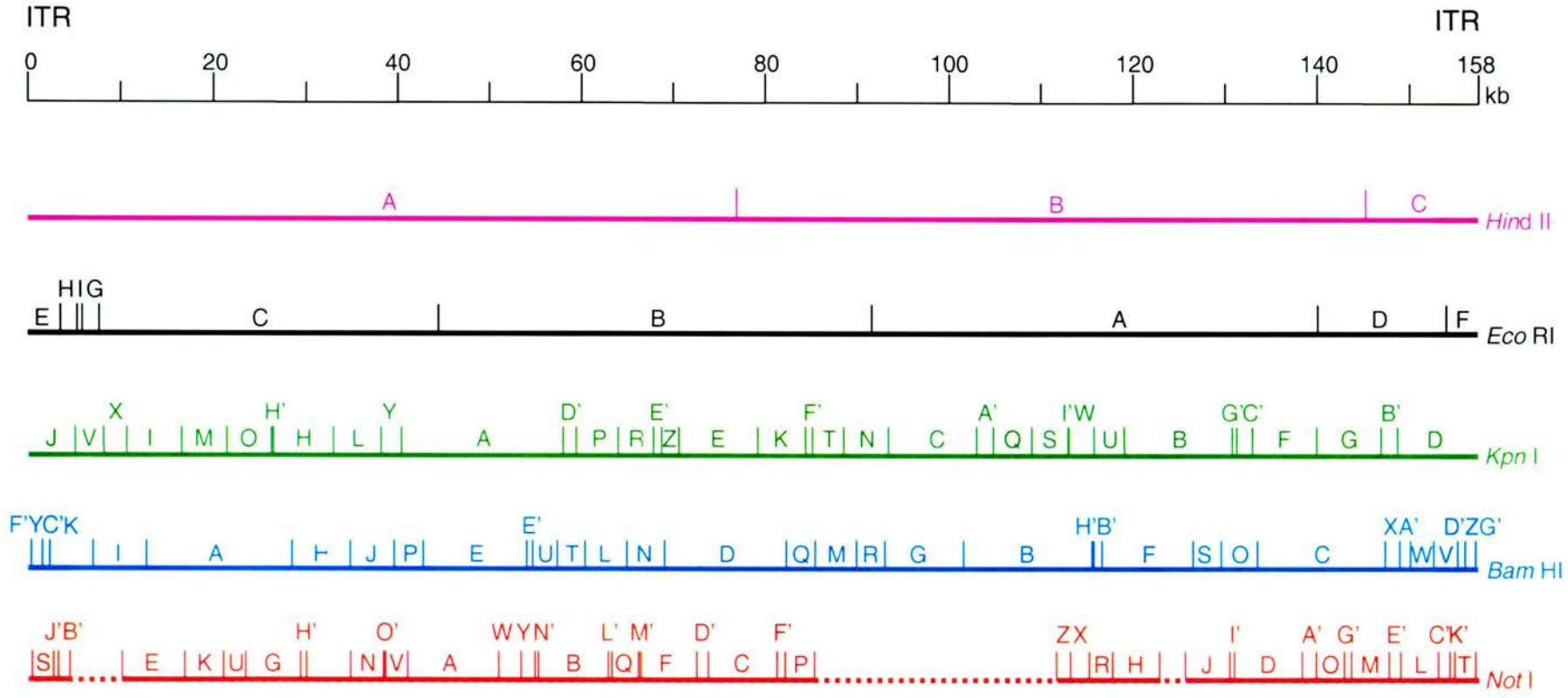

Figure 4.45 Schematic representation of the complete *Hind* III, *Eco* RI, *Kpn* I and *Bam* HI restriction endonuclease maps of SPPV and the partial map of the *Not* I sites. The regions of genome where the locations of *Not* I sites are unknown are represented by broken lines. Each fragment is labelled with a letter, which correspond to the approximate fragment sizes summarised in table 4.6. The inverted terminal repeats (ITR), which are approximately 4.96kb in size, are shaded in grey. Fragments were labelled A to Z, where there are more than 26 fragments subsequent fragments were assigned the nomenclature A', B' etc.

Fragments	*Not* I	*Kpn* I	*Bam* HI	*Eco* RI	*Hin*d III
A	10.1	17.5	15.8	48.9	76.8*
B	7.75	11.7	14.0	47.6	69.0
C	7.4	9.6	13.8	35.1	12.4*
D	7.25	9.0*	13.3	14.1	
E	6.6	8.4	11.35	3.9*	
F	5.75	7.1	9.9	3.9*	
G	5.45	6.85	8.6	1.9	
H	5.3	6.55	6.3	1.8	
I	5.15	5.9	5.7	0.6	
J	4.7	5.3*	4.75		
K	4.3	5.25	4.65		
L	4.15	5.05	4.6		
M	4.1	4.9	4.5		
N	3.75	4.85	4.1		
O	3.3	4.8	3.9		
P	3.1	4.65	3.15		
Q	2.8	4.3	3.15		
R	2.4	3.9	3.05		
S	2.4	3.85	3.05		
T	2.4	3.4	2.95		
U	2.35	3.25	2.65		
V	2.3	3.1	2.6		
W	2.3	2.8	2.55		
X	2.15	2.45	1.6		
Y	1.55	2.25	1.15		
Z	1.5	2.05	1.15		
A'	1.3	1.85	1.1		
B'	1.25	1.8	0.9		
C'	1.25	1.6	0.8		
D'	1.25	1.45	0.8		
E'	1.2	0.9	0.65		
F'	1.05	0.7	0.41*		
G'	0.9	0.55	0.41*		
H'	0.8	0.25	0.17		
I'	0.65	0.03			
J'	0.45				
K'	0.45				
L'	0.45				
M'	0.35				
N'	0.3				
O'	0.17				
Totals	**122.12**	**157.88**	**157.54**	**157.8**	**158.2**

Table 4.6 The approximate sizes of the *Kpn* I, *Bam* HI, *Eco* RI and *Hin*d III restriction fragments that comprise the complete genome of SPPV. The *Not* I restriction map is incomplete and therefore only the size of the fragments that have been mapped are presented here. An asterisk (*) indicates the end fragments, which are predicted to contain a terminal hairpin loop structure. For the location of each fragment refer to figure 4.45.

4.7 DISCUSSION

4.7.1 Restriction endonuclease mapping techniques

Hybridisation between overlapping cloned or isolated restriction fragments is a technique that has been successfully used to determine the restriction endonuclease maps of many poxviruses, albeit in conjunction with other techniques. For example; single restriction digests of genomic DNA to determine the number and the size of restriction fragments that constitute the genome, restriction profile analysis of singularly, doubly digested or partially digested genomic DNA, identification of the rapidly reannealing covalently linked end fragments performed by renaturing viral DNA singularly digested with a restriction enzyme and heat-denatured, and Southern blotting in order to identify and estimate the size of overlapping fragments too large to be cloned into plasmid vectors.

Extraction of SPPV DNA from scab material harvested from clinical cases consistently produced low quantities of viral DNA that appeared heavily contaminated with squirrel DNA. Hence, a clear restriction profile of SPPV could not be visualised. As a result, it was impossible to determine the number and size of restriction fragments that constitute the SPPV genome, or to map the genome using the restriction profile analysis of genomic DNA. However, Southern blotting of digested genomic DNA allowed the three restriction endonucleases: *Not* I, *Bam* HI and *Kpn* I to be selected on the basis that all the restriction fragments produced were estimated to be small enough to theoretically clone into the pBluescipt plasmid vector. It was envisaged that complete restriction endonuclease maps (with exception of the terminal fragments) could be constructed by identifying overlapping cloned fragments by hybridisation and aligning them accurately by restriction profile analysis of the cloned fragments.

This approach to mapping the genome was partially successful. In total, approximately 134kb of the SPPV genome was mapped, although in four non-contiguous blocks (termed clusters 1, 2, 3A and 3B), separated by three unmapped regions of unknown size. Extensive screening of the randomly cloned fragments by hybridisation failed to identify any restriction fragments situated adjacent to the mapped regions. Therefore, the regions between the mapped clusters could not be deduced. The reasons for the failure of hybridisation to identify adjacent to the mapped regions are numerous.

Firstly, it is likely that not all restriction fragments were cloned. The random cloning procedure was inefficient at generating large numbers of clones. Despite repeated cloning attempts, the total number of *Not* I, *Bam* HI and *Kpn* I clones generated was only 655. Physical damage such as shearing and fragmentation arising from natural decay processes or mechanical damage during the extraction procedure may have impaired the quality of the DNA, and impurities such as residual salt or phenol present in the extracted DNA preparation may have also reduced cloning efficiencies.

It is a reasonable assumption that a number of the clones generated using the random cloning procedure are not viral in origin. As previously explained, a proportion of the extracted DNA was squirrel genomic DNA, therefore cloning of the contaminating DNA would occur alongside the cloning of viral DNA. Although the percentage of contaminating clones within the genomic libraries was not determined, it is likely that the actual number of viral clones in the libraries is far less than the total number of clones. These problems could have been overcome by expanding the size of the genomic libraries and subsequently screening more clones, however this was not possible as the supply of scab from isolate 1296/99 was limited. Increasing the amount of DNA available by pooling material extracted from different scab isolates was not considered appropriate, as isolates of the same parapoxvirus species often exhibit heterogeneous restriction profiles (Wittek *et al.,* 1980; Robinson *et al.,* 1982; Rafii and Burger, 1985; Gassmann *et al.,* 1985; Robinson *et al.,* 1987; Gilray *et al.,* 1998; Mazur *et al.,* 2000), which must be the result of underlying genetic differences.

The possibility that some of the *Bam* HI and *Kpn* I fragments were too large to clone was ruled out. It was predicted from the southern blot of digested genomic SPPV DNA (figures 4.1 and 4.2) and later confirmed from the complete restriction endonuclease maps that none of the *Bam* HI and *Kpn* I restriction fragments were larger than could be theoretically cloned into the pBluescript vector. In fact the two largest fragments: *Kpn* I fragment A and *Bam* HI fragment A, were successfully cloned into pBluescript using the random cloning procedure (clones pK47-1 and pB3-1).

Secondly, it is possible that cloned fragments situated adjacent to the mapped regions were not detected by hybridisation because of the close proximity of two or more restriction sites. For example, at the left end of cluster 3A the *Not* I and *Bam* HI sites are located within 100bp of

each other. Theoretically the colormetric DIG-system is able to detect fragments overlapping by 100bp, however in practice, particularly when screening bacterial colonies sensitivity was much reduced. Improving the sensitivity of hybridisation and detection by using a sensitive detection system such as ^{32}P or confining library screening to purified cloned DNA rather than screening bacterial colonies would have been time-consuming, but may have overcome these problems.

Due to the limited success of restriction mapping the SPPV genome using restriction fragments cloned into a plasmid vector, a second method was sought in order to complete the restriction endonuclease maps. Contiguous stretches of DNA approximately 30kb to 42kb in length were cloned into a cosmid vector. The commercially available SuperCos I cosmid vector (Stratagene) was chosen due to the advantages that double *cos* site vectors offer over traditional single *cos* site vectors. The extra *cos* site eliminated the need to dephosphorylate the vector to prevent packaging of cosmid concatamers into the phage capsids. This allowed the insert DNA to be dephosphorylated, preventing the multiple insertion of fragments into the cloning site, thus removing the need to size fractionate the insert DNA. As size fractionation generally results in a large loss of DNA, the SuperCos I vector was particularly useful in this study where DNA was in short supply. Due to the limited quantity of SPPV, DNA extracted from the wild type scab isolate 1296/99 was mixed with a carrier DNA in a ratio of 1:4 prior to cloning. The carrier DNA source was rainbow trout (*Oncorhynchus mykiss*). This was selected due to the low G+C content: approximately 40 to 50% G+C (R. Sharif personal communication) and the abundance of fish tissue in the laboratory where this study was performed. It was predicted that the use of a carrier DNA with a low G+C content would allow differentiation between the G+C rich SPPV clones and the A+T-rich carrier DNA clones when the library was screened with DIG-labelled probes.

The previously mapped and cloned restriction fragments were utilised in screening the cosmid library. The selection of mapped restriction fragments from along the entire length of the SPPV genome enabled SPPV cosmid clones to be identified by hybridisation and their approximate location within the SPPV genome to be estimated. Furthermore, comparison of the previously mapped regions with the restriction profiles of the cosmid clones enabled ten cosmid clones to be selected that were predicted to overlap extensively with each other and span the entire length of the genome (with the exception of the end fragments containing hair pin loop structure). Detailed restriction endonuclease maps of the *Bam* HI, *Kpn* I and *Eco* RI were determined using

the partial digest and end-labelling method developed by Rackwitz *et al.,* (1984 and 1985). However, the *Not* I sites occurred too frequently for the partial digest and end-labelling method to be used successfully, therefore the *Not* I map was not completed. As only four cosmid clones possessed a *Hin*d III site, therefore the complete *Hin*d III map was easily determined using only restriction profile data.

The advantages of the cosmid mapping method were; it was rapid, and it was easily adapted for a number of restriction endonucleases. However, the plasmid cloning method enabled many locations along the SPPV genome to be easily sequenced without the need to perform time-consuming subcloning of the cosmid clones.

4.7.2 General structure of the genome

SPPV was formally classified as a parapoxvirus (van Regenmortel *et al.,* 2000) based upon the morphological similarities to parapoxvirus particles (Scott *et al.,* 1981), however, until now, no molecular evidence to support or disprove the classification of SPPV as a parapoxvirus has been provided. The average G+C content of the SPPV genome is estimated to be 66.4% (table 4.3), which is comparable to the G+C content found in parapox and molluscipox virus genomes (Wittek *et al.,* 1979; Senkevich *et al.,* 1997). The estimated size of the SPPV dsDNA genome is approximately 158kb, making it the largest of the classified parapoxviruses. The size of parapoxvirus genomes generally lie within a range of 130 to 150kb (van Regenmortel *et al.,* 2000). However this size range is misleading, as wild type parapoxviruses and low passaged tissue-cultured viruses generally range from 139kb to 145kb (Menna *et al.,* 1979; Robinson *et al.,* 1982; Robinson *et al.,* 1987; Horner *et al.,* 1987; Mercer *et al.,* 1987; McInnes *et al.,* 2001), whilst parapoxviruses exceeding 145kb in size are all virus strains that have been extensively passaged in tissue culture. The larger size of parapoxviruses serially passaged in tissue culture have been shown to be the result of genomic rearrangement of the terminal sequences by duplication, transposition and deletion events (Rafii and Burger, 1985; Fleming *et al.,* 1995; Cottone *et al.,* 1998; McInnes *et al.,* 2001). The SPPV used in this study was a wild type isolate and therefore its larger size is not the result of adaptation to tissue culture. The size of MOCV subtype 1 is approximately 190kb (Senkevich *et al.,* 1997) and little variation in size exists between different isolates and subtypes of MOCV (Burgert and Darai, 1991). SPPV is approximately 13kb larger than wild-type parapoxviruses and 32kb smaller than MOCV; hence the SPPV genome does not correspond in size to any of the G+C-rich poxviruses characterised

so far. The only poxviruses that correspond in size to SPPV belong to the leporipoxvirus genus, which are approximately 160kb in size (Delange AM, 1984; Russell and Robbins, 1989). However, the G+C content of leporipoxvirus genomes is approximately 40% (Cameron *et al.*, 1999; Willer *et al.*, 1999). To date, closely related viruses assigned to the same genera always have comparable G+C composition (van Regenmortel *et al.*, 2000). Therefore, on the basis of G+C content, SPPV is unlikely to belong in the leporipoxvirus genus.

The ITRs of SPPV were estimated to be approximately 4.96kb and they presumably terminate with hairpin loop structures, which are common to all poxviruses. The size of ORFV ITRs vary from 3.1kb to 3.4kb for the wild type viruses (Fraser *et al.*, 1990; McInnes *et al.*, 2001) and up to 18kb for the larger tissue-culture adapted viruses (Cottone *et al.*, 1998). The ITRs of MOCV are approximately 4.7kb (Senkevich *et al.*, 1997), whilst the ITRs of leporipoxviruses are much larger at approximately 11.5kb to 12.4kb (Upton *et al.*, 1987; Cameron *et al.*, 1999; Willer *et al.*, 1999). Therefore in terms of size the ITRs are most like the molluscipoxviruses. Analysis of nucleotide sequence derived from within the ITR of SPPV (figures 4.42A and B) suggested a G+C content of approximately 65.3%. Hence, the G+C content of the central region of the genome is maintained towards the termini as in molluscipoxviruses and parapoxviruses (Fraser *et al.*, 1990; Senkevich *et al.*, 1997). Further analysis of the right-terminal sequence of SPPV revealed that the DNA sequence that spans the ITR junction (extending 300bp left and right of the right-ITR junction) is extremely G+C-rich at 72.67%. This situation is also evident in ORFV, with the corresponding 600bp right-terminal region also extremely G+C-rich at 83.67% (EMBL accession number M30023). In contrast the same region in MOCV (EMBL accession number U60315) is less G+C-rich at 66.17%.

Fundamental differences in the frequency of restriction sites exist between SPPV and parapoxvirus genomes. For example, one striking difference is the frequency of *Bam* HI sites, in SPPV there are thirty-three sites whilst in ORFV isolates there are between ten and twelve sites (Robinson *et al.*, 1987; Mercer *et al.*, 1987; McInnes *et al.*, 2001). Consequently, the *Bam* HI, *Eco* RI, *Kpn* I and *Hin*d III restriction endonuclease maps of SPPV do not resemble restriction maps or correspond to restriction profiles of wild-type isolates or low passaged strains of ORFV, BPSV, PCPV and PNZV (Menna *et al.*, 1979; Wittek *et al.*, 1980; Robinson *et al.*, 1982; Rafii and Burger, 1985; Gassmann *et al.*, 1985; Robinson *et al.*, 1987; Horner *et al.*, 1987; Mercer *et al.*, 1987; Gilray *et al.*, 1998; McInnes *et al.*, 2001). This was not unexpected, because unlike the

orthopoxviruses, the different species of wild-type or low passaged parapoxviruses are highly divergent in restriction profiles (Wittek *et al.,* 1977; Esposito *et al.,* 1978; Mackett and Archard, 1979; Wittek *et al.,* 1980; Esposito and Knight, 1985; Gassmann *et al.,* 1985; Robinson and Mercer, 1995). Therefore, if SPPV is a separate species belonging to the parapoxvirus genus, the restriction map is unlikely to resemble previously characterised parapoxvirus species. Likewise, the restriction maps of SPPV did not correspond to any of the published profiles of MOCV subtypes 1, 2 and 3 (Porter and Archard, 1992). Therefore the use of restriction profile analysis to establish the relationship of SPPV to the parapoxviruses is unsuitable due to the lack conservation between the different parapoxvirus species.

In this chapter the base pair composition of the SPPV genome and restriction endonuclease maps are presented, however these alone are not sufficient to determine the genetic relationship of SPPV to other poxviruses. Therefore in the next chapter the general relationship of SPPV with parapoxviruses are investigated using cross-hybridisation between SPPV and ORFV. The relationship of SPPV to other poxviruses is also discussed, with reference to the establishment of a genetic map and direct comparison of the organisation of the SPPV genome with other poxviruses.

CHAPTER 5.0

GENETIC COMPOSITION OF THE SPPV GENOME AND ITS RELATIONSHIP WITH OTHER POXVIRUSES

5.1 INTRODUCTION

Restriction endonuclease profiles of viruses belonging to the orthopox, avipox and capripox virus genera have shown that the genomes are highly conserved in a genus-specific manner (Mackett and Archard, 1979; Esposito and Knight, 1985; Schnitzlein *et al.,* 1988; Gershon and Black, 1988). Whereas, restriction endonuclease maps are similar only in a species-specific or subtype-specific manner for poxviruses belonging to the parapox, molluscipox and leporipox virus genera (Wittek *et al.,* 1980; Porter and Archard, 1992; Cabirac *et al.,* 1985). As previously established the restriction profile of SPPV does not resemble that of any characterised parapoxvirus species to date (chapter 4.0). Therefore restriction mapping and profiling is a useful technique, but has limitations in determining the genetic relationship of a newly classified member of the parapoxvirus genus, like SPPV, with existing member species.

Cross-hybridisation of genomic DNA from different poxvirus species has been used to characterise the relationship between species and determine organisation of poxvirus genomes (Mackett and Archard, 1979; Esposito and Knight, 1985; Gershon and Black, 1988; Porter and Archard, 1992). However due to the disparate G+C composition of poxvirus genomes, comparison by hybridisation is only possible between viruses with similar G+C contents. For this reason hybridisation of the SPPV genome is only possible with the other G+C rich genomes found in the parapox and molluscipox viruses, and not with the orthopoxvirus genomes.

Cross-hybridisation of the genomes of different parapoxvirus species has demonstrated that the central regions of parapoxvirus genomes are highly related, however the terminal regions only cross-hybridise between isolates of the same species and are therefore species-specific (Gassmann *et al.,* 1985). Identification of the regions of the SPPV and ORFV genomes that hybridised extensively with each other would be useful in determining the level of conservation between the two genomes. Conversely, the identification of the regions of the SPPV genome which did not hybridise with ORFV DNA would be equally valuable as it would indicate regions which were relatively more divergent from ORFV or even unique to SPPV.

The complete DNA sequencing of several poxvirus genomes has increased our understanding of the relationship between different poxvirus genera and species (Goebel *et al.,* 1990; Massung *et al.,* 1994; Senkevich *et al.,* 1997; Cameron *et al.,* 1999; Willer *et al.,* 1999; Afonso *et al.,* 2000; Tulman *et al.,* 2001; Lee *et al.,* 2001; Afonso *et al.,* 2002; Shchelkunov *et al.,* 2002; Gubser and Smith, 2002). Taken together, restriction endonuclease maps, hybridisation and sequencing have revealed that poxvirus genomes consist of a conserved central core of genes that are generally essential for the replication of the virus and the production of infectious progeny virus. Flanking

the central core are the variable regions, which contain genes non-essential for replication and are often genus or species-specific. Many of these genes are homologues of cellular genes, some of which have been shown to confer a replication advantage to the virus *in vivo* (Bugert and Darai, 2000).

Sequencing at defined points along the genome was employed in this study to produce a genetic map of SPPV to allow a detailed comparison of the organisation of the SPPV genome with other poxviruses. In addition, sequence was obtained from the regions that were predicted to be divergent from ORFV by hybridisation (section 5.2) in order to investigate the presence of species-specific genes.

5.2 GENERAL RELATIONSHIP BETWEEN SPPV AND ORFV

SPPV cosmid clones 3, 5, 9, 24, 28, 43, 51, 54, 81 and 86 were previously characterised and shown to overlap extensively and span the entire genome of SPPV with the exception of the terminal 0.4kb (section 4.5.1). The cosmid clones were digested with the restriction endonuclease *Kpn* I and the resulting fragments separated by electrophoresis in a 0.5% agarose gel. Southern blots were prepared and hybridised with digoxygenin (DIG) labelled probes derived from eleven regions of the ORFV strain orf-11 genome and the ITR region of MRI scab isolate (McInnes *et al.*, 2001). The locations of the probes within the ORFV genomes are shown in figure 5.1.

ORFV was the parapoxvirus chosen for the comparison as it is the most well characterised species of the parapoxvirus genus, with preliminary genetic maps of ORFV strains NZ2 and D1701 having been published (Mercer *et al.*, 1995; Buttner and Rziha, 2002) and a preliminary genetic map of Orf-11 available in the laboratory where this study was performed.

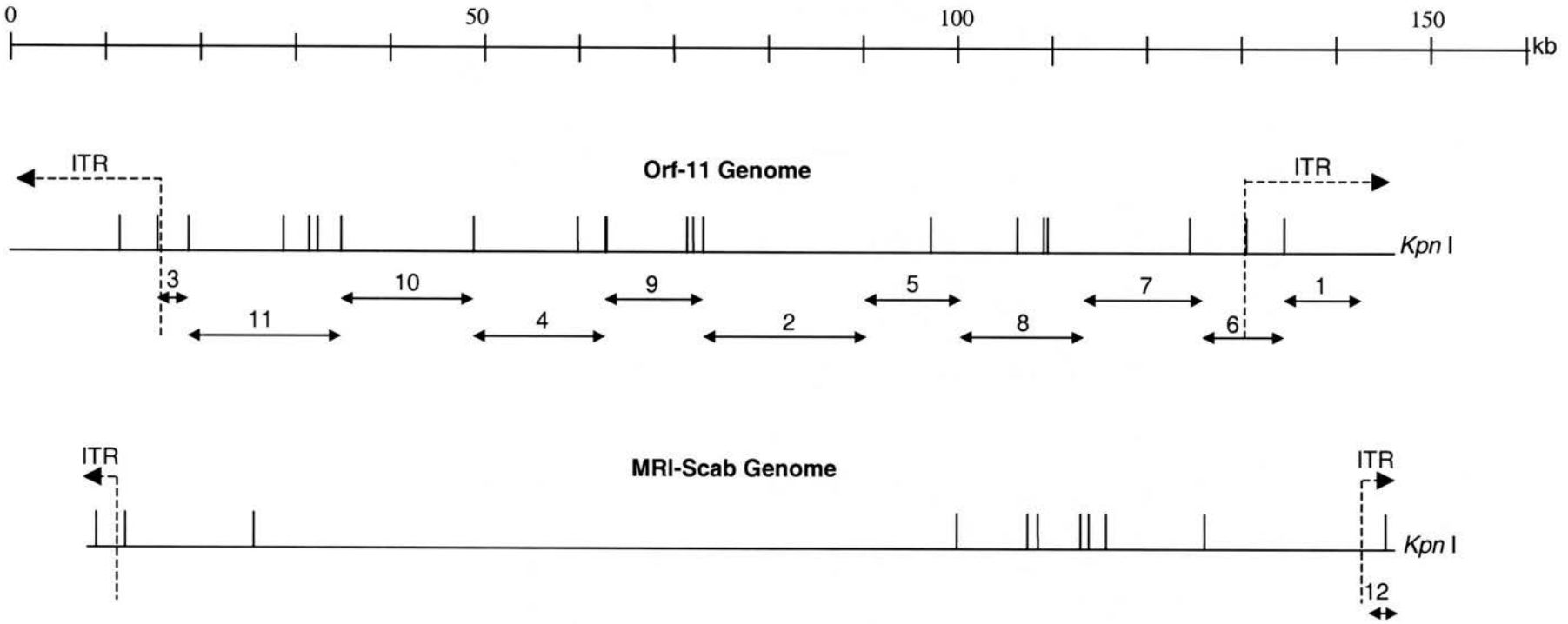

Figure 5.1 *Kpn* I restriction endonuclease maps of ORFV strain orf-11 and MRI-scab isolate (adapted from McInnes *et al.,* 2001, with permission). The broken lines indicate the position of the ITR junctions. The double-ended arrows below the ORFV genomes show the locations of the probes prepared from cloned ORFV restriction fragments labelled with digoxygenin (section 2.4.5.1.2). The number above each arrow corresponds to the identification number of each probe.

5.2.1 Hybridisation of SPPV with ORFV

The SPPV *Kpn* I fragments which hybridised with the ORFV probes are summarised in table 5.1. Probes 1, 2, 3, 4, 5, 7, 8, 9, 10 and 11 all hybridised with SPPV, however probes 6 and 12 did not. A schematic representation of which ORFV probes hybridised with which SPPV *Kpn* I restriction fragments is shown in figure 5.2, and is described in more detail in the text that follows.

Probes 2, 3, 4, 5, 7, 8, 9, 10 and 11 all hybridised with SPPV *Kpn* I fragments in an order identical to the order of the probes themselves, demonstrating a general genetic relationship and a high degree of collinearity between the SPPV and ORFV genomes. There were few *Kpn* I fragments within this region which did not hybridise with the ORFV probes. This collinear and cross-hybridising region in SPPV extended from approximately 17kb to 133kb and as a result is predicted to form the conserved central core of the genome. However several differences were noted between the viruses towards the ends of the genomes.

Probes 3, 7, 8 and 11, derived from the near terminal regions of the ORFV genome hybridised with several SPPV *Kpn* I fragments located towards the ends of the SPPV genome. However, the hybridisation signal between these ORFV probes and some of the SPPV *Kpn* I fragments was weak when compared with that of the control ORFV DNA. For example, probe 11 hybridised with SPPV *Kpn* I fragments extending from fragment O near the left end of the SPPV genome to fragment Y located towards the centre (figure 5.3A). Fragments Y, L and H (respective sizes 2.25, 5.05 and 6.55kb) hybridised strongly with probe 11, however fragment O (4.8kb) hybridised weakly. No hybridisation signal was detected with fragment H' (0.25kb), which is situated between fragments O and H. Likewise probe 3 hybridised weakly with a *Kpn* I fragment corresponding to *Kpn* I fragment M (figure 5.3B). A similar situation was also observed with probe 8. Probe 8 hybridised strongly with the SPPV *Kpn* I fragments corresponding in size to U and B. However, weak hybridisation was also detected with fragments corresponding in size to S and W. Fragment I', which is situated between fragments S and W, did not hybridise.

Probe 7, which spans a 12.7kb region of the ORFV genome hybridised with *Kpn* I fragment C', which is only 1.6kb in size. The fragments flanking C' did not hybridise with probe 7 (figure 5.3C).

Kpn I fragment	Size (kb)	*Kpn* I fragments spanned by the cosmid clones										Hybridisation ORFV probe
		86	43	54	51	5	3	9	24	81	28	
J	5.3	●	●	●								NH
V	3.1											NH
X	2.45											NH
I	5.9											1
M	4.9											3*
O	4.8				●							11*
H'	0.25											NH
H	6.55		●									11
L	5.05	●										11
Y	2.25											11
A	17.5			●		●						10
D'	1.45											4
P	4.65				●							4
R	3.9						●					4
E'	0.9											9
Z	2.05											9
E	8.4											9
K	5.25							●				9 and 2
F'	0.7					●						2
T	3.4											2
N	4.85											2
C	9.6											2
A'	1.85											5
Q	4.3						●		●			5
S	3.85											8*
I'	0.03											NH
W	2.8											8*
U	3.25									●		8
B	11.7							●			●	8
G'	0.55											NH
C'	1.6											7
F	7.1											NH
G	6.85								●			NH
B'	1.8											NH
D	9.0									●	●	NH

Table 5.1 Summary of the SPPV *Kpn* I fragments (listed in the first column from the left end to the right end of the genome with their sizes listed in column 2) which hybridised with the ORFV DIG-labelled probes depicted in figure 5.1. Hybridisations were performed with *Kpn* I digested cosmid clone DNAs, the region of the SPPV genome each cosmid clone overlaps is indicated in columns 3 to 12 by the bars (●——●). Column 13 summarises the ORFV probes that hybridised with SPPV *Kpn* I fragments, a * suffix indicates that the hybridisation was very weak and NH indicates that the *Kpn* I fragment did not hybridise with any of the ORFV probes. A schematic representation of this data is presented in figure 5.2.

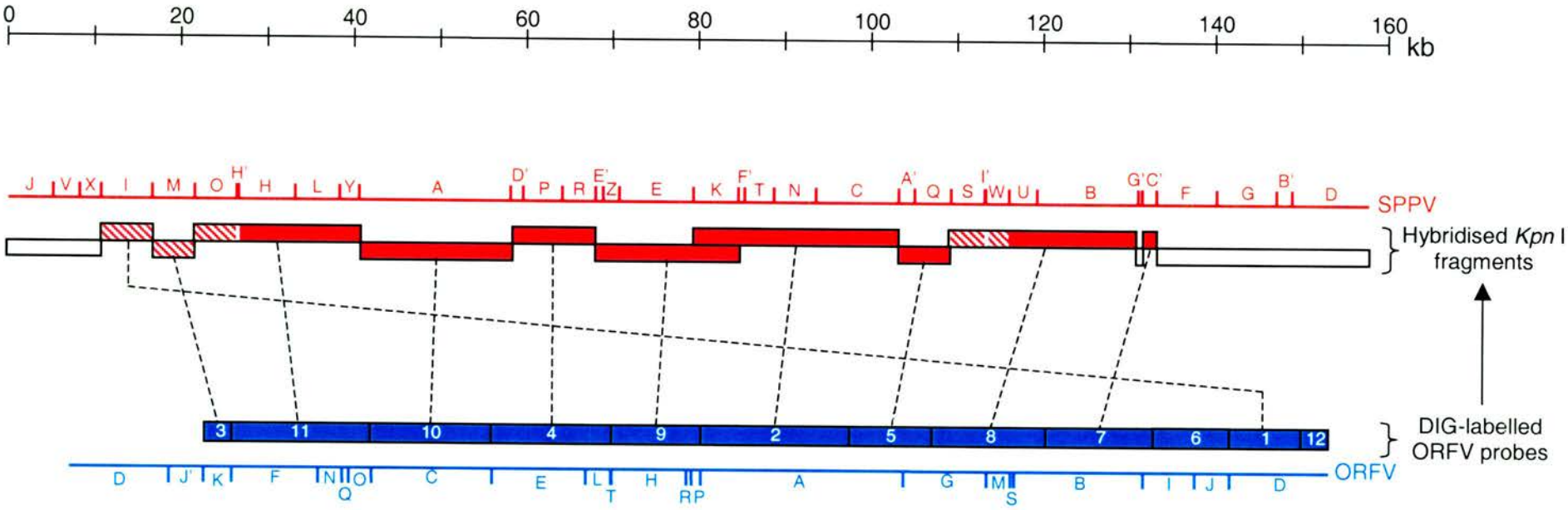

Figure 5.2 Schematic representation of the data presented in table 5.1, detailing the hybridisation of the ORFV genome (strain orf-11) with the SPPV genome (isolate 1296/99). The ORFV genome was subdivided into 12 regions (designated probes 1 to 12 and represented by the blue boxes). Each ORFV DIG-labelled probe was individually hybridised with Southern blots of cloned SPPV DNA digested with *Kpn* I (see figures 5.3 and 5.4). The boxes shaded in red denote the region of the SPPV genome that hybridised with each ORFV probe (except probes 6 and 12), as indicated by the broken lines. Areas of the boxes that are shaded in solid red represent *Kpn* I fragments that hybridised strongly, whilst the area that are crosshatched represent *Kpn* I fragments that hybridised weakly and the white areas *Kpn* I fragments that did not hybridise with any of the ORFV probes.

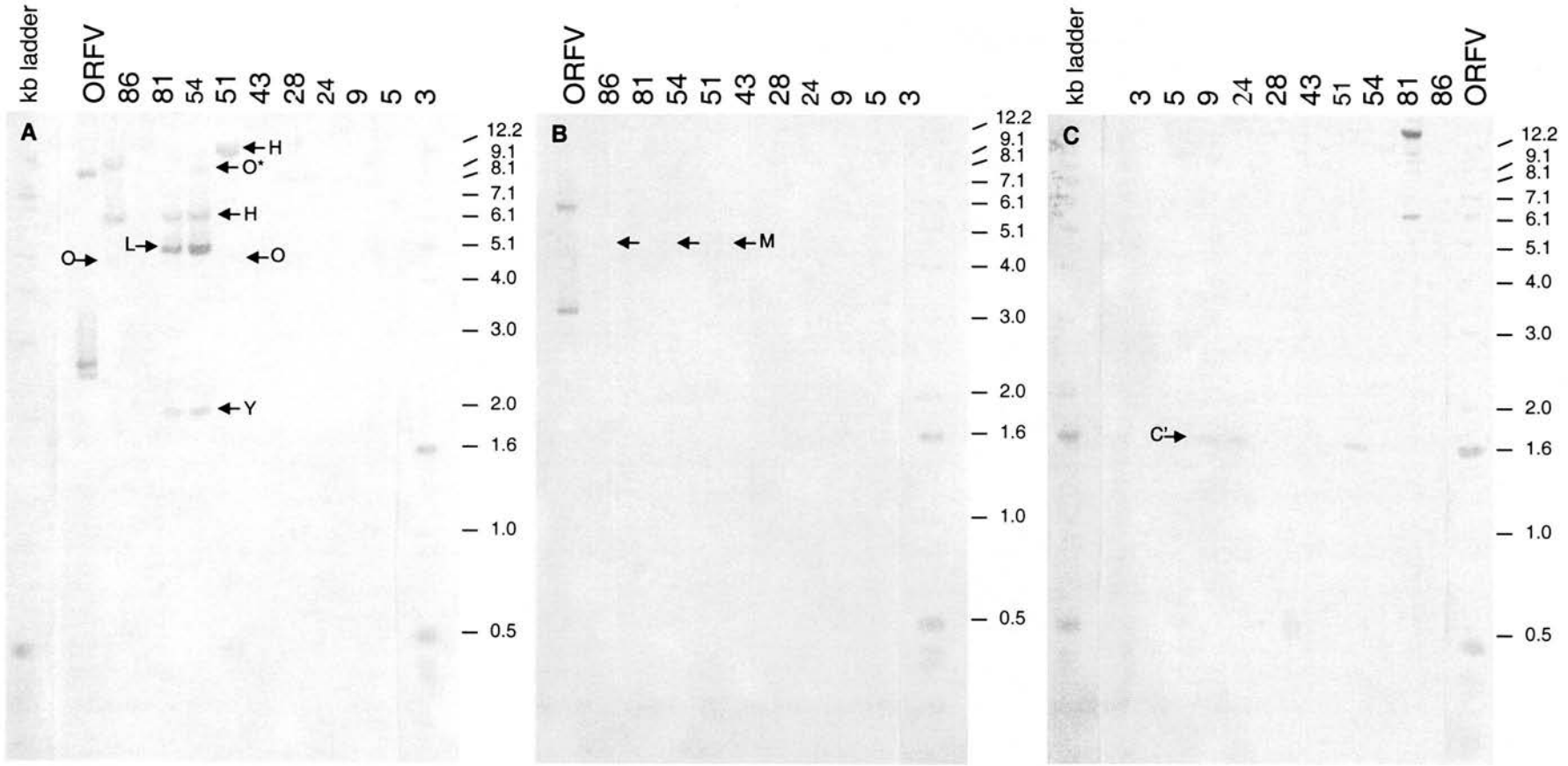

Figure 5.3 Southern blots of SPPV DNA cloned into cosmids and ORFV (orf-11) genomic DNA digested with *Kpn* I and hybridised with (A) ORFV probe 11, (B) ORFV probe 3 and (C) ORFV probe 7. The hybridised SPPV *Kpn* I fragments are indicated with arrows and their identification letter. The end fragments that partially overlap a *Kpn* I fragment and are attached to the cosmid vector have an asterisk suffix (eg. O*).

Seven consecutive *Kpn* I fragments (B', D, F, J, G, V and X) located at the ends of the SPPV genome did not hybridise with any of the ORFV probes. In addition, the ORFV probes 6 and 12, which are located at the ends of the ORFV genome also did not hybridise with SPPV. The lack of or weak hybridisation observed between the end fragments of ORFV and SPPV is probably due to divergence at the nucleotide level. In support of these observations, cloned SPPV DNA was labelled with DIG and hybridised with ORFV (orf-11) *Kpn* I restriction fragments using the same hybridisation conditions as hybridisation of SPPV with the ORFV probes. The results correlated well with the hybridisation of SPPV with ORFV in that the central region of the two genomes hybridised extensively, whilst the terminal regions showed little or no hybridisation (results not shown).

The hybridisation conditions employed in this study were relatively stringent. Hybridisation and the subsequent washes of the Southern blots were performed at high temperature (65°C) with a wash solution of a low salt concentration (0.5X SSC). It was predicted that the stringent conditions would enable the regions of the SPPV genome that are highly conserved with ORFV and those regions that are less so to be distinguished. Therefore, the SPPV *Kpn* I fragments that did not hybridise with ORFV DNA are not necessarily unique to SPPV. Instead they may just lack sufficient homology to ORFV to enable hybridisation to be detected at the stringency used. Hence, the regions that are unique to SPPV and regions divergent from ORFV cannot be distinguished using this hybridisation technique alone.

Interestingly probe 1, which is derived from the right-end of the ORFV genome hybridised with the *Kpn* I fragment I, which is situated at the left-end of SPPV (figure 5.4). Therefore it appears that the left-end of the SPPV genome shares DNA homology with the right-hand end of wild type ORFVs, suggesting a translocation of sequence in SPPV with respect to ORFV.

In summary the central region of SPPV extending from 17kb to 133kb generally hybridised with ORFV in a collinear order, suggesting a high degree of relatedness between the two viruses. However, the terminal regions of the SPPV genome consist of non-hybridising fragments and a possible translocation of sequence with respect to ORFV. On the basis of hybridisation, the terminal regions of the SPPV genome (extending from 0kb to 17kb and 133kb to 158kb) were predicted to be the most divergent from ORFV.

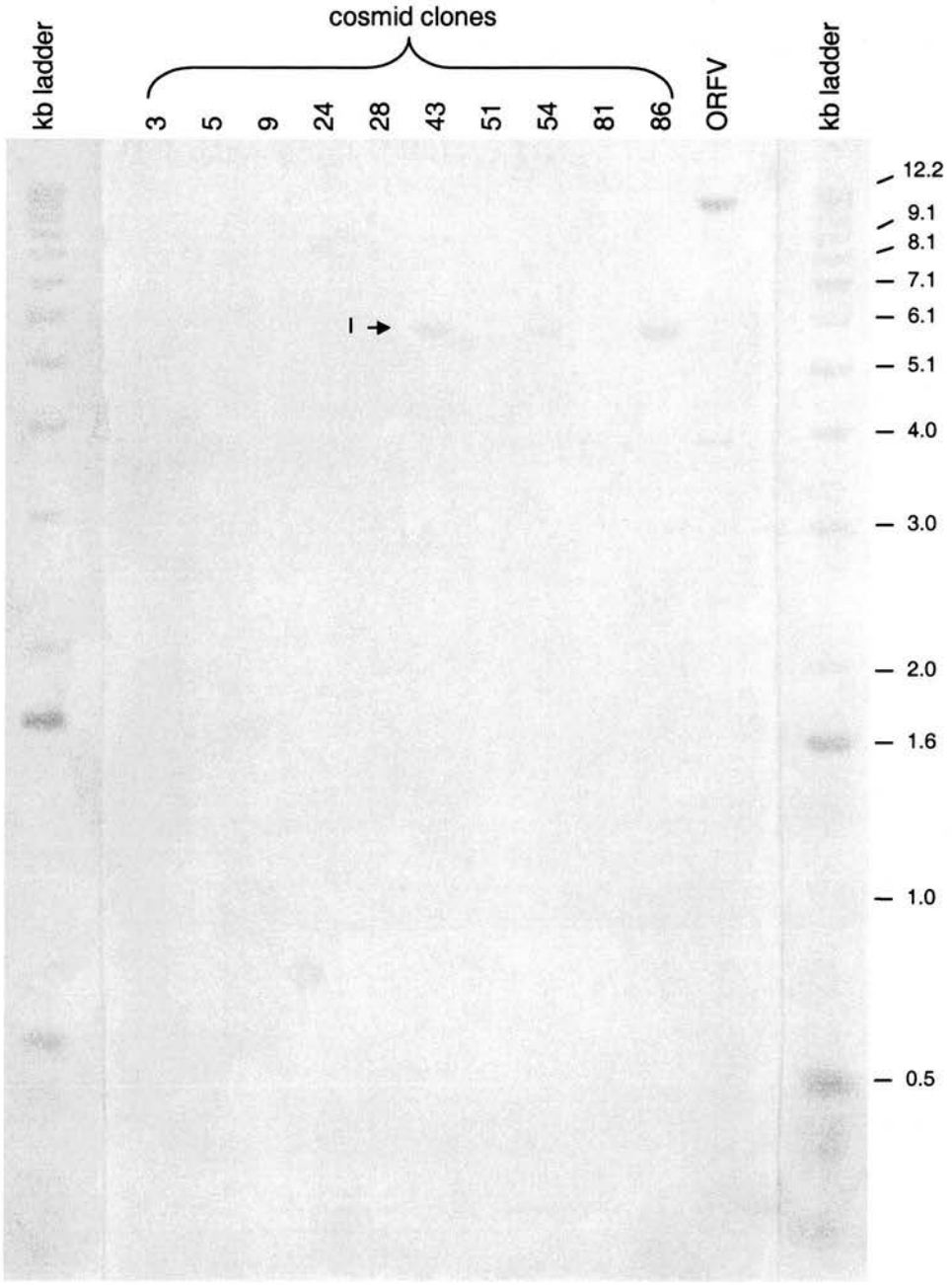

Figure 5.4 Southern blot of SPPV DNA cloned into the SuperCos I cosmid vector and ORFV (orf-11) genomic DNA digested with *Kpn* I and hybridised with ORFV probe 1. A strong hybridisation signal can be seen with the ORFV control DNA and a weak hybridisation signal with SPPV *Kpn* I fragment I.

5.3 DNA SEQUENCING OF THE SPPV GENOME

The differences noted between the SPPV and ORFV genomes, when compared by hybridisation (section 5.2) may be a result of differences in the complement of genes present, their homology at a nucleotide level and the order/spatial distribution of genes.

To further characterise these differences short lengths of DNA sequence were obtained from a number of defined locations in the SPPV genome. Particular attention was paid to the terminal regions of the genome in the hope of identifying genus-specific genes, which would aid in determining the taxonomic relationships of SPPV. In addition, the terminal regions may also contain genes associated with immuno-modulation and virulence. Identification of such genes may be of importance for future vaccine development. In total approximately 23kb of non-contiguous DNA of the SPPV genome was sequenced, which represent approximately 15% of the total genome. Analysis of the resulting data allowed the construction of a preliminary genetic map of SPPV.

5.3.1 Identification of homologous poxvirus genes in SPPV

Forty-seven sequences were obtained by sequencing the ends of cloned restriction endonuclease fragments (section 2.4.7). FastA analysis of each DNA sequence (section 2.4.8.1) revealed that most were homologous with the G+C rich genomes of MOCV and ORFV, however very few other poxviruses exhibited homology at the DNA level presumably because of the disparity in G+C content. Despite underlying divergence in nucleotide sequence, poxviruses encode proteins that are highly conserved in sequence (Fleming *et al.,* 1993; Mercer *et al.,* 1995). Therefore predicted amino acid sequences rather than nucleotide sequences were employed to search the databases for homologous sequence as it was considered more likely that a homologous poxvirus protein would be identified rather than a homologous DNA sequence (section 2.4.8.2).

A total of twenty-six poxvirus protein homologues were identified in this way. A further two poxvirus protein homologues (homologues of VACV F13L and MOCV 157R) were identified using targeted sequencing (sections 6.3.1 and 7.2) but are included in the genetic map and comparison with other poxviruses for completeness. In the absence of any previously described SPPV genes, the system of annotating ORFs used by Mercer *et al.,* (1995) in describing a genetic map of ORFV was adopted. Each putative protein was designated a co-ordinate code which corresponds to the location within the SPPV genome (SP) and combined with either L or R to indicate the direction (left or right) of transcription

(e.g. SP 29.9L). Whenever possible the location corresponded to the co-ordinate of the initiating methionine (indicated by a m-suffix, e.g. SP 72.2L^{m}) or the termination codon (indicated by a t-suffix, e.g. SP130.5L^{t}), when not possible the co-ordinate corresponds to the location of the restriction site at which the sequence was derived.

The nucleotide sequences that are predicted to encode poxvirus gene homologues are presented in figure 5.5 along with the translated frames, except for the homologues of VACV F13L and MOCV 157R, which are presented in sections 6.3.1 and 7.2. These data are summarised in table 5.2, along with the predicted structure and/or function of each protein. A further twenty-two DNA sequences did not contain any ORFs with recognisable identity to other poxviruses (sequences not presented).

Figure 5.5

Not I K right. SP 21.0L^{t}
MPV C21L (49.3% over 69aa). Homologues: VACV F15L/MOCV 025L

```
TCGCGAAGGAGGTATATTTATTTTATGTTTTTTTGCGGGCGGCGGCCTCAGTCGATCTCGAATGTGGCGGACCAGAAAGACCGGATGCGG
                                    21.0L^t →  .  D  I  E  F  T  A  S  W  F  S  R  I  R
AGCCCGATGACCACGTAGAGCTGGTTGGTGGCGGTCGGCACGAAGACGTTCAGGTTCAGGTCGTGGCGGTCGCTGTTGTCCCGGTGCACG
 L  G  I  V  V  Y  L  Q  N  T  A  T  P  V  F  V  N  L  N  L  D  H  R  D  S  N  D  R  H  V
ATGCAGTAGTGGCACGTCTTGTTGTTGCGGGCGGCCTCGTCGATGCAGGAGAGGACGAACCCCGGCAGCAGGTACTGGAACTGCGGCCGC
 I  C  Y  H  C  T  K  N  N  R  A  A  E  D  I  C  S  L  V  F  G  P  L  L  Y  Q  F  Q  P  R
```

Not I U left. SP 21.4L^{m} and SP 21.7L^{m}
YMTV 29L (55.1% over 78aa). Homologues SP 21.4L^{m}: VACV F15L/MOCV 025L
MOCV 026L (42.1% over 76aa). Homologues SP 21.7L^{m}: MOCV 026L only.

```
GCGGCCGCTGGAAGTGGAACAGCGAGAACAGCAGCTCCGAGAGCGTGAACTCGTGGTTGCGGAACCTGACCGTCTCGTCGGTGGTGACCG
  P  R  Q  F  H  F  L  S  F  L  L  E  S  L  T  F  E  H  N  R  F  R  V  T  E  D  T  T  V  A
CGTTGCGCGAGATGGCGCGCACCTGGGAGACCTTGACGAAGCAGCGGTTCGCCAGGACGCAGTCGCCGTCGCTGTTGATCTTGACCTTGG
  N  R  S  I  A  R  V  Q  S  V  K  V  F  C  R  N  A  L  V  C  D  G  D  S  N  I  K  V  K  T
TCATGCTCCTGAAGGGCTGCAGGGTCATCACGTCCGCCAGCTTGGAGACGTTCATGTCAGTCGGGTGATGATGCGGAGGCCGCGCAGGGG
  M  S  R  F  P  Q  L  T  M  V  D  A  L  K  S  V  N  M ← SP 21.4L^m
                                                .  T  L  R  T  I  I  R  L  G  R  L  P
CTCCCGGCAGACGTAGCAGACGGTGGCGCCCTCGGGCAGACAGTGGCGGTGGTACCCGTGCTTGCACTGGGACAAGAGAAACTCGCACTG
 E  R  C  V  Y  C  V  T  A  G  E  P  L  C  H  R  H  Y  G  H  K  C  Q  S  L  L  F  E  C  Q
GTTGCAGGAGGAGTCGCAATCGGAGCGGAGGCAGCTATCGGCGAACCTCTTACGGCATATGTAGCACGTGTCGTTGGCGGCGGGCAGGGA
 N  C  S  S  D  C  D  S  R  L  C  S  D  A  F  R  K  R  C  I  Y  C  T  D  N  A  A  P  L  S
CCACTGTATCACGGGGCTCAGAAATCTTATCGTGACTGACATTCTGAATGATCTTCAAGGTAGATTAGGATTTCACTTATTTCTGGTTGG
 W  Q  I  V  P  S  L  F  R  I  T  V  S  M ← SP 21.7L^m
```

Not I I left. SP 29.9L
VACV E4L (63% over 119aa) Homologues: MOCV 034L/ORFV 20.3L

```
GCGGCCGCCGCCTCGGCGTCCCCGGCGCCCTTCTTCTTCCGCCGCGGCGCCCGGTCCTCGTCCTCGTCGCGGCGGTCCAGTCGGTCGCGG
 A  A  A  A  E  A  D  G  A  G  K  K  K  R  R  P  A  R  D  E  D  E  D  R  R  D  L  R  D  R
AACCGCGGCGGCGCGAAGTGCTTCTGGCAGTCCCGGCACGTGTACCGGACCGTGGGCGGCTCGTCGGCCGCGCGCATCTGCACCATCATG
 F  R  P  P  A  F  H  K  Q  C  D  R  C  T  Y  R  V  T  P  P  E  D  A  A  R  M  Q  V  M  M
GGGATCGTGTTCTTGCTCCGGCACGAAGGGCAGCGGGGGTTGTACTTCTCGTCCAGGATGTTGAAGTAGGGCTTGTACTCGTGGTCCCGC
 P  I  T  N  K  S  R  C  S  P  C  R  P  N  Y  K  E  D  L  I  N  F  Y  P  K  Y  E  H  D  R
AGCTCCTCGATGTTGTACTCCACGCCCTTTCGCAGGCACTTGATGCCGAAGAGGGCGTAGCGCAGGATGTCCTTCTCGACGCCGCTGGTG
 L  E  E  I  N  Y  E  V  G  K  R  L  C  K  I  G  F  L  A  Y  R  L  I  D  K  E  V  G  S  T
GATCGGATCATGTCGCAGAGGTCCGTGTACTCCGCGTTCGTGGGGGATGAGCGGCTTGTTGCGGTACGAGA 431
 S  R  I  M  D  C  L  D  T  Y  E  A  N  T  P  S  S  R  S  T  A  T  R  S ← SP 29.9L
```

Not I I right SP 34.9R
MOCV 037R (49.7% over 193aa) Homologues: VACV E6R

```
GGCCCGGTCGTGCACAGCGCCATGACGGAGAAGTTCCGGCAGTTCATGTTCCCCGGGGACCGCACCAGCTACTGGGTCTGCTGCGCGAGC
 G  P  V  V  H  S  A  M  T  E  K  F  R  Q  F  M  F  P  G  D  R  T  S  Y  W  V  C  C  A  S
GGATCGCCAACGACGCGGACATCCTCAAGGGCGCCCGGCACGCTCCATGCACGAGCGGCTGCTGAGCTACGTCTACTCCGAGGTGAAGCA
 G  S  P  I  I  R  I  S  S  R  A  P  G  I  L  H  A  R  A  A  A  E  L  R  L  L  R  G  E  A
GGGGCGGGCCAACCGGAACATGCTCAAGCTGCGTACGCCTTCGAGACCGACCCCGAGATCCGGGCCATGCTCCTCGAGATCATCTACGGC
 G  A  G  Q  P  E  H  A  Q  A  A  Y  A  F  E  T  D  P  E  I  R  A  M  L  L  E  I  I  Y  G
GTCCCCGGGGACATCCTCGGCATCATCGACGCGGAGAACGAGGAGTGGAAGCGGTACTTCGTCTCCATGTACCGGGACAAGTTCGTCGAC
 V  P  G  D  I  L  G  I  I  D  A  E  N  E  E  W  K  R  Y  F  V  S  M  Y  R  D  K  F  V  D
GGGACCACCTTCGCCAGCGAGCGCACCTTCCGGGACGACCTCTTCCGCGTGGTGGCCGCCATCGACCCGGACTTCTTCGACGGGGACGTG
 G  T  T  F  A  S  E  R  T  F  R  D  D  L  F  R  V  V  A  A  I  D  P  D  F  F  D  G  D  V
ACCGCGCTCTTCAACGCCGCGCCCGAGACCGTGAAGCGCTTCGACGAGATGCCCATGAACTCCACCTTCGTCTCGCGCATGGTCTACGGA
 T  A  L  F  N  A  A  P  E  T  V  K  R  F  D  E  M  P  M  N  S  T  F  V  S  R  M  V  Y  G
TCCGCCGACGTGGACCTCGCGGCCGC 566
 S  A  D  V  D  L  A  A  A ← SP 34.9R
```

Not I N left SP 34.9R
MOCV 037R (63.3% over 49aa) Homologue: VACV E6R

GCGGCCGCGGAGCGGGAGTACACCTGCCAGATCTACCACGAGGACACGCTCTACCACATCCGCGAGTACAACACCTACCTCTTCCTCAAC
A A A E R E Y T C Q I Y H E D T L Y H I R E Y N T Y L F L N
GAGGAGGACCCGCTCGTCCTCGACGCGGGCGTCCTGGTGCGGCTCTCCTACGTGCCCGCC 150
E E D P L V L D A G V L V R L S Y V P A ← SP 34.9R

Not I N right SP 38.7L
VACV E9L (71.7% over 99aa) Homologues: MOCV 039L/ ORFV 26.4L

CGCCTCCAGGCGGTTGCCGCTCACCATCACGCCGACCAGCGTCTCCGGCGAGAGGTTGCCGAAGATGCAGACGTTGGGGTACAGGCTGTT
A E L R N G S V M V G V L T E P S L N G F I C V N P Y L S N
GTAGTCGAAGACCGCGACGTTGTTCTCGAACATCTTCTTCCTAGGCGCGAAGACCTTCCCGCCCTCGTAGAGGAACTTGGTCTTCCCGTC
Y D F V A V N N E F M K K R P A F V K G G E Y L F K T K G D
GTTGCGCACGAAGACCTTCCGCTGCTCCAGCATCATGCGCAGCAGCGGGCCCTTGATCAGCGTGCTCGCGCGGTACTCGAAGGCCAGGCA
N R V F V K R Q E L M M R L L P G K I L T S A R Y E F A L C
GTGCGGCAGCAGGTACGTCGCCGCGGCCGC 300
H P L L Y T A A A A ← SP 38.7L

Bam HI J right SP 39.7
CMPV C61L (68.9%over 196aa) Homologues: VACV E9L/MOCV 039L/ORFV 26.4L

TGAGTCCAGCTTGTACGAGTCCAGCTTCTCCGACTTCTGGATGTACGCGTAGAGGTCGAAGAAGATGGTGCCGTTGTTGTTGTTNACGTG
S D L K Y S D L K E S K Q I Y A Y L D F F I T G N N N N V H
GTAGGTCGTGTTGGCCACGCCGCCCTGGCCCCGGTGGCTGAGCAGGTTGCGCTCGTAGATGCACAGCTTCACCGTCTCGCTGTGGTCGGG
Y T T N A V G G Q G R H S L L N R E Y I C L K V T E S H D P
AAGCCGGAACGTCACGCTCTCCCCCGTGAGCAGCTCCAGCCGGTTGGCCACGTAGCGCAGGTCGAAGTTGTGTCCGTTGAAGGTGACCAC
L R F T V S E G T L L E L R N A V Y R L D F N H G N F T V V
GAAGTCGAAGGCGCTCTCGATCAGCAGCCGCGTGATCTGCAACATGACCACCTCGCTGCAGAGCACCACCTCGCGGCTCAGGTCCGCCTC
F D F A S E I L L R T I Q L M V V E S C L V V E R S L D A E
CGTGGCCGACCGCGCGCGCACGCACCCGCGGCGCAGCGCCTCCGCGCGGTCGGCCTCGCTCAGCATCTCCTCGTTCAGCAGCGTGAACCG
T A S R A R V C G R R L A E A R D A E S L M E E N L L T F R
GAACTCGGCGCCCGTCCGGTCCACGGTGCAGCAGCTGACGTGAGACACCGGGGTTGGTGAACACCGAGGGGAACTTCTTCTCGAAGTGGCA
F E A G T R D V T C C S V H S V P N T F V S P F K K E F H C
CTCGATGTCCATGAACAGGTAGGTGCGCTGGACGTCGAAGCGCGGGATCC 590
E I D M F L Y T R Q V D F R P I R ← SP 39.7

Kpn I A right SP 58.0L
YMTV 57L (52.9% over 102aa) Homologues: VACV G7L/MOCV 065L

GCCAGCGTACTCGGCCGAGTTGTTGGCGGGGGAGACTCCGCGCTGGATCAGGACCCGGTAGGCGTCCGATACGATGGTGGTGCGCACCGG
G A Y E A S N N A P S V G R Q I L V R Y A D S V I T T R V P
CAGCGAGAGCAGGCGCTCGGCCTCGCGCATGTACTCCCTCGGAGGAGTCGCTGCCGAAAGACGCCCGAGCCGCCCGCCCGGCGTGTCCTC
L S L L R E A E R M Y E R P P T A A S L R G L R G G P T D E
GCTCTCACCCAGCATCGCCGGCAGGAGCCGGTACTGCACCATGTTCACCAGCCCGTACTTCATCTCCAGCAGGTCCGCCACGTCCTGCGA
S E G L M A P L L R Y Q V M N V L G Y K M E L L D A V D Q S
GGGGGACTTCTGCACGTCGAAGAGGTACC 299
P S K Q V D F L Y R ← SP 58.0L

Kpn I A left SP 59.4R
VACV G9R (43.9% over 180aa) Homologues: MOCV 068R

GGTACCTGCCGGAGTTCGACGCCTACCCCACCGGCCCGGGGCTCGCGGGCCTGGTGCGGAAGGGGTACGCGGGGGAGGCCTCGCACTGCT
G Y L P E F D A Y P T G P G L A G L V R K G Y A G E A S H C
GCCGCTCCTTCGAGCGCACGCACTACTGGGAGGACGACGCCGGCCGCCGCTTCCCCGACTACGCGGAGGGGCGCGCGCTGCGGACGTGCG
C R S F E R T H Y W E D D A G R R F P D Y A E G R A L R T C
AGCCCGAGATGCACGCCCGGGGCGACTGCGACGTCGACCTCTTCGAGTGGTGCCGGGGCCCGGACGCGGACGCCGCCCTGTGCCGGCACT
E P E M H A R G D C D V D L F E W C R G P D A D A A L C R H
GGATCGGCGCCTCCGCGTACCGCGGGAACCTGGACGCCTCGACGGCGCAGGGCGGCTCGACGGCCATGGCGCTCTTCGGGCGCTTCGTGG
W I G A S A Y R G N L D A S T A Q G G S T A M A L F G R F V
CCGAGTGCTCGCAGGACGCGCTGCGGCCCATGTGCGCGGAGTGGCTGCACGCGCTGCGGATGGGGTCCCGCCCCGACTTCGACCTCATCG
A E C S Q D A L R P M C A E W L H A L R M G S R P D F D L I
TCGACGACGTGCTCGAGAGCCAGAGCCCCGAGTTCAAGGCCAAGTACATGCGGTGCAGCTACCCCTCGGGGCACGTGCTGGACGAGGCGC
V D D V L E S Q S P E F K A K Y M R C S Y P S G H V L D E A
TCCGG 545
L R ← SP 59.4R

Not I Q left SP 63.6R
YMTV I5R (40.0% over 60aa) Homologues: VACV L5R/MOCV 074R

```
GCGGCCGCTGATCCTGACGCCGGTCTTCGTGGAGCCGACCATCAAGCACACGCTCCTGCGCGAGACCCGGTACACCGGCCTGGTGGTCCT
  R  P  L  I  L  T  P  V  F  V  E  P  T  I  K  H  T  L  L  R  E  T  R  Y  T  G  L  V  V  L
GGAGCTGATCGTGGCCGTGCTGCTGCTCCTCATCTTCTTCCGGACCGAGCTGGGGTCCGTCTTCTCGCGCGCGGCCAGCGCCCGGACCCC
  E  L  I  V  A  V  L  L  L  L  I  F  F  R  T  E  L  G  S  V  F  S  R  A  A  S  A  R  T  P  ← SP 63.6R
CT 182
```

Kpn I P right SP 64.4R^{m}
MOCV 075R (58.3% over 103aa) Homologues: VACVJ1R

```
ACGCCCCATCCGGCCGGCGGACTGCGCGGCCGTTTTACGATCAGTAAATAATGGACCACTCGCAGTATCTCTTGACGATGTTCTTCGAGG
                                        SP 64.4R^m→  M  D  H  S  Q  Y  L  L  T  M  F  F  E
AGAGTAACTCCTTCTTCGCGTACCTCGCGGCGCAGGAGGACGACGCCGCCATGGACGACGTGACCACGGTCGTGCGGCACCTGGACGTGC
 E  S  N  S  F  F  A  Y  L  A  A  Q  E  D  D  A  A  M  D  D  V  T  T  V  V  R  H  L  D  V
TGCTGCACCTGCTCGTGCGCGGCAAGGAGAAGCTGGAGGCCATCGGGCACTGCTACGAGCCGCTGTCCGAGGACGTCACCGCGCTCTTCG
 L  L  H  L  L  V  R  G  K  E  K  L  E  A  I  G  H  C  Y  E  P  L  S  E  D  V  T  A  L  F
AGTTCCGGAACATGCGCGACGTGCGCCGCGTGCTCGACCGCGCGTCCGGGCCCGCGGCCGAGGGGCGCGTGGCCATCCGCCGCGGGTACC
 E  F  R  N  M  R  D  V  R  R  V  L  D  R  A  S  G  P  A  A  E  G  R  V  A  I  R  R  G  Y
```

Not I Q right SP 65.93R^{t} and SP 65.95L
MOCV 077R (61.4% over 70aa) Homologues SP 65.93R^{t}: VACV J4R/ORFV 53.1R^{m}
CPV v103 (61.1% over 126aa) Homologues SP 65.95L : VACV J5L/MOCV 078L

```
TTACCCACGATCTCCCGGCTCACCCCAAAGAGACGGCGGTGTGTCCACCATGCTGCAGGTGGACGGGAAGGACAGCTGCGGCTGCCCCGG
 L  P  T  I  S  R  L  T  P  K  R  R  R  C  V  H  H  A  A  G  G  R  E  G  Q  L  R  L  P  R
ATGCTGGAGACGGAGCTGGTGGCCAAGATCCTGCACCACCCCAACCTCCAGCTGAAGATCGTGCGCTTCTACCGGCGCAACATGATCACG
 M  L  E  T  E  L  V  A  K  I  L  H  H  P  N  L  Q  L  K  I  V  R  F  Y  R  R  N  M  I  T
                                                  SP 65.95L→  .  R  R  L  M  I  V
GGGATTGAGGTGACGGACCGCGCCGTGGTGGCGGTCCTGGAGTAGTCACCGGCACGCGACCACGACCAGCCGGCCACGGCCGCCAGCGCC
 G  I  E  V  T  D  R  A  V  V  A  V  L  E  .  ← SP 65.93R^t
P  I  S  T  V  S  R  A  T  T  A  T  R  S  Y  D  G  A  R  S  W  S  W  G  A  V  A  A  L  A
ACGGGCAGCCAGGCCGGGCGCAGCAGCGGGAGCACGATCTCCTGGTTCAGGTACGAGGTCTGGAACCGGGCGACGCGCGCCTCGAGCGAG
 V  P  L  W  A  P  R  L  L  P  L  V  I  E  Q  N  L  Y  S  T  Q  F  R  A  V  R  A  E  L  S
CCGCACGCGTTGTGCACGTTCAGGCGGCCGTTCACCAGCGCCACGTCCCCGAGGGACACGGTGCAGTCCGAGACGTTGCACCTAGAGATG
 G  C  A  N  H  V  N  L  R  G  N  V  L  A  V  D  G  L  S  V  T  C  D  S  V  N  C  R  S  I
TTTTTCTTCAGCGCCGCCGGGAGCATGGCGTCCGCGCGCTTGCATGGCTCGTACCAGCAGTAGTACGGCAGCAGCGTGTCCCGGCCGATC
 N  K  K  L  A  A  P  L  M  A  D  A  R  K  C  P  E  Y  W  C  Y  Y  P  L  L  T  D  R  G  I
CGCACCACCGAGCTGTCCGGGTGCAGGCAGAGGCAGCGCGGGTCGGCGGGGTGCGCGTCGCAGAAGGCGTAGATCTCCTCGTCGGTGAGG
 R  V  V  S  S  D  P  H  L  C  L  C  R  P  D  A  P  H  A  D  C  F  A  Y  I  E  E  D  T  L
TCGCGCCGCGCTGCGCCGGGCGGAGCCGCGCGGCCGC 667
 D  R  R  A  A  G  P  P  A  A  R  G
```

Not I M' and F SP 66.6R^{m}
MOCV 079R (82.9% over 135aa) Homologues: VACV J6R/ORFV 58.8R

```
GCGGCCGCGCTGACCGCCATCGATTTATAGCGCGTAAATAGCAACCGCCCGGTCGGCCCGGGGGCAGGGACGCGGTCCGGACGCCGGCGA
CCCGGGTTCGCGCCCGCAAAACTGAACTCCTATTCCGACGAGTGGACCCGCTCCTTTACGGAATCCTCAAAGGATATCAAAAATGGCAGT
                                                        SP 66.6R^m→  M  A  V
CATCGCTCGCGTGTCCTACAGCCTGTACACCCAGAATGAGATCAACGCCACGGACGTGCTCATCAACCACGTCAAGAACGACGACGACAT
  I  A  R  V  S  Y  S  L  Y  T  Q  N  E  I  N  A  T  D  V  L  I  N  H  V  K  N  D  D  D  I
CGGCACCGTCAAGGACAGCCGCCTGGGCGCCATCGACGGCGCGCTCTGCCGCACCTGCGGCCGCACGGAGCTGGAGTGCTTCGGGCACTG
  G  T  V  K  D  S  R  L  G  A  I  D  G  A  L  C  R  T  C  G  R  T  E  L  E  C  F  G  H  W
GGGCAAGGTGCGCCTCTACGAGACGCACGTGGTGAAGCCCGAGTACATCGGCGAGGTGATCCGCATCATGAACCACATCTGCGCGCGCTG
  G  K  V  R  L  Y  E  T  H  V  V  K  P  E  Y  I  G  E  V  I  R  I  M  N  H  I  C  A  R  C
CGGACTGCTGCGGTCCCGGGAGCCGTACGCGGTGGAGGACCTGGGGTCCATGTCGCTGCACGCGCTGCGGCGCCTGAAGGACCGCGTCTT
  G  L  L  R  S  R  E  P  Y  A  V  E  D  L  G  S  M  S  L  H  A  L  R  R  L  K  D  R  V  F
CTCCAAGAAGAAGTCGTGCTGGAACAAAAGTGCATGC 577
  S  K  K  K  S  C  W  N  K  S  A  C
```

Not I F right SP 72.2R^{m}
VACV H2R (58.9% over 73aa) Homologues: MOCV 083R

```
GGAGCAGCCCCCTCGTAGATGTTTTTCCCAATCCATTTAGATGATACAAATGGGGGACGCGACCACCCTCTCGGTCCACGGGCTGGATTT
                                        SP 72.2R^m→ M  G  D  A  T  T  L  S  V  H  G  L  D  L
AGAATACGCGCGCGAGCGGGAGGCGGAGAGCGTCCACGCCGCGCGCGCGTCTACGCTCTGCTTCTTCGTGCTGGTCCTGGCCGCCAGCGC
  E  Y  A  R  E  R  E  A  E  S  V  H  A  A  R  A  S  T  L  C  F  F  V  L  V  L  A  A  S  A
GGTGCTCCTGTGGCTGCAGGTCTCCGACAACGGCGTGGTGACGGAGCTCACGCGGTACGCGCGGATCAAGGAGTCGGTGCGCGGGCTGCG
  V  L  L  W  L  Q  V  S  D  N  G  V  V  T  E  L  T  R  Y  A  R  I  K  E  S  V  R  G  L  R
GCCGC 275
  P
```

Bam HI Q right SP 85.5R^{t}
LSDV 083 (62.4% over 141aa) Homologues: MOCV 094R/VACV D5R/ORFV 68.8R

```
TACGACGACGTCAAGCCCCTGGACGAGAGTCTGGACCGGAAGATCCAGCGGAACTACTTCAGGTTCGCCTTCCTGCACCTGCTGGTGCGC
 Y  D  D  V  K  P  L  D  E  S  L  D  R  K  I  Q  R  N  Y  F  R  F  A  F  L  H  L  L  V  R
TGGTACCAGCGGCACCACGTCCCCGCGCTGCGGCTGGAGGCGACGCCCGACGCCGTGCCCGACTTCGCGTTCCAGCGGCGCGTGGGCTCG
 W  Y  Q  R  H  H  V  P  A  L  R  L  E  A  T  P  D  A  V  P  D  F  A  F  Q  R  R  V  G  S
CTGCTGATCCCGAGTGGCTCCGCGCACGTGCCCATGATGCCGGAGCTCGCCAAGCTGGGGTACGTGCTGGTGGACGGGGCGGTGGGCCTG
 L  L  I  P  S  G  S  A  H  V  P  M  M  P  E  L  A  K  L  G  Y  V  L  V  D  G  A  V  G  L
CCGGCGCACACCTTCCAGCAGCGCCTGGCCAACCACTTCAACGCGCGGGCGTACGGTCACGACATGGAGAGCTTCGTGGCGCGCCACAAG
 P  A  H  T  F  Q  Q  R  L  A  N  H  F  N  A  R  A  Y  G  H  D  M  E  S  F  V  A  R  H  K
AAGTTCGGGTCCTCGAACGAGGAATACCTGGAGTACATATTCATAGAAGACGTAGCGTCTAAATGAATGTCGGGATCC 438
 K  F  G  S  S  N  E  E  Y  L  E  Y  I  F  I  E  D  V  A  S  K  . ← SP 85.5R^t
```

Not I Z left SP 111.7L
MOCV 121L (42.4% over 177aa) Homologues: VACV A16L

```
GCGGCCGCGCCGTCCGCAGCCACTTCAAACAGTTGCCGGAGCCCGGGTTCGCGCGGCAGAAGGTGGACATGACCTCGTCGCAGTCGGTGG
  P  R  A  T  R  L  W  K  L  C  N  G  S  G  P  N  A  R  C  F  T  S  M  V  E  D  C  D  T  T
TGGCGTAGTCGTTACAGAGCATCTTCGGGCACCCGGCCGTCCGCGCGCCCGTGCAGCACGGCACCCGGTCCGCGTCGGTGCCCAGGTCGT
  A  Y  D  N  C  L  M  K  P  C  G  A  T  R  A  G  T  C  C  P  V  R  D  A  D  T  G  L  D  D
CGTCGCGCACGAAGCGGCACAGGCGCCCGTCGGCCAGGTACTGCTGCGCGTTCGGGGGCAGGAAGTCGCGGAAGAGCACGTAGGACCCCG
  D  R  V  F  R  C  L  R  G  D  A  L  Y  Q  Q  A  N  P  P  L  F  D  R  F  L  V  Y  S  G  P
GGCGGAAGGTGATGGAGTGGCAGGGCGCGCCCAGGGTGAGGGTGTATTTGCCGGCGATGGACGGGTCCACGAACGAGCCGCAGCTGCTCG
  R  F  T  I  S  H  C  P  A  G  L  T  L  T  Y  K  G  A  I  S  P  D  V  F  S  G  C  S  S  P
GGTCCATGTCCGGCGTGAGGCAGAAGTGCGGCACGATCTCCGCCTGCGTTCCGTCCTTGAAGACGTCGCTCTCCTCGTAGAACCGCACGA
  D  M  D  P  T  L  C  F  H  P  V  I  E  A  Q  T  G  D  K  F  V  D  S  E  E  Y  F  R  V  F
ACTCGGGGGAGTCCTGGCCGCCGAGCCGGAAGACCATGAACTTCTTCCACGGCACGCCGGCCGACACCACGCTCACGCTCTCGACCGGGA
  E  P  S  D  Q  G  G  L  R  F  V  M  F  K  K  W  P  V  G  A  S  V  V  S  V  S  E  V  P  L
GG 542
← SP 111.7L
```

Not I Z right SP 112.9L^{m} and SP 112.9R^{m}
MPV A18L (51.2% over 82aa) Homologues SP 112.9L^{m}: VACV A17L/MOCV 122L
FPV 183 (51.2% over 86aa) Homologues SP 112.9R^{m}: VACV A18R/MOCV123R

```
CGACGACAGGGCCAGGACGAAGAGCACCAGCCCCAGCAGGGTGCGGATGTCCATGTGCGCCAGCAACGCGCGCCCGAAGTCGTTCATGCT
 S  S  L  A  L  V  F  L  V  L  G  L  L  T  R  I  D  M  H  A  L  L  A  R  G  F  D  N  M  S
GCTGACGGCGCCGTAGGGTGCGTCGGCCAGCACGTTCCCGCCCGGGTTCTTGGGCAGGAAGGCCTCCTTCTCGTCGGGGGTGTAGAGCTC
 S  V  A  G  Y  P  A  D  A  L  V  N  G  G  P  N  K  P  L  F  A  E  K  E  D  P  T  Y  L  E
GTCCTCGAGCACCCCCGCCCCGCCATCGAAGTCGTCTAATATGCTATAGTAACTTAAATAACTCATTTATATATAAAAAAATGTCTGTCT
 D  E  L  V  G  A  G  G  D  F  D  D  L  I  S  Y  Y  S  L  Y  S  M ← SP 112.9L^m  M  S  V
ACACCGAGATAGACGATAAACTCTTTTCAGAGCTTCGAAACCTGGTGGGCGAACAGCAGCTGAACCTCTTCACGCAGAAGGGGGAGCTGA
 Y  T  E  I  D  D  K  L  F  S  E  L  R  N  L  V  G  E  Q  Q  L  N  L  F  T  Q  K  G  E  L
CCGAGGTCTTCCAGGGGTCCTCCTTCCGGTTCCTGGTACCGGTCGGGTTCTTCGCGGGCCTCCCGGTACCGCCCCGCGGGCGGCGCTTCC
 T  E  V  F  Q  G  S  S  F  R  F  L  V  P  V  G  F  F  A  G  L  P  V  P  P  R  G  R  R  F
GCCGGCCCGCCAACCCCATGCCCGACGCGGAGAAGGTGTCGGTGCCCGAGCTGTACCCGGTGCAGCGCCCGTGGTCGAGGAGGTGGAGGC
 R  R  P  A  N  P  M  P  D  A  E  K  V  S  V  P  E  L  Y  P  V  Q  R  P  W  S  R  R  W  R
GGCCGC 546
 R  P ← SP 112.9R^m
```

Not I X left SP 113.2R
VACV A18R (62.3% over 146aa) Homologues: MOCV 123R

```
GCGGCCGCCAAGCGCAAGGCGCGGGAGGGCCGGCCGCCGTACGTGACCCTGCACCTGGCGTGCGGGTTCGGCAAGACGGTGACCGCCTGC
 A  A  A  K  R  K  A  R  E  G  R  P  P  Y  V  T  L  H  L  A  C  G  F  G  K  T  V  T  A  C
CACCTGATCGCCAAGCACCGCCTGCGCGCGGTGGTCTGCGTCCCCAACAAGATGATCATCCCCCAGTGGCGGGCGGCCGTGGAGGCGACG
 H  L  I  A  K  H  R  L  R  A  V  V  C  V  P  N  K  M  I  I  P  Q  W  R  A  A  V  E  A  T
GGGCGCGAGCACCTCGTCTCCGTCGACGGCGTGAGCAGCCTGCTGCGGGAGCTGCGCACCGTCACGCCCAGCGTGCTGGTGGTGGTCAGC
 G  R  E  H  L  V  S  V  D  G  V  S  S  L  L  R  E  L  R  T  V  T  P  S  V  L  V  V  V  S
CGCCATTTCGGGAACGAGGAGTTCTGCCGCCTGGTCGACGAGCGGTACGACGTCCTGGTCGTGGACGAGTCGCACACGCACAACCTCATG
 R  H  F  G  N  E  E  F  C  R  L  V  D  E  R  Y  D  V  L  V  V  D  E  S  H  T  H  N  L  M
AACAACACCGCCATGGCGCGGTTCCTGGCCTTCCACCCTCCCCGCGTCTGCTACTTCCTCACGGCCACGCCGCGCGCGGTCAACCGG 447
 N  N  T  A  M  A  R  F  L  A  F  H  P  P  R  V  C  Y  F  L  T  A  T  P  R  A  V  N  R ← SP 113.2R
```

Not I X right SP 115.3R
MOCV 126R (44.4% over 108aa) Homologues: VACV A20R

```
AAAGAGCTGGCTCGAGTGAGCCGGTGCCTGGCACGGGCCAACGACGCGACCGTCCAGAAGTACAACGCGCTCGTGGAGTGGGCCACCCGC
 K  E  L  A  R  V  S  R  C  L  A  R  A  N  D  A  T  V  Q  K  Y  N  A  L  V  E  W  A  T  R
ACGTACTGGACGGTGGGGGTGGCGCCCAGCGAGGGCGGCTCGGTCTCCGTGGCGCGGTACTACGCCGAGCCCGAGAGGCGCGAGTTCGAG
 T  Y  W  T  V  G  V  A  P  S  E  G  G  S  V  S  V  A  R  Y  Y  A  E  P  E  R  R  E  F  E
ATGGCGGCCGGCGAGTACGTCTTCTCGCTGGCCTTCTTCGGGACCGTCCTTCTCTTCACCAACGGGTCCCTGATGGAGGTCGGCGGGCGC
 M  A  A  G  E  Y  V  F  S  L  A  F  F  G  T  V  L  L  F  T  N  G  S  L  M  E  V  G  G  R
GCGGCGGCGACGAACGAGCGCGTGGTCGCGGCGTGCCGCGCGGTGGCGGCCGC 323
 A  A  A  T  N  E  R  V  V  A  A  C  R  A  V  A  A  A ← SP 115.3R
```

Not I H left SP 118.1R^{t} and SP 118.1R^{m}
MOCV 128R (58.6% over 116aa) Homologues SP 118.1R^{t}: VACV A23R
MYXV M114R (82.4% over 17aa) Homologues SP 118.1R^{m}: VACV A24R/MOCV 129R/ ORFV 103.3R

```
GCGGCCGCCGCCCGCGTGGCCGCGCCGGCGGAGCTTCGACGAGAAGATGGCGCTGATCGCCGACGGCCCGGGGACTACGGCGTGGGCAAC
 A  A  A  A  R  V  A  A  P  A  E  L  R  R  E  D  G  A  D  R  R  R  P  G  D  Y  G  V  G  N
TTCCGCGTGGGCATGTTCAACCTGACACACACGCGGCAGATCGCCTCGACCGTCTTCCCCTCGCTGCTCGACGACGCCAGCAAGATCAAG
 F  R  V  G  M  F  N  L  T  H  T  R  Q  I  A  S  T  V  F  P  S  L  L  D  D  A  S  K  I  K
TTCTTCAAGGGCAAGAAGCTCAACATCGTCGCCATCGGGTCCCTGGAGGAGTGCCGCCGCTACGTGGAGCAGGCGGACTGGCTCCTGGAC
 F  F  K  G  K  K  L  N  I  V  A  I  G  S  L  E  E  C  R  R  Y  V  E  Q  A  D  W  L  L  D
GTCATGGCGCGGCGGTCCGCGACGCTGGACGCGCTGGACATCGCCCGCGCCCCCGTGGACGCGCTCAAAGACCTTTTAAAGTGAAAGAAA
 V  M  A  R  R  S  A  T  L  D  A  L  D  I  A  R  A  P  V  D  A  L  K  D  L  L  K  . ← SP 118.1R$^{t}$
ACAACGCCCACAAATGGAGCAGCGTCTCGGTTACAAGTTCCTGGGGGCCGACCCGAAGGCCGGCGT 426
SP 118.1R$^{m}$→ M  E  Q  R  L  G  Y  K  F  L  G  A  D  P  K  A  G
```

Not I J right SP 130.5L^{m} and SP 130.5L^{t}
MPV A29L (38.0% over 50aa) Homologues SP 130.5L^{m}: VACV A27L/MOCV 133L/ORFV 108.2L^{m}
MOCV 134L (42.6% over 47aa) Homologues SP 130.5L^{t}: VACV A28L

```
TTTCCGCAGCGTGTCCGCGTGCTTCTCCAGCCGGGTCAGGCGGTCGTCGGCGTGCTCGCAGCACTCGATGACGCGCTCCTGCTCCTCCAG
 K  R  L  T  D  A  H  K  E  L  R  T  L  R  D  D  A  H  E  C  C  E  I  V  R  E  Q  E  E  L
CAGCCGCTTCAGCCGCTCCCTGTTCCGGTCGGTGACGCGCAGCAGCATGGGCTCCTCGTTCTCCATCCTATTTAGATGACGGATTTTAGA
 L  R  K  L  R  E  R  N  R  D  T  V  R  L  L  M  P  E  E  N  E  M ← SP 130.5L$^{m}$  I  V  S  K  L
AACACGCAATCGGCGTCTCCGGGCCCGCGGGGAGGCGCGCACGGGTTGATGATGGAGGACGCGTTGCCCGGGGTGAAGGTGAAGTCCTGG
 F  V  C  D  A  D  G  P  G  R  P  P  A  C  P  N  I  I  S  S  A  N  G  P  T  F  T  F  D  Q
CAGCTCTCCTCGTCGGGGAAGAGCTTGACGCGGCCGC 307
 C  S  E  E  D  P  F  L  K  V  R  G ← SP 130.5L$^{t}$
```

Not I D left SP 131.2L
VARV A32L (56.2% over 73aa) Homologues: VACV A29L/MOCV 135L/ORFV 109.5L

```
GCGGCCGCGCGGCGCGACGGCGATAAAGGGGACCTCGCCGCGGAAGCCGTCCCGCAGCACCGGGCGCACGTTGCCGTACTCGCGGTTGAA
 R  G  R  P  A  V  A  I  F  P  V  E  G  R  F  G  D  R  L  V  P  R  V  N  G  Y  E  R  N  F
GACCTCGGCGTCGAGGAAGGTCAGCCGGGCCACGAGCGCGTCGTTGACGACCGTGCCGGAGCTGAAGGCGACCAGCTCCACGGCCTGCTC
 V  E  A  D  L  F  T  L  R  A  V  L  A  D  N  V  V  T  G  S  S  F  A  V  L  E  V  A  Q  E
GTTGGACATGCGGTACTCCTGGAAGGTGTGCAGGAGCGT 219
 N  S  M  R  Y  E  Q  F  T  H  L  L  T ← SP 131.2L
```

Kpn I C' right SP 131.7L^{m}
MOCV 136L (54.7% over 64aa) Homologues: VACV A30L

GGTACCCGTGCTTGATGAAGGACGCGAGGCCGGGGTCGAGGTCAGCGACGATCTCCACTTCGTCCCGGGGCATGCTGCGGCTGCTCCGGA
. R R D G S R G P A H Q P Q E P
CCCTTGGTGTTCTTTTTCGATCTTTTATTGATGGCCATCAACTTCAAATTGATGGCGTTGATGAGCTCCCGGACCGCGGCCACCGTGCAG
G K T N K K S R K N I A M L K L N I A N I L E R V A A V T C
GCGAACTCGCTGTCCCCGCACTCCGAGAGCTTCTCCAGCAGGTGGTTGAGGTTGGCCTCGTCGATGTCCTCCTCCATTTAAGTGCTGTAA
A F E S D G C E S L K E L L H N L N A E D I D E E M ← SP 131.7L^{m}
AGCTCGGTGCGCCGACAAAAAGGGAAGTT 299

Bam HI O right SP 133.2L^{m}
MOCV 140L (76.7% over 60aa) Homologues: VACV A32L

GTAGGCCGGGTTGGCCACCGGCGTGAAGAGCAGGACGTGCCGGTACCCGTCCACCAGCGTGCCGAGAAGCGAGAGCAGGTAGGCCGTCTT
Y A P N A V P T F L L V H R Y G D V L T G L L S L L Y A T K
GCCGGACCCCGAGCCGCCCACCATGGCGATCCTGAAGGGCGCCCGCAGAAGGCTTTTACGACAGAACCGCTTCTCTTGAACGCGGTCCAT
G S G S G G V M A I R F P A R L L S K R C F R K E Q V R D M ← SP 133.2L^{m}
TTCGATATTTACAGTTACTAAATTAAACCTTCGGGGGTTGGAAAGTGGAAATTCAAGCCCCACTTAGCTTCTGCAAACAACGGCACACAC
GACTGTCGTTGTTGATCTTCCCTCAGCCTTCCCAGCCATGGCAGATGTGGAGCAGCAGGCCGACACCCTGCCCCTCAACATCCCCGAGAA
GCCGCGACGCCACCCGCTCGCCGCCCGGGGAATGGCGTGTGCAATCATCACCCTGCGCATAATGGTGCTCGTCTCGCTGGTCTCCCTGAC
CACAATCGTGGCCGCGCTGGCGGGTGCAGCTGCGCGCCTGTCGCCAGCAACACGAGGGGTCGGCGTGCGCCGTCACCGGCACGCCCAGGA
TCC 543

Not I D right SP 138.3R^{t}
LSDV 127R (26.3% over 99aa) Homologues: VACV 37R/MOCV 149R

ATCGCCTTCGCCATGCGCCTGCTGACGGACAAGATCACCGGCCGCGTCGTCTGCGAGCAGTCTGATGGTCGGCGGGGACTGGTTCACCGT
I A F A M R L L T D K I T G R V V C E Q S D G R R G L V H R
CGTGGTCTACGGCAAGCGCTGCGGCGGCTGGCCATCCCCGCCGTCTGCGTCGGCAGCACCTCCATGGACCGCATCTGTTCGTCCAGCGCG
R G L R Q A L R R L A I P A V C V G S T S M D R I C S S S A
AGCGACGAGGAGCGGAACATGATCGTCTCCGTGAACCCGCCCTACGAGATCAGCACCCCCGCGCCCTGCATCTACGAGAGCGTGTGCGTG
S D E E R N M I V S V N P P Y E I S T P A P C I Y E S V C V
GGAGAGGAGCGCGTGGTCTACGGGCGCGTGCTCCGCTCGGCGGAGGGGGAAATGGACGTGGACCTGACGCCTCCCGCGGCCGAGCCCGGC
G E E R V V Y G R V L R S A E G E M D V D L T P P A A E P G
GCCGCGGCGGCCCCGACCGAGGGCGCTGAGGCCGCCGCGCCGAGCGTGCGTCTGCAGCACTCCGCGACCCTGGTCTAAATGAAAAACAAT
A A A A P T E G A E A A A P S V R L Q H S A T L V . ← SP 138.3R^{t}
CCGGCCTTTTTGTAGCCCGAGAGGCGCGACTCACAATGGGGTTCCTCTGTGCGCTCTTCCGCCGGTGCCTCCGTCCCTCCGTCCCCCAGG
AGTCGCGAGGGGACCCGATCGTGGTGGTGAAGGCGGCGGCCGC 583

Figure 5.5 SPPV sequence derived from the ends of cloned restriction endonuclease fragments. Sequencing was performed by the Functional Genomic Unit (Moredun Research Institute) using PE Biosystems 377 DNA sequencer. The nucleotide sequences are presented along with the translated ORFs that are predicted to encode homologues of poxvirus proteins as determined by FastA analysis. The text immediately above each sequence details the restriction fragment and the left or right end that each sequence derived from, and the location co-ordinate of each putative SPPV protein [e.g. SP 19.05L (see section 5.3.1 for an explanation)]. The closest homologue is also indicated with the percentage identity between the two proteins, together with known homologues from VACV, MOCV and ORFV (see appendix 2.0 for the protein alignments performed by the FastA algorithm). The sequences that did not appear to encode known poxvirus genes are not shown here.

SPPV location[a]	Sequence length (aa)[b]	Homologues[c]	% identity/length[d]	VACV homologue	Predicted function and/or structure[e]	Reference[f]
19.05L	220	**ORFV B2L**	51.4%/216aa	F13L	Major EEV protein, membrane	Sullivan *et al.*, 1994
		MOCV 021L	57.2%/215aa		wrapping of IMV	Husain and Moss, 2002
21.0L[t]	73	**MPV C21L**	49.3%/69aa	F15L	TM protein	Shchelkunov *et al.*, 2001
		MOCV 025L	54.4%/68aa			
21.7L[m]	86	**MOCV 026L**	42.1%/76aa	none	Putative protein	Senkevich *et al.*, 1997
29.9L	39	**VACV E4L**	67.6%/37aa	E4L	RNA polymerase subunit RPO30	Ahn *et al.*, 1990
		ORFV	56.8%/37aa			
		MOCV	54.3%/35aa			
34.9R	188	**MOCV 037R**	49.7%/193aa	E6R	Putative protein	Senkevich *et al.*, 1997
38.7L	100	**VACV E9L**	71.7%/99aa	E9L	DNA polymerase	Earl *et al.*, 1986
		MOCV 039L	72.0&/100aa			Mercer *et al.*, 1996
		ORFV	68.0%/100aa			
58.0L	99	**YMTV 57L**	52.9%/102aa	G7L	Virion core protein, TM	Takahashi *et al.*, 1994
		MOCV 065L	49.0%/100aa			
59.4R	181	**VACV G9R**	43.9%/180aa	G9R	Myristylated protein	Martin *et al.*, 1997
		MOCV 068R	44.3%/183aa			
63.6R	60	**YMTV I5R**	40.0%/60aa	L5R	Putative TM protein	Lee *et al.*, 2001
		MOCV 074R	45.3%/53aa			
64.4R[m]	103	**MOCV 075R**	58.3%/103aa	J1R	Virion protein, morphogenesis	Senkevich *et al.*, 1997
						Chiu and Chang, 2002
65.93L[t]	73	**MOCV 077R**	61.4%/70aa	J4R	RNA polymerase subunit RPO22	Broyles and Moss, 1986
65.95L	168	**CPV v103**	61.1%/126aa	J5L	Essential protein	Dietrich *et al.*, 2002
		MOCV 078L	57.8%/128			
66.6R[m]	135	**MOCV 079R**	82.9%/135aa	J6R	RNA polymerase subunit RPO147	Broyles and Moss, 1986
72.2R[m]	75	**VACV H2R**	58.9%/73aa	H2R	TM N-terminus	Johnson *et al.*, 1993
		MOCV 083R	61.3%/75aa			
85.5R[t]	141	**LSDV 083**	62.4%/141aa	D5R	NTPase DNA replication	Evans *et al.*, 1995
		MOCV 094R	61.9%/139aa			
111.7L	180	**MOCV 121L**	42.4%/177aa	A16L	TM, myristylated	Martin *et al.*, 1997
112.9L[m]	82	**MPV A18L**	51.2%/82aa	A17L	IMV membrane protein	Wallengren *et al.*, 2001

SPPV location[a]	Sequence length (aa)[b]	Homologues[c]	% identity/length[d]	VACV homologue	Predicted function and/or structure[e]	Reference[f]
112.9R[m]	95	**FPV 183** MOCV 123R	51.2%/86aa 48.8%/86aa	A18R	DNA helicase, transcription elongation	Simpson and Condit, 1995
115.3R	108	**MOCV 126R**	44.4%/108aa	A20R	DNA polymerase processivity factor	Klemperer *et al.*, 2001
118.1R[t]	117	**MOCV 128R**	58.6%/116aa	A23R	Intermediate transcription factor VITF-3	Sanz and Moss, 1999
118.1R[m]	17	**MYXV 114R** ORFV MOCV 129R	82.4%/17aa 80.0%/15aa 66.7%/15aa	A24R	RNA polymerase subunit RPO132	Patel and Pickup, 1989 Amegadzie *et al.*, 1991a
130.2L	52	**MPV A29L** ORFV MOCV 133L	38.0%/50aa 44.4%/36aa 36.4%/44aa	A27L	IMV fusion protein, IMV transport and attachment protein	Sanderson *et al.*, 2000 Chung *et al.*, 1998 Rodriguez and Smith, 1990
130.5L[t]	47	**MOCV 134L**	42.6%/47aa	A28L	Signal peptide	Senkevich *et al.*, 1997
131.2L	73	**VARV A32L** MOCV 135L	56.2%/73aa 48.6%/74aa	A29L	RNA polymerase subunit RPO35	Amegadzie *et al.*, 1991b
131.7L[m]	71	**MOCV 136L**	54.7%/60aa	A30L	Putative protein	Senkevich *et al.*, 1997
133.2L[m]	60	**MOCV 140L**	76.7%/60aa	A32L	ATPase, DNA packaging	Koonin *et al.*, 1993 Cassetti *et al.*, 1998
138.3R[t]	145	**LSDV 127R** MOCV 149R	26.3%/99aa	A37R	Putative TM protein	Afonso *et al.*, 2002
155.0R[t]	333	**MOCV 157R**	27.6%/214	MOCV 157R	Putative plasma membrane receptor	Senkevich *et al.*, 1997

Table 5.2 Summary of the SPPV sequence analysis data (as determined by the FastA algorithm), detailing:

[a] The location coordinate of the putative protein in the SPPV genome (see section 5.3.1 for an explanation).
[b] The length of sequence used to perform the FastA alignments.
[c] The closest homologue (presented in bold type) as calculated by the FastA algorithm. The alignment values for MOCV and ORFV are also presented. Viruses are abbreviated according to their standard nomenclature (van Regenmortel *et al.*, 2000) and are defined in the summary of abbreviations (located at the beginning of this thesis).
[d] The percentage identity of the two aligned proteins and the size of the overlap.
[e] The predicted function or predicted structure of each putative protein as determined by functional/structural studies carried out with homologous poxvirus proteins.
[f] The literature reference relating to the structure/function of the poxvirus proteins are presented in the last column.

5.3.2 The comparison of putative SPPV proteins to those encoded by other poxviruses

Twenty-six of the twenty-eight poxvirus protein homologues identified in SPPV are conserved across the genera and have been identified in many individual species including; VACV, VARV, MOCV, SFV, MYXV, FPV, LSDV, YLDV, MPV and SWPV (Johnson *et al.*, 1993; Massung *et al.*, 1994; Senkevich *et al.*, 1997; Cameron *et al.*, 1999; Willer *et al.*, 1999; Afonso *et al.*, 2000; Tulman *et al.*, 2001; Lee *et al.*, 2001; Afonso *et al.*, 2002; Shchelkunov *et al.*, 2002; Gubser and Smith, 2002); except for homologues of the VACV genes A27L and A37R which are absent in the FPV genome. SPPV ORFs SP21.7L^{m} and SP155.0R^{t} have one poxvirus match each in the database to the putative MOCV proteins 026L and MOCV 157R, which were previously believed to be unique to MOCV (Senkevich *et al.*, 1996 and 1997).

As SPPV is classified as a parapoxvirus (van Regenmortel *et al.*, 2000), it was therefore expected that the putative SPPV proteins would exhibit the greatest identity to the ORFV proteins. However the complete genome sequence of ORFV has yet to be determined, and possibly as a result, only five of the SPPV sequences resulted in a direct match with ORFV proteins during database searching. Four other SPPV sequences corresponded with genes putatively identified in the ORFV genome by comparison of each with VACV rather than by direct comparison with each other. Direct comparison with each other was not possible because sequence obtained from SPPV and the sequence published for the four ORFV genes do not overlap as they correspond to different regions of the same gene.

A broad view of the data revealed that the closest alignment of twelve of the twenty-eight putative SPPV proteins were with MOCV proteins. Orthopoxviruses accounted for nine of the closest alignments, whilst the remaining seven ORFs aligned with parapox, avipox, leporipox, capripox and yatapox viruses. The availability of the complete DNA sequence of MOCV and its high G+C content (Senkevich *et al.*, 1997) may account for the high level of protein alignment with SPPV. Codons in G+C rich genomes will naturally have a bias towards a G or a C in the first or second position of a codon, which will invariably alter the amino acid coded for when compared to A+T rich genomes. It then follows that proteins from two different poxvirus species are more likely to show a high amino acid identity if they have comparable G+C contents.

Despite the differences in G+C content, the closest alignment of nine SPPV proteins were with orthopoxvirus proteins. However, most of these proteins were also highly conserved in MOCV and little difference in the percentage identity (as calculated by the FastA algorithm) of SPPV with MOCV and orthopoxvirus proteins was observed. Likewise, six of the seven SPPV proteins that appeared to be most closely related to parapox, avipox, leporipox, capripox and yatapox viruses all had a similar percentage identity with MOCV, suggesting that these proteins are also highly conserved within the poxvirus family. The exception was ORF SP138.3R^{t}. This protein aligned only with LSDV and SFV homologues of VACV A37R. Further analysis revealed that homologues of the VACV A37R gene are poorly conserved at the protein level between different poxviruses.

Of the five sequences derived from SPPV that overlap with published ORFV genes, only one protein, SP19.05L (section 7.2) was the most closely related to ORFV. This ORF corresponded to the major EEV protein (homologue of VACV F13L). However many orthopox, molluscipox and capripox virus F13L homologues also gave similar percentage identities, suggesting that this is a highly conserved gene. The remaining four SPPV ORFs, SP29.9L, SP38.7L, SP118.1R^{m} and SP130.2L, which corresponding to the VACV proteins E4L, E9L, A24R and A27L aligned with published ORFV sequence but not as the closest homologue.

To refine the analysis, some of the SPPV sequences were trimmed such that they corresponded to the region for the ORFV protein present in the databases. The FastA analysis was then performed again with the shorter sequence. Despite this, VACV proteins remained the closest homologues. For example, ORF SP38.7L most closely resembled the VACV E9L DNA polymerase gene, despite trimming the sequence. However, comparison of SP38.7L with all the vertebrate poxvirus E9L sequences suggests that the poxvirus DNA polymerase genes are highly conserved.

ORF SP130.2L is predicted to encode the IMV fusion protein based on homology to other poxvirus homologues of the VACV A27L. However, the percentage identity of SP130.2L with other poxviruses A27L homologues is low suggesting this gene may be poorly conserved in SPPV.

In summary the results discussed in this section indicate that putative SPPV proteins are most homologous with proteins derived from G+C rich poxviruses such as MOCV. The

restricted volume of sequence published for the parapoxviruses may have limited the number of matches observed with putative SPPV proteins. Comparison of complete gene sequences and/or phylogenetic analysis may be more accurate in determining the evolutionary relationship of SPPV to the poxviruses (chapter 7.0).

5.4 GENETIC MAP OF SPPV

The locations of the predicted poxvirus homologues were plotted onto a schematic representation of the genome (figure 5.6). The location of each homologue corresponds to those summarised in table 5.2, and where possible the location corresponds to the initiating methionine or the termination codon of putative SPPV genes; where this was not possible the location of restriction site the sequence originates from is given.

5.4.1 Comparison of the genetic map of SPPV with the regions hybridised with ORFV

All of the sequences derived from the region of the genome extending from approximately 30kb to 118kb, exhibited identity with at least one previously described poxvirus protein. Hence the sequencing results correlate well with the hybridisation data described in section 5.2.1, in that the region of SPPV, which hybridised strongly with ORFV contains many conserved poxvirus genes.

Twenty-two sequences derived from near the genome ends (0kb to 30kb and 124kb to 158kb) did not exhibit nucleotide or protein homology with any of the poxvirus sequences deposited in the databases. Hence, the locations of these sequences correspond well with regions of the SPPV genome that did not hybridise with ORFV, suggesting the presence of sequence possibly unique to SPPV, absent from ORFV or too divergent from ORFV for hybridisation to occur. However a number of differences were noted between the hybridisation and sequence data and these are discussed in the text that follows.

We have identified homologues of the VACV genes A29L, A32L and A37R located within SPPV *Kpn* I fragments G'and F. Comparison of the completely sequenced poxvirus genomes has revealed that homologues of the VACV genes A30L, A32L, A37R are present in one or more species belonging to each genus, except FPV which lacks A37R (Afonso *et al.,* 2000). It is therefore likely that these genes will be present in ORFV. However, no visible hybridisation signal was observed between the restriction fragments of ORFV and SPPV predicted to contain these genes. This suggests that the DNA sequence of these genes may be

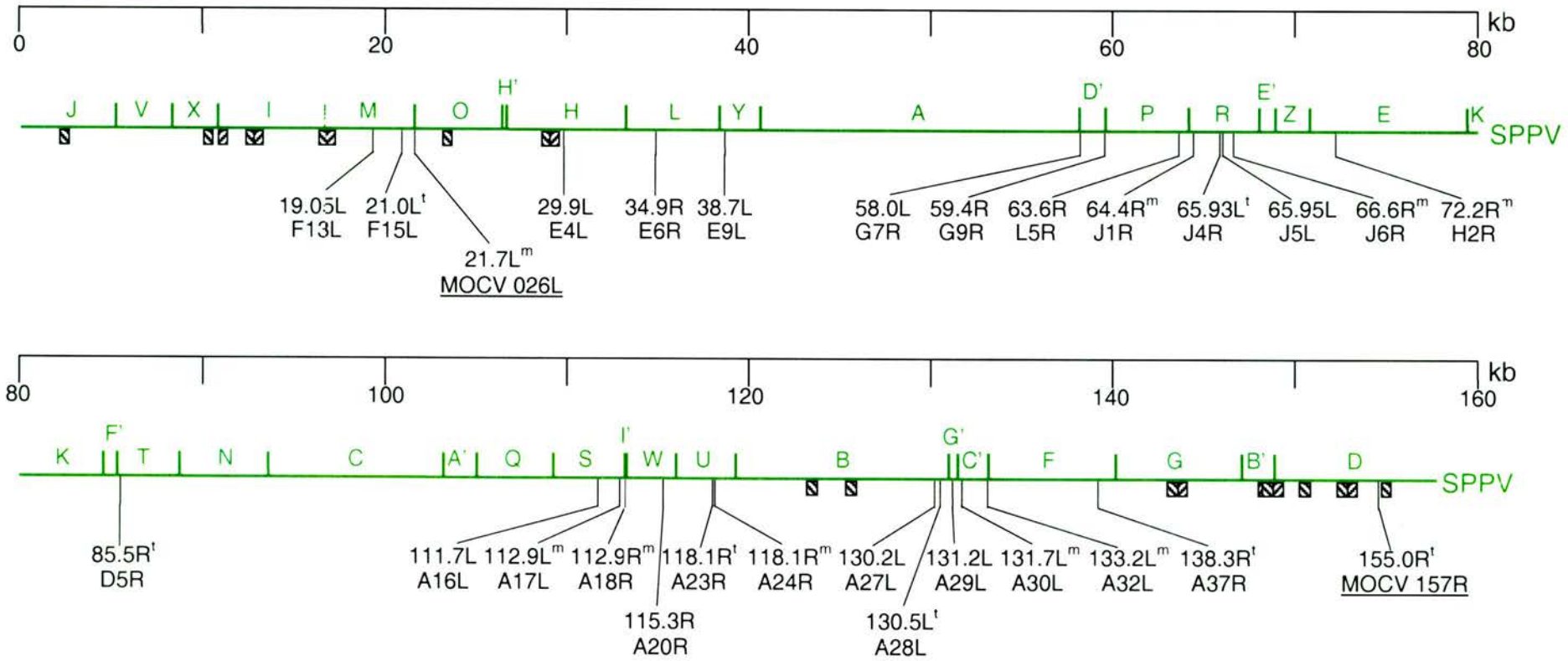

Figure 5.6 Genetic map of SPPV. The *Kpn* I restriction endonuclease map of SPPV is depicted in green. The location coordinates and the predicted direction of transcription are indicated below the genome for each of the 28 homologues of previously described poxvirus proteins (see section 5.3.1 for an explanation of the nomenclature used). The corresponding homologue of VACV is also indicated below the location coordinates, with the exception of MOCV 026L and MOCV 157R (underlined), which were previously thought to be unique to MOCV. The crosshatched boxes represent sequenced regions of the SPPV genome that do not encode previously described poxvirus genes.

too divergent in ORFV and SPPV for hybridisation to be visualised at the hybridisation stringency used. Unfortunately direct comparison of the sequence of the corresponding homologues in SPPV and ORFV was not possible because the ORFV sequences are not available in the databases.

A number of SPPV *Kpn* I fragments (S, I', W and M) hybridised weakly with ORFV DNA. Analysis of sequence obtained from within these fragments identified homologues of the VACV genes F13L, F15L, A16L, A17L, A18R and A20R. Homologues of these genes have been identified in all the completely sequenced vertebrate poxvirus genomes to date and are therefore likely to be present in ORFV. The weak hybridisation signals visualised suggest that these genes are divergent at the nucleotide level between ORFV and SPPV. However due to the absence of ORFV sequence in the databases no direct comparison of these genes could be performed between ORFV and SPPV, except for the F13L homologue. FastA alignment of the SPPV and ORFV F13L homologues revealed that they are only 61.6% homologous at the nucleotide level. Low levels of homology between SPPV and ORFV may explain the weak hybridisation signals with *Kpn* I restriction fragments S, I', W and M when using stringent hybridisation conditions.

As previously discussed probe 1, which is derived from the right end of the ORFV genome hybridised with *Kpn* I fragment I, which is situated at the left end of SPPV, suggesting a translocation of sequence (section 5.2.1). Sequencing of ORFV has revealed that the homologue of mammalian vascular endothelial growth factor (VEGF), interleukin-10 (IL-10), F9L, F10L and several ORFs without homologues in the databases are located within the region spanned by ORFV probe 1 (Mercer *et al.,* 1995; Fleming *et al.,* 1997; Rziha *et al.,* 2003). Four short lengths of sequence were obtained from within SPPV *Kpn* I fragment I, totalling approximately 2kb. Analysis of these sequences failed to identify homologues of the characterised ORFV genes. However if one or more of these genes are present within *Kpn* I fragment I they may be located between the regions sequenced and result in hybridisation between ORFV and SPPV. Alternatively, the hybridisation between probe 1 and *Kpn* I fragment I may be the result of one or more the unpublished genes being conserved in both viruses, but in different locations.

5.5 COMPARISON OF THE GENOME ORGANISATION OF SPPV WITH OTHER POXVIRUSES

To better understand the relationship of SPPV with other poxviruses, the genetic organisation of the SPPV genome was compared to the poxvirus genomes: ORFV (NZ2), VACV (Tian Tian) and MOCV (subtype 2).

A genome alignment of SPPV with ORFV (NZ2) was performed because SPPV is classified as a parapoxvirus (van Regenmortel *et al.,* 2000) and ORFV is the most characterised member of this genus. However, in the absence of a complete sequence of ORFV, only a preliminary alignment could be produced as only nine genes were identified as being common to both viruses. Mercer *et al.,* (1995) showed that ORFV is essentially collinear with VACV in the order and spatial distribution of genes, although several differences do exist in the terminal regions of the genomes. VACV has been completely sequenced; consequently a detailed alignment of SPPV and VACV could be produced using twenty-six genes predicted to be common to both viruses. Due to the collinearity of ORFV and VACV, the alignment of SPPV with ORFV could be extrapolated from an alignment of SPPV with VACV. Initially, SPPV was aligned with the Tian Tian strain of VACV, however since then, mistakes in the annotation of the Tian Tian genome have been noted (communication C Upton, XIVth International Poxvirus and Iridovirus Workshop, 2002). These mistakes concern the incorrect annotation of methionine and termination codons of a small number of ORFs. However, as no mistakes are apparent with the VACV ORFs that correspond with those identified in SPPV and it is the location of homologous points within a gene that concerns us here, the Tian Tian genome was deemed sufficiently accurate for the purpose of genome alignment with SPPV.

Due to the extensive protein homology between SPPV and MOCV (section 5.3.2) and as MOCV belongs to the only G+C rich genus other than the parapoxvirus genus; an alignment with MOCV was performed to assess the relatedness of SPPV with the molluscipoxviruses. MOCV has been completely sequenced, therefore a detailed alignment using twenty-seven genes predicted to be common to both viruses could be produced.

SPPV was aligned with ORFV, VACV and MOCV using the locations of genes predicted to be common to both genomes in the alignment as points of homology. As MOCV and VACV have been completely sequenced and the coding segments (CDS) of each ORF identified, it was possible to calculate the location in the MOCV or VACV genomes that corresponded

with SPPV co-ordinate by examining the FastA protein alignments of SPPV with MOCV and VACV.

The alignment of SPPV with the ORFV genome was more difficult because often the sequence obtained from SPPV and the sequence published for the corresponding ORFV genes did not overlap as the sequences are derived from different regions of the same genes. In this situation the homologous location in ORFV corresponding to a SPPV co-ordinate had to be estimated; this was achieved by extrapolating the alignment of the SPPV and ORFV protein via alignment with protein from a third poxvirus.

Once all the homologous co-ordinates in the ORFV, VACV and MOCV genomes were calculated or estimated, SPPV was manually aligned with each genome to allow visual comparison of organisation and spacing of genes (figure 5.7). In addition, the distance between a number of conserved poxvirus genes identified in SPPV, ORFV, MOCV and VACV were calculated and compared (table 5.3).

The ORFs in SPPV predicted to encode poxvirus proteins are identical in order to the homologues found in ORFV, VACV and MOCV. Therefore SPPV is highly collinear to other poxviruses in the order of genes that have been identified so far. However, the spatial distribution of genes is different in SPPV when compared with ORFV, MOCV and VACV. By visual comparison of the genome alignments (figure 5.7), the intervals between the corresponding genes in MOCV are greater than in SPPV. In contrast the distances between the corresponding genes in VACV and ORFV are smaller than in SPPV. The intervals between the nine genes homologues identified in SPPV, ORFV, MOCV and VACV demonstrate this spacing difference (table 5.3).

The size of the intervals between genes in MOCV, VACV and ORFV that most closely resemble those calculated in SPPV are highlighted in grey in table 5.3. The interval between VACV genes A27L and A29L and the homologues in ORFV are identical to those found in SPPV. However, the intervals between four pairs of genes in VACV are more like those calculated for SPPV than ORFV or MOCV. In comparison the intervals between two pairs of genes in ORFV and the interval between one pair of genes in MOCV are most like SPPV. Therefore from this data it appears that the organisation of genes in SPPV is more consistent with VACV than with ORFV or MOCV.

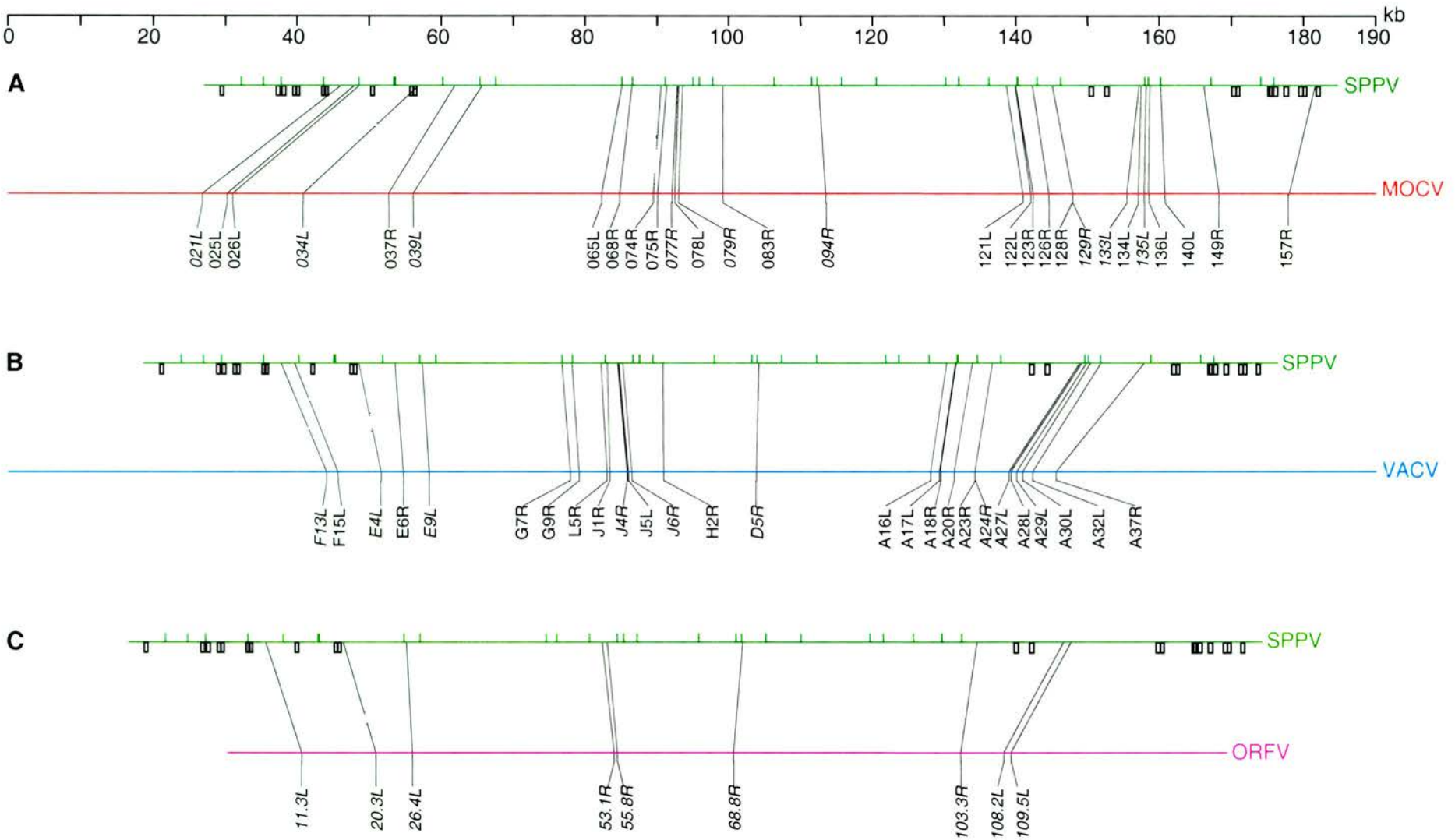
kb
0
20
40
60
80
100
120
140
160
180
190
A
SPPV
MOCV
021L
025L
026L
034L
037R
039L
065L
068R
074R
075R
077R
078L
079R
083R
094R
121L
122L
123R
126R
128R
129R
133L
134L
135L
136L
140L
149R
157R
B
SPPV
VACV
F13L
F15L
E4L
E6R
E9L
G7R
G9R
L5R
J1R
J4R
J5L
J6R
H2R
D5R
A16L
A17L
A18R
A20R
A23R
A24R
A27L
A28L
A29L
A30L
A32L
A37R
C
SPPV
ORFV
11.3L
20.3L
26.4L
53.1R
55.8R
68.8R
103.3R
108.2L
109.5L

Figure 5.7 Alignment of the SPPV genome with (A) MOCV subtype 2, (B) VACV Tian Tian and (C) ORFV NZ2 via several genes predicted to be homologous. The black lines connecting two aligned genomes indicate the locations of corresponding genes within each genome. The names of the homologous genes identified in MOCV, VACV and ORFV are indicated below each connector using the nomenclature previously described (Senkevich *et al.,* 1997; Johnson *et al.,* 1993; Mercer *et al.,* 1995). The locations of the nine genes which have been identified in SPPV, MOCV, VACV and ORFV and the distances between these genes examined further (see table 5.3) are indicated in italics (e.g. *021L*). The boxes situated below the SPPV genome indicate the regions of the SPPV genome that are sequenced but do not appear to encode known poxvirus genes.

SPPV co-ordinate	SPPV interval	ORFV homologue	ORFV co-ordinate	ORFV interval	VACV homologue	VACV co-ordinate	VACV interval	MOCV homologue	MOCV co-ordinate	MOCV interval
19.05L	/	11.3L^{m}	10.27	/	F13L	44.03	/	021L	26.81	/
29.9L	10.9	20.3L	20.62	10.4	E4L	51.63	7.6	034L	40.79	14.0
38.7L	8.8	26.4L	25.73	5.1	E9L	58.34	6.7	039L	56.13	15.3
65.93R^{t}	27.2	53.1R^{m}	53.66	27.9	J4R	85.93	27.6	077R	92.15	36.0
66.6R^{m}	0.7	55.8R	54.18	0.5	J6R	86.5	0.6	079R	93.01	0.9
85.5R^{t}	18.9	68.8R	70.30	16.1	D5R	103.78	17.3	094R	113.51	20.5
118.1R^{m}	32.6	103.3R	102.0	31.7	A24R	134.34	30.6	129R	147.99	34.5
130.2L	12.1	108.2L^{m}	108.0	6.0	A27L	139.06	4.7	133L	155.53	7.5
131.2L	1.0	109.5L	109.0	1.0	A29L	140.10	1.0	135L	157.89	2.4

Table 5.3 Summary of the distances between homologous genes in the SPPV, ORFV (NZ2), VACV (Tian Tian) and MOCV (subtype 2) genomes. The data shaded grey indicated the intervals between genes in ORFV, VACV and MOCV that are closest to the interval in SPPV.

The notable difference in distribution of genes is the interval between homologues of the VACV genes A24R and A27L. In SPPV the distance is 12.1kb, in ORFV, VACV and MOCV this distance is much smaller at 6.0kb, 4.7kb and 7.5kb respectively. Sequence was obtained from the SPPV genome from two locations situated between the homologues of A24R and A27L. FastA analysis of the nucleotide sequence and putative translated ORFs failed to reveal homology with previously described poxvirus genes.

5.6 DISCUSSION

Homologues of the VACV genes extending from F9L to A34R are generally found in all poxviruses and represent the conserved central core and is likely contains to the minimal gene complement required for viral replication (Gubser and Smith, 2002). The region of the SPPV genome extending from 17kb to 133kb hybridised with the central region of ORFV, demonstrating a genetic relationship between the central regions of the two poxviruses (figure 5.2). The establishment of a genetic map of SPPV revealed that the cross-hybridisation regions of ORFV and SPPV contain homologues of the VACV genes extending from F13L to A32L. Therefore cross-hybridisation data corresponds extremely well with the region representing the conserved central core of genes. Many of the twenty-six genes located within the central region of the SPPV genome are predicted to be essential for the replication of poxviruses as they encode for proteins involved in viral transcription and DNA replication (table 5.2). The sequences derived from within the central region of SPPV genome shares greater than 60% homology at the DNA level with the G+C rich poxviruses MOCV or ORFV, which would account for the hybridisation of this region with ORFV. The general organisation of the central region of SPPV (17kb to 133kb) was predicted to be collinear with ORFV based upon the identical order which the ORFV probes and SPPV *Kpn* I fragments hybridised. The order and orientation of the twenty-six genes located in the central core of the genome were identical to the homologues described in all characterised poxviruses except FPV, which has undergone rearrangement of the central regions (Afonso *et al.*, 2000). Therefore SPPV is collinear with most other poxviruses.

The spacing of genes in SPPV is more similar to the spacing of genes in ORFV and VACV, although considerable differences do exist. VACV and ORFV have previously been described as being highly collinear, although minor differences in the spacing of genes do exist (Mercer *et al.*, 1995). From the data (table 5.3), it appears that the spacing of genes in SPPV is more like that

found in VACV than ORFV. However, due to the limited amount of ORFV sequence data only a total of nine homologous points between ORFV and SPPV could be established and therefore it is not possible to determine, with certainty, if SPPV is more consistent with VACV or ORFV in genome organisation.

Towards the ends of the central core in SPPV the gene content and organisation is less conserved than in the centre, when compared with other poxviruses. For example, at the left end of the conserved central core of SPPV a homologue of the MOCV unique gene 026L was identified (Senkevich *et al.,* 1997). One major difference in the organisation of genes located towards the right end of the SPPV central core is the distance between the homologues of the VACV genes A24L and A27L. Here the distance is much larger in SPPV than in ORFV, VACV or MOCV. Sequence derived from two locations situated between A24L and A27L did not match with any known poxvirus DNA or protein sequence deposited in the databases. The closest DNA homologies of this G+C rich region were with rodent sequence (EMBL accession numbers AF292401 and AC013622). This indicates that approximately 7kb of DNA, possibly host in origin, may have been incorporated into the SPPV genome during in the evolution of this virus. Towards the termini several sequences also gave the closest FastA matches with rodent DNA. Homologues of cellular genes are found in all poxviruses characterised to date and many of these genes confer an advantage to the virus *in vivo* by interfering with the host immune response (Bugert and Darai, 2000). The transfer mechanism of host genes to poxvirus genomes is unclear. However, VACV DNA ligase has been shown to efficiently ligate the 3'-hydroxyl group of RNA with the 5'-phosphate group of DNA, hence providing a possible route in which cellular mRNA could be incorporated into poxvirus genomes (Sekiguchi and Shuman, 1997). The direct incorporation of RNA based genetic information into poxvirus genomes may also explain the absence of host derived introns within poxvirus genomes.

The terminal regions of parapoxvirus genomes only cross-hybridise in a species-specific manner (Gassmann *et al.,* 1985). Therefore it is not surprising that ORFV did not hybridise with 10kb at the left end and 25kb at the right end of the SPPV genome, suggesting that the ends of the two genomes diverge at the DNA level.

Analysis of sequences obtained from the terminal (non-hybridising) regions of SPPV failed to match with known poxviruses sequences, except for sequence corresponding to the VACV gene

A37R and MOCV 157R. MOCV 157R is not present in ORFV in a comparable location (Rziha *et al.*, 2003) and therefore will not result in cross-hybridisation between SPPV and ORFV. Homologues of the A37R are not well conserved at the protein or nucleotide level across the poxvirus genera. The lack of hybridisation of the SPPV restriction fragment containing A37R (*Kpn* I fragment F) with ORFV suggests that the genes expected to be located within this fragment (homologues of VACV A33R to A37R) are divergent from ORFV at the DNA level. The rarity of identifiable homologues of poxvirus genes located at the ends of the SPPV genome indicates that the terminal regions may be mostly unique to SPPV. Further analysis of the terminal regions may result in the identification of genes associated with host range or immune modulation, knowledge that is essential for future production of a vaccine.

DNA hybridisation suggests that the 10kb to 17kb region of the SPPV genome consists of DNA sequence that is homologous to the right end of ORFV genome (spanned by probe 1) (section 5.4.1). Several genes have been identified in ORFV from the probe 1 region, including homologues of the VACV F9L and F10L (Rziha *et al.*, 2003). Sequence analysis of several parapoxvirus species has revealed that F9L and F10L are translocated to the right-end of the genome close to the ITR junction, with respect to other poxviruses (Mercer *et al.*, 1995; Rziha *et al.*, 2003; Ueda *et al.*, 2003). The hybridisation of ORFV DNA containing the F9L and F10L homologues with the left end of the SPPV genome may suggest that the translocation event, which is common to all parapoxviruses characterised to date, may not have occurred in SPPV. Therefore it is probable that F9L and F10L homologues in SPPV may be found at the left end of the genome within *Kpn* I fragment I. However mapping the location of these genes in SPPV using DNA sequencing or hybridisation is required to confirm this.

In summary, the genome of SPPV consists of a central core region containing conserved genes essential for virus replication, which is flanked by non-conserved terminal regions. These terminal regions may encode for SPPV-specific genes that were acquired from the host during in co-evolution. Hence, the organisation of SPPV is consistent with other poxvirus genomes (Gubser and Smith, 2002). Hybridisation studies using DNA templates of specific ORFV genes and phylogenetic analysis was performed in order to further characterise the relationship of SPPV with ORFV and to possibly identify genes associated with immune modulation that are common to both viruses. This is discussed in chapter 6.0.

CHAPTER 6.0

GENES ASSOCIATED WITH IMMUNO-MODULATION OR VIRUS VIRULENCE AND TRANSCRIPTION CONTROL SIGNALS PRESENT IN THE GENOME OF SPPV

6.1 INTRODUCTION

Random sequencing of SPPV enabled a preliminary genetic map to be determined, however only nine of the SPPV genes matched published ORFV genes (section 5.3.1). Therefore comparison of the genomic organisation of the two genomes was limited. Characterisation of the ORFV genome is ongoing in the laboratory where this study was performed. A preliminary map of the early genes of ORFV (strain orf-11) has been produced and cDNAs encoding ORFV early genes isolated (C McInnes personal communication). A series of DNA hybridisations, using several cloned ORFV early genes as probes, were performed in order to investigate the presence of homologous sequences in the SPPV genome and clarify the organisational relationship between SPPV and ORFV. The presence of four genes in SPPV encoding for: a homologue of interleukin-10 (IL-10), homologue of vascular endothelial growth factor (VEGF-E), the interferon resistance protein (E3L) and the granulocyte macrophage colony stimulating factor/interleukin-2 inhibitory factor (GIF), was investigated in the first instance using hybridisation.

Three of these genes, IL-10, GIF and E3L are implicated in modulation of the host immune response (Haig *et al.*, 1998; Deane *et al.*, 2000; Fleming *et al.*, 2000; Haig *et al.*, 2002). The fourth gene (VEGF-E) is believed to enhance virulence by stimulating epidermal proliferation and increasing cellular permeability, thereby increasing the number of target cells available for ORFV infection and attributing to scab formation (Savory *et al.*, 2000). To date, GIF and VEGF genes have only been identified in parapoxviruses (Lyttle *et al.*, 1994; Deane *et al.*, 2000; Mercer *et al.*, 2002; Buttner and Rziha, 2002; Rziha *et al.*, 2003; Ueda *et al.*, 2003), whilst the E3L gene is a highly conserved in most poxviruses sequenced to date, except for MOCV and FPV (Senkevich *et al.*, 1997; Afonso *et al.*, 2000). Recently a homologue of the IL-10 gene was also identified in the capripoxvirus LSDV (Tulman *et al.*, 2001).

It was hypothesised that SPPV was likely to possess a homologue of the ORFV VEGF-E, due to the superficial similarities between SPPV and ORFV dermal lesion pathology. Erythmatous response and extensive scab production are a general feature of both diseases and the lesions are often haemorrhagic in nature (Edwards, 1962; Keymer, 1983; Reid, 1991; Sainsbury and Gurnell, 1995; Sainsbury and Ward, 1996; Buttner and Rziha, 2002). The haemorrhaging associated with SPPV lesions would suggest an underlying vascularisation, however

histopathological examination of SPPV-induced lesions have not been performed to confirm this.

DNA sequencing was also employed to investigate whether homologues of the VACV E3L and the ORFV VEGF-E genes are present in the SPPV genome. The characterisation of the SPPV genome structure (chapter 4.0) and the construction of a genetic map (section 5.4) enabled targeted sequencing of the regions of the SPPV genome that may contain homologues of these genes. However, the probable locations of the homologues of the ORFV genes IL-10 and GIF in the SPPV genome could not be sufficiently determined to enable targeted sequencing. This was due to insufficient data concerning the regions flanking the ORFV genes IL-10 and GIF and the corresponding regions in SPPV at the time this study was performed.

Sequence located upstream of putative translation initiation (ATG) and downstream of putative termination (TAG, TAA, TGA) codons that were identified during random or targeted sequencing was assessed for poxvirus-like promoter and termination signals. The identification of transcription control elements is a positive indicator of the likelihood that the ORFs identified encode genuine genes.

Phase-specific transcriptional control sequences have been extensively characterised in VACV. Analysis of VACV promoters revealed that both early and intermediate gene promoters are organised into three functional regions; a transcription initiator, the promoter core and a spacer region (Davison and Moss, 1989a; Baldick *et al.,* 1992) (figure 6.1). Although the two promoters are similar in organisation and have comparable A+T contents, several differences do exist. Mutational analysis of the core regions of early and intermediate promoters has revealed that several conserved nucleotides are essential for strong promoter function. The sequence of the VACV late promoter is quite different from early and intermediate promoters and consists of the conserved initiator sequence TAAAT (figure 6.1), which is often preceded by an A+T-rich track approximately 20nt in length (Davison and Moss, 1989b).

Early gene transcription ceases approximately 50nt downstream of a conserved TTTTTNT signal (Yuen and Moss, 1987). No termination signals have been identified for intermediate and

late transcription, which would explain the heterogeneous lengths of intermediate and late transcripts (Weir and Moss, 1984; Baldick and Moss, 1993).

The A+T-rich transcription control sequences of VACV are remarkably well conserved in the G+C rich genomes of parapox and molluscipox viruses (Mercer *et al.,* 1989; Fraser *et al.,* 1990; Naase *et al.,* 1991; Blake *et al.,* 1991; Fleming *et al.,* 1991; Sullivan *et al.,* 1994; Sullivan *et al.,* 1995b; Sullivan *et al.,* 1995a; Mercer *et al.,* 1996b; Senkevich *et al.,* 1997). Therefore it was hypothesised that similar sequences would also be found in SPPV. Hence putative SPPV promoter sequences located up stream of several putative ORFs were identified and compared with those preceding comparable MOCV and VACV genes. The relevance of putative SPPV promoters in determining genuine SPPV genes and transcription mechanism in SPPV is discussed.

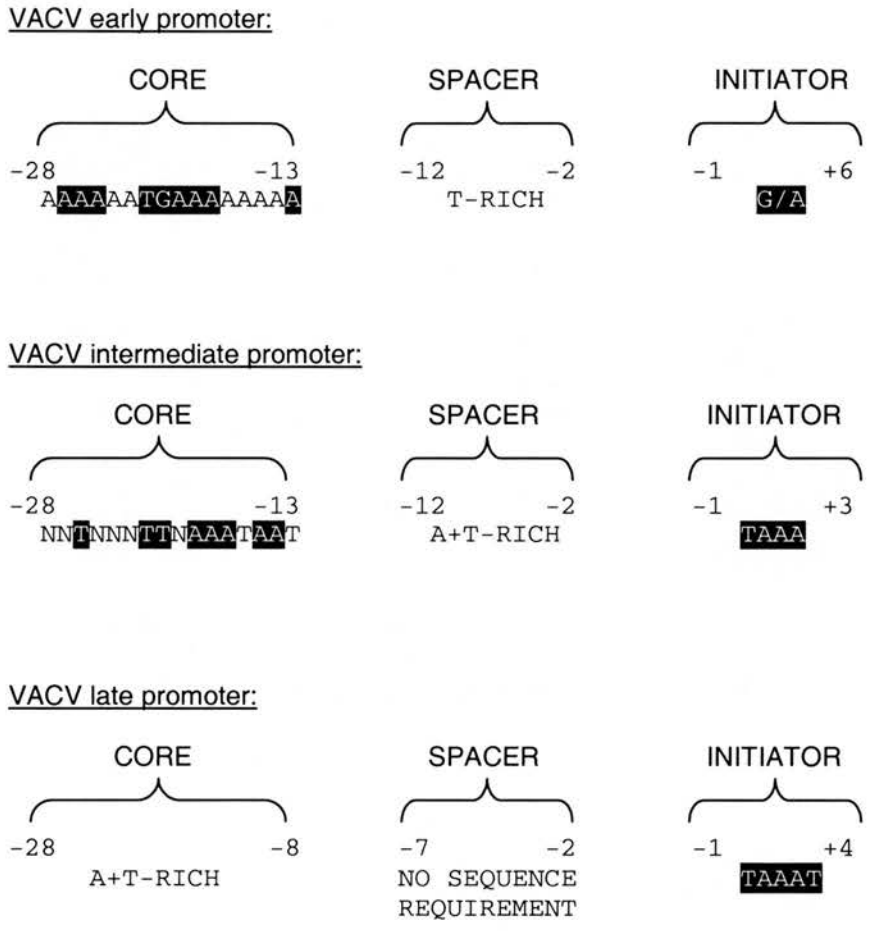

Figure 6.1 Schematic representation of the VACV early, intermediate and late promoters adapted from Davison and Moss (1989a and 1989b) and Baldick *et al.,* (1992). Transcription occurs with a purine (G or A) located within the initiator element of the early promoter and within the AAA initiator sequence for intermediate and late promoters. An 11nt A+T rich spacer region separates the A-rich conserved cores of early and intermediate promoters from the initiators. In late promoters the spacer is only 6nt and does not have any sequence requirement. The nucleotides essential for strong promoter function are highlighted in black.

6.2 HYBRIDISATION OF SPPV WITH ORFV GENES

Cloned DNAs (cDNAs) encoding for ORFV homologues of the VACV genes: E3L, I3L, G2R, L2R, J4R, H5R, A8R, A33R and the ORFV genes IL-10, VEGF-E and GIF (table 6.1 for a summary of the gene functions) were excised from their plasmid vector and radio-labelled with [α-^{32}P] dCTP using the random prime method outlined in section 2.4.5.2.1.

SPPV cosmid clones 5, 9, 28, 51 and 86, which span the SPPV genome (section 4.6) and ORFV genomic DNA (strain orf-11) were digested with *Kpn* I. 1.5μg of each digested DNA sample was electrophoresed on a 0.6% (w/v) agarose gel (figure 6.2). The gel was depurinated, denatured, neutralised and the DNA transferred to nylon membrane using the Southern blotting procedure (section 2.4.5.3.1).

Membranes were incubated at 60°C with the [α-^{32}P] dCTP-labelled ORFV cDNAs for approximately 16 hours. The hybridised membranes were sequentially washed with increasing stringency until a positive hybridisation signal could be visualised with minimal background hybridisation (section 2.4.5.5) and the resulting autoradiographs can be seen in figure 6.3.

A homologue of the VACV gene J4R, which encodes for the RNA polymerase subunit RPO22, was previously identified in SPPV by sequencing (section 5.3.1). Hence cDNA encoding for the ORFV homologue of the VACV gene J4R was used as a control probe to verify that homologues of the ORFV genes could be detected in SPPV with the hybridisation conditions used. Hybridisation of SPPV *Kpn* I digested cloned DNA with labelled J4R ORFV cDNA and subsequent washing at high stringency resulted in the detection of the SPPV J4R homologue (figure 6.3). However, the hybridisation signal of ORFV J4R with SPPV is much weaker when compared with the control ORFV DNA, suggesting underlying sequence divergence at the nucleotide level. The hybridised SPPV fragment is situated within cosmid clone 5 and corresponds to *Kpn* I fragment R, which is the predicted location from DNA sequencing (refer to figure 5.6).

Gene[1/2]	Function	References
Genes conserved in several poxviruses:		
E3L[1]	dsRNA binding, PKR inhibitor, IFNγ resistance	Davies *et al.*, 1993.
I3L[1]	ssDNA-binding protein, interacts with R2 subunit of ribonucleotide reductase.	Rochester and Traktman, 1998.
G2R[1]	Late transcription elongation factor	Condit *et al.*, 1996.
L2R[1]	unknown	
J4R[1]	RNA polymerase subunit RPO22	Broyles and Moss, 1986.
H5R[1]	Late transcription factor VLTF-4	Kovacs and Moss, 1996.
A8R[1]	Intermediate transcription factor VTLF-3	Sanz and Moss, 1999.
A33R[1]	EEV glycoprotein, promotes cell to cell spread	Roper *et al.*, 1996 and 1998.
IL-10[2]	Functional homologue of IL-10	Fleming *et al.*, 1997; Tulman *et al.*, 2001.
Genes unique to parapoxviruses:		
VEGF-E[2]	Functional homologue of VEGF	Lyttle *et al.*, 1994.
GIF[2]	IL-2 and GM-CSF inhibitor	Deane *et al.*, 2000.

Table 6.1 Summary of the gene function and level of conservation within the poxvirus family of the ORFV cDNA used to probe SPPV DNA.

[1] The ORFV cDNAs are referred to by the VACV homologue nomenclature,

[2] or are referred by the nomenclature used for ORFV.

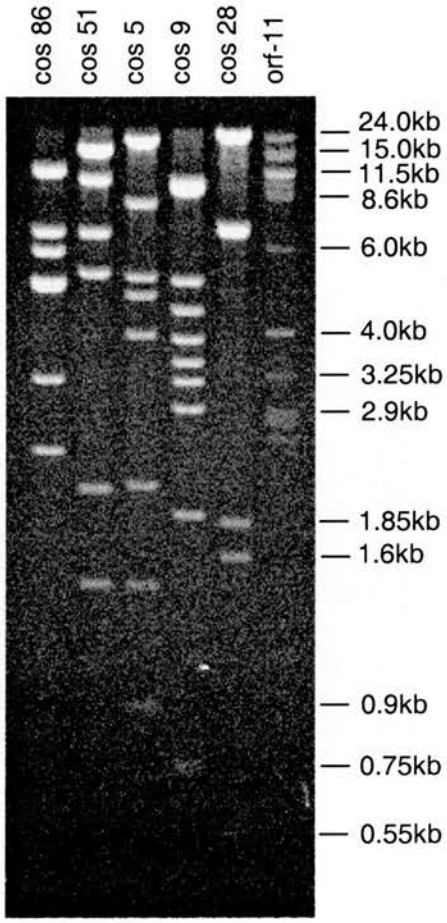

Figure 6.2 SSPV DNA cosmid clones 86, 51, 5, 9 and 28 and ORFV strain orf-11 DNA, digested with *Kpn* I and electrophoresed on a 0.6% (w/v) agarose gel. The DNA bands were visualised by Ethidium bromide staining and illumination under UV light.

Figure 6.3

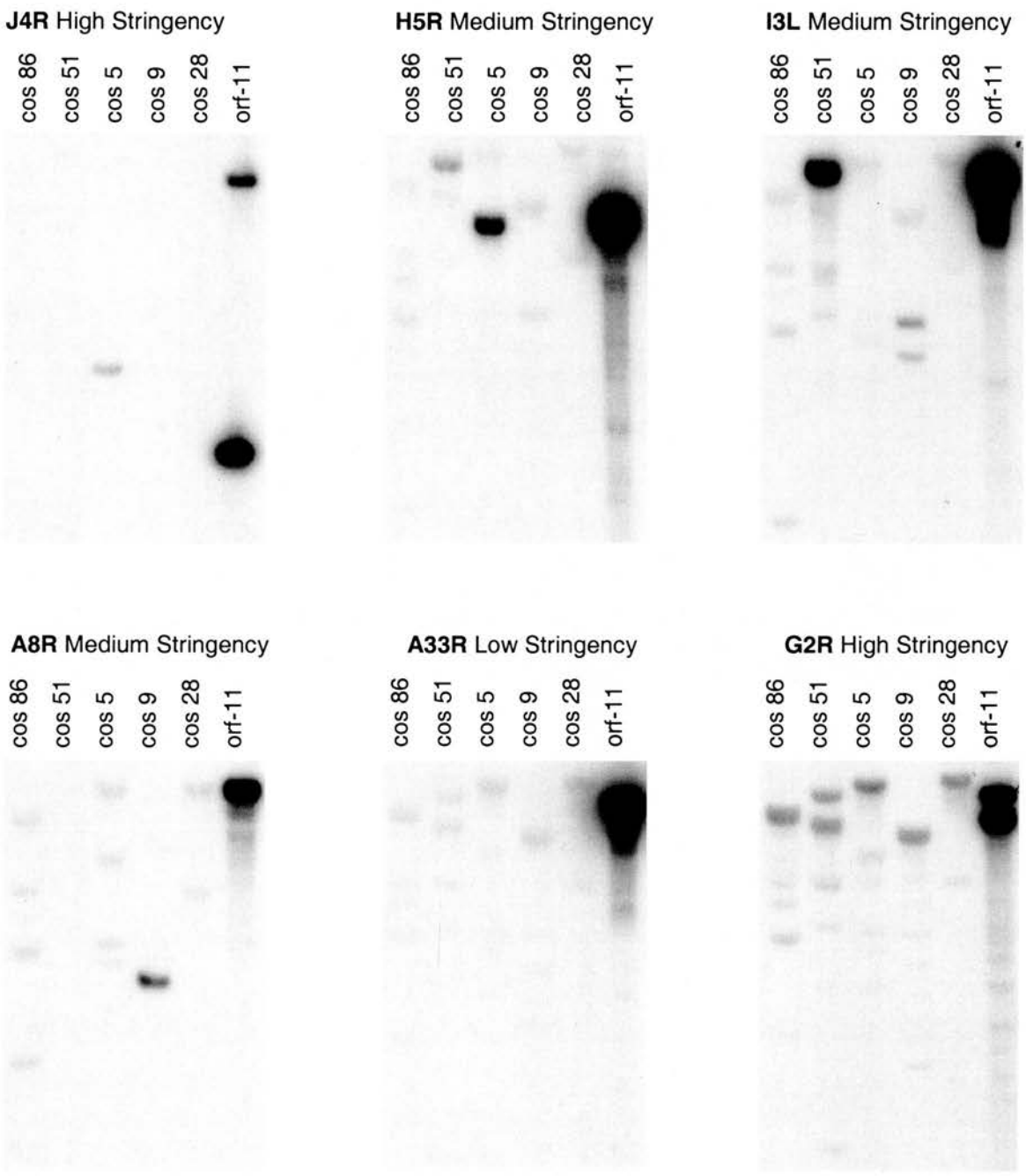
J4R High Stringency
cos 86
cos 51
cos 5
cos 9
cos 28
orf-11
H5R Medium Stringency
cos 86
cos 51
cos 5
cos 9
cos 28
orf-11
I3L Medium Stringency
cos 86
cos 51
cos 5
cos 9
cos 28
orf-11
A8R Medium Stringency
cos 86
cos 51
cos 5
cos 9
cos 28
orf-11
A33R Low Stringency
cos 86
cos 51
cos 5
cos 9
cos 28
orf-11
G2R High Stringency
cos 86
cos 51
cos 5
cos 9
cos 28
orf-11

L2R Low Stringency

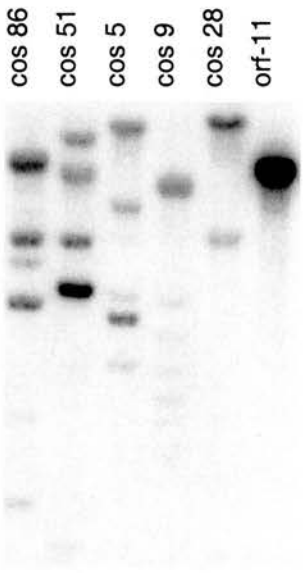

L2R Medium Stringency

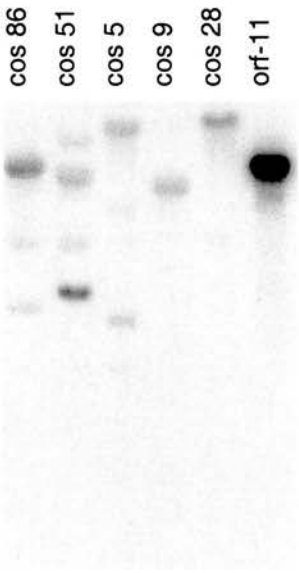

E3L Low Stringency

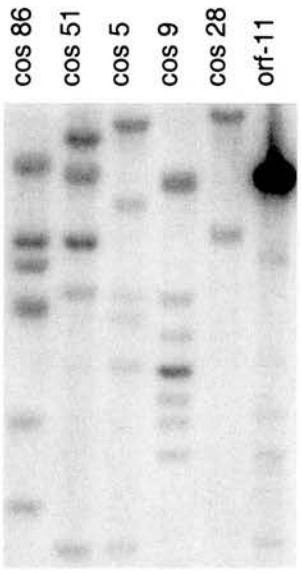

E3L Medium Stringency

VEGF-E Low Stringency

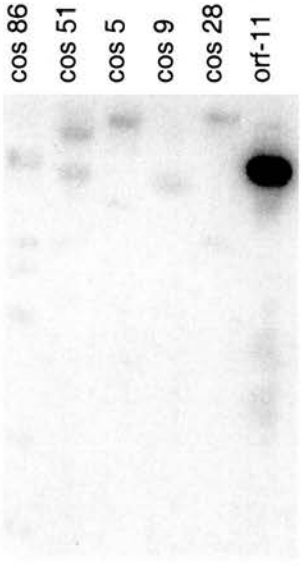

VEGF-E Medium Stringency

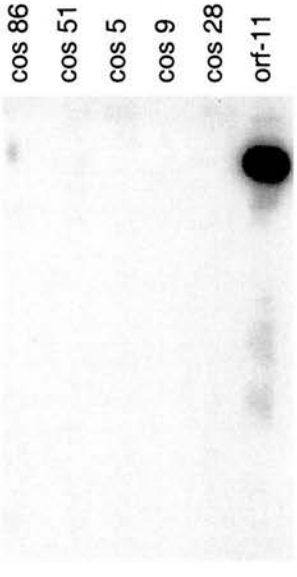

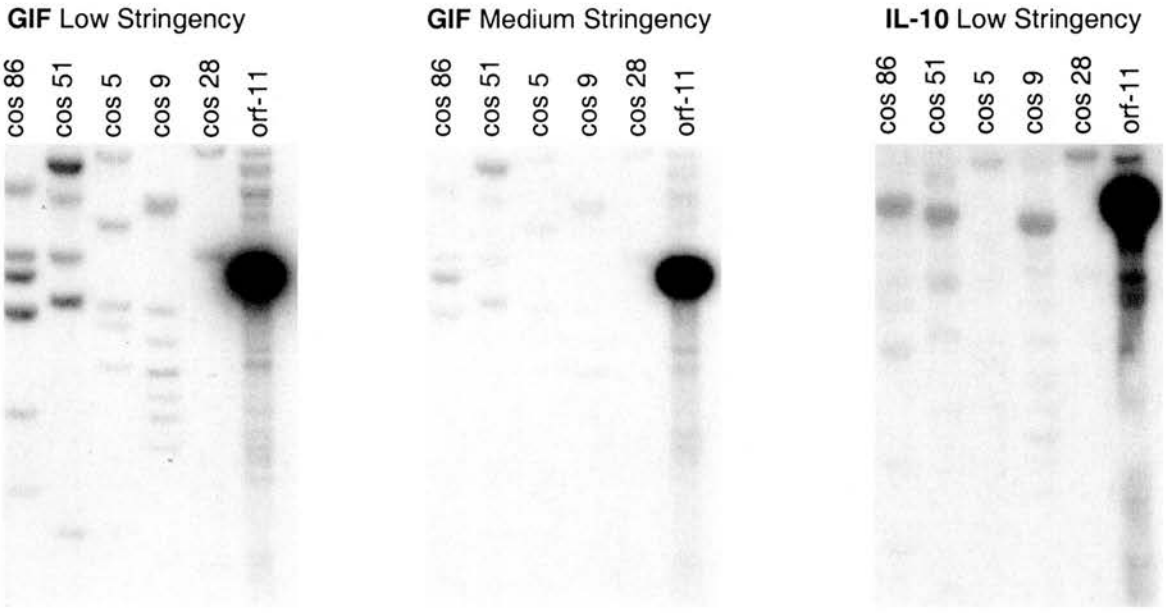

Figure 6.3 Southern blots of *Kpn* I digested SPPV cosmid clones and *Kpn* I digested ORFV DNA (strain orf-11) (depicted in figure 6.2) hybridised with several [α-32P] dCTP-labelled ORFV cDNAs. All hybridisations were performed at 60°C for 16 hours and the hybridised membranes sequentially washed twice for 30 minutes each using low stringency conditions (2XSSC/0.1%SDS at room temperature), medium stringency conditions (2XSSC/0.1%SDS at 60°C) or high stringency conditions (0.2XSSC/0.1%SDS at 60°C). The membranes were then exposed to medical X-ray film for 30 minutes and the developed using a compact X2 automated film processor (X-Ograph imaging systems). Autoradiographs were scanned and digitised using scanner and Image Master LabScan v3.01 software (Amersham Pharmacia Biotech).

Homologues of the VACV genes H5R, I3L and A8R were also clearly detected in SPPV by hybridisation with ORFV cDNAs (figure 6.3). The intensity of the hybridised *Kpn* I fragments was sufficient to be able to clearly distinguish between hybridised fragments and background at medium stringency. The ORFV cDNA H5R probe hybridised with SPPV *Kpn* I fragment E (located within cosmid clone 5 and 8.4kb in size), probe I3L hybridised with *Kpn* I fragment A (located within cosmid clone 51 and 17kb in size) and probe A8R hybridised with *Kpn* I fragment Q (located within cosmid clone 51 and 5.05kb in size). The mapped locations of homologues of H5R, I3L and A8R correspond well with their predicted locations extrapolated from the genetic map of SPPV (section 5.4 and figure 5.2) and are comparable to the locations found in other poxvirus genomes.

Hybridisation of SPPV DNA with the ORFV cDNA probes G2R and L2R resulted in non-specific hybridisation, which could not be eliminated with stringent washing. Though *Kpn* I fragment L appeared to hybridise more intensely with ORFV L2R, it is likely to be non-specific hybridisation as the putative location of L2R within *Kpn* I fragment L does not correspond with the location in any of the characterised poxviruses. Hybridisation of SPPV DNA with the ORFV cDNA probe A33R did not produce a visible signal. The absence of a clear hybridisation signal with the ORFV probes G2R, L2R and A33R would indicate these genes are absent in SPPV, however homologues of these three gene have been identified in all poxviruses sequenced to date, except FPV, which lacks L2R and A33R (Afonso *et al.*, 2000). Therefore homologues of L2R, G2R and A33R were thought likely to be present in the SPPV genome, but they may not be sufficiently conserved with the corresponding ORFV genes at the nucleotide level to be detected by DNA hybridisation.

Hybridisation of cloned SPPV DNA with ORFV cDNA probes E3L, GIF, VEGF-E and IL-10, with washes performed at medium stringency, did not produce any intense hybridisation signals, except with the control ORFV DNA. When the membranes were washed at low stringency, heavy background hybridisation was visible on all four blots. However, four SPPV *Kpn* I fragments, located within cosmid clones 51 and 86, hybridised more intensely with the GIF probe at low stringency than other fragments. The four fragments correspond to the *Kpn* I fragments, A, L, O and I. These *Kpn* I fragments are not adjacent and therefore the hybridisation seen is unlikely to be the result of a GIF homologue overlapping one or more of the SPPV *Kpn* I fragments. Furthermore, the GIF gene is located near the right end of the genome in ORFV (Deane *et al.*, 2000; Buttner and Rziha, 2002) and the cosmid clones 51 and 86 are derived from the left end of the SPPV genome. These observations suggest that the SPPV DNA fragments that seemingly hybridise with the GIF probe are likely to represent non-specific hybridisation.

6.3 TARGETED SEQUENCING

In the absence of clear hybridisation signals between SPPV genomic DNA and ORFV cDNA encoding VEGF-E and E3L, regions of the SPPV genome were sequenced in order to investigate the presence or absence of these genes.

6.3.1 Sequencing the region predicted to contain a homologue of the ORFV vascular endothelial growth factor (VEGF-E)

In parapoxviruses the VEGF-E genes are located close to the right ITR (Lyttle *et al.,* 1994; Rziha *et al.,* 2003; Ueda *et al.,* 2003). Therefore DNA sequence was obtained from the comparable region in SPPV and analysed for the presence of a homologue of the ORFV VEGF-E gene. Overlapping sequences were obtained from the cloned restriction fragments *Bam* HI W and *Not* I L by sequencing the ends of the cloned fragments or with specifically designed oligonucleotide primers. The contiguous sequence extends leftwards from the right-ITR junction for 1050bp (figure 6.4) and spans the region comparable to ORFV that contains the VEGF-E gene.

FastA analysis was performed with the nucleotide sequence, but no homologous poxvirus DNA sequence was detected. Likewise, no VEGF protein was detected with any of the translated putative ORFs. However, one ORF (designated SP 155.0R^{t}) aligned with two related MOCV proteins MOCV 003L and MOCV 157R (Senkevich *et al.,* 1997). SP 155.0R^{t} exhibited 29.9% and 27.5% identity at the amino acid level with MOCV proteins 003L and 157R respectively. Although the location of the termination codon for SP 155.0R^{t}, MOCV 003L and MOCV 157R all approximately correspond, the C-terminal 80 to 100 amino acids were highly heterogeneous.

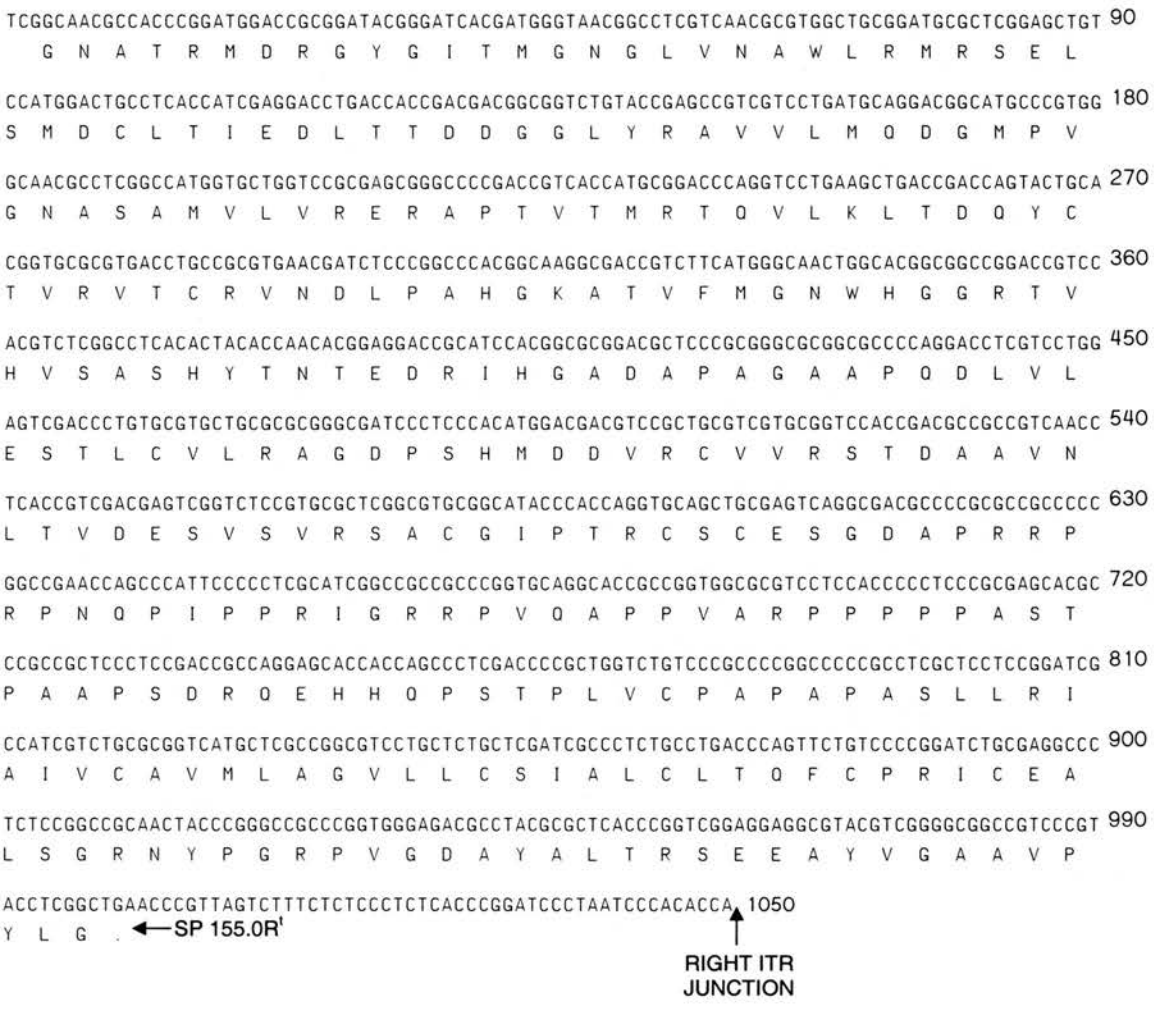

Figure 6.4 DNA sequence derived from the unique region situated immediately out-with ITR at the right end of the SPPV genome presented in the same orientation as the SPPV genome (5' to 3'). The right ITR junction is indicated in the figure and is located at nucleotide position 1050 on the sequence presented. The predicted amino acid sequence of the putative ORF SP 155.0R' is presented below the DNA sequence.

6.3.2 Sequencing the region predicted to contain homologues of the ORFV interferon (IFN) resistance and RNA polymerase subunit RPO 030 genes

The homologue of the VACV RNA polymerase subunit RPO 030 gene (E4L) was identified by sequencing the left end of *Not* I fragment I (section 5.3.2), however the sequence did not contain either the E4L initiation or termination codons. In most poxviruses a homologue of VACV gene E3L is located immediately downstream of E4L. Therefore it was important to establish the location of the E4L termination codon so that the region downstream of the E4L homologue could be analysed to determine if a homologue of E3L is present within the SPPV genome in a location comparable to other poxviruses.

The *Not* I fragment located left of fragment I was predicted to contain the termination codon of E4L. In order to identify the termination codon and obtain DNA sequence from the region of the genome to the left of the E4L homologue, the *Not* I fragment H' was completely sequenced using vector-specific T3 and T7 primers. In addition, the left end sequencing of *Not* I fragment I was repeated using the T7 primer and extended further by sequencing *Not* I fragment I using oligonucleotide primer (E4L-1) in order to identify the initiation codon of E4L. Additional DNA sequences were also obtained by sequencing the overlapping *Bam* HI fragment H using the oligonucleotide primers, E4L-2 and E4L-3 (figure 6.5 for schematic representation of the sequenced regions of *Not* I fragments I and H' and the *Bam* HI fragment H). Using the overlapping sequences, a 1.6kb contiguous sequence was obtained and is presented in figure 6.6.

Putative ORFs were identified using the analysis software DNASTAR MapDraw v5.00 (DNASTAR Inc.). The translated putative ORFs were compared to protein sequences deposited in the SWALL library using the FastA algorithm to identify homologous sequences (section 2.4.8.2). Two ORFs, designated SP 30.72L^{m} and SP 29.55L^{m} exhibited identity with previously characterised poxvirus proteins. ORF SP 30.72L^{m} corresponded with homologues of the VACV gene E4L and is discussed further in section 6.3.2.1. ORF SP 29.55L^{m} exhibited limited identity with the homologues of the VACV gene E3L and is discussed in section 6.3.2.2.

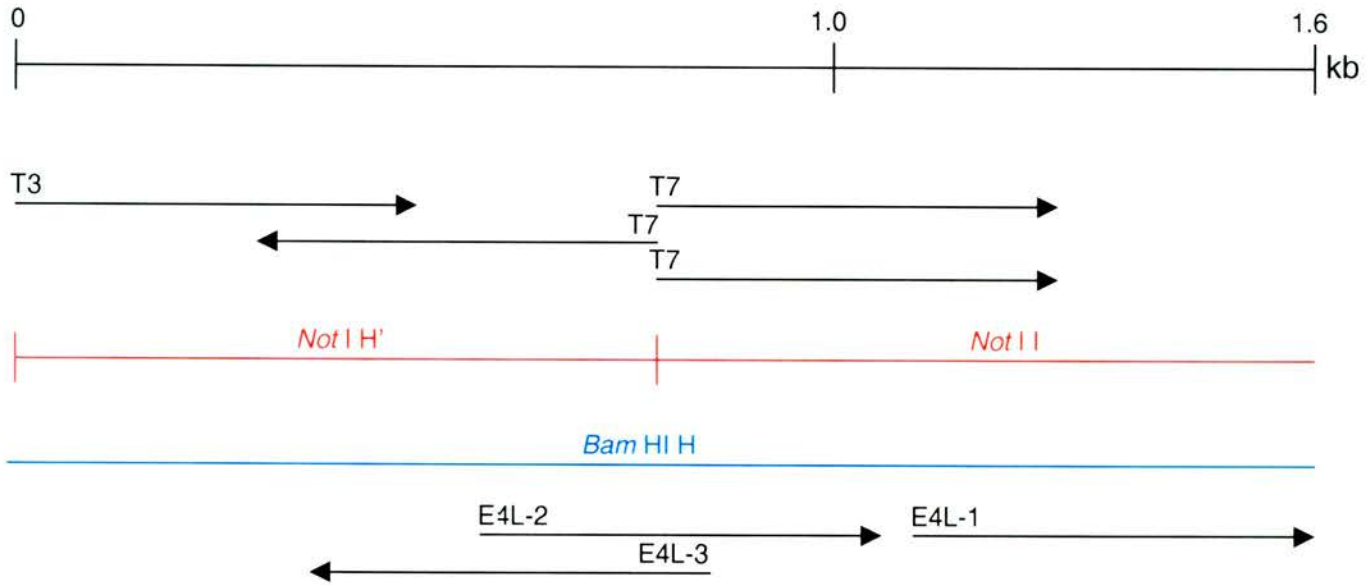

Figure 6.5 Schematic representation of the regions of the *Not* I fragment I and H' (depicted in red) and *Bam* HI H (depicted in blue) sequenced. The ends of the fragments were sequenced using the ol gonucleotide primers T3 and T7; and overlapping sequence obtained by sequencing the *Bam* HI fragment H with the primers E4L-2 and E4L-3, and *Not* I fragment I with primer E4L-1. The black arrows represent individual sequences, which were combined to determine the 1.6kb contiguous sequence that is presented in figure 6.6.

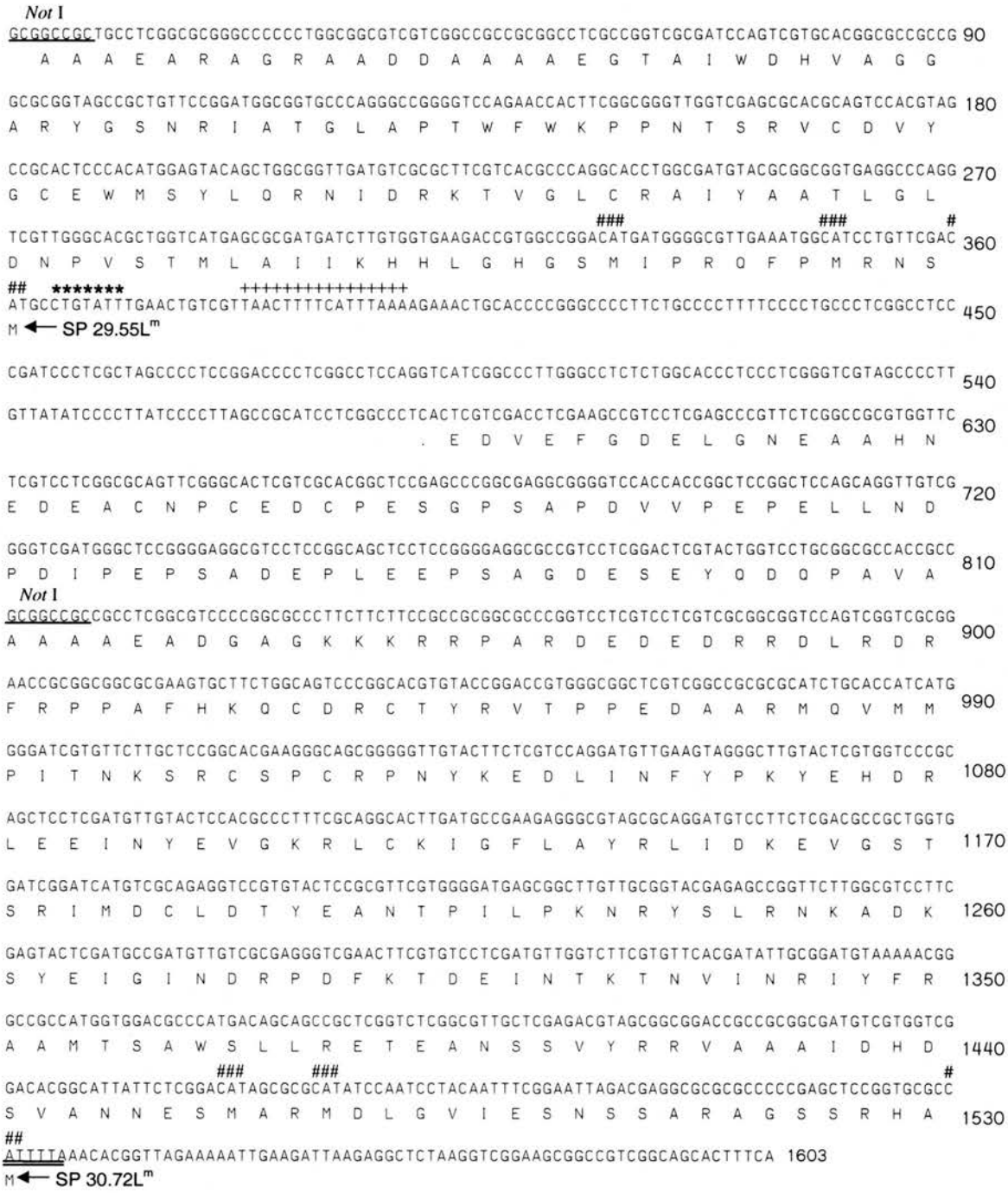

Figure 6.6 Contiguous nucleotide sequence of the region spanning *Not* I fragment H' and the left end of *Not* I fragment I (see figure 6.5) presented in the same orientation as the SPPV genome (5' to 3'). The predicted amino acid sequences, which are encoded by the reverse complement DNA strand (not shown), of the homologue of the VACV gene E4L (SP 30.72L$^{m)}$ and putative ORF SP 29.55L^{m} are present below the DNA sequence. The potential initiating methionines are indicated with the # symbols for each ORF. Putative early transcription control sequences are indicated by the symbol + for the promoter core and the symbol * for the initiator and a putative late promoter initiator is double underlined.

6.3.2.1 SPPV homologue of the VACV gene E4L

FastA analysis of the putative ORF SP 30.72L^{m} revealed the closest matches were with poxvirus homologues of the VACV E4L gene. The precise length of the putative protein cannot be accurately determined from sequence data alone, because there are three possible initiating methionine codons located in the N-terminal region of ORF SP 30.72L^{m}, at amino acid positions 1, 21 and 24 (indicated by # symbols in figure 6.6). However, FastA analysis of the predicted amino acid sequence, which included the three putative initiating methionines, revealed that the initiating methionines of all poxvirus E4L homologues aligned with the SPPV sequence between amino acid position 11 to 33. This suggests that the methionine at position 1 is unlikely to be the initiating methionine and the actual protein will be shorter at the N-terminus. Only the initiating methionine of the MYXV homologue aligned with SPPV sequence at a location corresponding with one of the three methionines, at amino acid 21. Therefore it is hypothesised that the methionine at position 21 is the most likely to be the initiating methionine of the SPPV homologue of E4L.

A termination codon (TGA) is located at nucleotide position 581 (figure 6.6). When the ORF is translated, beginning with the methionine at position 21, the putative homologue of the E4L protein is predicted to be 297 amino acids in length. This does not correspond in length with any of the poxvirus E4L homologues characterised to date. To ensure that the location of the termination codon at position 581 and the resulting length of the ORF are not due to sequencing errors; this region was re-sequenced three times. The location of a termination codon at nucleotide position 581 was confirmed, and therefore, the predicted length of the SPPV homologue is likely to be genuine.

The SPPV homologue of E4L is 38 amino acids longer than the orthopoxvirus E4L genes, which have a uniform length of 259 amino acids. Likewise, the SPPV homologue is longer than the E4L genes characterised in capripox, leporipox, suipox, avipox and yatapox virus genera by 96, 75, 75, 115 and 108 amino acids respectively. Only the terminal 89 amino acid sequence of the parapoxvirus ORFV E4L homologue is available (McInnes *et al.*, 1998). The FastA alignment of the SPPV homologue with partial sequence ORFV homologue demonstrated that the C-terminus of ORFV E4L aligned with the amino acid at position 200 in the SPPV sequence (figure 6.7). This suggests that the ORFV E4L is truncated by approximately 97 amino acids at the C-

terminus with respect to SPPV. In contrast, the corresponding MOCV gene is much longer than the SPPV gene by approximately 147 amino acids.

FastA alignment of the SPPV E4L protein with other poxviruses revealed considerable identity between the central regions of all poxvirus E4L homologues. However identity was only maintained to the "FRD" motif located at amino acid positions 191 to 193 (figure 6.7). The E4L proteins of ORFV, FPV, YLDV and the capripoxviruses terminated within 1 to 7 amino acids after the FRD motif. The leporipox and orthopoxvirus E4L genes were longer but significant gapping was required to align them with SPPV and identity was much reduced. In contrast, identity from the FRD motif onwards is maintained with MOCV until the end of the SPPV protein but is much reduced.

E4L plays an important role throughout infection and is likely to be expressed at more than one transcriptional phase. The homologues of the E4L ORF in SFV, SWPV, MYXV and LSDV are preceded by early promoter like elements (Willer *et al.*, 1999; Cameron *et al.*, 1999; Tulman *et al.*, 2001; Afonso *et al.*, 2002). However, the MOCV and MPV E4L homologues are preceded by both early and late promoters (Senkevich *et al.*, 1997; Shchelkunov *et al.*, 2002). A deviation of late promoter initiator (TAAAAT) shown to be functional in VACV by mutational analysis of the TAAAT sequence (Davison and Moss, 1989b) was identified in the SPPV sequence upstream of the putative methionine codons (indicated on figure 6.6). Furthermore, approximately 6nt upstream of the TAAAAT sequence an A+T-rich region extends for 20nt. However, no early or intermediate promoter elements corresponding with the VACV promoter consensi could be identified. In addition, no termination signal was apparent downstream of the SPPV E4L homologue. The absence of a termination signal is consistent with VACV and ORFV (Broyles and Pennington, 1990; McInnes *et al.*, 1998).

Therefore, in summary the E4L gene in SPPV is unique in terms of length. Minor sequence heterogeneity at the N-terminus is apparent when compared with other poxviruses. The C-terminus is however considerably different to other poxviruses with respect the length and predicted amino acid sequence. In addition, the transcription promoter sequences preceding other poxviruses E4L genes are not conserved in SPPV.

SPPV with ORFV

```
              150       160       170       180       190       200
SPPV:  ILDEKYNPRCPSCRSKNTIPMMVQMRAADEPPTVRYTCRDCQKHFAPPRFRDRLDRRDED
       .:::::.:  ::::.::::.::::.: :.:::::: ..:.:..::: : ::.: ..
ORFV:  VLDEKFNLPCPSCQSKNTMPMMIQTRSADEPPLIKYACKNCQKSFNPPKFCEKKGKPKS
                40        50        60        70        80
```

SPPV with SPV

```
          180       190       200       210       220       230
SPPV:  RYTCRDCQKHFAPPRFRDRLDRRDEDEDRAPRRKKKGAGDAEAAAAAVAPQDQYESEDGA
        ..:::::.:.: ::.::
SPV :  MHSCRDCKKNFKPPKFRAVEK
200
```

SPPV with VACV

```
              180       190       200       210       220       230
SPPV:  PPTVRYTCRDCQKHFAPPRFRDRLDRRDEDEDRAPRRKKKGAGDAEAAAAAVAPQDQYES
       :: ::.:::::.:: ::.::     :. .      ...:         . . :
VACV:  PPLVRHACRDCKQHFKPPKFRAF---RNLNVTTQSIHENK-------EITEILP------
     180       190       200          210               220

              240       250       260       270       280       290
SPPV:  EDGASPEELPEDASPEPIDPDNLLEPEPVVDPASPGSEPCDECPNCAEDENHAAENGLED
       ... :: : :: :::  :: :.:..
VACV:  DNNPSPPESPEPASP--ID-DGLIRATFDRNDEPPEDDE
           230       240       250
```

SPPV with MOCV

```
          180       190       200       210       220       230
SPPV:  VRYTCRDCQKHFAPPRFRDRLDRRDEDEDRAPRRKKKGAGDAEAAAAAVAPQD-QYESED
       :::.:.::::::.::.:::.   :  . :   :.  ..:.  ..: :.   :.    . .
MOCV:  VRYVCKDCNKHFSPPKFRS--PRGGHAEPGPPEGVSRGTQGSHAPAGEGEPEHVARRPRT
              190       200       210       220       230

           240       250       260       270       280       290
SPPV:  GASPEELPEDASPEPIDPDNLLEPEPVVDPASPGSEPCDECPNCAEDENHAAENGLEDGF
        :. .    ..  :  .   . : .  . :.:  .  : :    ::.  :. .. . :
MOCV:  RAKERACKCEVESEKAETKAVAEAKEET-PVSEEAAQCLENAASAENVAHSDDEEFADDP
      240       250       260       270       280       290
```

```
SPPV:  EVDE

MOCV:  GPVPVPEVLSADDAAAAAAVADALDNANDVTTGNADDEDASEKDADEDAEKDTDGDAEDN
       300       310       320       330       340       350
```

Figure 6.7 FastA alignment of the terminal region of the SPPV E4L homologue with the E4L homologues of ORFV, SPV, VACV and MOCV. Considerable homology between SPPV and other poxvirus E4L homologues is apparent prior to the FRD motif (highlighted in grey). The alignments degenerate after the FRD motif, which can be seen as the truncation of the aligned sequence, extensive gapping or reduced homology. The C-terminal amino acids, when shown, are highlighted in black.

6.3.2.2 Putative ORF SP 29.55L^{m}

The putative ORF SP 29.55L^{m} was compared to amino acid sequences deposited in the SWALL library databases. The only matches detected were with parapox and capripoxvirus homologues of the VACV E3L. However identity was limited to the region of the SPPV sequence extending from 29 to 75 amino acids (figure 6.8). Beyond amino acid 75, identity was not detected with any poxvirus E3L sequence. The relevance of the homology or lack of with the different domains of the E3L protein with respect to function is discussed further in section 6.5.

The sequence preceding the putative ORF SP 29.55L^{m} contains sequence corresponding to VACV early promoters (indicated on figure 6.6). The sequence of the putative early promoter compares favourably with the consensus sequence of the VACV early promoter (Davison and Moss, 1989a). The putative coding region of ORF SP29.55L^{m} cannot be precisely determined because three possible methionine sites (indicated on figure 6.6) are located downstream of the putative early promoter.

```
10         20         30         40         50         60
SPPV:  MSNRMPFQRPIMSGHGLHHKIIALMTSVPNDLGLTAAYIARCLGVTKRDINRQLYSMWEC
                                    .:  : :  ::. ::..:.. ::::: : :
GPPV:                 MACECASLILELLRKSDDKLPAKQIAKELGISKHEANRQLYRMLEL
                                10         20         30         40

               70         80         90        100        110        120
SPPV:  GYVDCVRSTNPPKWFWTPALGTAIRNSGYRAGGAVHDWIATGEAAAADDAARGARAEAAA
         : : .. :::.::
GPPV:  DDV-CCEDGNPPRWFVECAPSAPTEEDENSDTEPMETEAGCDTLFGGDIDIMTQSAVMRL
          50         60         70         80         90        100
```

Figure 6.8 FastA alignment of the predicted amino acid sequence of SPPV ORF SP 29.55L^{m} with the most significant match, the interferon resistance protein (homologue of VACV E3L) of the parapoxvirus (GPPV), which causes proliferative dermatitis in goats. The percentage identity of the two putative proteins is 47.8% over a 46 amino acid overlap.

6.4 TRANSCRIPTION CONTROL SEQUENCES

When putative translation initiation (ATG) and termination (TAG, TAA, TGA) codons were identified during DNA sequencing, the DNA sequence up or downstream of the putative genes were examined for poxvirus-like promoter and termination signals. Examples of poxvirus-like transcription promoters identified in SPPV and termination signals are presented in figures 6.9 to 6.13 and are discussed in the text that follows.

6.4.1 Early gene transcription control sequences

6.4.1.1 Early promoters

An example of a putative early promoter preceding the homologue of the MOCV 026L gene in SPPV is presented in figure 6.9. The putative promoter core region of SPPV corresponds extremely well with early promoter consensus sequences of VACV and MOCV (Davison and Moss, 1989a; Senkevich *et al.*, 1997). No specific transcriptional analysis has been performed on the MOCV 026L gene. However, transcriptional analysis of several putative early genes of parapox and molluscipox viruses has shown that VACV-like early promoters are functional in G+C rich genomes (Fleming *et al.*, 1991; Fleming *et al.*, 1992; Fleming *et al.*, 1993; Sullivan *et al.*, 1995b; Sullivan *et al.*, 1995a; Mercer *et al.*, 1996b; Bugert *et al.*, 1999). This suggests that the VACV-like early promoter sequences identified in SPPV may also be function in a manner similar to other poxviruses.

6.4.1.2 Early termination signals

The sequence downstream of several putative SPPV genes were analysed in order to identify putative early genes termination signals (TTTTTNT), which terminate transcription 20 to 118nt downstream of the signal in VACV and G+C rich poxviruses (Yuen and Moss, 1987; Fleming *et al.*, 1991; Fleming *et al.*, 1992; McInnes *et al.*, 1998; Bugert *et al.*, 1998; Bugert *et al.*, 1999). Only one T_5NT signal was identified in SPPV, 22nt downstream of the putative stop codon of the SPPV homologue of the VACV early gene A37R (figure 6.10).

MCV 026L putative early promoter

```
                          -28       -20       -13             -1      +6
SPPV : ACCTGACCAACCAGAAATAAGTGAAATCCTAATCTACCTTGAAGATCAT---TCAGAATG
MOCV : CCCGAGCCCGAGCCGCAAAAGTGAAAAGCTAGTTACCAGAGGGTGGCTTGCTGCAGTATG
```

Figure 6.9 Example of an early putative gene promoter identified in SPPV preceding the homologue of the putative MOCV gene 026L. The sequences of SPPV and MOCV immediately preceding the gene are presented in a pileup format with gapping to allow alignment. Note the sequences are presented as the complement and reverse of their actual situation within the genomes. The putative initiating methionine codons (ATG) are underlined. The region predicted to form the core region of the early promoter (-28 to –13) is highlighted in black. The spacer element (-12 to -2) is highlighted in light grey with black text and the region predicted to contain the transcription initiation element (-1 to +6) is highlighted in dark grey with white text.

A37R putative early termination signal

```
                 *         20          *         40          *         60
SPPV : TAAATGAAAAACAATCCGGCCTTTTTGTAGCCCGAGAGGCGCGACTCACAATGGGGTTCC
MOCV : TGAAAGCACGCGGGCCCACCGCGCCAGCGACAGACACCGGCCTTTTGTCGTTCTCGTTCG
VACV : TAATAGATTTCTAGTATGGGGATCATTAATCATCTCTAATCTCTAAATACCTCATAAAAC

                 *         80          *        100          *        120
SPPV : TCTGTGCGCTCTTCCGCCGGTGCCTCCGTCCCTCCGTCCCCCAGGAGTCGCGAGGGGACC
MOCV : CGACCTGGCGCGTGCGAGCAGAGGCATGCTTTTTGTTCTGCGCAGGGACGCGCTTTTCGC
VACV : GAAAAAAAAGCTATTATCAAATACTGTACGGAATGGATTCATTCTCTTCTCTTTTTATGA
```

Figure 6.10 Example of a putative early gene transcription termination sequence found in SPPV. 120bp of DNA sequence located after the termination codon of the homologues of the VACV A37R found in SPPV, MOCV and VACV are presented in a pileup format without alignment. Putative early termination sequences are highlighted in black.

6.4.2 Intermediate promoters

An example of a putative intermediate promoter identified in SPPV is presented in figure 6.11. The promoter precedes the homologue of the A18R VACV gene, which encodes a transcription cofactor (Simpson and Condit, 1995; Xiang *et al.,* 1998; Lackner and Condit, 2000). The sequence is highly conserved with MOCV, VACV and MYXV in all three regions of the putative promoter. Although no transcriptional analysis of the intermediate genes have been performed for any the G+C-rich poxviruses, the level of conservation of putative MOCV, SPPV and ORFV putative promoters with VACV (Baldick *et al.,* 1992; Senkevich *et al.,* 1997; Deane *et al.,* 2000) would suggest that transcription occurs by the same mechanism as in VACV.

6.4.3 Late promoters

DNA sequence was obtained from the regions preceding several putative late genes in SPPV (figure 6.12). In the case of the homologues of VACV A17L and A32L genes, late promoter initiator sequences are present either in combination or upstream of the putative initiating methionine codon. The VACV late gene initiator sequence (TAAAT) is also conserved in the G+C-rich genomes of MOCV and ORFV (Naase *et al.,* 1991; Klemperer *et al.,* 1995; Senkevich *et al.,* 1997). No transcriptional analysis has been performed to determine the location of the 5' end of mRNAs in MOCV; however transcription is initiated with an A-residue within the TAAAT sequence in ORFV and VACV (Davison and Moss, 1989b; Fleming *et al.,* 1993; Sullivan *et al.,* 1994). The long A+T-rich track preceding the TAAAT sequence are associated with strong promoter activity in VACV (Davison and Moss, 1989b), these also appear to be conserved in SPPV despite the overall high G+C composition of the SPPV genome.

6.4.4 Dual function promoters

Often, more than one promoter type is identified in the sequence preceding multiphase genes that are therefore expressed throughout infection. An example of a multiphase gene is presented in figure 6.13. Putative early, intermediate and late promoters have been identified preceding homologues of the A18R genes in many poxviruses (Johnson *et al.,* 1993; Massung *et al.,* 1994; Senkevich *et al.,* 1997; Cameron *et al.,* 1999; Willer *et al.,* 1999; Afonso *et al.,* 2000; Tulman *et al.,* 2001; Lee *et al.,* 2001; Afonso *et al.,* 2002). In addition, A18R is reportedly transcribed and functions throughout the replication cycle in VACV (Simpson and Condit, 1995; Xiang *et al.,* 1998; Lackner and Condit, 2000; Condit and Niles, 2002). A putative intermediate (section 6.4.2) and late promoter precede the SPPV homologue of the VACV gene A18R.

A18R putative intermediate promoter

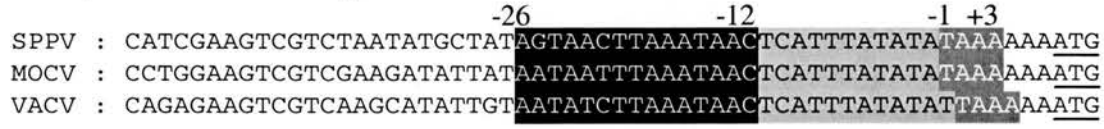

Figure 6.11 Example of a putative intermediate promoter found in SPPV. The highly conserved DNA sequence immediately preceding the ATG codons (underlined) of the homologues of the VACV A18R in SPPV, MOCV and VACV are aligned using ClustalW. The region predicted to form the core region of the promoter is highlighted in black. The spacer element is highlighted in light grey with black text, and the initiator is highlighted in dark grey with white text.

A17L putative late promoter

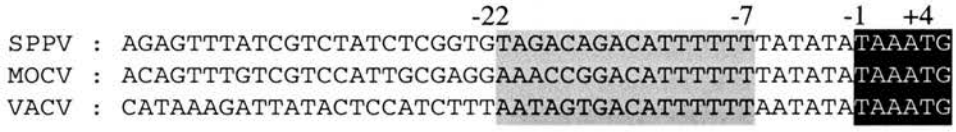

A32L putative late promoter

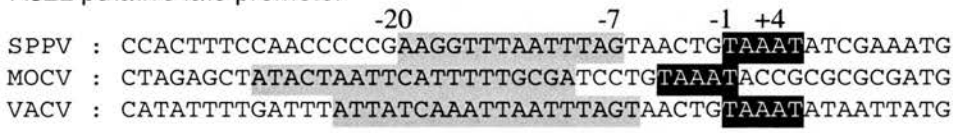

Figure 6.12 Examples of homologues found in SPPV of the VACV genes A17L and A32L that possess VACV-like late promoters. The sequences of SPPV MOCV and VACV immediately preceding the genes are presented in a pileup format without alignment with the initiating codon (ATG) on the right. Putative late promoters are highlighted in black and the A+T rich tracks preceding the promoter are shaded in grey.

A18R putative intermediate/late promoter

Figure 6.13 Example of the homologue of VACV gene A18R identified in SPPV that possess a VACV-like intermediate/late promoter. The DNA sequences of SPPV MOCV and VACV immediately preceding the A18R gene are aligned using ClustalW with the initiating codon (ATG) on the right. Putative late promoters are highlighted in black and the A+T rich tracks preceding the promoter are shaded in grey. The core region of the putative intermediate promoter is indicated with the symbol + and the initiator is indicated with the symbol *.

6.5 DISCUSSION

Hybridisation of SPPV DNA with several ORFV cDNAs resulted in the identification of homologues of the VACV genes I3L, J4R, H5R and A8R. SPPV DNA did not hybridise with ORFV cDNA encoding for VEGF-E, IL-10, GIF and the homologue of the VACV E3L gene, suggesting that these genes are absent in SPPV. In addition, ORFV cDNAs encoding for G2R, L2R and A33R also did not hybridise with SPPV DNA, even at low hybridisation stringency. The three genes, G2R, L2R and A33R are conserved in all poxviruses sequenced to date, except for FPV which lacks L2R and A33R (Afonso *et al.,* 2000). Consequently it was predicted that these genes would also be conserved in SPPV. This indicates that some SPPV and ORFV genes may not be sufficiently conserved at the nucleotide level for hybridisation to occur, and therefore cross-hybridisation, or lack of, cannot determine with certainty the presence or absence of specific genes in the SPPV genome. Therefore a second approach was used involving DNA sequencing to investigate the existence of homologues of defined ORFV genes in the SPPV genome. The construction of a genetic map of SPPV (see section 5.4) and establishing the locations of the ITR junctions (see section 4.5.2.1) enabled the regions of the SPPV genome comparable to the regions of ORFV that contain the VEGF-E and E3L genes to be identified and extensively sequenced.

Little is known about the immuno-modulator/virulence genes and their locations in parapoxvirus genomes other than ORFV. As a consequence, it is unknown if a homologue of the VACV E3L gene is conserved in all parapoxviruses. However, recent studies have confirmed that the VEGF gene is present in PCPV in a location comparable to ORFV, but absent in BPSV (Rziha *et al.,* 2003; Ueda *et al.,* 2003). A homologue of the ORFV IL-10 gene is situated in the BPSV genome in a location conserved with ORFV (Fleming *et al.,* 1997; Rziha *et al.,* 2003). It is unknown if a homologue of IL-10 is present in the PCPV genome, although a homologue of the GIF gene has been identified in PCPV and BPSV (C. McInnes personal communication). These data suggest that VEGF, GIF and IL-10 genes may be semi-conserved in parapoxvirus genomes. However the hybridisation data suggests that all four ORFV genes are absent in SPPV.

DNA sequencing identified the termination codon of the E4L homologue in SPPV and the region of the genome further downstream was sequenced in order to investigate if a homologue of E3L was present. In all poxviruses sequence to date the initiation codons of the E3L homologues are generally located within 66nt of the E4L termination codons (Johnson *et al.,*

1993; Massung *et al.*, 1994; McInnes *et al.*, 1998; Senkevich *et al.*, 1997; Cameron *et al.*, 1999; Willer *et al.*, 1999; Afonso *et al.*, 2000; Tulman *et al.*, 2001; Lee *et al.*, 2001; Afonso *et al.*, 2002; Shchelkunov *et al.*, 2002; Gubser and Smith, 2002). No comparable ORF was identified in SPPV within 66nt of the termination codon of E4L. However a putative ORF (SP 29.55L^{m}) that is preceded by early promoter-like sequence was identified 216nt downstream of the E4L termination codon. FastA analysis of SP 29.55L^{m} revealed amino acid homology with parapox and capripox virus E3L homologues over the first 75 amino acids, but not beyond. The abrupt cessation of identity at amino acid 75 strongly suggests that VACV E3L gene homologue is disrupted in SPPV.

Characterisation of the VACV E3L protein has revealed that the N-terminal region is associated with nuclear localisation of the protein (Chang *et al.*, 1995a) and the C-terminal is essential for dsRNA binding and the inhibition of the IFN-induced, dsRNA-dependent protein kinase pathway (PKR) (Chang and Jacobs, 1993). Both the C and N-terminal regions of the VACV E3L protein are required for full virus pathogenesis in the mouse model (Brandt and Jacobs, 2001). The apparent lack of homology of the SP 29.55L^{m} ORF with the C-terminal regions of poxvirus homologues of the E3L gene strongly suggests that SP 29.55L^{m} is not involved in PKR inhibition (reviewed in section 1.6.1). ORF SP 29.55L^{m} may represent a disrupted and therefore non-functional homologue of E3L or alternatively a gene unique to SPPV that may localise in the nucleus of infected cells, but without the capability of binding dsRNA. The presence of early promoter elements that are highly conserved with strong VACV early promoters suggests that this putative gene is transcribed.

Characterisation of poxvirus genomes from all genera suggests that VEGF homologues are unique to the parapoxvirus genus. Two distinct forms of the VEGF-E protein have been identified, one in ORFV isolate NZ2 and one in ORFV isolate NZ7. The two forms exhibit only 41.1% amino acid identity to each other (Lyttle *et al.*, 1994). In addition, extensive phylogenetic analysis of VEGF-E genes sequenced from twenty-two ORFV strains and isolates supported the existence of two distinct forms of VEGF-E but also revealed considerable heterogeneity in sequence within VEGF-Es that group together phylogenetically (Mercer *et al.*, 2002). The genetic heterogeneity of VEGF-Es may explain the inability to identify a homologue of VEGF-E in SPPV using hybridisation. However, sequence analysis of the SPPV genome near to the right ITR junction also failed to identify a homologue of ORFV VEGF-E. Taken together these data

indicate that SPPV does not possess a homologue of ORFV VEGF-E, which is surprising considering the haemorrhagic pathology exhibited by SPPV lesions.

In the right terminal region of SPPV, instead of a VEGF-E gene, a homologue of the putative MOCV proteins 003L and 157R was identified in the ORF designated SP155.0R^{t}. These two MOCV are related to each other at the amino acid level. Each MOCV protein contains a putative signal peptide, a transmembrane helix, and an immunoglobulin domain and may function as a plasma membrane receptor with as yet unknown specificity (Senkevich *et al.,* 1997). The putative MOCV 157R and MOCV 003L proteins have not been identified in any other poxvirus. Therefore the data published to date suggests this ORF is unique to SPPV and MOCV.

Transcriptional control sequences have been extensively characterised in the A+T-rich genome of VACV and the promoter and termination signals are invariably A+T-rich (Yuen and Moss, 1987; Davison and Moss, 1989a; Davison and Moss, 1989b; Baldick *et al.,* 1992). Despite the disparity in G+C content, the VACV A+T-rich transcriptional control sequences are also extremely well conserved SPPV. This is consistent with the conservation of VACV transcriptional control sequences in the other G+C rich genomes of parapox and mollusci poxviruses (Mercer *et al.,* 1989; Fraser *et al.,* 1990; Naase *et al.,* 1991; Fleming *et al.,* 1991; Fleming *et al.,* 1992; Fleming *et al.,* 1993; Sullivan *et al.,* 1994; Sullivan *et al.,* 1995b; Sullivan *et al.,* 1995a; Mercer *et al.,* 1996b; Senkevich *et al.,* 1997; Deane *et al.,* 2000). Remarkably, the conserved nature of the transcriptional control sequences is reflected in the ability of poxviruses, which are divergent in overall G+C content, to transcribe genes in a cross-species manner. For example, VACV extracts are able transcribe an ORFV early gene *in vitro* (Vos *et al.,* 1992). Likewise, Fleming *et al.,* (1992) reported that a recombinant VACV containing three ORFV early genes produced transcripts of a length comparable to ORFV; and the sites of transcription initiation were highly conserved in the recombinant VACV and the native ORFV. However quantitative differences in transcripts were noted and Fleming *et al.,* (1992) postulated that generically different transcription factors have specific promoter sequence requirement for optimal transcription. Therefore it is a reasonable assumption considering the high degree of homology shown between SPPV, MOCV and VACV transcription control signals that the mechanism of transcription in SPPV and the associated factors will be relatively well conserved with other poxviruses, despite differences in overall G+C content.

The data presented in chapters 4.0 to 6.0 has described several differences between SPPV and other parapoxviruses, including genome size, restriction profiles, genetic organisation and the apparent absence of all parapoxvirus-specific immuno-modulating/virulence genes in the SPPV genome. The lack of a homologue of VACV E3L gene is also surprising considering that all poxviruses completely sequenced to date possess this gene, except for MOCV and FPV (Senkevich *et al.,* 1997; Afonso *et al.,* 2000). The existence of two putative MOCV specific-genes in SPPV, one of which is located within the species-specific terminal regions, suggests that SPPV may not be so closely related to the parapoxviruses as initial morphological observation suggest. Therefore in chapter 7.0 the investigations undertaken pertaining to the phylogenetic relationships of SPPV are discussed.

CHAPTER 7.0

PHYLOGENETIC ANALYSIS OF SPPV

7.1 INTRODUCTION

Several differences exist between SPPV and the other parapoxviruses (discussed in section 6.5). Taken together they suggest that the classification of SPPV as a parapoxvirus may be incorrect. Therefore to clarify this issue, phylogenetic analysis was performed on two genes, homologues of VACV genes F13L and E4L, which are conserved across all members of the poxvirus family.

The VACV F13L gene encodes the 37KDa major membrane protein, which is absent in intracellular mature virus (IMV), but is abundant in the additional membranes of intracellular and extracellular enveloped virus (IEV and EEV) (Payne, 1978; Hirt *et al.,* 1986; Goebel *et al.,* 1990). F13L localises in the membranes of the trans-golgi network and is believed to facilitate the wrapping of IMV in the additional membranes possibly by the direct interaction with an unidentified protein(s) on the surface of IMV (Blasco and Moss, 1991; Grosenbach and Hruby, 1998; Sanderson *et al.,* 2000).

Most published parapoxvirus sequences are derived from ORFV, however the homologue of VACV F13L has been partially sequence in several accepted and tentative parapoxvirus species. The F13L gene was initially sequenced in ORFV (Sullivan *et al.,* 1994). Inoshima *et al.,* (2000) developed a diagnostic polymerase chain reaction (PCR) assay for the detection of parapoxvirus using oligonucleotide primers designed from the sequence of the ORFV F13L gene. The pan-parapoxvirus primers (PPP-1 and PPP-4) were shown to be capable of amplifying a 600bp region of the F13L genes in ORFV, BPSV, PCPV, PVNZ and several parapoxvirus isolates from cattle, sheep, Japanese serows, reindeer (reindeerPPV) and seals (sealPPV), but not from VACV or FPV (Inoshima *et al.,* 2000; Tryland *et al.,* 2001; Inoshima *et al.,* 2001; Becher *et al.,* 2002).

Phylogenetic analysis with the F13L gene has recently been performed to infer speciation within the parapoxvirus genus (Inoshima *et al.,* 2001), and to provide evidence supporting the inclusion of sealPPV and reindeerPPV as separate species belonging within the parapoxvirus genus (Becher *et al.,* 2002; M. Tikkenan personal communication). Due to the availability of F13L sequences derived from several parapoxvirus species, the F13L gene was specifically chosen for phylogenetic analysis. As the pan-parapoxvirus primers have successfully been used to amplify the F13L homologues of all parapoxviruses tested so far, it was predicted that the PCR approach would also be successful in amplifying the SPPV homologue (section 7.2).

The evolutionary relationships of eucaryotic viruses have been previously investigated using phylogenetic analysis of DNA-dependent RNA polymerase subunits (Sonntag and Darai, 1996). Several RNA polymerase subunit genes have been partially sequenced in SPPV (section 5.3.1, table 5.2), and the SPPV homologue of the RNA polymerase subunit RPO 030 (homologue of the VACV E4L gene) was completely sequenced (section 6.3.2.1). Complete E4L gene sequences have been published for at least one representative member from each genus, except the parapoxvirus genus. Only a partial E4L sequence has been published for ORFV (Mercer *et al.,* 1995). However the complete E4L gene sequence of the ORFV isolate MRI has recently been determined in the laboratory where this study was performed (C. McInnes personal communication); enabling phylogenetic analysis to be performed using complete E4L gene sequences of at least one species from each genus.

The VACV E4L gene encodes the DNA-dependent RNA polymerase subunit predicted to have a molecular mass of 30KDa and exhibits structural similarity with the eucaryotic transcription elongation factor TFIIS (Ahn *et al.,* 1990). The homology with TFIIS suggests that E4L may play a role in transcription elongation. E4L also has an additional role as an intermediate transcription factor (VACV intermediate transcription factor, VITF-1) (Rosales *et al.,* 1994a), however the precise function of E4L in intermediate transcription has yet to be determined.

7.2 IDENTIFICATION AND SEQUENCING OF THE GENE ENCODING THE MAJOR EEV MEMBRANE PROTEIN (F13L)

7.2.1 Amplification of F13L by polymerase chain reaction

A homologue of the VACV F15L gene was identified during DNA sequencing of the right end of the SPPV *Not* I fragment K (section 5.3). Because of the size of the *Not* I K fragment, it was hypothesised that it would also contain a homologue of the VACV F13L gene. Amplification of the SPPV F13L by PCR was attempted using the oligonucleotide primers PPP-1 and PPP-4 [PPP-1 (5'-GTC GTC CAC GAT GAG CAG CT-3') and PPP-4 (5'-TAC GTG GGA AGC GCC TCG CT-3') (Inoshima *et al.,* 2000)] using the cloned SPPV restriction fragment *Not* I K as template DNA and ORFV NZ2 DNA as the positive control. Reaction volumes of 50µl contained the DNA template ranging in concentration from 100ng to 1µg, 50pmol of each oligonucleotide primer, 200µM of each dNTP and 2 units of DNA Taq polymerase. DNA was amplified using the cycle parameters: denaturation at 95°C for 10 minutes followed by 25 cycles

of denaturation at 95°C for 1 minute, annealing at 50°C for 1 minute and extension at 72°C for 1 minute (section 2.4.6.1).

In all of the ORFV NZ2 positive control reactions, a PCR product of approximately 600bp was amplified, which indicates that the PCR reaction conditions were suitable for the amplification of the F13L gene (results not shown). However no PCR product was obtained with the SPPV, thus suggesting that the DNA sequence of the F13L in SPPV is different from the parapoxviruses in the regions corresponding to the PCR primers, or that the F13L gene was not present in the *Not* I K fragment.

7.2.2 Mapping of the F13L gene

Despite no PCR product being amplified, it was still expected that the homologue of the F13L gene would be situated at the left end of the SPPV genome within *Not* I fragment K and so the location was mapped using DNA hybridisation. Plasmid DNA containing the *Not* I fragment K was digested with the restriction enzyme *Pst* I, which cleaved the DNA once within the vector and three times within the insert (figure 7.1). The digested DNA products were electrophoresed on a agarose gel along with the *Kpn* I-digested SPPV cosmid clones 5, 9, 28, 51 and 86 (section 4.6) and ORFV NZ2 genomic DNA also digested with *Kpn* I. A Southern blot was prepared (section 2.4.5.3.1) from the agarose gel depicted in figure 7.1. The 0.6kb PCR product that was amplified from the positive control ORFV NZ2 DNA (section 7.2.1) was labelled with digoxygenin (DIG) and used to hybridised with the Southern blot (sections 2.4.5.1.2 and 2.4.5.4).

The DIG-labelled ORFV PCR product hybridised with a *Kpn* I fragment located within SPPV cosmid clone 86 and the 5kb *Pst* I digest product of the plasmid clone containing SPPV *Not* I fragment K (figure 7.2), confirming that F13L is located at the left end of the SPPV genome within the *Not* I fragment K as predicted. The 5kb *Pst* I fragment was predicted to consist of 3kb plasmid DNA attached to the right-terminal 2kb of SPPV *Not* I K fragment. The 5kb fragment was purified from an agarose gel (section 2.4.4.1) and the plasmid clone re-circularised by ligating the ends together using DNA ligase.

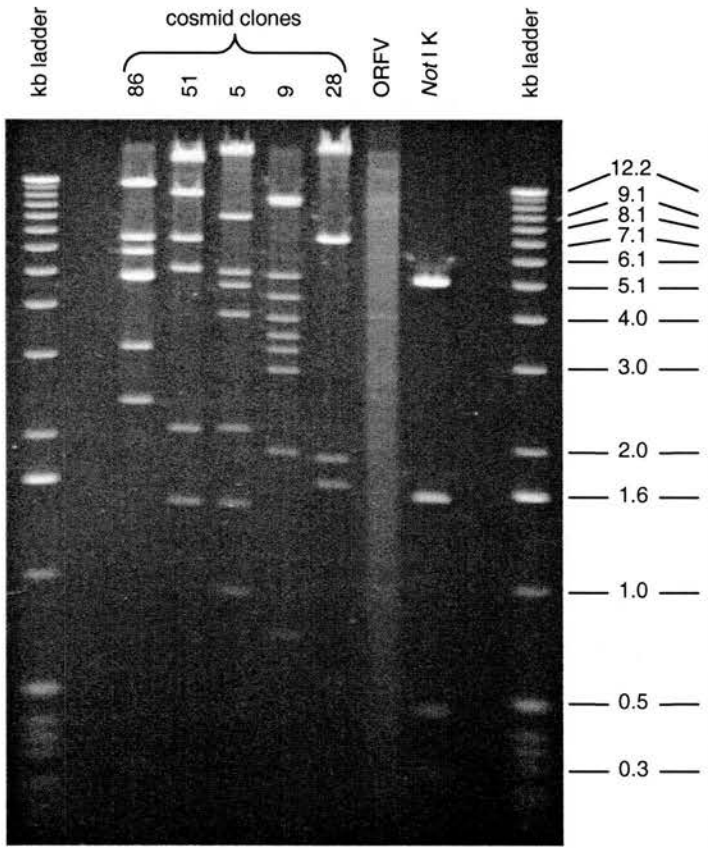

Figure 7.1 Agarose gel electrophoresis of the *Kpn* I digested cosmids clones (5, 9, 28, 51, and 86), *Kpn* I digested ORFV genomic DNA (isolate NZ2) and the *Not* I fragment K cloned into pBluescript SK$^-$ plasmid vector and digested with *Pst* I.

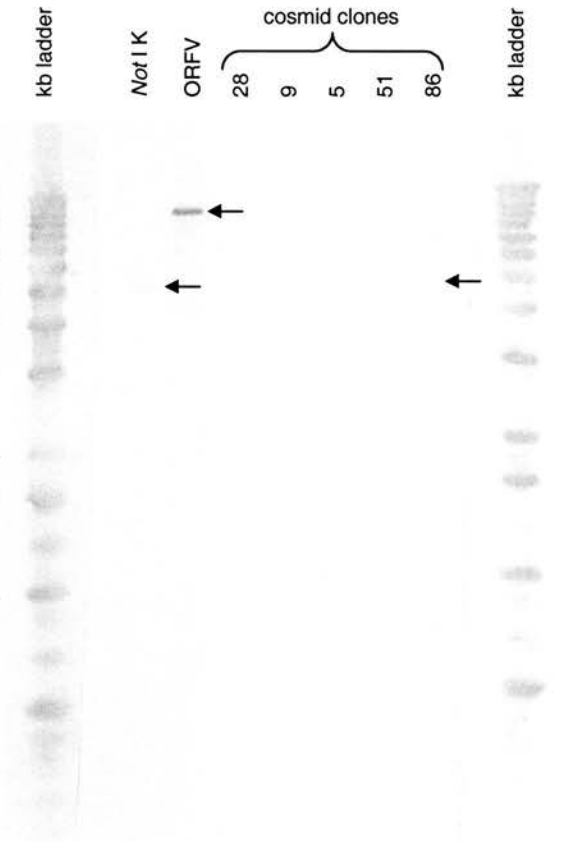

Figure 7.2 Southern blot of the agarose gel depicted in figure 7.1 probed with the DIG-labelled F13L PCR product that was amplified from ORFV NZ2 DNA with PPP-1 and PPP-4 oligonucleotide primers (Inoshima *et al.,* 2000). The F13L probe hybridised with ORFV and the SPPV clones Not I K and cosmid 86 (←).

7.2.3 Sequence analysis of F13L

DNA sequence was obtained from both ends of the SPPV DNA sequence contained within this new clone. Sequence derived with the T3 primer corresponded with the sequence previously obtained from the right end of *Not* I fragment K (encoding a homologue of the VACV gene F15L). Hence, confirming that the 2kb *Pst* I fragment corresponds with the right end of *Not* I fragment K. Sequence derived with the T7 primer was translated into all six ORF and the sequence databases searched for homologous proteins. The most significant match with the predicted amino acid sequence of the SPPV ORF designated SP 19.05L (figure 7.3) was with the ORFV NZ2 homologue of VACV F13L. The partial sequence of the SPPV F13L homologue corresponded with the published sequence of several parapoxvirus (Inoshima *et al.,* 2000; Becher *et al.,* 2002). The regions in ORFV and SPPV, which corresponded to the PCR primers PPP-1 and PPP-4 exhibited considerable differences in nucleotide sequence. Suggesting that the pan-parapoxvirus primers were unlikely to anneal with the SPPV DNA templates under the conditions used. Hence explaining the inability to amplify a product from the SPPV DNA by the PCR.

7.3 MULTIPLE SEQUENCE ALIGNMENT OF THE E4L AND F13L GENES

The majority of the DNA sequences that are published for the parapoxvirus F13L homologues are derived from the pan-parapoxvirus PCR products (Inoshima *et al.,* 2000; Becher *et al.,* 2002) and correspond to the central region of the ORFV F13L homologue, extending from amino acids 137 to 320 (Sullivan *et al.,* 1994). The F13L sequence derived from SPPV DNA (section 7.2.3) also spans this region (ORFV amino acids 129 to 344). Therefore it was aligned with all the known parapoxvirus F13L homologues and a further 15 sequences, with at least one member from each of the remaining chordopoxvirus genera being represented. The multiple alignment programme ClustalW (section 2.4.8.4.1) was used with the window of alignment corresponding to the ORFV amino acids 137 to 320 (figure 7.4).

The multiple sequence alignment generated by ClustalW was validated by shading the amino acids according to their physiochemical properties. Despite the obvious differences between the SPPV sequence and that of the other poxviruses at the amino acid level, the F13L homologues were conserved at the physiochemical level. The percentage identity values (section 2.4.8.4.1) of SPPV sequence with those derived from viruses belonging to all eight defined poxvirus genera are summarised in table 7.1. Surprisingly, the percentage identities of the SPPV sequence with the parapoxviruses were the lowest at 48% to 50%, along with the capripox and avipox viruses.

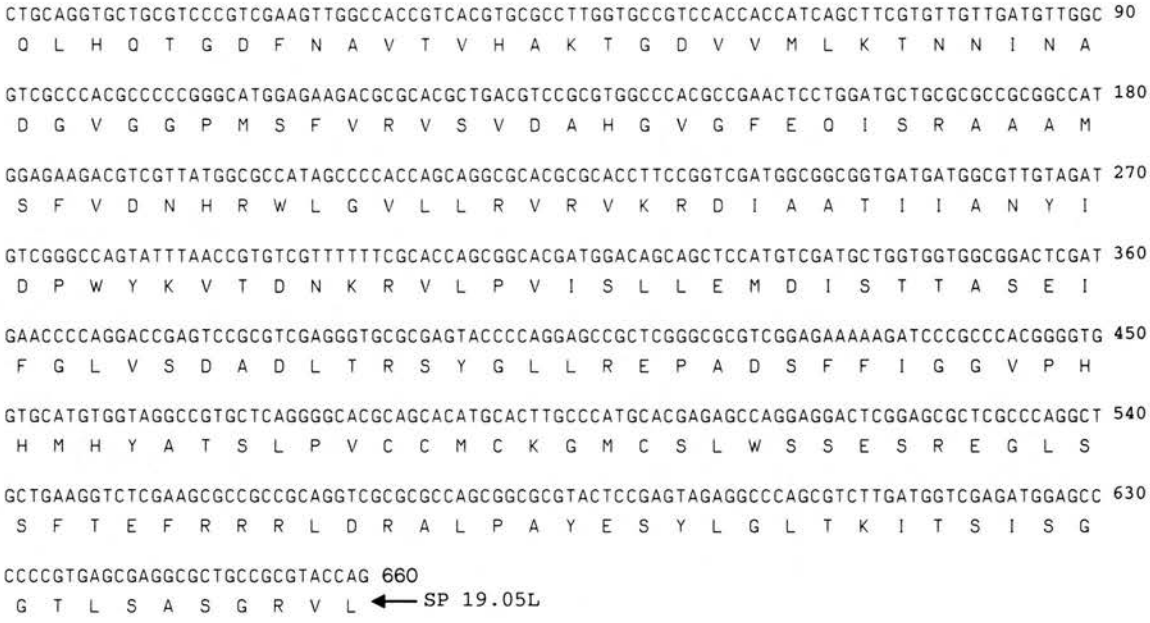

Figure 7.3 DNA sequence corresponding to the SPPV F13L homologue. The sequence is presented in the same direction as the SPPV genome (5' to 3'). The predicted amino acid sequence of the putative ORF SP 19.05L, which is encoded by the reverse complement DNA strand (not shown) is presented below the DNA sequence.

Genera	Percentage identity with SPPV	
	F13L	E4L
Parapox	48-50%	55%
Molluscipox	54%	58%
Orthopox	54-55%	59-60%
Capripox	53%	61-62%
Leporipox	48-49%	62%
Avipox	35%	55%
Suipox	52%	64%
Yatapox	51%	61%

Table 7.1 The percentage identities of the putative SPPV major membrane protein (F13L) and the RNA polymerase subunit RPO030 (E4L) with homologues derived from virus species belonging to the eight defined poxvirus genera. The percentage identities were obtained from the multiple sequence alignment data as described in section 2.4.8.4.1.

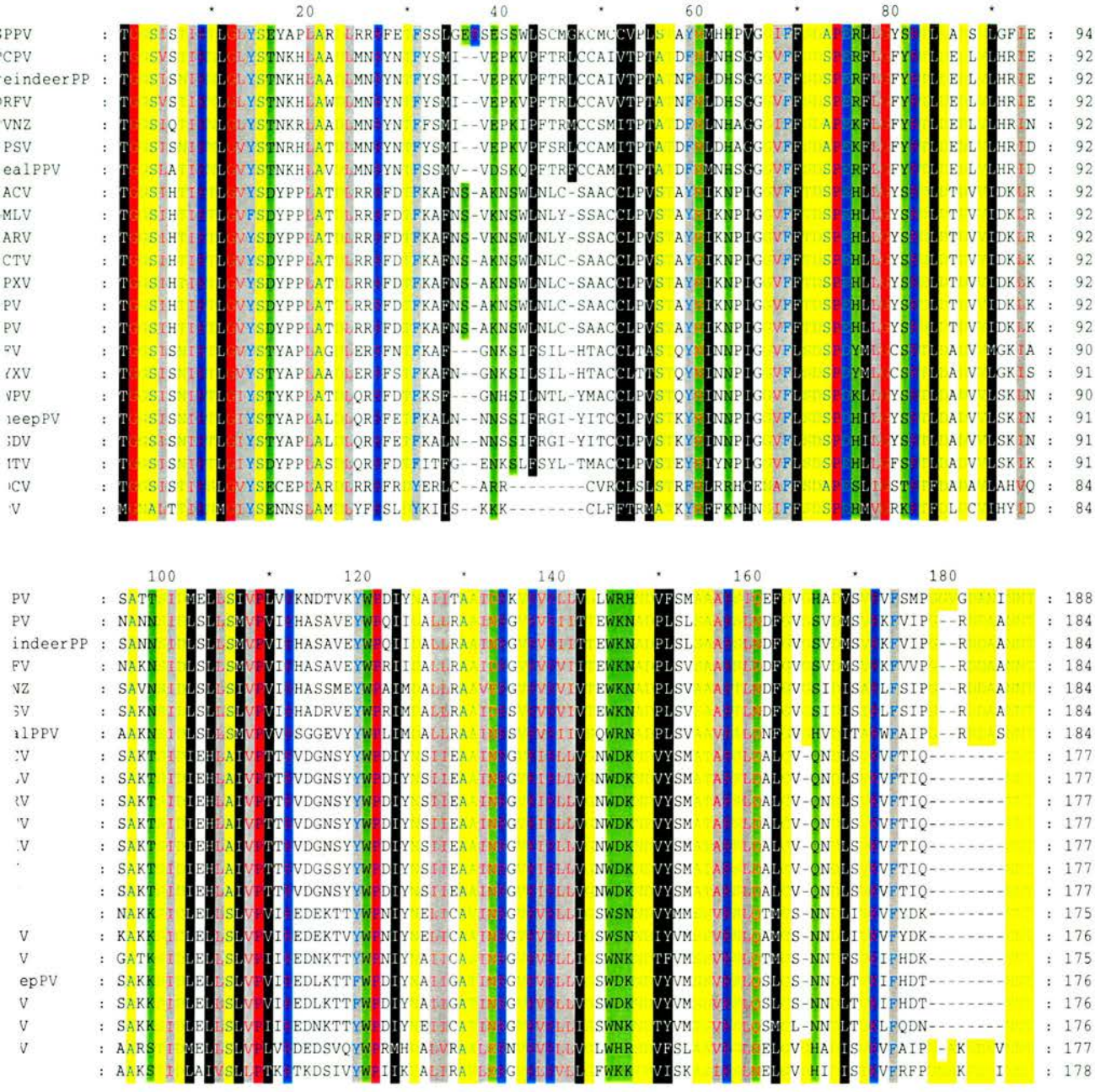

gure 7.4 Multiple sequence alignment of the predicted amino acid sequences of poxvirus F13L genes, luding several accepted and tentative species of the parapoxvirus genus. The multiple sequence gnment was performed using the Clustal W alignment algorithm (Thompson *et al.*, 1994) and aligned ino acids shaded according to their physio-chemical properties (Taylor, 1986). The identity of each virus ndicated by its standard abbreviation (van Regenmortel *et al.*, 2000) or as defined in the summary of breviations (located at the beginning of this thesis).

The precise length of the SPPV homologue of the VACV E4L gene could not be determined, however estimates suggest that it does not correspond in length with any of the characterised poxvirus E4L genes (section 6.3.2.1). A preliminary multiple sequence alignment was performed with the complete amino acid sequence of the SPPV and several other poxvirus E4L genes representing all eight defined genera (results not shown). As expected there was considerable variability at both ends of the E4L alignment, however a conserved "core" of approximately 180 amino acids was identified. Thus a second multiple sequence alignment was performed with amino acids 34 to 211 of the SPPV sequence and the comparable regions of 16 other E4L homologues representing all of the defined poxvirus genera (figure 7.5).

As with the F13L alignment, the E4L alignment was also validated by shading the aligned amino acids according to their physio-chemical properties. At the physio-chemical level all sequences were completely conserved, although gaps were inserted into some sequences at enable alignment. The percentage identities of the SPPV E4L sequence with the 16 aligned poxvirus sequences were calculated (table 7.1). Identity ranged from 58% to 64% for most genera, however SPPV exhibited the lowest identity with the parapox and avipox viruses (ORFV and FPV) at 55%.

7.4 PHYLOGENETIC TREE CONSTRUCTION

Phylogenetic trees were constructed from the multiple sequence alignments depicted in figures 7.4 and 7.5 using the maximum likelihood algorithm PROML (section 2.4.8.1.3). The trees are presented in radial form in figures 7.6 and 7.7. Bootstrap resampling, based on 100 data sets (section 2.4.8.1.4) was used to examine the statistical significance of the observed clades.

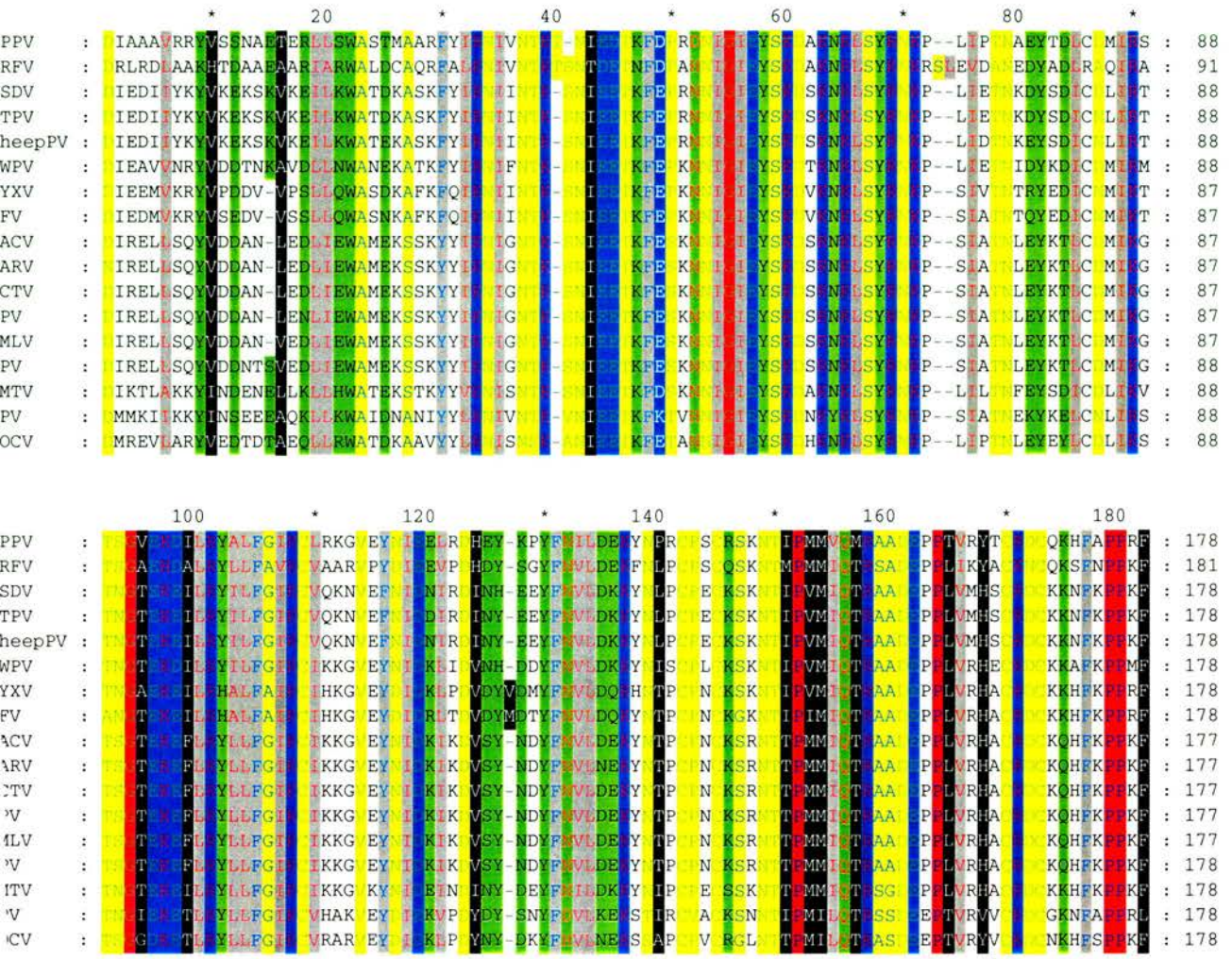

gure 7.5 Multiple sequence alignment of the central region of the SPPV RNA polymerase subunit ?O030 (homologue of VACV E4L gene) with sixteen other poxvirus E4L homologues, representing at ast one member of each defined poxvirus genera. The alignment was performed using the ClustalW gorithm (Thompson *et al.*, 1994) and the aligned sequences shaded according to their physio-chemical operties (Taylor, 1986). The identity of each virus is indicated by its standard abbreviation (van genmortel *et al.*, 2000) or as defined in the summary of abbreviations (located at the beginning of this sis).

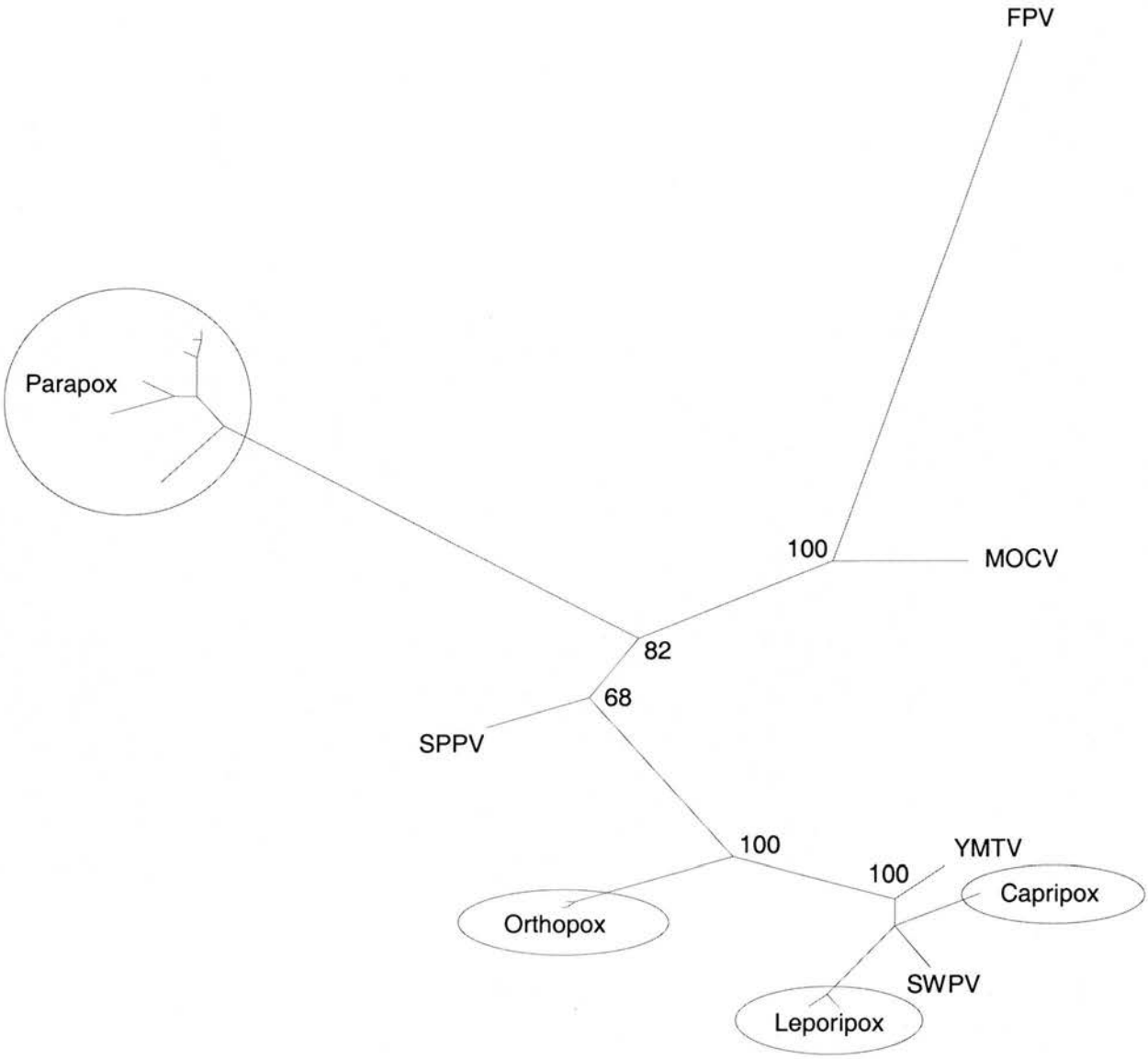

Figure 7.6 Phylogenetic tree of the *Chordopoxviridae* based upon analysis of the predicted amino acid sequence of the major membrane protein (homologues of the VACV F13L gene). The tree was constructed from multiple sequence alignment data (figure 7.4) using the maximum likelihood algorithm PROML and evaluated by bootstrap analysis of a hundred resampled data sets. Defined genera where two or more member species were included in the analysis are circled. Genera where only one representative member species was included are not circled and are referred to by their standard abbreviation. Relevant bootstrap percentages supporting diverging branches are shown where appropriate.

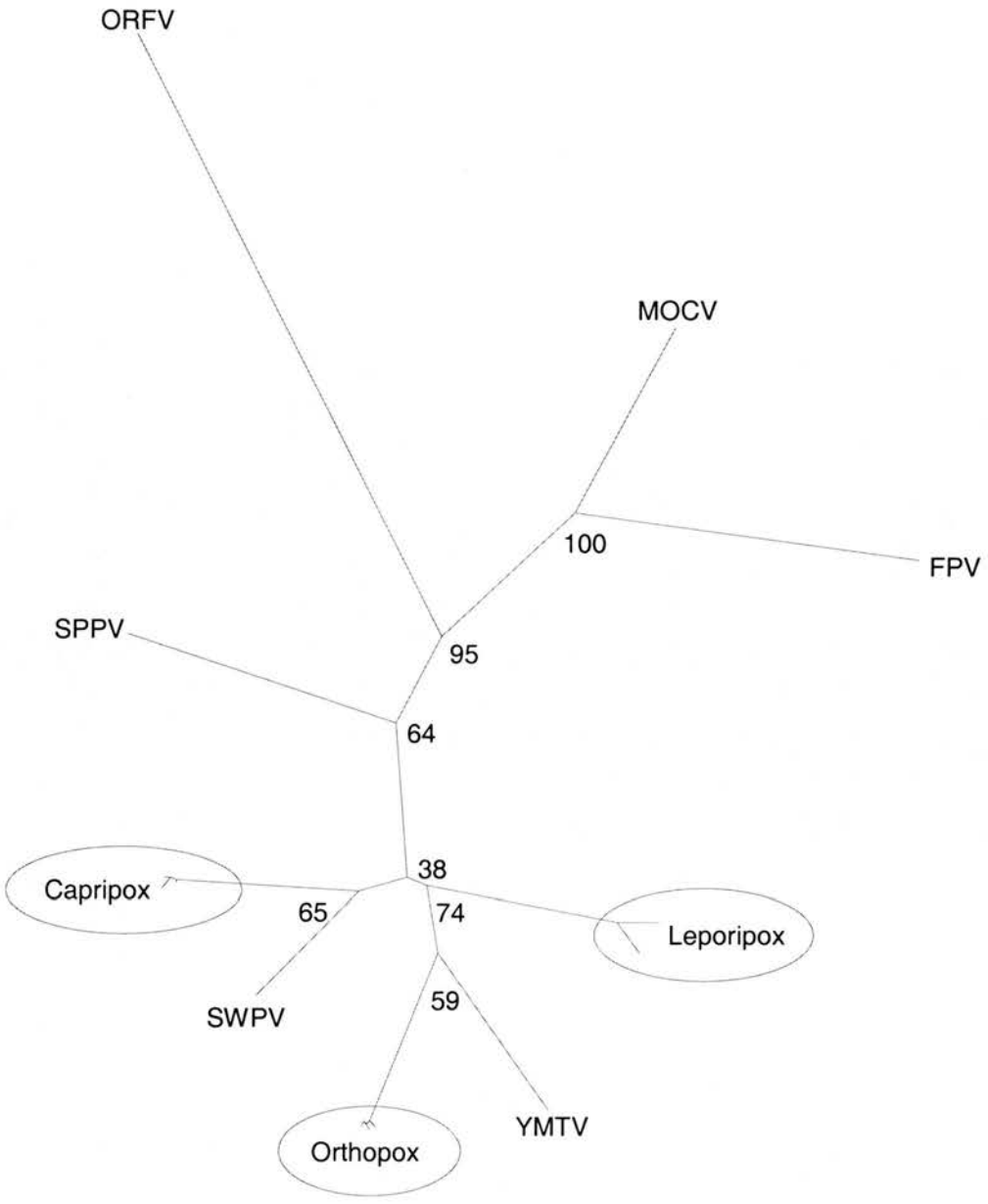

Figure 7.7 Phylogenetic tree of the C*hordopoxviridae* based upon analysis of the predicted amino acid sequence of the RNA polymerase subunit RPO030 (homologues of the VACV E4L gene). The tree was constructed from multiple sequence alignment data (figure 7.5) using the maximum likelihood algorithm PROML and evaluated by bootstrap analysis of a hundred resampled data sets. Defined genera where two or more member species were included in the analysis are circled. Genera where only one representative member species was included are not circled and are referred to by their standard abbreviation. Relevant bootstrap percentages supporting diverging branches are shown where appropriate.

7.5 DISSCUSSION

The pan-parapoxvirus primers (Inoshima *et al.*, 2000) were successfully used to amplify a region of the F13L homologue in all parapoxvirus species tested to date except for SPPV, which casts further doubt on the validity of including SPPV in the parapoxvirus genus. Furthermore, the percentage identity between the SPPV F13L homologue and other poxviruses was generally greater with species belonging to genera other than the parapoxviruses. This was also true for the percentage identities between the SPPV E4L homologue and those derived from species belonging to genera other than the parapoxviruses. Indeed the percentage identity between SPPV E4L and ORFV E4L was only 55%, whereas all other poxvirus species, except for FPV, shared at least 58% identity. These differences between SPPV and the parapoxviruses are also reflected in the phylogenetic trees.

Phylogenetic analysis of the F13L protein grouped the five recognised species of parapoxvirus (ORFV, BPSV, PCPV and PVNZ) and the tentative species of sealPPV and reindeerPPV together, with 82% support from the bootstrap resampling (figure 7.6). The SPPV sequence branched off from the parapoxvirus clade along with five other genera and was placed on a separate branch of the tree with 68% support from the bootstrap resampling. Indeed, the placement of SPPV on a branch separate from all other defined poxvirus genera suggests that SPPV may represent a separate genus of the poxvirus family.

Phylogenetic analysis of the E4L sequences also supports the inferred phylogeny of SPPV as a virus that is distinct from all defined poxvirus genera (figure 7.7). Once again ORFV was placed on a distinct branch, with 95% support from bootstrap resampling, whilst SPPV appeared on a branch of its own, supported by 64% from bootstrap analysis. This again supports the observation that the SPPV does not partition neatly into any of the recognised *Poxvirus* genera.

CHAPTER 8.0

GENERAL DISCUSSION

8.1 COMPARISON OF SPPV TO OTHER POXVIRUSES

This thesis describes the morphology and the characterisation of the genome of the SPPV isolate 1296/99, which has subsequently been shown to be highly virulent and cause severe disease in all red squirrels challenged with this isolate (Thomas *et al.*, 2003, accepted for publication). The general surface morphology of the SPPV isolate 1296/99 (section 3.2) was similar to that of the parapoxviruses and consistent with observations previously reported for SPPV (Scott *et al.*, 1981). The dsDNA genome was estimated to be 158kb in length and consists of approximately 66.4% G+C. The central core region of SPPV hybridised strongly with the central core region of the ORFV genome, suggesting that the central regions of the two genomes are highly conserved at the nucleotide level. Furthermore, DNA sequencing putatively identified twenty-six genes, which are highly conserved within the poxvirus family and are generally essential for viral replication, located towards the centre of the SPPV genome. The order of these genes in SPPV is also identical to the order found in other poxviruses, which indicates that SPPV is consistent with other poxviruses in terms of genome organisation. However, the terminal regions of the SPPV genome did not hybridise with ORFV suggesting that the two genomes are divergent towards the termini. This was not unexpected as the terminal regions of the different parapoxvirus species do not cross-hybridise (Gassmann *et al.*, 1985).

Despite exhibiting a similar surface morphology and a comparable genomic G+C content, SPPV differs from the parapoxviruses in several important areas. 1) The size of the SPPV genome is approximately 18kb larger than all known wild type parapoxviruses (Menna *et al.*, 1979; Robinson *et al.*, 1982; Robinson *et al.*, 1987; Horner *et al.*, 1987; Mercer *et al.*, 1987; McInnes *et al.*, 2001). 2) No parapoxvirus genus-specific genes were identified in the SPPV genome despite extensive DNA sequencing of the regions predicted to contain such genes. 3) The distances between the putative genes in SPPV are considerably different from the distances observed in ORFV (Mercer *et al.*, 1995), particularly towards the ends of the genome. Moreover, there appeared to be a greater similarity between the ORFV and VACV genomes than between SPPV and ORFV. 4) The translocation (with respect to other poxviruses) of the F9L and F10L homologues from the left to the right end of the ORFV genome (Mercer *et al.*, 1995) may not have occurred in SPPV, although the identification and mapping of these genes in SPPV is required to confirm this assumption. The translocation of these two genes is also apparent in the genomes of PCPV and BPSV (Ueda *et al.*, 2003; Rziha *et al.*, 2003) and therefore may prove to be a defining feature of parapoxviruses. 5) The VACV E3L and the three ORFV genes, IL-10,

GIF and VEGF that are associated with immuno-modulation and virulence appear to be absent in SPPV. This was most surprising for the E3L gene, which is conserved in nearly all poxviruses characterised to date except for MOCV and FPV (Senkevich *et al.,* 1997; Afonso *et al.,* 2000). 6) Two genes believed to be unique to MOCV (026L and 157R) were identified in the SPPV genome in comparable locations to MOCV. Taken together this data indicates that genomic divergence between SPPV and ORFV is greater than the level of divergence observed between the other parapoxvirus species. This may suggest that SPPV does not belong in the parapoxvirus genus.

The comparable genomic G+C content between SPPV and MOCV and the presence of two MOCV specific genes in the SPPV genome raises the possibility that SPPV may belong in the molluscipoxvirus genus. However this is unlikely as the clinical pathology of the two diseases is quite different. MOCV causes small self-limiting epithelial tumours in the dermis of humans (Diven, 2001). In the red squirrel, SPPV produces large necrotic dermal lesions, which are often haemorrhagic (figure 8.1). In addition to the different pathologies, the MOCV genome is approximately 32kb larger than SPPV and when the two genomes are compared, the spatial distribution of genes is markedly different.

In an attempt to clarify the taxonomic relationships of SPPV, phylogenetic analysis of two putative SPPV proteins that are conserved across all eight genera was employed (chapter 7.0). Contrary to the formal classification of SPPV as a parapoxvirus (van Regenmortel *et al.,* 2000), the analysis provided no evidence to support its classification as such. Indeed the SPPV sequences did not group with any of the clades representing defined poxvirus genera, suggesting that SPPV may represent a separate genus of the poxvirus family. In view of data presented in this thesis it may be appropriate to remove SPPV from the parapoxvirus genus and place it into a new genus on its own. In addition, the misleading name of squirrel parapoxvirus (SPPV) should be changed to squirrel poxvirus (SQPV).

Figure 8.1 Red squirrel 1296/99 found dead during in an outbreak of SQPV in Gateshead, Northumbria. The animal has severe necrotic and haemorrhagic lesions on the face, hands, feet and thorax attributed to SQPV. Negative contrast electron microscopy revealed parapoxvirus-like particles in the lesions and sera collected from this animal tested positive for antibodies against SQPV by ELISA (Sainsbury *et al.*, 2000).

8.2 FURTHER CONSIDERATIONS

The red squirrel is now all but extinct from England and Wales with just a few isolated populations remaining. The remaining stronghold in Scotland is now under threat from interloping grey squirrels and SQPV (Pepper and Paterson, 1998; P. Nettleton personal communication). This situation is mirrored in Italy where the red squirrel is being rapidly displaced by the greys in deciduous woodland (Lurz *et al.,* 2001). Conservation strategies encompass several areas including; habitat management, translocation and reintroduction of red squirrels, supplemental feeding programmes and grey squirrel control (reviewed in section 1.8.4). However, in the UK, many conservation programmes have encountered problems due to SQPV (Venning *et al.,* 1997; Jackson, 1999). Whether SQPV is present in the red and grey squirrel populations of continental Europe is at present not clear. A vaccine may prove to be essential for the continuation and success of many red squirrel conservation programmes and ultimately the survival of the red squirrel species.

On the basis of the inclusion of SQPV into the parapoxvirus genus, many assumptions were made regarding viral transmission, host range and genes associated with immuno-modulation that SQPV might possess. All of these are critically important for the development of effective vaccine and conservation strategies, and in view of the findings reported in this thesis, many of these assumptions may prove to be incorrect.

Circumstantial evidence suggests that the grey squirrel is the source of SQPV which was introduced to the UK with the grey squirrel (Middleton, 1930). Serological evidence and computer modelling also implicates the grey squirrel as a reservoir for SQPV, capable of transmitting the disease to the susceptible red squirrel (Sainsbury *et al.,* 2000; Rushton *et al.,* 2000; Tompkins *et al.,* 2003). In addition, the rapid clinical progression of the disease (Tompkins *et al.,* 2002) and the high mortality rate seen in the red squirrel suggests that it is not the natural host species for SQPV. The grey squirrel's resistance to SQPV may be due to the co-evolution of host and virus resulting in genetic resistance. Conversely, the lack of previous exposure to SQPV would suggest that the red squirrel lacks genetic resistance and is therefore susceptible to SQPV. In this, SQPV may have many parallels with MYXV. MYXV is primarily a disease of North and South American brush and jungle rabbits and infection of the host species causes a non-lethal localised cutaneous fibroma. MYXV was recently introduced to Europe and

Australia where, in the naïve European rabbit, it causes a fatal systemic infection (Robinson and Kerr, 2001).

Further research is required to confirm that infected grey squirrels are capable of transmitting the virus to susceptible red squirrels and the route(s) of transmission needs to be identified. In addition alternative reservoir species cannot be ruled out. A preliminary study assessing different rodent species for their potential as reservoir hosts has been carried out (section 3.3). The data suggests that the wood mice and bank voles are not involved in the epidemiology of SQPV. However this work is not conclusive for rodents as a whole as only two species were assessed. In future, several species of rodent should be assessed and these should preferably be sampled from an area during in an outbreak of SQPV.

Previously it was assumed that the mode of transmission of SQPV was similar to that of the parapoxviruses; via direct contact with infectious scab material either between individuals and/or environmental contamination (Sainsbury and Gurnell, 1997). These routes are feasible between red squirrels where infection results in extensive cutaneous lesions, although the rarity of clinical symptoms in the grey squirrel would suggest that transmission from the grey to the red squirrel via the scab route is unlikely. However, in parapoxvirus infections, transmission from asymptomatic animals has not been ruled out (Nettleton *et al.*, 1996b). An alternative route of transmission is passive transmission via biting insects, which is known to occur in leporipoxviruses. A report of an unusual epizootic of squirrel fibroma virus (SQFV) in America described large numbers of grey squirrels with proliferative lesions around the eyes and ears (Terrell *et al.*, 2002). The facial lesions were attributed to biting insects favouring hairless region of the body and the eyelids were proposed to be the site of inoculation. In SQPV the onset of clinical symptom also occurs around the hairless eyes, nose and mouth (Edwards, 1962; Sainsbury and Gurnell, 1995). Clearly the potential involvement of insect vectors in the epidemiology of SQPV warrants further investigation. In addition, grey squirrels need to be assessed to see if virus is present despite the absence of pathology. Now that DNA sequence of SQPV is available, a diagnostic PCR could be developed and utilised in these studies. A greater understanding of the transmission of SQPV may provide insight into control measures that could be implemented during epidemics to reduce infection rates.

Numerous examples exist of successful vaccination strategies involving the use of one poxvirus to provide protection against another. However vaccination within a genus is more successful than between genera. For example, VACV cross-protects against other orthopoxviruses such as VARV and the emerging MPV (section 1.1), however it does not cross-protect sheep against ORFV (Robinson and Mercer, 1988). Therefore, in terms of vaccination strategy, it is important to establish the relationship between SQPV with the other poxviruses. As SQPV is formally included in the parapoxvirus genus, it was a possibility that SQPV vaccination strategies would encounter the same problems as ORFV vaccination. ORFV vaccines routinely comprise of live attenuated ORFV strains such as D1701 and scabby mouth or live unattenuated virus such as Scabivax™. However, vaccination only provides partial protection and the vaccinees are susceptible to reinfection with a virulent ORFV although the severity of the disease is reduced (Nettleton *et al.,* 1996a). The lack of complete protection may be due to the array of immuno-modulating factors that parapoxviruses possess. However, as SQPV appears to be only distantly related to the parapoxviruses, the application of a live attenuated strain of SQPV may provide complete protection.

Attenuation of poxviruses is most often achieved through prolonged passage in tissue culture. Evidence suggests that an attenuated strain of SQPV may arise from the extensive passage of the tissue culture isolate of SQPV. This is one option that could be pursued in the development of a vaccine against SQPV. Alternatively manually disrupting known virulence or immuno-modulating genes has also been demonstrated as a method to attenuate a poxviruses (Rziha *et al.,* 2000). Obviously such genes will need to be identified in SQPV, however the ongoing DNA sequencing of the terminal 30kb of the SQPV genome should help to resolve this matter.

An undesirable effect of vaccination with live attenuated VACV and ORFV is that secondary contacts are susceptible to infection with the vaccine strain. In the case of VACV this has promoted safety concerns (Moss, 1996a). With ORFV secondary contacts often develop lesions around the mouth comparable to those seen in natural infections (Haig and Mercer, 1998). Infection of secondary contacts, which is considered undesirable in VACV and ORFV vaccination, may actually be beneficial in terms of a wildlife vaccination strategy. A transmissible vaccine will readily disseminate amongst the unvaccinated individuals within a vaccinated population, thereby avoiding the need to individually trap and vaccinate each animal. In addition, the virus may continuously circulate within a population thereby maintaining a high

degree of protection. An attenuated and transmissible isolate of MYXV was shown to confer protection against challenge with virulent MYXV in vaccinated European rabbits and in secondary contacts (Barcena *et al.*, 2000). This transmissible MYXV strain was exploited as a vaccine vector expressing the capsid protein of the calicivirus rabbit haemorrhagic disease virus (RHDV). Field trial vaccination demonstrated that all inoculated rabbits and 50% of uninoculated rabbits seroconverted to both MYXV and RHDV (Torres *et al.*, 2001).

The use of an attenuated and transmissible SQPV strain may warrant further investigation as a vaccine strategy for the immunisation of red squirrels against SQPV. Obviously the release of any virus into the wild should be undertaken only after rigorous safety testing to ensure that there are no adverse effects of the vaccine and that the live vaccine has a limited host range. Experimental release should take place in contained environment, as the effects of the virus in wild animals may differ from the effects in laboratory animals due to stresses such as other diseases, predators, nutritional stress and competitors (Torres *et al.*, 2001).

In summary the data presented in this thesis strongly suggests that SQPV is not a parapoxvirus. Therefore previous assumptions regarding transmission of SQPV in the wild, the possession of parapoxvirus virulence and immuno-modulation factors and the efficacy of potential attenuated vaccines clearly need to be reassessed.

CHAPTER 9.0

BIBLIOGRAPHY

Afonso, C. L., Tulman, E. R., Lu, Z., Zsak, L., Kutish, G. F. and Rock, D. L. (2000). The genome of fowlpox virus. Journal of Virology, 74, 3815-3831.

Afonso, C. L., Tulman, E. R., Lu, Z., Zsak, L., Osorio, F. A., Balinsky, C., Kutish, G. F. and Rock, D. L. (2002). The genome of swinepox virus. Journal of Virology, 76, 783-790.

Ahn, B. Y., Gershon, P. D., Jones, E. V. and Moss, B. (1990). Identification of rpo30, a vaccinia virus RNA polymerase gene with structural similarity to a eucaryotic transcription elongation factor. Molecular and Cell Biology, 10, 5433-5441.

Ahn, B. Y., Gershon, P. D. and Moss, B. (1994). RNA polymerase-associated protein Rap94 confers promoter specificity for initiating transcription of vaccinia virus early stage genes. Journal of Biological Chemistry, 269, 7552-7557.

Ahn, B. Y. and Moss, B. (1989). Capped poly(A) leaders of variable lengths at the 5' ends of vaccinia virus late mRNAs. Journal of Virology, 63, 226-232.

Ahn, B. Y. and Moss, B. (1992). RNA polymerase-associated transcription specificity factor encoded by vaccinia virus. Proceeding of the National Academy of Science USA, 89, 3536-3540.

Alcami, A. and Koszinowski, U. H. (2000). Viral mechanisms of immune evasion. Immunology Today, 21, 447-455.

Amegadzie, B. Y., Ahn, B. Y. and Moss, B. (1991a). Identification, sequence, and expression of the gene encoding a Mr 35,000 subunit of the vaccinia virus DNA-dependent RNA polymerase. Journal of Biological Chemistry, 266, 13712-13718.

Amegadzie, B. Y., Holmes, M. H., Cole, N. B., Jones, E. V., Earl, P. L. and Moss, B. (1991b). Identification, sequence, and expression of the gene encoding the second-largest subunit of the vaccinia virus DNA-dependent RNA polymerase. Virology, 180, 88-98.

Anderson, I. E., Reid, H. W., Nettleton, P. F., McInnes, C. J. and Haig, D. M. (2001). Detection of cellular cytokine mRNA expression during orf virus infection in sheep: differential interferon-gamma mRNA expression by cells in primary versus reinfection skin lesions. Veterinary Immunology and Immunopathology, 83, 161-176.

Bairoch, A. and Apweiler, R. (2000). The SWISS-PROT protein sequence database and its supplement TrEMBL in 2000. Nucleic Acids Research, 28, 45-48.

Baldick, C. J. Jr., Keck, J. G. and Moss, B. (1992). Mutational analysis of the core, spacer, and initiator regions of vaccinia virus intermediate-class promoters. Journal of Virology, 66, 4710-4719.

Baldick, C. J. Jr. and Moss, B. (1993). Characterization and temporal regulation of mRNAs encoded by vaccinia virus intermediate-stage genes. Journal of Virology, 67, 3515-3527.

Barcena, J., Pages-Mante, A., March, R., Morales, M., Ramirez, M. A., Sanchez-Vizcaino, J. M. and Torres, J. M. (2000). Isolation of an attenuated myxoma virus field strain that can confer protection against myxomatosis on contacts of vaccinates. Archives of Virology, 145, 759-771.

Baroudy, B. M., Venkatesan, S. and Moss, B. (1982). Incompletely base-paired flip-flop terminal loops link the two DNA strands of the vaccinia virus genome into one uninterrupted polynucleotide chain. Cell, 28, 315-324.

Barratt, E. M., Malarky, G., Boddy, S., Gurnell, J. and Bruford, M. W. (1997). Genetic diversity among fragmented populations of red squirrel *Sciurus vulgaris*: a preliminary study. In "The conservation of red squirrels, *Sciurus vulgaris* L.". (Gurnell, J. and Lurz, P.). pp61-76. Peoples Trust for Endangered Species, London.

Beattie, E., Tartaglia, J. and Paoletti, E. (1991). Vaccinia virus-encoded eIF-2 alpha homolog abrogates the antiviral effect of interferon. Virology, 183 , 419-422.

Becher, P., Konig, M., Muller, G., Siebert, U. and Thiel, H. J. (2002). Characterization of sealpox virus, a separate member of the parapoxviruses. Archives of Virology, 147, 1133-1140.

Berns, K. I. and Silverman, C. (1970). Natural occurrence of cross-linked vaccinia virus deoxyribonucleic acid. Journal of Virology, 5, 299-304.

Biron, C. A., Nguyen, K. B., Pien, G. C., Cousens, L. P. and Salazar-Mather, T. P. (1999). Natural killer cells in antiviral defence: function and regulation by innate cytokines. Annual Review of Immunology, 17, 189-220.

Black, E. P. and Condit, R. C. (1996). Phenotypic characterization of mutants in vaccinia virus gene G2R, a putative transcription elongation factor. Journal of Virology, 70, 47-54.

Blake, N. W., Porter, C. D. and Archard, L. C. (1991). Characterization of a molluscum contagiosum virus homolog of the vaccinia virus p37K major envelope antigen. Journal of Virology, 65, 3583-3589.

Blasco, R. and Moss, B. (1991). Extracellular vaccinia virus formation and cell-to-cell virus transmission are prevented by deletion of the gene encoding the 37,000-Dalton outer envelope protein. Journal of Virology, 65, 5910-5920.

Blasco, R. and Moss, B. (1992). Role of cell-associated enveloped vaccinia virus in cell-to-cell spread. Journal of Virology, 66, 4170-4179.

Brandt, T. A. and Jacobs, B. L. (2001). Both carboxy- and amino-terminal domains of the vaccinia virus interferon resistance gene, E3L, are required for pathogenesis in a mouse model. Journal of Virology, 75, 850-856.

Brown, F., Schild, G. C. and Ada, G. L. (1986). Recombinant vaccinia viruses as vaccines. Nature, 319, 549-550.

Broyles, S. S. and Moss, B. (1986). Homology between RNA polymerases of poxviruses, prokaryotes, and eukaryotes: nucleotide sequence and transcriptional analysis of vaccinia virus genes encoding 147-kDa and 22-kDa subunits. Proceeding of the National Academy of Science USA, 83, 3141-3145.

Broyles, S. S. and Pennington, M. J. (1990). Vaccinia virus gene encoding a 30-kilodalton subunit of the viral DNA-dependent RNA polymerase. Journal of Virology, 64, 5376-5382.

Bryce, J. M. (1999). Habitat use by red and grey squirrels in the Dunkeld area 1996-1999, In "3rd NPI Red Alert Forum for Red Squirrel Conservation, Forum Proceedings" (Collins, L. M. and Cooper, J. A.). pp3-9. Scottish Natural Heritage, Perth.

Buddle, B. M. and Pulford, H. D. (1984). Effect of passively-acquired antibodies and vaccination on the immune response to contagious ecthyma virus. Veterinary Microbiology, 9, 515-522.

Bugert, J. J., Lohmuller, C., Damon, I., Moss, B. and Darai, G. (1998). Chemokine homolog of molluscum contagiosum virus: sequence conservation and expression. Virology, 242, 51-59.

Bugert, J. J., Lohmuller, C. and Darai, G. (1999). Characterization of early gene transcripts of molluscum contagiosum virus. Virology, 257, 119-129.

Bugert, J. J. and Darai, G. (2000). Poxvirus homologues of cellular genes. Virus Genes, 21, 111-133.

Buller, R. M., Chakrabarti, S., Moss, B. and Fredrickson, T. (1988a). Cell proliferative response to vaccinia virus is mediated by VGF. Virology, 164, 182-192.

Buller, R. M. L., Chakrabarti, S., Cooper, J. A., Twardzik, D. R. and Moss, B. (1988b). Deletion of the vaccinia virus growth-factor gene reduces virulence. Journal Of Virology, 62, 866-874.

Burgert, J. J. and Darai, G. (1991). Stability of molluscum contagiosum virus DNA amongst patient isolates: evidence for variability of sequences in the terminal regions. Journal of Medical Virology, 33, 211-217.

Buttner, M. and Rziha, H. J. (2002). Parapoxviruses: from the lesion to the viral genome. Journal of Veterinary Medicine, B49, 7-16.

Cabirac, G. F., Strayer, D. S., Sell, S. and Leibowitz, J. L. (1985). Characterization, molecular cloning, and physical mapping of the Shope fibroma virus genome. Virology, 143, 663-670.

Cameron, C., Hota-Mitchell, S., Chen, L., Barrett, J., Cao, J. X., Macaulay, C., Willer, D., Evans, D. and McFadden, G. (1999). The complete DNA sequence of myxoma virus. Virology, 264, 298-318.

Cassetti, M. A. and Moss, B. (1996). Interaction of the 82-kDa subunit of the vaccinia virus early transcription factor heterodimer with the promoter core sequence directs downstream DNA binding of the 70-kDa subunit. Proceeding of the National Academy of Science USA, 93, 7540-7545.

Cassetti, M. C., Merchlinsky, M., Wolffe, E. J., Weisberg, A. S. and Moss, B. (1998). DNA packaging mutant: repression of the vaccinia virus A32 gene results in noninfectious, DNA-deficient, spherical, enveloped particles. Journal of Virology, 72, 5769-5780.

Chang, H. W. and Jacobs, B. L. (1993). Identification of a conserved motif that is necessary for binding of the vaccinia virus E3L gene products to double-stranded RNA. Virology, 194, 537-547.

Chang, H. W., Uribe, L. H. and Jacobs, B. L. (1995a). Rescue of vaccinia virus lacking the E3L gene by mutants of E3L. Journal of Virology, 69, 6605-6608.

Chang, W., Hsiao, J. C., Chung, C. S. and Bair, C. H. (1995b). Isolation of a monoclonal antibody which blocks vaccinia virus infection. Journal of Virology, 69, 517-522 .

Chiu, W. L. and Chang, W. (2002). Vaccinia virus J1R protein: a viral membrane protein that is essential for virion morphogenesis. Journal of Virology, 76, 9575-9587.

Chung, C. S., Hsiao, J. C., Chang, Y. S. and Chang, W. (1998). A27L protein mediates vaccinia virus interaction with cell surface heparan sulfate. Journal of Virology, 72, 1577-1585.

Cohen, E. P., Delong, S. S., Sanders, J. and Moscovici, C. (1964). Aspects of the morphologic development of pseudocowpox virus. Virology, 23, 56-64.

Cohen, S. N., Chang, A. C. and Hsu, L. (1972). Nonchromosomal antibiotic resistance in bacteria: genetic transformation of *Escherichia coli* by R-factor DNA. Proceeding of the National Academy of Science USA, 69, 2110-2114.

Collins, L. (1999). Workshop on dealing with a disease outbreak, In "3rd NPI Red Alert Forum for Red Squirrel Conservation, Forum Proceedings" (Collins, L. M. and Cooper, J. A.). pp117. Scottish Natural Heritage, Perth.

Condit, R. C. and Niles, E. G. (2002). Regulation of viral transcription elongation and termination during vaccinia virus infection. Biochimica et Biophysica Acta, 1577, 325-336.

Condit, R. C., Xiang, Y. and Lewis, J. I. (1996). Mutation of vaccinia virus gene G2R causes suppression of gene A18R ts mutants: implications for control of transcription. Virology, 220, 10-19.

Cottone, R., Buttner, M., Bauer, B., Henkel, M., Hettich, E. and Rziha, H. J. (1998). Analysis of genomic rearrangement and subsequent gene deletion of the attenuated Orf virus strain D1701. Virus Research, 56, 53-67.

Cottone, R., Buttner, M., McInnes, C. J., Wood, A. R. and Rziha, H. J. (2002). Orf virus encodes a functional dUTPase gene. Journal of General Virology, 83, 1043-1048.

Cudmore, S., Cossart, P., Griffiths, G. and Way, M. (1995). Actin-based motility of vaccinia virus. Nature, 378, 636-638.

da Fonseca, F. G., Silva, R. L., Marques, J. T., Ferreira, P. C. and Kroon, E. G. (1999). The genome of cowpox virus contains a gene related to those encoding the epidermal growth factor, transforming growth factor alpha and vaccinia growth factor. Virus Genes, 18, 151-160.

Davies, M. V., Chang, H. W., Jacobs, B. L. and Kaufman, R. J. (1993). The E3L and K3L vaccinia virus gene products stimulate translation through the inhibition of the double-stranded RNA-dependent protein kinase by different mechanisms. Journal of Virology, 67, 1688-1692.

Davies, M. V., Elroy-Stein, O., Jagus, R., Moss, B. and Kaufman, R. J. (1992). The vaccinia virus K3L gene product potentiates translation by inhibiting double-stranded-RNA-activated protein kinase and phosphorylation of the alpha subunit of eukaryotic initiation factor 2. Journal of Virology, 66, 1943-1950.

Davison, A. J. and Moss, B. (1989a). Structure of vaccinia virus early promoters. Journal of Molecular Biology, 210 , 749-769.

Davison, A. J. and Moss, B. (1989b). Structure of vaccinia virus late promoters. Journal of Molecular Biology, 210, 771-784.

Deane, D., McInnes, C. J., Percival, A., Wood, A., Thomson, J., Lear, A., Gilray, J., Fleming, S., Mercer, A. and Haig, D. (2000). Orf virus encodes a novel secreted protein inhibitor of granulocyte- macrophage colony-stimulating factor and interleukin-2. Journal of Virology, 74, 1313-1320.

Delange AM (1984). Tumorigenic poxviruses: construction of the composite physical map of the Shope fibroma virus genome. Journal of Virology, 50(2), 408-416.

Deng, L. and Shuman, S. (1998). Vaccinia NPH-I, a DExH-box ATPase, is the energy coupling factor for mRNA transcription termination. Genes and Development., 12, 538-546.

Dietrich, F. S. Ray, C. A., Sharma, A. D., Allen, A. and Pickup, D. J. (2002). Complete genome of cowpoxvirus Brighton red strain, direct submission. National Center for Biotechnology Information.

Diven, D. G. (2001). An overview of poxviruses. Journal of the American Academy of Dermatology, 44, 1-16.

Doms, R. W., Blumenthal, R. and Moss, B. (1990). Fusion of intra- and extracellular forms of vaccinia virus with the cell membrane. Journal of Virology, 64, 4884-4892.

Driven, D. G. (2001). Continuing medical education: an overview of poxviruses. Journal of American Academy of Determatology, 44, 1-16.

Dubochet, J., Adrian, M., Richter, K., Garces, J. and Wittek, R. (1994). Structure of intracellular mature vaccinia virus observed by cryoelectron microscopy. Journal of Virology, 68, 1935-1941.

Duff, J. P., Higgins, R. J., Sainsbury, A. W. and Macgregor, S. K. (2001). Zoonotic infections in red squirrels. Veterinary Record, 148, 123-124.

Duff, J. P., Scott, A. and Keymer, I. F. (1996). Parapox virus infection of the grey squirrel. The Veterinary Record, 138, 527 -527.

Earl, P. L., Jones, E. V. and Moss, B. (1986). Homology between DNA polymerases of poxviruses, herpesviruses, and adenoviruses: nucleotide sequence of the vaccinia virus DNA polymerase gene. Proceeding of the National Academy of Science USA, 83, 3659-3663.

Earnshaw, W. C. (1995). Nuclear changes in apoptosis. Current Opinion in Cell Biology, 7, 337-343.

Edwards, F. B. (1962). Red squirrel disease. The Veterinary Record, 74, 739-741.

Engelstad, M. and Smith, G. L. (1993). The vaccinia virus 42-KDa envelope protein is required for the envelopment and egress of extracellular virus and for virus virulence. Virology, 194, 627-637.

Esposito, J. J. and Knight, J. C. (1985). Orthopoxvirus DNA - a comparison of restriction profiles and maps. Virology, 143, 230-251.

Esposito, J. J., Obijeski, J. F. and Nakano, J. H. (1978). Orthopoxvirus DNA:Strain differentiation by electrophoresis of restiction endonuclease fragmented virion DNA. Virology, 89, 53-66.

Evans, E., Klemperer, N., Ghosh, R. and Traktman, P. (1995). The vaccinia virus D5 protein, which is required for DNA replication, is a nucleic acid-independent nucleoside triphosphatase. Journal of Virology, 69, 5353-5361.

Everett, H. and McFadden, G. (1999). Apoptosis: an innate immune response to virus infection. Trends in Microbiology, 7, 160-165.

Falk, E. S. (1978). Parapoxvirus infections of reindeer and musk ox associated with unusual human infections. British Journal of Dermatology, 99, 647-654.

Felsenstein, J. (1985). Confidence intervals on phylogenies: An approach using the bootstrap. Evolution, 39, 783-791.

Felsenstein, J. (1993). PHYLIP (Phylogeny Inference Package) version 3.5c. Department of Genetics. University of Washington, Seattle.

Fenner, F. (1996). Poxviruses. *In* "Fields Virology". (Fields, B. N., Knipe, D. M., and Howley, P. M.). Third ed., 2637-2671. Lippcott-Raven Publishers, Philadelphia.

Fleming, S. B., Blok, J., Fraser, K. M., Mercer, A. A. and Robinson, A. J. (1993). Conservation of gene structure and arrangement between vaccinia virus and orf virus. Virology, 195, 175-184.

Fleming, S. B., Fraser, K. M., Mercer, A. A. and Robinson, A. J. (1991). Vaccinia virus-like early transcriptional control sequences flank an early gene in orf virus. Gene, 97, 207-212.

Fleming, S. B., Haig, D. M., Nettleton, P., Reid, H. W., McCaughan, C. A., Wise, L. M. and Mercer, A. (2000). Sequence and functional analysis of a homolog of interleukin-10 encoded by the parapoxvirus orf virus. Virus Genes, 21, 85-95.

Fleming, S. B., Lyttle, D. J., Sullivan, J. T., Mercer, A. A. and Robinson, A. J. (1995). Genomic analysis of a transposition-deletion variant of orf virus reveals a 3.3 kbp region of non-essential DNA. Journal of General Virology, 76 (Pt 12), 2969-2978.

Fleming, S. B., McCaughan, C. A., Andrews, A. E., Nash, A. D. and Mercer, A. A. (1997). A homolog of interleukin-10 is encoded by the poxvirus orf virus. Journal of Virology, 71, 4857-4861.

Fleming, S. B., Mercer, A. A., Fraser, K. M., Lyttle, D. J. and Robinson, A. J. (1992). In vivo recognition of orf virus early transcriptional promoters in a vaccinia virus recombinant. Virology, 187, 464-471.

Forestry Commission. (2002). Grey squirrel contraception research put on hold. News release number 5148, Edinburgh.

Fraser, K. M., Hill, D. F., Mercer, A. A. and Robinson, A. J. (1990). Sequence analysis of the inverted terminal repetition in the genome of the parapoxvirus, orf virus. Virology, 176, 379-389.

Frischknecht, F., Moreau, V., Rottger, S., Gonfloni, S., Reckmann, I., Superti-Furga, G. and Way, M. (1999). Actin-based motility of vaccinia virus mimics receptor tyrosine kinase signalling. Nature, 401, 926-929.

Galmiche, M. C., Goenaga, J., Wittek, R. and Rindisbacher, L. (1999). Neutralizing and protective antibodies directed against vaccinia virus envelope antigens. Virology, 254, 71-80.

Garcia, A. D., Aravind, L., Koonin, E. V. and Moss, B. (2000). Bacterial-type DNA holliday junction resolvases in eukaryotic viruses. Proceeding of the National Academy of Science USA, 97, 8926- 8931.

Garcia, A. D. and Moss, B. (2001). Repression of vaccinia virus Holliday junction resolvase inhibits processing of viral DNA into unit-length genomes. Journal of Virology, 75, 6460-6471.

Garon, C. F., Barbosa, E. and Moss, B. (1978). Visualization of an inverted terminal repetition in vaccinia virus DNA. Proceeding of the National Academy of Science USA, 75, 4863-4867.

Gassmann, U., Wyler, R. and Wittek, R. (1985). Analysis of parapoxvirus genomes. Archives of Virology, 83, 17-31 .

Geada, M. M., Galindo, I., Lorenzo, M. M., Perdiguero, B. and Blasco, R. (2001). Movements of vaccinia virus intracellular enveloped virions with GFP tagged to the F13L envelope protein. Journal of General Virology, 82, 2747-2760.

Gerdes, G. H. (1991). Morphology of poxviruses from reptiles. Veterinary Record, 128, 452

Gershon, P. D., Ahn, B. Y., Garfield, M. and Moss, B. (1991). Poly(A) polymerase and a dissociable polyadenylation stimulatory factor encoded by vaccinia virus. Cell, 66, 1269-1278.

Gershon, P. D., Ansell, D. M. and Black, D. N. (1989). A comparison of the genome organization of capripoxvirus with that of the orthopoxviruses. Journal of Virology, 63, 4703-4708.

Gershon, P. D. and Black, D. N. (1988). A comparison of the genomes of capripoxvirus isolates of sheep, goats, and cattle. Virology, 164, 341- 349.

Gershon, P. D. and Moss, B. (1990). Early transcription factor subunits are encoded by vaccinia virus late genes. Proceeding of the National Academy of Science USA, 87, 4401-4405.

Geshelin, P. and Berns, K. I. (1974). Characterization and localization of the naturally occurring cross-links in vaccinia virus DNA. Journal of Molecular Biology, 88, 785 -796.

Gilray, J. A., Nettleton, P. F., Pow, I., Lewis, C. J., Stephens, S. A., Madeley, J. D. and Reid, H. W. (1998). Restriction endonuclease profiles of orf virus isolates from the British Isles. Veterinary Record, 143, 237-240.

Goebel, S. J., Johnson, G. P., Perkus, M. E., Davis, S. W., Winslow, J. P. and Paoletti, E. (1990). The complete DNA sequence of vaccinia virus. Virology, 179, 247-266.

Goodbourn, S., Didcock, L. and Randall, R. E. (2000). Interferons: cell signalling, immune modulation, antiviral response and virus countermeasures. Journal of General Virology, 81, 2341-2364.

Grist, G. E., Bell, E. J., Follet, E. A. C. and Urquhart, G. E. D. (1979). Diagnostic methods in clinical virology. 3rd ed., Blackwell Scientific Publications, Oxford.

Grosenbach, D. W. and Hruby, D. E. (1998). Analysis of a vaccinia virus mutant expressing a nonpalmitylated form of p37, a mediator of virion envelopment. Journal of Virology, 72, 5108-5120.

Grunstein, M. and Hogness, D. S. (1975). Colony hybridization: a method for the isolation of cloned DNAs that contain a specific gene. Proceeding of the National Academy of Science USA, 72, 3961-3965.

Gubser, C. and Smith, G. L. (2002). The sequence of camelpox virus shows it is most closely related to variola virus, the cause of smallpox. Journal of General Virology, 83, 855-872.

Gunasinghe, S. K., Hubbs, A. E. and Wright, C. F. (1998). A vaccinia virus late transcription factor with biochemical and molecular identity to a human cellular protein. Journal of Biological Chemistry, 273, 27524-27530.

Gurnell, J. and Pepper, H. (1991). Conserving the red squirrel, Research information note. Forestry commission, Edinburgh.

Gurnell, J. and Pepper, H. (1993). A critical look at conserving the British red squirrel *Sciurus vulgaris*. Mammal Review, 23, 127-137.

Gurnell, J., Nettleton, P. and Sainsbury, A. W. (1999). The conservation of the red squirrel in Britain: problems of disease. In "3rd NPI Red Alert Forum for Red Squirrel Conservation, Forum Proceedings" (Collins, L. M. and Cooper, J. A.). pp99-100. Scottish Natural Heritage, Perth.

Haig, D., Entrican, G., Yirrell, D., Deane, D., Miller, H. R. P., Norval, M. and Reid, H. W. (1992). Differential appearance of interferon-γ and colony stimulating activity in afferent versus efferent lymph following orf virus infection of sheep. Veterinary Dermatology, 3, 221-229.

Haig, D. M., Hutchinson, G., Green, I., Sargan, D. and Reid, H. W. (1995a). The effect of intradermal injection of GM-CSF and TNF-α on the accumulation of dendritic cells in the ovine skin. Veterinary Dermatology, 6, 211-220.

Haig, D. M., Percival, A., Mitchell, J., Green, I. and Sargan, D. (1995b). The survival and growth of ovine afferent lymph dendritic cells in culture depends on tumour necrosis factor-alpha and is enhanced by granulocyte-macrophage colony-stimulating factor but inhibited by interferon-gamma. Veterinary Immunology and Immunopathology, 45, 221-236.

Haig, D., Deane, D., Percival, A., Myatt, N., Thomson, J., Inglis, L., Rothel, J., Heng-Fong Seow, Wood, P., Miller, H. R. P. and Reid, H. W. (1996a). The cytokine response of affent lymph following orf virus reinfection of sheep. Veterinary Dermatology, 7, 11-20.

Haig, D. M., Hutchinson, G., Thomson, J., Yirrell, D. and Reid, H. W. (1996b). Cytolytic activity and associated serine protease expression by skin and afferent lymph CD8+ T cells during orf virus reinfection. Journal of General Virology, 77 (Pt 5), 953-961.

Haig, D. M., McInnes, C. J., Hutchison, G., Seow, H. F. and Reid, H. W. (1996c). Cyclosporin A abrogates the acquired immunity to cutaneous reinfection with the parapoxvirus orf virus. Immunology, 89, 524-531.

Haig, D. M., McInnes, C. J., Thomson, J., Wood, A., Bunyan, K. and Mercer, A. (1998). The orf virus OV20.OL gene product is involved in interferon resistance and inhibits an interferon-inducible, double- stranded RNA-dependent kinase. Immunology, 93, 335-340.

Haig, D. M. and Mercer, A. A. (1998). Ovine diseases. Orf. Veterinary Research, 29, 311-326.

Haig, D. M., Hopkins, J. and Miller, H. R. (1999). Local immune responses in afferent and efferent lymph. Immunology, 96, 155-163.

Haig, D. M. (2001). Subversion and piracy: DNA viruses and immune evasion. Research in Veterinary Science, 70, 205-219.

Haig, D. M. and McInnes, C. J. (2002). Immunity and counter-immunity during infection with the parapoxvirus orf virus. Virus Research, 88, 3-16.

Haig, D. M., Thomson, J., McInnes, C. J., Deane, D. L., Anderson, I. E., McCaughan, C. A., Imlach, W., Mercer, A. A., Howard, C. J. and Fleming, S. B. (2002). A comparison of the anti-inflammatory and immuno-stimulatory activities of orf virus and ovine interleukin-10. Virus Research, 90, 303-316.

Hale, M. L., Lurz, P. W., Shirley, M. D., Rushton, S., Fuller, R. M. and Wolff, K. (2001). Impact of landscape management on the genetic structure of red squirrel populations. Science, 293, 2246-2248.

Hamilton, J. A. (2002). GM-CSF in inflammation and autoimmunity. Trends in Immunology, 23, 403-408 .

Heymann, D. L., Szczeniowski, M. and Esteves, K. (1998). Re-emergence of monkeypox in Africa: a review of the past six years. British Medical Bulletin, 54, 693-702.

Hiller, G. and Weber, K. (1985). Golgi-derived membranes that contain an acylated viral polypeptide are used for vaccinia virus envelopment. Journal of Virology, 55, 651-659.

Hirt, P., Hiller, G. and Wittek, R. (1986). Localization and fine structure of a vaccinia virus gene encoding an envelope antigen. Journal of Virology, 58, 757-764.

Hollinshead, M., Rodger, G., van Eijl, H., Law, M., Hollinshead, R., Vaux, D. J. and Smith, G. L. (2001). Vaccinia virus utilizes microtubules for movement to the cell surface. Journal of Cell Biology, 154, 389-402.

Hollinshead, M., Vanderplasschen, A., Smith, G. L. and Vaux, D. J. (1999). Vaccinia virus intracellular mature virions contain only one lipid membrane. Journal of Virology, 73, 1503-1517.

Horner, G. W., Robinson, A. J., Hunter, R., Cox, B. T. and Smith, R. (1987). Parapoxvirus infections in New Zealand farmed red deer (*Cervus elaphus*). New Zealand Veterinary Journal, 35, 41-45.

Housawi, F. M. T. (1997). Studies on parapoxvirus antigens through the development of monoclonal antibodies to orf virus. PhD thesis, University of Edinburgh.

Hsiao, J. C., Chung, C. S. and Chang, W. (1999). Vaccinia virus envelope D8L protein binds to cell surface chondroitin sulfate and mediates the adsorption of intracellular mature virions to cells. Journal of Virology, 73, 8750-8761.

Husain, M. and Moss, B. (2002). Similarities in the induction of post-Golgi vesicles by the vaccinia virus F13L protein and phospholipase D. Journal of Virology, 76, 7777-7789.

Ichihashi, Y. (1996). Extracellular enveloped vaccinia virus escapes neutralization. Virology, 217, 478-485.

Imlach, W., McCaughan, C. A., Mercer, A. A., Haig, D. and Fleming, S. B. (2002). Orf virus-encoded interleukin-10 stimulates the proliferation of murine mast cells and inhibits cytokine synthesis in murine peritoneal macrophages. Journal of General Virology, 83, 1049-1058.

Inoshima, Y., Morooka, A. and Sentsui, H. (2000). Detection and diagnosis of parapoxvirus by the polymerase chain reaction. Journal of Virological Methods, 84, 201-208.

Inoshima, Y., Murakami, K., Yokoyama, T. and Sentsui, H. (2001). Genetic heterogeneity among parapoxviruses isolated from sheep, cattle and Japanese serows (Capricornis crispus). Journal of General Virology, 82, 1215-1220.

Isaacs, S. N., Kotwal, G. J. and Moss, B. (1992). Vaccinia virus complement-control protein prevent antibody-dependent complement-enhanced neutralisation of infectivity and contributes to virulence. Proceedings of the National Academy of Sciences USA, 89, 628-632.

Jackson, N. L. (1999). The reds return - project update to 31 May 1998, In "3rd NPI Red Alert Forum for Red Squirrel Conservation, Forum Proceedings" (Collins, L. M. and Cooper, J. A.). pp67-78. Scottish Natural Heritage, Perth.

Jenkinson, D. M., McEwan, P. E., Onwuka, S. K., Moss, V. A., Elder, H. Y., Hutchinson, G. and Reid, H. W. (1990). The pathological changes and polymorphonuclear and mast cell responses in the skin of specific-pathogen free lambs following primary and secondary challenge with orf virus. Veterinary Dermatology, 1, 139-150 .

Jenkinson, D. M., Hutchinson, G., Onwuka, S. K. and Reid, H. W. (1991). Changes in the MHC class II^+ dendritic cell population of ovine skin in response to orf virus infection. Veterinary Dermatology, 2, 1-9.

Jenkinson, D. M., Hutchinson, G. and Reid, H. W. (1992). The B and T responses to orf virus infection of ovine skin. Veterinary Dermatology, 3, 57-64.

Jensen, O. N., Houthaeve, T., Shevchenko, A., Cudmore, S., Ashford, T., Mann, M., Griffiths, G. and Krijnse, L. J. (1996). Identification of the major membrane and core proteins of vaccinia virus by two-dimensional electrophoresis. Journal of Virology, 70, 7485-7497.

Johnson, D. C. and Huber, M. T. (2002). Directed egress of animal viruses promotes cell-to-cell spread. Journal of Virology, 76, 1-8.

Johnson, G. P., Goebel, S. J. and Paoletti, E. (1993). An update on the vaccinia virus genome. Virology, 196, 381- 401.

Joklik, W. K. (1964). The intracellular uncoating of poxvirus DNA. II. The molecular basis of the uncoating process. Journal of Molecular Biology, 8, 277-288.

Jones, D. T., Taylor, W. R. and Thornton, J. M. (1992). The rapid generation of mutation data matrices from protein sequences. Computer Applications in the Biosciences, 8, 275-282.

Kates, J. R. and McAuslan, B. R. (1967a). Messenger RNA synthesis by a "coated" viral genome. Proceeding of the National Academy of Science USA, 57, 314-320.

Kates, J. R. and McAuslan, B. R. (1967b). Poxvirus DNA-dependent RNA polymerase. Proceeding of the National Academy of Science USA, 58, 134-141.

Kates, J. R. and Beeson, J. (1970). Ribonucleic acid synthesis in vaccinia virus. II. Synthesis of polyriboadenylic acid. Journal of Molecular Biology, 50, 19-33.

Keck, J. G., Baldick, C. J. and Moss, B. (1990). Role of DNA replication in vaccinia virus gene expression: a naked template is required for transcription of three late trans-activator genes. Cell, 61, 801-809.

Kenward, R. E. and Holm, J. L. (1989). What future for British red squirrels? Biological Journal of the Linnean Society, 38, 83-89 .

Keymer, I. F. (1976). Report of the pathologist, 1973 and 1974. Journal of Zoology, 178, 456-508.

Keymer, I. F. (1983). Diseases of squirrels in Britain. Mammal Review, 13, 155-158.

Klemperer, N., Lyttle, D. J., Tauzin, D., Traktman, P. and Robinson, A. J. (1995). Identification and characterization of the orf virus type I topoisomerase. Virology, 206, 203-215.

Klemperer, N., McDonald, W., Boyle, K., Unger, B. and Traktman, P. (2001). The A20R protein is a stoichiometric component of the processive form of vaccinia virus DNA polymerase. Journal of Virology, 75, 12298-12307.

Koonin, E. V., Senkevich, T. G. and Chernos, V. I. (1993). Gene A32 product of vaccinia virus may be an ATPase involved in viral DNA packaging as indicated by sequence comparisons with other putative viral ATPases. Virus Genes, 7, 89-94.

Kovacs, G. R. and Moss, B. (1996). The vaccinia virus H5R gene encodes late gene transcription factor 4: purification, cloning, and overexpression . Journal of Virology, 70, 6796-6802.

Lackner, C. A. and Condit, R. C. (2000). Vaccinia virus gene A18R DNA helicase is a transcript release factor. Journal of Biological Chemistry, 275, 1485-1494.

Lateef, Z., Fleming, S., Halliday, G., Faulkner, L., Mercer, A. and Baird, M. (2003). Orf virus-encoded interleukin-10 inhibits maturation, antigen presentation and migration of murine dendritic cells. Journal of General Virology, 84, 1101-1109.

Latner, D. R., Xiang, Y., Lewis, J. I., Condit, J. and Condit, R. C. (2000). The vaccinia virus bifunctional gene J3 (nucleoside-2'-O-)-methyltransferase and poly(A) polymerase stimulatory factor is implicated as a positive transcription elongation factor by two genetic approaches. Virology, 269, 345-355.

Lear, A., Hutchison, G., Reid, H. W., Norval, M. and Haig, D. M. (1996). Phenotypic characterisation of the dendritic cells accumulating in ovine dermis following primary and secondary orf virus infections. European Journal Of Dermatology, 6, 135-140.

Lee, H. J., Essani, K. and Smith, G. L. (2001). The genome sequence of Yaba-like disease virus, a yatapoxvirus. Virology, 281, 170-192.

Li, J., Pennington, M. J. and Broyles, S. S. (1994). Temperature-sensitive mutations in the gene encoding the small subunit of the vaccinia virus early transcription factor impair promoter binding, transcription activation, and packaging of multiple virion components. Journal of Virology, 68, 2605-2614.

Lin, C. L., Chung, C. S., Heine, H. G. and Chang, W. (2000). Vaccinia virus envelope H3L protein binds to cell surface heparan sulfate and is important for intracellular mature virion morphogenesis and virus infection in vitro and in vivo. Journal of Virology, 74, 3353-3365.

Lindahl, T. (1993). Instability and decay of the primary structure of DNA. Nature, 362, 709-715.

Lloyd, H. G. (1983). Pat and present distribution of red and grey squirrels. Mammal Review, 13, 69-80.

Lloyd, J. B., Gill, H. S., Haig, D. M. and Husband, A. J. (2000). In vivo T-cell subset depletion suggests that CD4+ T-cells and a humoral immune response are important for the elimination of orf virus from the skin of sheep. Veterinary Immunology and Immunopathology, 74, 249-262.

Locker, J. K., Kuehn, A., Schleich, S., Rutter, G., Hohenberg, H., Wepf, R. and Griffiths, G. (2000). Entry of the two infectious forms of vaccinia virus at the plasma membane is signaling-dependent for the IMV but not the EEV. Molecular Biology of the Cell, 11, 2497-2511.

Luo, Y., Mao, X., Deng, L., Cong, P. and Shuman, S. (1995). The D1 and D12 subunits are both essential for the transcription termination factor activity of vaccinia virus capping enzyme. Journal of Virology, 69, 3852-3856.

Lurz, P. W. W. and Garson, P. J. (1997). Forest management for red squirrel in conifer woodlands: a northern perspective. In "The conservation of red squirrels, *Sciurus vulgaris* L.". (Gurnell, J. and Lurz, P.). pp145-152. Peoples Trust for Endangered Species, London.

Lurz, P. W. W., Rushton, S., Wauters, L. A., Bertolini, S., Mazzoglio, P. and Shirley, M. D. F. (2001). Predicting grey squirrel expansion in North Italy: a spatially explicit modelling approach. Landscape Ecology, 16, 407-420.

Lurz, P. W., Shirley, M. D., Shirley, M. D. and Rushton, S. P. (2002). Evaluation of immunocontraception as a publicly acceptable form of vertebrate pest species control: the introduced grey squirrel in Britain as an example. Environmental Management, 30, 342-351.

Lyttle, D. J., Fraser, K. M., Fleming, S. B., Mercer, A. A. and Robinson, A. J. (1994). Homologs of vascular endothelial growth factor are encoded by the poxvirus orf virus. Journal of Virology, 68, 84-92.

Mackett, M. and Archard, L. C. (1979). Conservation and variation in Orthopoxvirus genome structure. Journal of General Virology, 45, 683-701.

Marsland, B. J., Tisdall, D. J., Heath, D. D. and Mercer, A. A. (2003). Construction of a recombinant orf virus that expresses an Echinococcus granulosus vaccine antigen from a novel genomic insertion site. Archives of Virology, 148, 555-562.

Martin, K. H., Grosenbach, D. W., Franke, C. A. and Hruby, D. E. (1997). Identification and analysis of three myristylated vaccinia virus late proteins. Journal of Virology, 71, 5218-5226.

Massung, R. F., Liu, L. I., Qi, J., Knight, J. C., Yuran, T. E., Kerlavage, A. R., Parsons, J. M., Venter, J. C. and Esposito, J. J. (1994). Analysis of the complete genome of smallpox variola major virus strain Bangladesh-1975. Virology, 201, 215-240.

Maxam, A. M. and Gilbert, W. (1977). A new method for sequencing DNA. Proceeding of the National Academy of Science USA, 74, 560-564.

Mazur, C., Ferreira, I. I., Rangel Filho, F. B. and Galler, R. (2000). Molecular characterization of Brazilian isolates of orf virus. Veterinary Microbiology, 73, 253-259.

Mazur, C., Rangel Filho, F. B. and Galler, R. (1991). Molecular analysis of contagious pustular dermatitis virus: a simplified method for viral DNA extraction from scab material. Journal of Virological Methods, 35, 265-272.

McDonald, W. F., Crozel-Goudot, V. and Traktman, P. (1992). Transient expression of the vaccinia virus DNA polymerase is an intrinsic feature of the early phase of infection and is unlinked to DNA replication and late gene expression. Journal of Virology, 66, 534-547.

McInnes, C. J., Wood, A. R. and Mercer, A. A. (1998). Orf virus encodes a homolog of the vaccinia virus interferon-resistance gene E3L. Virus Genes, 17, 107-115.

McInnes, C. J., Wood, A. R., Nettleton, P. E. and Gilray, J. A. (2001). Genomic comparison of an avirulent strain of Orf virus with that of a virulent wild type isolate reveals that the Orf virus G2L gene is non-essential for replication. Virus Genes, 22, 141-150.

McIntosh, A. A. and Smith, G. L. (1996). Vaccinia virus glycoprotein A34R is required for infectivity of extracellular enveloped virus. Journal of Virology, 70, 272-281.

McKeever, D. J., Jenkinson, D. M., Hutchison, G. and Reid, H. W. (1988). Studies of the pathogenesis of orf virus infection in sheep. Journal of Comparitive Pathology, 99, 317-328.

McKeever, D. J. and Reid, H. W. (1986). Survival of orf virus under British winter conditions. Veterinary Record, 118, 613-614.

Medzon, E. L. and Bauer, H. (1970). Structural features of vaccinia virus revealed by negative staining, sectioning, and freeze-etching. Virology, 40, 860-867.

Menna, A., Wittek, R., Bachmann, P. A., Mayr, A. and Wyler, R. (1979). Physical characterization of a stomatitis papulosa virus genome: a cleavage map for the restriction endonucleases HindIII and EcoRI. Archives of Virology, 59, 145-156.

Mercer, A. A., Fraser, K., Barns, G. and Robinson, A. J. (1987). The structure and cloning of orf virus-DNA. Virology, 157, 1-12.

Mercer, A. A., Fraser, K. M., Stockwell, P. A. and Robinson, A. J. (1989). A homologue of retroviral pseudoproteases in the parapoxvirus, orf virus. Virology, 172, 665-668.

Mercer, A. A., Yirrell, D. L., Reid, H. W. and Robinson, A. J. (1994). Lack of cross-protection between vaccinia virus and orf virus in hysterectomy-procured, barrier-maintained lambs. Veterinary Microbiology, 41, 373-382.

Mercer, A. A., Lyttle, D. J., Whelan, E. M., Fleming, S. B. and Sullivan, J. T. (1995). The establishment of a genetic map of orf virus reveals a pattern of genomic organization that is highly conserved among divergent poxviruses. Virology, 212, 698-704.

Mercer, A. A., Fraser, K. M. and Esposito, J. J. (1996a). Gene homology between orf virus and smallpox variola virus. Virus Genes, 13, 175-178.

Mercer, A. A., Green, G., Sullivan, J. T., Robinson, A. J. and Drillien, R. (1996b). Location, DNA sequence and transcriptional analysis of the DNA polymerase gene of orf virus. Journal of General Virology, 77 (Pt 7), 1563-1568.

Mercer, A., Fleming, S., Robinson, A., Nettleton, P. and Reid, H. (1997a). Molecular genetic analyses of parapoxviruses pathogenic for humans. Archives of Virology Supplemental, 13, 25-34.

Mercer, A. A., Yirrell, D. L., Whelan, E. M., Nettleton, P. F., Pow, I., Gilray, J. A., Reid, H. W. and Robinson, A. J. (1997b). A novel strategy for determining protective antigens of the parapoxvirus, orf virus. Virology, 229, 193- 200.

Mercer, A. A., Wise, L. M., Scagliarini, A., McInnes, C. J., Buttner, M., Rziha, H. J., McCaughan, C. A., Fleming, S. B., Ueda, N. and Nettleton, P. F. (2002). Vascular endothelial growth factors encoded by Orf virus show surprising sequence variation but have a conserved, functionally relevant structure. Journal of General Virology, 83, 2845-2855.

Meyer, H., Ropp, S. L. and Esposito, J. J. (1995). Poxvirus diagnostic protocols. In "Diagnostic virology protocols". pp199-211. Humana Press Inc., Totowa, New Jersey.

Meyer, M., Clauss, M., Lepple-Wienhues, A., Waltenberger, J., Augustin, H. G., Ziche, M., Lanz, C., Buttner, M., Rziha, H. J. and Dehio, C. (1999). A novel vascular endothelial growth factor encoded by Orf virus, VEGF- E, mediates angiogenesis via signalling through VEGFR-2 (KDR) but not VEGFR-1 (Flt-1) receptor tyrosine kinases. EMBO Journal, 18, 363-374.

Middleton, A. D. (1930). The ecology of the American grey squirrel (*Sciurus carolinensis* Gmelin) in the British Isles. Proceedings of the Zoological Society of London, 2, 809-843.

Mohamed, M. R., Christen, L. A. and Niles, E. G. (2002). Antibodies directed against an epitope in the N-terminal region of the H4L subunit of the vaccinia virus RNA polymerase inhibit both transcription initiation and transcription termination, in vitro. Virology, 299, 142-153.

Mohamed, M. R., Latner, D. R., Condit, R. C. and Niles, E. G. (2001). Interaction between the J3R subunit of vaccinia virus poly(A) polymerase and the H4L subunit of the viral RNA polymerase. Virology, 280, 143-152.

Mohamed, M. R. and Niles, E. G. (2000). Interaction between nucleoside triphosphate phosphohydrolase I and the H4L subunit of the viral RNA polymerase is required for vaccinia virus early gene transcript release. Journal of Biological Chemistry, 275, 25798-25804.

Mohamed, M. R. and Niles, E. G. (2001). The viral RNA polymerase H4L subunit is required for Vaccinia virus early gene transcription termination. Journal of Biological Chemistry, 276, 20758-20765.

Moore, H. D., Jenkins, N. M. and Wong, C. (1997). Immunocontraception in rodents: a review of the development of a sperm-based immunocontraceptive vaccine for the grey squirrel (*Sciurus carolinensis*). Reproduction Fertility and Development., 9, 125-129.

Morgan, C. (1976). Vaccinia virus reexamined: development and release. Virology, 73, 43-58.

Moss, B. (1990). Regulation of vaccinia virus transcription. Annual Review of Biochemistry, 59, 661-688.

Moss, B. (1996a). Genetically engineered poxviruses for recombinant gene expression, vaccination, and safety. Proceeding of the National Academy of Science USA, 93, 11341-11348.

Moss, B. (1996b). *Poxviridae*: The viruses and their replication. In "Fields Virology". (Fields, B. N., Knipe, D. M., and Howley, P. M.). 3rd ed., pp2637-2671. Lippcott-Raven Publishers, Philadelphia.

Moss, B., Shisler, J. L., Xiang, Y. and Senkevich, T. G. (2000). Immune-defence molecules of molluscum contagiosum virus, a human poxvirus. Trends in Microbiology, 8, 473-477.

Munyon, W., Paoletti, E. and Grace, J. T. (1967). RNA polymerase activity in purified infectious vaccinia virus. Proceeding of the National Academy of Science USA, 58, 2280-2287.

Naase, M., Nicholson, B. H., Fraser, K. M., Mercer, A. A. and Robinson, A. J. (1991). An orf virus sequence showing homology to the 14K 'fusion' protein of vaccinia virus. Journal of General Virology, 72, 1177-1181.

Nagington, J. and Horne, R. W. (1962). Morphological studies on orf and vaccinia viruses. Virology, 16, 248-260.

Nagington, J., Plowright, W. and Horne, R. W. (1962). The morphology of bovine papular stomatitis virus. Virology, 17, 361-364.

Nagington, J., Newton, A. A. and Horne, R. W. (1964). The structure of orf virus. Virology, 23, 461-472.

Nettleton, P. F., Brebner, J., Pow, I., Gilray, J. A., Bell, G. D. and Reid, H. W. (1996a). Tissue culture-propagated orf virus vaccine protects lambs from orf virus challenge. Veterinary Record, 138, 184-186.

Nettleton, P. F., Gilray, J. A., Yirrell, D. L., Scott, G. R. and Reid, H. W. (1996b). Natural transmission of orf virus from clinically normal ewes to orf- naive sheep. Veterinary Record, 139, 364-366.

Nicholas, K. B., Nicholson, H. B. and Deerfield, D. W. (1997). GeneDoc: analysis and visualization of genetic variation. EMBNET News, 4, 1-4.

Ochsenbein, A. F. and Zinkernagel, R. M. (2000). Natural antibodies and complement link innate and acquired immunity. Immunology Today, 21, 624-630.

Ogawa, S., Oku, A., Sawano, A., Yamaguchi, S., Yazaki, Y. and Shibuya, M. (1998). A novel type of vascular endothelial growth factor, VEGF-E (NZ-7 VEGF), preferentially utilizes KDR/Flk-1 receptor and carries a potent mitotic activity without heparin-binding domain. Journal of Biological Chemistry, 273, 31273-31282.

Onwuka, S. K., Jenkinson, D. M., Inglis, L., Pow, I., Gray, E. W. and Reid, H. W. (1995). Ultrastructural studies of orf virus infection and replication in fetal lamb fibrocytes. Veterinary Dermatology, 6, 85-92.

Page, R. D. M. (1996). TREEVIEW: An application to display phylogenetic trees on personal computers. Computer Applications in the Biosciences, 12, 357-358.

Panicali, D., Davis, S. W., Mercer, S. R. and Paoletti, E. (1981). Two major DNA variants present in serially propagated stocks of the WR strain of vaccinia virus. Journal of Virology, 37, 1000-1010.

Paoletti, E. (1996). Applications of pox virus vectors to vaccination: an update. Proceeding of the National Academy of Science USA, 93, 11349-11353.

Patel, D. D. and Pickup, D. J. (1989). The second-largest subunit of the poxvirus RNA polymerase is similar to the corresponding subunits of procaryotic and eucaryotic RNA polymerases. Journal of Virology, 63, 1076-1086.

Payne, L. (1978). Polypeptide composition of extracellular enveloped vaccinia virus. Journal of Virology, 27, 28-37.

Payne, L. G. and Norrby, E. (1978). Adsorption and penetration of enveloped and naked vaccinia virus particles. Journal of Virology, 27, 19-27.

Pearson, W. R. and Lipman, D. J. (1988). Improved tools for biological sequence comparison. Proceeding of the National Academy of Science USA, 85, 2444-2448.

Pedley, C. B. and Cooper, R. J. (1987). The assay, purification and properties of vaccinia virus-induced uncoating protein. Journal of General Virology, 68 (Pt 4), 1021 -1028.

Pepper, H. and Paterson, G. (1998). Red squirrel conservation, Practice note. Forestry Commission, Edinburgh.

Porter, C. D. and Archard, L. C. (1992). Characterisation by restriction mapping of three subtypes of molluscum contagiosum virus. Journal of Medical Virology, 38, 1-6.

Pye, D. (1990). Vaccination of sheep with cell culture grown orf virus. Australian Veterinary Journal, 67, 182-186 .

Rackwitz, H. R., Zehetner, G., Frischauf, A. M. and Lehrach, H. (1984). Rapid restriction mapping of DNA cloned in lambda phage vectors. Gene, 30, 195-200.

Rackwitz, H. R., Zehetner, G., Murialdo, H., Delius, H., Chai, J. H., Poustka, A., Frischauf, A. and Lehrach, H. (1985). Analysis of cosmids using linearization by phage lambda terminase. Gene, 40, 259-266.

Rafii, F. and Burger, D. (1985). Comparison of contagious ecthyma virus genomes by restriction endonucleases. Archives of Virology, 84, 283-289.

Regnery, R. L. (1975). Preliminary studies on an unusual poxvirus of the western grey squirrel (*Sciurus griseus griseus*) of North America. Intervirology, 5, 364-366.

Reid, H. W. (1991). Orf. *In* "Diseases of sheep". (Martin, W. B. and Aitkin, I. D.). 2nd ed., pp265-268. Blackwell scientific publications

Risau, W. (1997). Mechanisms of angiogenesis. Nature, 386, 671-674.

Risco, C., Rodriguez, J. R., Demkowicz, W., Heljasvaara, R., Carrascosa, J. L., Esteban, M. and Rodriguez, D. (1999). The vaccinia virus 39-kDa protein forms a stable complex with the p4a/4a major core protein early in morphogenesis. Virology, 265, 375-386.

Rivas, C., Gil, J., Melkova, Z., Esteban, M. and Diaz-Guerra, M. (1998). Vaccinia virus E3L protein is an inhibitor of the interferon (IFN) induced 2-5A synthetase enzyme. Virology, 243, 406-414.

Robinson, A. J. and Balassu, T. C. (1981). Contagious pustular dermatitis (orf). The Veterinary Bulletin, 51, 771-782.

Robinson, A. J., Ellis, G. and Balassu, T. (1982). The genome of orf virus: restriction endonuclease analysis of viral DNA isolated from lesions of orf in sheep. Archives of Virology, 71, 43-55.

Robinson, A. J., Barns, G., Fraser, K., Carpenter, E. and Mercer, A. A. (1987). Conservation and variation in orf virus genomes. Virology, 157, 13-23.

Robinson, A. J. and Mercer, A. A. (1988). Orf virus and vaccinia virus do not cross-protect sheep. Archives of Virology, 101, 255-259.

Robinson, A. J. and Mercer, A. A. (1995). Parapoxvirus of red deer: evidence for its inclusion as a new member in the genus parapoxvirus. Virology, 208, 812-815.

Robinson, A. J. and Kerr, P. (2001). Poxvirus infections. In "Infectious diseases of wild mammals". (Williams, E. S. and Barker, I. K.). 3rd ed., pp179. Manson Publishing and The Veterinary Press, London.

Rochester, S. C. and Traktman, P. (1998). Characterization of the single-stranded DNA binding protein encoded by the vaccinia virus I3 gene. Journal of Virology, 72, 2917-2926.

Rodriguez, D., Esteban, M. and Rodriguez, J. R. (1995). Vaccinia virus A17L gene product is essential for an early step in virion morphogenesis. Journal of Virology, 69, 4640-4648.

Rodriguez, J. F. and Smith, G. L. (1990). IPTG-dependent vaccinia virus: identification of a virus protein enabling virion envelopment by Golgi membrane and egress. Nucleic Acids Research, 18, 5347-5351.

Rodriguez, J. R., Risco, C., Carrascosa, J. L., Esteban, M. and Rodriguez, D. (1998). Vaccinia virus 15-kilodalton (A14L) protein is essential for assembly and attachment of viral crescents to virosomes. Journal of Virology, 72, 1287- 1296.

Roitt, I., Brostoff, J. and Male, D. (1998). Immunology. 5th ed., Mosby International Limited, London.

Roper, R. L., Payne, L. G. and Moss, B. (1996). Extracellular vaccinia virus envelope glycoprotein encoded by the A33R gene. Journal of Virology, 70, 3753-3762.

Roper, R. L., Wolffe, E. J., Weisberg, A. and Moss, B. (1998). The envelope protein encoded by the A33R gene is required for formation of actin-containing microvilli and efficient cell-to-cell spread of vaccinia virus. Journal of Virology, 72, 4192-4204.

Rosales, R., Harris, N., Ahn, B. Y. and Moss, B. (1994a). Purification and identification of a vaccinia virus-encoded intermediate stage promoter-specific transcription factor that has homology to eukaryotic transcription factor SII (TFIIS) and an additional role as a viral RNA polymerase subunit. Journal of Biological Chemistry , 269, 14260-14267.

Rosales, R., Sutter, G. and Moss, B. (1994b). A cellular factor is required for transcription of vaccinia viral intermediate-stage genes. Proceeding of the National Academy of Science USA, 91, 3794-3798.

Rottger, S., Frischknecht, F., Reckmann, I., Smith, G. L. and Way, M. (1999). Interactions between vaccinia virus IEV membrane proteins and their roles in IEV assembly and actin tail formation. Journal of Virology, 73, 2863-2875.

Rushton, S. P., Lurz, P. W. W., Gurnell, J. and Fuller, R. (2000). Modelling the spatial dynamics of a parapoxvirus disease in red and grey squirrels: a possible cause of the decline of the red squirrel in the UK. Journal of Applied Ecology, 37, 997-1012.

Russell, R. J. and Robbins, S. J. (1989). Cloning and molecular characterization of the myxoma virus genome. Virology, 170, 147-159.

Rziha, H., Henkel, M., Cottone, R., Bauer, B., Auge, U., Gotz, F., Pfaff, E., Rottgen, M., Dehio, C. and Buttner, M. (2000). Generation of recombinant parapoxviruses: non-essential genes suitable for insertion and expression of foreign genes. Journal of Biotechnology, 83, 137-145.

Rziha, H. J., Bauer, B., Adam, K. H., Rottgen, M., Cottone, R., Henkel, M., Dehio, C. and Buttner, M. (2003). Relatedness and heterogeneity at the near-terminal end of the genome of a parapoxvirus bovis 1 strain (B177) compared with parapoxvirus ovis (Orf virus). Journal of General Virology, 84, 1111-1116.

Rziha, H. J., Henkel, M., Cottone, R., Meyer, M., Dehio, C. and Buttner, M. (1999). Parapoxviruses: potential alternative vectors for directing the immune response in permissive and non-permissive hosts. Journal of Biotechnology, 73, 235-242.

Saiki, R. K., Gelfand, D. H., Stoffel, S., Scharf, S. J., Higuchi, R., Horn, G. T., Mullis, K. B. and Erlich, H. A. (1988). Primer-directed enzymatic amplification of DNA with a thermostable DNA polymerase. Science, 239, 487-491.

Sainsbury, A. W. and Gurnell, J. (1995). An investigation into the health and welfare of red squirrels, Sciurus vulgaris, involved in reintroduction studies. Veterinary Record, 137, 367-370.

Sainsbury, T. and Ward, L. (1996). Parapoxvirus infection in red squirrels. Veterinary Record, 138, 400

Sainsbury, A. W. and Gurnell, J. (1997). Disease risks associated with the translocation of squirrels, *Sciuridae,* in Europe. Journal of the British Veterinary Zoological Society, 2, 5-8.

Sainsbury, A. W., Nettleton, P. and Gurnell, J. (1997). Recent developments in the study of a parapoxvirus in red and grey squirrels. In "The conservation of red squirrels, *Sciurus vulgaris* L.". (Gurnell, J. and Lurz, P.), pp105-108. Peoples Trust for Endangered Species, London.

Sainsbury, A. W., Nettleton, P., Gilray, J. and Gurnell, J. (2000). Grey squirrels have a high seroprevalence to a parapoxvirus associated with deaths in red squirrels. Animal Conservation, 3, 229-233.

Sambrook, J. (1989). Molecular cloning. (Fritsch, E. F. and Maniatis, T.). 2nd ed., Cold Spring Harbour Laboratory Press, New York.

Sanderson, C. M., Hollinshead, M. and Smith, G. L. (2000). The vaccinia virus A27L protein is needed for the microtubule-dependent transport of intracellular mature virus particles. Journal of General Virology, 81, 47-58.

Sands, J. J., Scott, A. C. and Harkness, J. W. (1984). Isolation in cell culture of a poxvirus from the red squirrel (*Sciurus vulgaris*). Veterinary Record, 114, 117- 118.

Sanger, F., Nicklen, S. and Coulson, A. R. (1977). DNA sequencing with chain-terminating inhibitors. Proceeding of the National Academy of Science USA, 74, 5463-5467.

Sanz, P. and Moss, B. (1998). A new vaccinia virus intermediate transcription factor. Journal of Virology, 72 , 6880-6883.

Sanz, P. and Moss, B. (1999). Identification of a transcription factor, encoded by two vaccinia virus early genes, that regulates the intermediate stage of viral gene expression. Proceeding of the National Academy of Science USA, 96, 2692-2697.

Savory, L. J., Stacker, S. A., Fleming, S. B., Niven, B. E. and Mercer, A. A. (2000). Viral vascular endothelial growth factor plays a critical role in orf virus infection. Journal of Virology, 74, 10699-10706.

Schmidt, H. A., Strimmer, K., Vingron, M. and von Haeseler, A. (2002). TREE-PUZZLE: maximum likelihood phylogenetic analysis using quartets and parallel computing. Bioinformatics., 18, 502-504.

Schnitzlein, W. M., Ghildyal, N. and Tripathy, D. N. (1988). Genomic and antigenic characterization of avipoxviruses. Virus Research, 10, 65-75.

Scott, A. C., Keymer, I. F. and Labram, J. (1981). Parapoxvirus infection of the red squirrel (*Sciurus vulgaris*). Veterinary Record, 109, 202

Sekiguchi, J., Cheng, C. and Shuman, S. (2000). Resolution of a Holliday junction by vaccinia topoisomerase requires a spacer DNA segment 3' of the CCCTT/ cleavage sites. Nucleic Acids Research, 28, 2658-2663.

Sekiguchi, J. and Shuman, S. (1997). Ligation of RNA-containing duplexes by vaccinia DNA ligase. Biochemistry, 36, 9073-9079.

Senkevich, T. G., Bugert, J. J., Sisler, J. R., Koonin, E. V., Darai, G. and Moss, B. (1996). Genome sequence of a human tumorigenic poxvirus: prediction of specific host response-evasion genes. Science, 273, 813-816.

Senkevich, T. G., Koonin, E. V., Bugert, J. J., Darai, G. and Moss, B. (1997). The genome of molluscum contagiosum virus: analysis and comparison with other poxviruses. Virology, 233, 19-42.

Senkevich, T. G. and Moss, B. (1998). Domain structure, intracellular trafficking, and beta2-microglobulin binding of a major histocompatibility complex class I homolog encoded by molluscum contagiosum virus. Virology, 250, 397-407.

Senkevich, T. G., Weisberg, A. S. and Moss, B. (2000). Vaccinia virus E10R protein is associated with the membranes of intracellular mature virions and has a role in morphogenesis. Virology, 278, 244-252.

Shchelkunov, S. N., Totmenin, A. V., Safronov, P. F., Mikheev, M. V., Gutorov, V. V., Ryazankina, O. I., Petrov, N. A., Babkin, I. V., Uvarova, E. A., Sandakhchiev, L. S., Sisler, J. R., Esposito, J. J., Damon, I. K., Jahrling, P. B. and Moss, B. (2002). Analysis of the monkeypox virus genome. Virology, 297, 172-194.

Short, J. M., Fernandez, J. M., Sorge, J. A. and Huse, W. D. (1988). Lambda ZAP: a bacteriophage lambda expression vector with in vivo excision properties. Nucleic Acids Research, 16, 7583-7600.

Shorten, M. (1946). A survey of the distribution of the American grey squirrel (Sciurus carolinenesis) and the British red squirrel (Scirus vulgaris leucourus) in England and Wales in 1944-1945. Journal of Animal Ecology, 15, 82-92.

Shorten, M. (1957). Squirrels in England, Wales and Scotland, 1955. Journal of Animal Ecology, 26, 287-294.

Shorten, M. (1964). Introduced menace: American gray squirrel poses threat to British woodlands. Journal of the American Museum of Natural History, 73, 42-49.

Shpaer, E. G., Robinson, M., Yee, D., Candlin, J. D., Mines, R. and Hunkapiller, T. (1996). Sensitivity and selectivity in protein similarity searches: a comparison of Smith-Waterman in hardware to BLAST and FASTA. Genomics, 38, 179-191.

Shuman, S., Broyles, S. S. and Moss, B. (1987). Purification and characterization of a transcription termination factor from vaccinia virions. Journal of Biological Chemistry, 262, 12372-12380.

Shuman, S. and Moss, B. (1988). Factor-dependent transcription termination by vaccinia virus RNA polymerase. Evidence that the cis-acting termination signal is in nascent RNA. Journal of Biological Chemistry, 263, 6220-6225.

Shuttleworth, C. M. (1997). The effects of supplimental feeding on the diet, population density and reproduction of red squirrels (*Sciurus vulgaris*). In "The conservation of Red squirrels, *Sciurus vulgaris* L.". (Gurnell, J. and Lurz, P.). pp13-24. Peoples Trust for Endangered Species, London.

Simpson, D. A. and Condit, R. C. (1995). Vaccinia virus gene A18R encodes an essential DNA helicase. Journal of Virology, 69, 6131-6139.

Simpson, V. R., Stuart, N. C., Stack, M. J., Ross, H. A. and Head, J. C. (1994). Parapox infection in grey seals (Halichoerus grypus) in Cornwall. Veterinary Record, 134, 292-296.

Skelcher, G. (1997). The ecological replacement of red by grey squirrels. In "The conservation of red squirrels, *Sciurus vulgaris* L.". (Gurnell, J. and Lurz, P.). pp67-78. Peoples Trust for Endangered Species, London.

Smith, G. E. and Summers, M. D. (1980). The bidirectional transfer of DNA and RNA to nitrocellulose or diazobenzyloxymethyl-paper. Analytical Biochemistry, 109, 123 -129.

Smith, G. L., Symons, J. A., Khanna, A., Vanderplasschen, A. and Alcami, A. (1997). Vaccinia virus immune evasion. Immunological Reviews, 159, 137- 154.

Smith, G. L. and Vanderplasschen, A. (1998). Extracellular enveloped vaccinia virus, entry, egress and evasion. Advances in Experimental Medicine and Biology, 440, 395-414.

Smith, G. L., Vanderplasschen, A. and Law, M. (2002). The formation and function of extracellular enveloped vaccinia virus . Journal of General Virology, 83, 2915-2931.

Smith, G. L. and McFadden, G. (2002). Smallpox: anything to declare? National Review of Immunology, 2, 521-527.

Sodeik, B., Doms, R. W., Ericsson, M., Hiller, G., Machamer, C. E., van 't, H. W., van Meer, G., Moss, B. and Griffiths, G. (1993). Assembly of vaccinia virus: role of the intermediate compartment between the endoplasmic reticulum and the Golgi stacks. Journal of Cell Biology, 121, 521-541.

Sodeik, B., Griffiths, G., Ericsson, M., Moss, B. and Doms, R. W. (1994). Assembly of vaccinia virus: effects of rifampin on the intracellular distribution of viral protein p65. Journal of Virology, 68, 1103-1114.

Sodeik, B. and Krijnse-Locker, J. (2002). Assembly of vaccinia virus revisited: de novo membrane synthesis or acquisition from the host? Trends in Microbiology, 10, 15-24.

Sonntag, K. C. and Darai, G. (1996). Evolution of viral DNA-dependent RNA polymerases. Virus Genes, 11, 271-284.

Southern, E. M. (1975). Detection of specific sequences among DNA fragments separated by gel electrophoresis. Journal of Molecular Biology, 98, 503-517.

Stoesser, G., Baker, W., van den, B. A., Camon, E., Garcia-Pastor, M., Kanz, C., Kulikova, T., Leinonen, R., Lin, Q., Lombard, V., Lopez, R., Redaschi, N., Stoehr, P., Tuli, M. A., Tzouvara, K. and Vaughan, R. (2002). The EMBL Nucleotide Sequence Database. Nucleic Acids Research, 30, 21-26.

Sullivan, J. T., Mercer, A. A., Fleming, S. B. and Robinson, A. J. (1994). Identification and characterization of an orf virus homologue of the vaccinia virus gene encoding the major envelope antigen p37K. Virology, 202, 968-973.

Sullivan, J. T., Fleming, S. B., Robinson, A. J. and Mercer, A. A. (1995a). Sequence and transcriptional analysis of a near-terminal region of the orf virus genome. Virus Genes, 11, 21-29.

Sullivan, J. T., Fraser, K. M., Fleming, S. B., Robinson, A. J. and Mercer, A. A. (1995b). Sequence and transcriptional analysis of an orf virus gene encoding ankyrin-like repeat sequences. Virus Genes, 9, 277-282.

Szajner, P., Jaffe, H., Weisberg, A. S. and Moss, B. (2003). Vaccinia virus G7L protein Interacts with the A30L protein and is required for association of viral membranes with dense viroplasm to form immature virions. Journal of Virology, 77, 3418-3429.

Szybalski, W., Erikson, R. L., Gentry, G. A., Gafford, L. G. and Randall, C. C. (1963). Unusual properties of fowlpox virus DNA. Virology, 19, 386- 389.

Takahashi, T., Oie, M. and Ichihashi, Y. (1994). N-terminal amino acid sequences of vaccinia virus structural proteins . Virology, 202, 844-852.

Tangney, D. and Montgomery, W. L. (1995). Distribution and habitat associations of red and grey squirrels in Northern Ireland, In "2nd NPI Red Alert Forum for Red Squirrel Conservation, Forum Proceedings" (Hughes, D. G. and Tew, T.). pp73-76. Ferderation of Zoological Gardens of Great Britain and Ireland, and Joint Nature Conservation Committee,

Taylor, W. R. (1986). The classification of amino acid conservation. Journal of Theoretical Biology, 119, 205-218.

Teangara, D. O., Reilly, S. and Lawton, C. (1999). Red and grey squirrels in Ireland; and overview, In "3rd NPI Red Alert Forum for Red Squirrel Conservation, Forum Proceedings" (Collins, L. M. and Cooper, J. A.). pp79-85. Scottish Natural Heritage, Perth.

Terrell, S. P., Forrester, D. J., Mederer, H. and Regan, T. W. (2002). An epizootic of fibromatosis in gray squirrels (Sciurus carolinensis) in Florida. Journal of Wildlife Diseases, 38, 305-312.

Thomas, V., Flores, L. and Holowczak, J. A. (1980). Biochemical and electron microscopic studies of the replication and composition of milker's node virus. Journal of Virology, 34, 244-255 .

Thompson, J. D., Higgins, D. G. and Gibson, T. J. (1994). CLUSTAL W: improving the sensitivity of progressive multiple sequence alignment through sequence weighting, position-specific gap penalties and weight matrix choice. Nucleic Acids Research, 22, 4673-4680.

Tompkins, D. M., Sainsbury, A. W., Nettleton, P., Buxton, D. and Gurnell, J. (2002). Parapoxvirus causes a deleterious disease in red squirrels associated with UK population declines. Proceeding of the Royal Society of London Biological Sciences, 269, 529- 533.

Tompkins, D. M., White, A. R. and Boots, M. (2003). Ecological replacement of native red squirrels by invasive greys driven by disease. Ecology Letters, 6, 1-8.

Torres, J. M., Sanchez, C., Ramirez, M. A., Morales, M., Barcena, J., Ferrer, J., Espuna, E., Pages-Mante, A. and Sanchez-Vizcaino, J. M. (2001). First field trial of a transmissible recombinant vaccine against myxomatosis and rabbit haemorrhagic disease. Vaccine, 19, 4536-4543.

Traktman, P., Caligiuri, A., Jesty, S. A., Liu, K. and Sankar, U. (1995). Temperature-sensitive mutants with lesions in the vaccinia virus F10 kinase undergo arrest at the earliest stage of virion morphogenesis. Journal of Virology, 69, 6581-6587.

Tryland, M., Josefsen, T. D., Oksanen, A. and Aschfalk, A. (2001). Parapoxvirus infection in Norwegian semi-domesticated reindeer (Rangifer tarandus tarandus). Veterinary Record, 149, 394-395.

Tulman, E. R., Afonso, C. L., Lu, Z., Zsak, L., Kutish, G. F. and Rock, D. L. (2001). Genome of lumpy skin disease virus. Journal of Virology, 75, 7122-7130.

Twardzik, D. R., Brown, J. P., Ranchalis, J. E., Todaro, G. J. and Moss, B. (1985). Vaccinia virus-infected cells release a novel polypeptide functionally related to transforming and epidermal growth factors. Proceeding of the National Academy of Science USA, 82, 5300-5304.

Ueda, N., Wise, L. M., Stacker, S. A., Fleming, S. B. and Mercer, A. A. (2003). Pseudocowpox virus encodes a homolog of vascular endothelial growth factor. Virology, 305, 298-309.

Upton, C., DeLange, A. M. and McFadden, G. (1987). Tumorigenic poxviruses: genomic organization and DNA sequence of the telomeric region of the Shope fibroma virus genome. Virology, 160, 20-30.

van den Broek, M. F., Muller, U., Huang, S., Zinkernagel, R. M. and Aguet, M. (1995). Immune defence in mice lacking type I and/or type II interferon receptors. Immunological Reviews, 148, 5-18.

van Eijl, H., Hollinshead, M., Rodger, G., Zhang, W. H. and Smith, G. L. (2002). The vaccinia virus F12L protein is associated with intracellular enveloped virus particles and is required for their egress to the cell surface. Journal of General Virology, 83, 195-207.

van Eijl, H., Hollinshead, M. and Smith, G. L. (2000). The vaccinia virus A36R protein is a type Ib membrane protein present on intracellular but not extracellular enveloped virus particles. Virology, 271, 26-36.

van Regenmortel, M. H. V., Fauquet, C. M., Bishop, D. H. L., Carstens, E. B., Estes, M. K., Lemon, S. M., Maniloff, J., Mayo, M. A., McGeoch, D. J., Pringle, C. R. and Wickner, R. B. (2000). Family *Poxviridae*. In "Virus Taxonomy. Seventh Report of the International Committee on Taxonomy of Viruses.". (van Regenmortel, M. H. V., Fauquet, C. M., Bishop, D. H. L., Carstens, E. B., Estes, M. K., Lemon, S. M., Maniloff, J., Mayo, M. A., McGeoch, D. J., Pringle, C. R., and Wickner, R. B.). pp137- 157. Academic Press, California.

Vanderplasschen, A., Hollinshead, M. and Smith, G. L. (1997). Antibodies against vaccinia virus do not neutralize extracellular enveloped virus but prevent virus release from infected cells and comet formation. Journal of General Virology, 78, 2041-2048.

Vanderplasschen, A., Hollinshead, M. and Smith, G. L. (1998). Intracellular and extracellular vaccinia virions enter cells by different mechanisms. Journal of General Virology, 79, 877-887.

Vanderplasschen, A. and Smith, G. L. (1997). A novel virus binding assay using confocal microscopy: demonstration that the intracellular and extracellular vaccinia virions bind to different cellular receptors. Journal of Virology, 71, 4032-4041.

Vazquez, M. I. and Esteban, M. (1999). Identification of functional domains in the 14-kilodalton envelope protein (A27L) of vaccinia virus. Journal of Virology, 73, 9098-9109.

Venning, T., Sainsbury, A. W. and Gurnell, J. (1997). Red squirrel translocation and population reinforcement as a conservation tactic. In "The conservation of red squirrels, *Sciurus vulgaris* L.". (Gurnell, J. and Lurz, P.). pp133-143. Peoples Trust for Endangered Species, London.

Vizoso, A. D., Vizoso, M. R. and Hay, R. (1964). Isolation of a virus resembling encephalomyocarditis from a red squirrel. Nature, 201, 849-850.

Vizoso, A. D. (1968). A red squirrel disease. Symposium of the Zoological Society of London, 24, 29-38.

Vos, J. C., Sasker, M. and Stunnenberg, H. G. (1991). Vaccinia virus capping enzyme is a transcription initiation factor. EMBO Journal, 10, 2553-2558.

Vos, J. C., Mercer, A. A., Fleming, S. B. and Robinson, A. J. (1992). In vitro recognition of an orf virus early promoter in a vaccinia virus extract. Archives of Virology, 123, 223- 228.

Wallengren, K., Risco, C., Krijnse-Locker, J., Esteban, M. and Rodriguez, D. (2001). The A17L gene product of vaccinia virus is exposed on the surface of IMV. Virology, 290, 143-152.

Ward, B. M. and Moss, B. (2000). Golgi network targeting and plasma membrane internalization signals in vaccinia virus B5R envelope protein. Journal of Virology, 74, 3771-3780.

Warns, E. (1995). Characterisation of squirrel sera and a red squirrel parapoxvirus isolate. MSc thesis, University of London.

Warren, R. (1999). Supplementary feeding workshop, In "3rd NPI Red Alert Forum for Red Squirrel Conservation, Forum Proceedings" (Collins, L. M. and Cooper, J. A.). pp112-116. Scottish Natural Heritage, Perth.

Watson, J. C., Chang, H. W. and Jacobs, B. L. (1991). Characterization of a vaccinia virus-encoded double-stranded RNA-binding protein that may be involved in inhibition of the double-stranded RNA-dependent protein kinase. Virology, 185, 206-216.

Wauters, L. A. (1997). Replacement of red squirrels by introduced grey squirrels in Italy: evidence from a distribution survey. In "The conservation of red squirrels, *Sciurus vulgaris* L.". (Gurnell, J. and Lurz, P.). Peoples Trust for Endangered Species, London.

Weir, J. P. and Moss, B. (1984). Regulation of expression and nucleotide sequence of a late vaccinia virus gene. Journal of Virology, 51, 662-669.

WHO. (1980). The global erradication of smallpox. Final report of the global commission for the certification of smallpox erradication, In "History of Inetrnational Public Health". World Health Organisation, Geneva.

Wilcock, D. and Smith, G. L. (1996). Vaccinia virions lacking core protein VP8 are deficient in early transcription. Journal of Virology, 70, 934-943.

Willer, D. O., McFadden, G. and Evans, D. H. (1999). The complete genome sequence of shope (rabbit) fibroma virus. Virology, 264, 319-343.

Willer, D. O., Yao, X. D., Mann, M. J. and Evans, D. H. (2000). In vitro concatemer formation catalyzed by vaccinia virus DNA polymerase. Virology, 278, 562-569.

Wilson, T. M. and Sweeney, P. R. (1970). Morphological studies of seal poxvirus. Journal of Wildlife Diseases, 6, 94-97.

Wise, L. M., Veikkola, T., Mercer, A. A., Savory, L. J., Fleming, S. B., Caesar, C., Vitali, A., Makinen, T., Alitalo, K. and Stacker, S. A. (1999). Vascular endothelial growth factor (VEGF)-like protein from orf virus NZ2 binds to VEGFR2 and neuropilin-1. Proceeding of the National Academy of Science USA, 96, 3071-3076.

Wittek, R., Menna, A., Schumperli, D., Stoffel, S., Muller, H. K. and Wyler, R. (1977). *Hind*III and *Sst*I restiction sites mapped on rabbit poxvirus and vaccinia virus DNA. Journal Of Virology, 23, 669-678.

Wittek, R., Menna, A., Muller, H. K., Schumperli, D., Bosley, P. G. and Wyler, R. (1978a). Inverted terminal repeats in rabbit poxvirus and vaccinia virus DNA. Journal Of Virology, 28, 171-181.

Wittek, R., Muller, H. K. and Wyler, R. (1978b). Length heterogeneity in the DNA of vaccinia virus is eliminated on cloning the virus. FEBS Lett., 90, 41-46.

Wittek, R., Kuenzle, C. C. and Wyler, R. (1979). High C + G content in parapoxvirus DNA. Journal of General Virology, 43, 231-234.

Wittek, R., Herlyn, M., Schumperli, D., Bachmann, P. A., Mayr, A. and Wyler, R. (1980). Genetic and antigenic heterogeneity of different Parapoxvirus strains. Intervirology, 13, 33-41.

Wolffe, E. J., Isaacs, S. N. and Moss, B. (1993). Deletion of the vaccinia virus B5R-gene encoding a 42-kilodalton membrane glycoprotein inhibits extracellular virus envelope formation and dissemination. Journal of Virology, 67, 4732-4741.

Wolffe, E. J., Katz, E., Weisberg, A. and Moss, B. (1997). The A34R glycoprotein gene is required for induction of specialized actin-containing microvilli and efficient cell-to-cell transmission of vaccinia virus. Journal of Virology, 71, 3904-3915.

Wolffe, E. J., Weisberg, A. S. and Moss, B. (1998). Role for the vaccinia virus A36R outer envelope protein in the formation of virus-tipped actin-containing microvilli and cell-to-cell virus spread. Virology, 244, 20-26.

Wright, C. F. and Coroneos, A. M. (1995). The H4 subunit of vaccinia virus RNA polymerase is not required for transcription initiation at a viral late promoter. Journal of Virology, 69, 2602-2604.

Wright, C. F., Hubbs, A. E., Gunasinghe, S. K. and Oswald, B. W. (1998). A vaccinia virus late transcription factor copurifies with a factor that binds to a viral late promoter and is complemented by extracts from uninfected HeLa cells. Journal of Virology, 72, 1446-1451.

Xiang, Y., Simpson, D. A., Spiegel, J., Zhou, A., Silverman, R. H. and Condit, R. C. (1998). The vaccinia virus A18R DNA helicase is a postreplicative negative transcription elongation factor. Journal of Virology, 72, 7012-7023.

Yeh, W. W., Moss, B. and Wolffe, E. J. (2000). The vaccinia virus A9L gene encodes a membrane protein required for an early step in virion morphogenesis. Journal of Virology, 74, 9701-9711.

Yirrell, D. L., Reid, H. W., Norval, M. and Howie, S. E. (1989). Immune response of lambs to experimental infection with Orf virus. Veterinary Immunology and Immunopathology, 22, 321-332.

Yirrell, D. L., Reid, H. W., Norval, M. and Miller, H. R. P. (1991a). Qualitative and quantitative changes in ovine afferent lymph draining the site of epidermal orf virus infection. Veterinary Dermatology, 2 , 133-141.

Yirrell, D. L., Reid, H. W., Norval, M., Entrican, G. and Miller, H. R. (1991b). Response of efferent lymph and popliteal lymph node to epidermal infection of sheep with orf virus. Veterinary Immunology and Immunopathology, 28, 219-235.

Yirrell, D. L., Vestey, J. P. and Norval, M. (1994). Immune responses of patients to orf virus infection. British Journal of Dermatology., 130, 438-443.

Yuen, L. and Moss, B. (1987). Oligonucleotide sequence signalling transcriptional termination of vaccinia virus early genes. Proceeding of the National Academy of Science USA, 84, 6417-6421.

APPENDIX 1.0

RESTRICTION ENDONUCLEASE MAPPING DATA

Not I DIG-Labelled Probes	*Bam* HI Clones and Fragments																										
		B1A-1	B2-1	B3-1	B5-2	B6A-1	B7D-1	B7C-1	B8-1	B11-1	B12-1	B13-1	B16C-1	B19-1	B20B-1	B20A-1	B24-1	B25-1	B26-1	B30-2	B51-2	B70-2	B98-2	B164-2
	N1-1	-	-	-		-	-	-	-	-	-	-	-	-	-	-				-	-	-	-	
	N2-1	-	-	-	-	-	-	-	-	-	-	-	-	-	-	-				-	-	-	-	-
	N3-1	-	-	-	-	-	-	-	-	-	-	-	-	-	-	-	-	-	-	-	-	-	+	+
	N4-1	-	-	-		-	-	-	+	-	-	-	-	-	-	-								
	N5-2								+															
	N5-1	-	-	-	-	-	+	-	-	-	-	-	-	-	-	-					+	-		
	N6-1	-	-	-		-	-	-	-	-	-	-	-	-	-	-								
	N7-1	-	-	-		+	-	-	-	-	-	-	-	+	-	-								
	N9B-1	-	-	-		-	-	-	-	-	-	+	-	-	-	-		+						
	N9A-1	-	-	-		-	-	-	-	-	-	+	+	-	-	-								
	N10B-1																							
	N11A-1	-	-	-		-	-	-	-	-	-	-	-	-	-	+	+	+						
	N11H-1	-	-	-	+	-	-	+	-	-	-	-	-	-	-	-				-		-		
	N12-1	-	-	-	-	-	-	-	-	-	-	-	+	-	-	-								
	N13-1	-	-	-	-	-	-	-	-	+	-	-	-	-	-	-								
	N14D-1																							
	N14A-1																							
	N14C-1																							
	N15D-1	+	-	+		-	-	-	-	-	-	-	-	-	-	-								
	N15H-1																							
	N15A-1	-	-	+		-	-	-	-	-	-	-	-	-	-	-								
	N16-1	-	-	-		-	+	-	-	-	-	-	-	-	-	-								
	N22A-1	-	-	+	-	-	-	-	-	-	-	-	-	-	-	-				-	-	-	-	+
	N22B-1																			-	-	-		
	N24-1	-	-	-		-	+	-	-	-	-	-	-	-	-	-								
	N26A-1	-	-	-		+	-	-	+	-	-	-	-	-	-	-			+					
	N30-1														-	-	-	+						
	N31-1																							
	N33-1																							
	N34-1																							
	N42-2	-	-	-		-	-	-	-	-	-	-	-	-	+	+							+	
	N55-2	-	+	-	+	-	-	+	-	-	-	-	-	-	-	-	-	-	-	-	-	+	-	-
	N65-2	-	-	-	+	-	-	+	-	-	+	-	-	-	-	-	-	-	-	+	-	-	-	-
	N74-1																							

Table A1.1 Summary of hybridisation results produced by dot-blot, Southern blot and colony screening of the *Bam* HI clones and fragments with *Not* I DIG-labelled fragments. Positive and negative signals are depicted with the symbols: + and – respectively. Blank cells indicate that the *Not* I DIG-labelled fragments were not used to screen the *Bam* HI clones.

Not I DIG-Labelled Probes	*Kpn* I Clones and Fragments																
		K1-1	K1-TC	K4-1	K11-1	K11-2	K13-1	K18-1	K19-1	K21-1	K24-1	K31-1	K32-1	K43-1	K45-1	K46-1	K47-1
	N1-1	-	-	+	-		-	-	-	-	-	-	-	-	-	-	-
	N2-1	-	-	-	-	-	-	-	+	-	-	-	-	-	-	-	-
	N3-1	-	+	-	-	-	-	-	-	-	-	-	-	-	-	-	-
	N4-1	+	-	-	-		-	-	-	-	-	-	-	-	-	-	-
	N5-2	+	-	+	-		-	-	-	-	-	-	-	-	-	-	-
	N5-1	-	-	-	-	-	+	-	-	+	-	-	-	-	-	-	-
	N6-1	-	-	+	-		-	-	-	-	-	-	+	-	-	-	-
	N7-1																
	N9B-1	-	-	-	-		-	-	-	-	-	-	-	-	+	-	-
	N9A-1	-	-	-	-		-	-	-	-	-	-	-	-	+	-	-
	N10B-1																
	N11A-1														+		
	N11H-1					-											
	N12-1																
	N13-1																
	N14D-1																
	N14A-1																
	N14C-1																
	N15D-1	-	-	-	-	-	-	-	-	-	-	-	-	-	-	-	+
	N15H-1	-	-	-	-		-	-	-	-	-	-	-	-	-	-	-
	N15A-1	-	-	-	-		-	-	-	-	-	-	-	-	-	-	+
	N16-1	-	-	-	-		+	-	-	-	-	-	-	-	-	-	-
	N22A-1	-	-	-	-	+	-	-	-	-	-	-	-	-	-	-	-
	N22B-1																
	N10A-1						+							+			
	N26A-1	-	-	-	-		-	-	-	-	-	-	-	-	-	-	-
	N30-1		-												+		
	N31-1																
	N33-1																
	N34-1																
	N42-2	-	+	-	-		-	-	-	-	-	-	-	-	+	-	-
	N55-2	-	-	-	-	-	-	-	-	-	-	-	-	-	-	-	-
	N65-2	-	-	-	-	-	-	-	-	-	-	-	-	-	-	-	-
	N74-1																

Table A1.2 Summary of hybridisation results produced by dot-blot, Southern blot and colony screening of the *Kpn* I clones and fragments and fragments with *Not* I DIG-labelled fragments.

	***Kpn* I Clones and Fragment**																
***Bam* HI DIG-Labelled Probes**		K1-1	K1-TC	K4-1	K11-1	K11-2	K13-1	K18-1	K19-1	K21-1	K24-1	K31-1	K32-1	K43-1	K45-1	K46-1	K47-1
	B1A-1	-	-	-	-	-	-	-	-	-	-	-	-	-	-	-	+
	B2-1	-	-	-	-		-	-	-	-	-	-	-	-	-	-	-
	B3-1	-	-	-	-	+	-	-	-	-	-	-	-	-	-	-	+
	B5-2					-											
	B6A-1	-	-	-	+		-	+	-	-	+	-	-	-	-	-	-
	B7D-1	-	-	-	-		+	-	-	+	-	-	-	+	-	+	-
	B7C-1	-	-	-	-	-	-	-	-	-	-	-	-	-	-	-	-
	B8-1	+	-	-	-		-	-	-	-	-	-	-	-	-	-	-
	B11-1	-	-	-	-		-	-	-	-	-	-	-	-	-	+	-
	B12-1																
	B13-1	-	-	-	-		-	-	-	-	-	-	-	-	+	-	-
	B16C-1	-	-	-	-		-	-	-	-	-	-	-	-	-	-	-
	B19-1	-	-	-	-		-	+	+	-	-	+	-	-	-	-	-
	B20B-1	-	+	-	-	-	-	-	-	-	-	-	-	-	+	-	-
	B20A-1		-												+		
	B24-1		-												+		
	B25-1														+		
	B26-1																
	B30-2																
	B51-2	-	-	-	-	-	-	-	-	+	-	-	-	-	-	-	-
	B70-2																
	B98-2		+														
	B164-2																

Table A1.3 Summary of hybridisation results produced by dot-blot, Southern blot and colony screening of the *Kpn* I clones and fragments with *Bam* HI DIG-labelled fragments

Bam HI DIG-Labelled Probes	***Not* I Clones and Fragments**																																							
	N1-1	N2-1	N3-1	N4-1	N5-2	N5-1	N6-1	N7-1	N9B-1	N9A-1	N10B-1	N11A-1	N11H-1	N12-1	N13-1	N14D-1	N14A-1	N14C-1	N15D-1	N15H-1	N15A-1	N16-1	N22A-1	N22B-1	N24-1	N26A-1	N30-1	N31-1	N33-1	N34-1	N42-2	N55-2	N65-2	N74-2
B1A-1	-	-	-	-	-	-	-	-	-	-	-	-	-	-	-	-	-	-	+	-	-	-	-	-	-	-					-	-	-	-
B2-1	-	-	-	-		-	-	-	-	-	-	-	-	-	-	-	-	-	-	-	-	-	-	-	-	-						+	-	
B3-1	-	-	-	-		-	-	-	-	-	-	-	-	-	-	-	-	-	+	-	+	-	+	-	-	-								
B5-2													+																		-	+	+	-
B6A-1	-	-	-	-		-	-	+	-	-	-	-	-	-	-	-	-	-	-	-	-	-	-	-	-	+								
B7D-1	-	-	-	-		+	-	-	-	-	+	-	-	-	-	-	-	-	-	-	-	+	-	-	+	-								
B7C-1	-	-	-	-	-	-	-	-	-	-	-	-	+	-	-	-	-	-	-	-	-	-	-	-	-	-					-	+	+	-
B8-1	-	-	-	+	+	-	-	-	-	-	-	-	-	-	-	-	-	-	-	+	-	-	-	-	-	+				+				
B11-1	-	-	-	-		-	-	-	-	-	+	-	-	-	+	-	-	-	-	-	-	-	-	-	-	-								
B12-1																																		
B13-1	-	-	-	-		-	-	-	+	+	-	-	-	-	-	-	-	-	-	-	-	-	-	-	-	-								
B16C-1	-	-	-	-		-	-	-	-	+	-	-	-	+	-	-	-	-	-	-	-	-	-	-	-	-								
B19-1	-	-	-	-		-	-	+	-	-	-	-	-	-	-	+	+	+	-	-	-	-	-	-	-	-								
B20B-1	-	-	-	-	-	-	-	-	-	-	-	-	-	-	-	-	-	-	-	-	-	-	-	-	-	-	-	-			+			
B20A-1												+	-														-	+			+			
B24-1												+	-														-	-			-			
B25-1									+			+															+							
B26-1																																		
B30-2																																		
B51-2	-	-	-	-	-	+	-	-	-	-	-	-	-	-	-	-	-	-	-	-	-	-	-	-	-	-					-	-	-	-
B70-2			+										-																			+		
B98-2			+																												+			
B164-2																																		

Table A1.4 Summary of hybridisation results produced by dot-blot, Southern blot and colony screening of the *Not* I clones and fragments with *Bam* HI DIG-labelled fragments.

Kpn I DIG-Labelled Probes	***Not* I Clones and Fragments**																																								
	N1-1	N2-1	N3-1	N4-1	N5-2	N5-1	N6-1	N7-1	N9B-1	N9A-1	N10B-1	N11A-1	N11H-1	N12-1	N13-1	N14D-1	N14A-1	N14C-1	N15D-1	N15H-1	N15A-1	N16-1	N22A-1	N22B-1	N24-1	N26A-1	N30-1	N31-1	N33-1	N34-1	N42-2	N55-2	N65-2	N74-2
K1-1	-	-	-	+	+	-	-	-	-	-	-	-	-	-	-	-	-	-	-	-	-	-	-	-	-	-					-	-	-	-
K1-TC	-	-	+	-		-	-	-	-	-	-	-	-	-	-	-	-	-	-	-	-	-	-	-	-	-								
K4-1	+	-	-	-		-	+	-	-	-	-	-	-	-	-	-	-	-	-	-	-	-	-	-	-	-								
K11-1																																		
K11-2																																		
K13-1	-	-	-	-		+	-	-	-	-	-	-	-	-	-	-	-	-	-	-	-	+	-	-	+	-								
K18-1	-	-	-	-		-	-	+	-	-	-	-	-	-	-	+	+	-	-	-	-	-	-	-	-	-								
K19-1	-	+	-	-		-	-	-	-	-	-	-	-	-	-	-	-	-	-	-	-	-	-	-	-	-								
K21-1	-	-	-	-		+	-	-	-	-	-	-	-	-	-	-	-	-	-	-	-	-	-	-	-	-								
K24-1								+																		-								
K31-1		-						-								+	-	+																
K32-1	-	-	-	-		-	+	-	-	-	-	-	-	-	-	-	-	-	-	-	-	-	-	-	-	-					-	-	-	-
K43-1	-	-	-	-		-	-	-	-	-	+	-	-	-	-	-	-	-	-	-	-	-	-	-	+	-								
K45-1	-	-	-	-	-	-	-	-	+	+	-	+	-	-	-	-	-	-	-	-	-	-	-	-	-	-								
K46-1	-	-	-	-		-	-	-	-	-	+	-	-	-	+	-	-	-	-	-	-	-	-	-	-	-								
K47-1	-	-	-	-		-	-	-	-	-	-	-	-	-	-	-	-	-	+	-	+	-	-	-	-	-								

Table A1.5 Summary of hybridisation results produced by dot-blot, Southern blot and colony screening of the *Not* I clones and fragments with *Kpn* I DIG-labelled clones.

Kpn I DIG-Labelled Probes	*Bam* HI Clones and Fragments																								
		B1A-1	B2-1	B3-1	B5-2	B6A-1	B7D-1	B7C-1	B8-1	B11-1	B12-1	B13-1	B16C-1	B19-1	B20B-1	B20A-1	B24-1	B25-1	B26-1	B30-2	B51-2	B70-2	B98-1	B164-2
	K1-1	-	-	-	-	-	-	-	+	-	-	-	-	-	-	-				-	-	-		
	K1-TC	-	-	-		-	-	-	-	-	-	-	-	-	+	-				-	-	-	+	-
	K4-1	-	-	-		-	-	-	-	-	-	-	-	-	-	-							-	-
	K11-1																							
	K11-2																							
	K13-1																							
	K18-1	-	-	-		+	-	-	-	-	-	-	-	+	-	-								
	K19-1	-	-	-	-	-	-	-	-	-	-	-	-	+	-	-				-	-	-		
	K21-1	-	-	-		-	+	-	-	-	-	-	-	-	-	-								
	K24-1					+			-															
	K31-1													+										
	K32-1	-	-	-	-	-	-	-	-	-	-	-	-	-	-	-				-	-	-	-	-
	K43-1																							
	K45-1	-	-	-		-	-	-	-	-	-	+	-	-	+	+								
	K46-1	-	-	-		-	+	-	-	+	-	-	-	-	-	-								
	K47-1	+	-	+		-	-	-	-	-	-	-	-	-	-	-								

Table A1.6 Summary of hybridisation results produced by dot-blot, Southern blot and colony screening of the *Bam* HI clones and fragments with *Kpn* I DIG-labelled fragments.

Kpn I Clones	*Bam* HI Fragment Sizes (kb)	*Not* I Fragments Sizes (kb)
pK45-1	11.5, 5.3*, 2.45, 0.65, 0.55	10.1, 3.6*, 2.7, 2.3, 1.55, 0.3
pK46-1	4.9*, 4.6	5.2*, 3.5, 0.8
pK18-1	6.4, 3.5*	8.0*, 1.3, 0.7
pK31-1	9.85*	6.1*, 2.85, 0.85
pK21-1	6.7*, 2.1	8.8*
pK47-1	6.2*, 2.05	4.6*, 2.5, 1.05
pK1-TC	3.95*, 3.65	6.6*, 0.75, 0.45
pK13-1	7.8*	4.4, 3.1*, 0.4
pK43-1	7.75*	4.9*, 2.95
pK32-1	6.85*	3.2*, 1.45, 1.1, 0.65, 0.45
pK1-1	3.8*, 2.4	4.75*, 1.5
pK4-1	2.97*, 2.7, 0.17	3.5*, 2.15, 0.25
pK11-2	3.2*, 1.85	5.0*
pK19-1	3.6*,1.3	3.9*, 0.9
pK11-1	4.6*	4.6*
pK24-1	3.5*	2.9*, 0.6

Table A1.7 Summary of the fragment sizes produced when *Kpn* I clones were digested singularly with *Bam* HI or *Not* I restriction endonucleases. Fragments with the * suffix denote those that include the 2.96kb pBluescript SK⁻ vector.

Bam HI Clones	*Kpn* I Fragment Sizes (kb)	*Not* I Fragments Sizes (kb)
pB7D-1	6.7*, 4.9, 4.8, 2.0, 0.25	8.0*, 4.4, 4.05, 2.35
pB19-1	9.3*, 6.8, 0.65	6.6*, 4.6, 3.3, 1.3, 0.9
pB3-1	8.4, 4.7*, 3.1	7.4, 3.4*, 3.2, 1.24, 1.05
pB25-1	14.3*	11.5*, 2.3, 0.65
pB8-1	7.6, 5.3*	5.3, 4.0*, 1.35, 1.05, 0.85, 0.25, 0.14
pB11-1	7.6*, 1.75	8.0*, 0.8, 0.4
pB5-2	4.7*, 3.0	3.5*, 2.45, 1.2, 0.45
pB98-1	6.6*, 0.9	4.5*, 2.65, 0.45
pB51-2	4.15*, 2.45, 2.1	5.5, 3.25
pB16C-1	6.3*, 1.4	3.75, 3.8*, 0.17, <0.075
pB164-2	2.95, 3.15*, 0.9	4.2*, 2.65, 0.32
pB6A-1	4.1*, 1.6, 0.6, 0.55	5.6*, 0.65, 0.65
pB26-1	6.0*	6.0*
pB13-1	5.3*, 0.85	4.4*, 1.65
pB1A-1	3.25*, 2.05, 0.7	5.55*, 0.5
pB20A-1	5.5*	3.25*, 2.05, 0.3
pB20B-1	3.5*, 1.45, 1.0	5.85*
pB7C-1	5.55*	3.4*, 1.2, 0.55, 0.45
pB30-2	5.5*	5.5*
pB12-1	4.1*	4.1*
pB70-2	4.15*	3.1*, 1.1
pB2-1	3.76*	3.75*
pB24-1	3.55*	3.55*

Table A1.8 Summary of the fragment sizes produced when *Bam* HI clones were digested singularly with *Kpn* I or *Not* I restriction endonucleases. Fragments with the * suffix denote those that include the 2.96kb pBluescript SK$^-$ vector.

Not I Clones	*Kpn* I Fragment Sizes (kb)	*Bam* HI Fragments Sizes (kb)
N9B-1	12.8*	11.5*, 1.65
N7-1	8.0*, 1.6, 0.55	7.6*, 2.65
N5-1	5.9, 3.1*, 0.5	7.0*, 2.55
N42-2	6.5*, 2.65, 1.45	5.6*, 2.95, 2.05
N22A-1	4.3*, 2.05, 1.4, 0.9	5.5*, 3.2
N13-1	3.5, 4.7*	5.1, 3.0*
N26A-1	7.8*	4.0*, 3.0, 0.65
N10B-1	5.7*, 2.45, 0.25	8.0*, 0.4
N4-1	6.8*, 1.5	8.25*
N65-2	7.1*	3.4*, 2.6, 1.1, 0.1
N16-1	7.3*	7.3*
N12-1	3.55*, 3.25	6.7*,
N14D-1	5.6*, 0.7	5.9*
N15D-1	3.5*, 2.6	5.5*, 0.47
N3-1	5.0*, 0.75	4.2*, 1.5
N24-1	3.25*, 2.1	5.25*
N55-2	5.4*	3.5*, 1.05, 0.8
N9A-1	4.4*, 0.8	3.75*, 1.5
N5-2	3.6*, 1.8	3.35*, 0.95, 0.85, 0.17
N30-1	5.3*	5.3*
N1-1	5.1*	5.1*
N6-1	3.1*, 1.45, <0.075	4.45*
N11A-1	4.5*	3.25*, 0.65, 0.65
N15H-1	4.3*	4.3*
N14A-1	4.2*	4.3*
N2-1	3.3*, 0.85	4.15*
N11H	4.2*	4.2*
N15A-1	4.1*	4.1*
N74-1	4.0*	4.0*
N34-1	4.0*	4.0*
N14C-1	3.8*	3.8*
N33-1	3.8*	3.8*
N22B-1	3.3*	3.3*
N31-1	3.2*	3.2*

Table A1.9 Summary of the fragment sizes produced when *Not* I clones were digested singularly with *Kpn* I or *Bam* HI restriction endonucleases. Fragments with the * suffix denote those that incorporate the 2.96kb pBluescript SK⁻ vector.

APPENDIX 2.0

PUBLICATIONS ARISING FROM THIS THESIS

paper no. vir19464 charlesworth ref: vir29161 »

dnavi

rnal of General Virology (2003), 84, 000–000 DOI 10.1099/vir.0.19464-0

Short Communication

A novel poxvirus lethal to red squirrels (*Sciurus vulgaris*)

Kathryn Thomas,[1] Daniel M. Tompkins,[2]† Anthony W. Sainsbury,[3] Ann R. Wood,[1] Robert Dalziel,[4] Peter F. Nettleton[1] and Colin J. McInnes[1]

[1]Moredun Research Institute, Pentlands Science Park, Bush Loan, Penicuik EH26 0PZ, UK

[2]University of Stirling, UK

[3]Institute of Zoology, London, UK

[4]University of Edinburgh, UK

orrespondence
olin McInnes
cinc@mri.sari.ac.uk

A parapoxvirus has been implicated in the decline of the red squirrel in the United Kingdom. Virus was isolated from an outbreak of lethal disease in red squirrels in the north-east of England. Experimental infection of captive-bred red squirrels confirmed that this virus was the cause of the severe skin lesions observed. Electron microscopic examination of the virus showed that it had a morphology typical of parapoxviruses whilst preliminary sequence data suggested a genomic G+C composition of approximately 66 %, again similar to that found in other parapoxviruses. However Southern hybridization analysis failed to detect three known parapoxvirus genes, two of which have been found so far only in the genus *Parapoxvirus*. Comparative sequence analysis of two other genes, conserved across the eight recognized chordopoxvirus genera, suggests that the squirrel virus represents a previously unrecognized genus of the *Chordoxviridae*. Chordopoxviridae

ceived 26 June 2003
cepted 1 September 2003

prognosis for the survival of the red squirrel (*Sciurus aris*) in the United Kingdom is poor. Numbers have in decline for the last 150 years (Lloyd, 1983; Gurnell epper, 1993), with extinction in mainland England ible within the next 20 years (Kenward & Holm, 1989; ıell & Pepper, 1993). Competition between red and squirrels for habitat and food undoubtedly plays a in replacement of the red species by the grey squirrel lcher, 1997). However several authors have attributed ɛxtinction of local populations of red squirrels to the ɛnce of an epidemic disease that causes high mortality ısbury *et al.*, 1997, 2000; Rushton *et al.*, 2000; Tompkins , 2003). The disease is characterized by ulcerated and ıorrhagic scabs affecting the skin around the eyes, nose lips which later spread to the ventral thorax, inguinal and feet (Edwards, 1962; Sainsbury & Gurnell, 1995). causative agent was identified tentatively by electron oscopy as a parapoxvirus (SPPV) (Scott *et al.*, 1981). origin of the virus is not clear, but no clinical disease ɛcorded until the introduction of grey squirrels to the (Sainsbury & Gurnell, 1995). A serological survey of ınd grey squirrels from across the UK revealed that of 223 apparently healthy grey squirrels had antibodies ?PV, whereas only 3·2 % of 140 red squirrels were ɔsitive (Sainsbury *et al.*, 2000). All the seropositive red rels were found dead or dying with symptoms typical ɛ poxvirus disease. There has only been one confirmed report of SPPV-induced disease in a wild grey squirrel (Duff *et al.*, 1996), and generally grey squirrels are thought to be unaffected clinically. However, the high seroprevalence of antibodies to the virus and low incidence of disease in grey squirrels suggest that they may be a reservoir for SPPV, which is then transmitted to red squirrels causing lethal disease.

Experimental infection with a mixture of isolates from various outbreaks of scab disease confirmed that SPPV is the agent responsible for the disease observed in red squirrels. In contrast, infection of grey squirrels failed to induce disease although all developed antibodies to the virus (Tompkins *et al.*, 2002). We have taken a single isolate of the virus from an outbreak of disease in northern England and shown that it alone causes a deleterious disease in red squirrels. Sequencing and subsequent phylogenetic analysis of genes from this virus casts doubt over its relationship to the parapoxviruses.

Virus was isolated from a red squirrel (see supplementary data at JGV Online: http://vir.sgmjournals.org) with typical SPPV-induced haemorrhagic erythematous dermatitis about the face and on the feet and was visualized by negative-staining transmission electron microscopy. The SPPV particles were generally ovoid with approximate dimensions of 275 × 175 nm, similar to the parapoxviruses. The regular basket-weave surface morphology characteristic of the parapoxviruses was also observed (Fig. 1A). However, the angle at which the SPPV basket-weave ridges cross each other

ɛnt address: University of Otago, Dunedin, New Zealand.

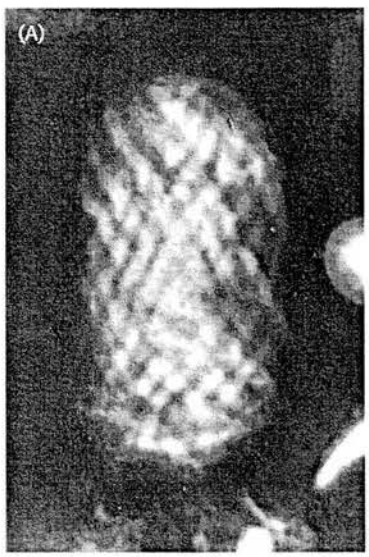

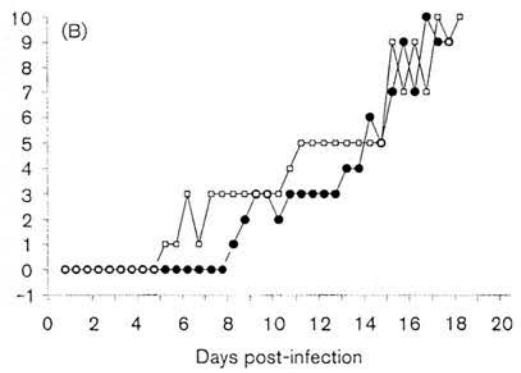

(A) Virus from the scabs on a squirrel (1296/99) found Northumberland, England, exhibiting typical poxvirus-like on the head, hands and feet (see supplementary data at line: http://vir.sgmjournals.org), was visualized by negative- transmission electron microscopy. (B) Two captive-bred irrels were infected with virus isolated directly from scab taken from squirrel 1296/99. Scabs were homogenized in d after clarification at 2000 *g* for 30 min at 4 °C, the virus rified by centrifugation at 71 000 *g* for 30 min at 4 °C a sucrose cushion (36 %, w/w, in PBS). The virus pellet suspended in PBS, the concentration estimated by electron opy and adjusted to approximately 10^5 virus particles ml^{-1}. iirrels were infected with the virus suspension and their vas monitored every 12 h according to the clinical scoring of Tompkins *et al.* (2002). Animals exhibiting a clinical 8 or more on three consecutive occasions were removed experiment.

to differ from that of other parapoxviruses, support- previous observations made by Scott *et al.* (1981).

nation that this virus could induce scab disease was d by experimental infection of two captive-bred red squirrels. Virus was isolated directly from scab material and its concentration was estimated by electron microscopy and adjusted to approximately 10^5 virus particles ml^{-1} in PBS. Squirrels were challenged by topical application of 0·2 ml virus suspension to a scarification site on the right thigh and also by subcutaneous injection of 0·2 ml into the right thigh. The progression of disease in each animal was assessed every 12 h using the clinical scoring system described by Tompkins *et al.* (2002). Individuals scoring eight or more on three consecutive occasions were removed from the experiment, as it was predetermined that this severity of disease would cause mortality in the wild. Both squirrels succumbed to disease within 10 days. Severe secondary lesions appeared within 2 weeks and the animals exhibited lethargy and poor condition, appetite loss by up to 100 % and reduction in body weight by up to 12 %. The progression of disease in both individuals (Fig. 1B) was not significantly different from that reported previously (ANOVA $F_{1,3}=0{\cdot}06$, $P=0{\cdot}83$), with animals being removed from the experiment at days 17·5 and 18·0, compared to days 15·0, 17·0 and 18·5 in the previous study with the mixture of viruses. The overall pathological symptoms were consistent with those reported previously in wild red squirrels (Edwards, 1962; Sainsbury & Gurnell, 1995), and confirmed that the isolated virus was virulent.

SPPV has been formally classified as a *Parapoxvirus* (van Regenmortel *et al.*, 2000), although Sands *et al.* (1984) concluded that SPPV and *Orf virus* (ORFV) were antigenically distinct. Furthermore, in a study of 27 monoclonal antibodies (mAbs) raised against ORFV, only two were found to cross-react with SPPV (Housawi *et al.*, 1998). This contrasts with 17 mAbs that cross-reacted with both *Pseudocowpox virus* (PCPV) and *Bovine papular stomatitis virus* (BPSV) and six that cross-reacted with Sealpox virus, suggesting that SPPV is more divergent from ORFV than from these other parapoxviruses. To study the relationship between SPPV and the other parapoxviruses we attempted to identify genes within the SPPV genome that were related to known ORFV genes and in particular to those associated with modulation of the host immune response and/or virulence. Five cosmid clones that span the SPPV genome were screened for the presence of sequence related to the ORFV *GIF* gene (encoding a protein capable of binding interleukin-2 and granulocyte–macrophage colony-stimulating factor; Deane *et al.*, 2000), the *VEGF-E* gene (encoding a protein related to mammalian vascular endothelial growth factor; Lyttle *et al.*, 1994), the *IL-10* gene (encoding a protein closely related to mammalian interleukin-10; Fleming *et al.*, 1997) and the orthologue of the *H5R* gene of *Vaccinia virus* (VACV) (encoding a late transcription factor, VLTF-4; Kovacs & Moss, 1996). Two of these genes, *VEGF-E* and *GIF*, have been found so far only in parapoxviruses whilst the IL-10 gene has also been found in the capripoxvirus *Lumpy skin disease virus* (LSDV) (Tulman *et al.*, 2001). Orthologues of *H5R* are found in each of the chordopoxvirus genera. No specific hybridization between the ORFV probes and

'V DNA was detected with the exception of that corres-
ıding to the *H5R* gene (results not shown). On the basis
this it was hypothesized that SPPV does not encode
ıologues of any of the ORFV *GIF*, *VEGF* or *IL-10* genes
that the corresponding SPPV sequences have diverged
iciently so as to prevent cross-hybridization. Com-
ative sequence analysis of 22 ORFV strains and isolates
ıonstrated that the *VEGF-E* gene varies considerably
ı within a single species of virus (Mercer *et al.*, 2002).
s heterogeneity could explain our inability to identify
ɔrthologue of *VEGF-E* in SPPV by hybridization. *VEGF-*
:nes are present close to the right ITR junctions in two
he three parapoxviruses for which there is sequence
ı available, that is in ORFV and PCPV, but not in BPSV
.tle *et al.*, 1994; Rziha *et al.*, 2003; Ueda *et al.*, 2003).
sequenced approximately 1 kb of the corresponding
on of the SPPV genome, but were unable to identify an
ıologue of *VEGF-E*. Instead an ORF with similarity to
003L and *157R* genes of *Molluscum contagiosum virus*
)CV) was found (results not shown). These genes appear
epresent paralogues of each other although they do
:r at their 3′ ends (Senkevich *et al.*, 1997). The SPPV
: (GenBank accession no. AY312570) is approximately
ɔ identical to the MOCV sequences, with the predicted
no acid sequences sharing approximately 28 % identity.

hybridization and sequence data taken together sug-
that SPPV probably does not possess an orthologue
)RFV *VEGF-E*. This was unexpected because the
:arance of SPPV-induced lesions suggests an underlying
ularization similar to that of ORFV-induced lesions.
vascularization appears to be a function of VEGF-E
: knockout viruses lacking this protein produced lesions
had lower blood vessel formation in the dermis than
ns induced with wild-type virus and as a consequence
: considerably less erythematous and florid (Savory
., 2000).

e we were unable to identify known parapoxvirus
s associated with immunomodulation or virulence
in the SPPV genome we sought alternative genes with
h to explore the relationship between SPPV and other
poxviruses. Phylogenetic analysis with the partial
ence of the major outer envelope protein (orthologue
ACV F13L) has been used to infer speciation within
genus *Parapoxvirus* (Becher *et al.*, 2002). Previous
ysis was based on the alignment of amino acids 137 to
(numbering with respect to the ORFV protein) because
lata produced for the majority of parapoxviruses are
ed from PCR products using primers considered to
pecific for all parapoxviruses (Inoshima *et al.*, 2000).
mpts to obtain a PCR product from SPPV DNA using
: primers failed. Nevertheless we identified, by DNA
idization with the ORFV gene, a plasmid containing the
:sponding SPPV sequence. Sequence analysis revealed
resence of an ORF (GenBank accession no. AY312569)
:sponding to amino acids 129 to 344 of the ORFV
:in. Pairwise alignment of the predicted SPPV amino acid sequence with that of the four recognized species of *Parapoxvirus*, ORFV, PCPV, BPSV and *Parapoxvirus of red deer in New Zealand* (PVNZ), and the tentative member of the genus, Sealpox virus, indicated that the SPPV protein shared approximately 49 % identity to each. This was less than with VACV F13L (57 % identity). We aligned our sequence with all known chordopoxvirus orthologues of the F13L protein, representing all eight chordopoxvirus genera, and constructed a phylogenetic tree based on a maximum-likelihood algorithm (Fig. 2A). The analysis grouped ORFV, BPSV, PCPV and PVNZ together with Sealpox virus, but the SPPV sequence was placed on a separate branch of the tree with 82 % support from the bootstrap resampling. Indeed, the SPPV sequence was placed on a branch of its own and did not partition with any of the other poxvirus genera, suggesting that SPPV represents a separate genus of the *Poxviridae*.

To gather support for this theory we performed a similar phylogenetic analysis on a second SPPV gene. The orthologue of the VACV *E4L* gene (encoding the 30 kDa RNA polymerase subunit; Ahn *et al.*, 1990) was identified by random sequencing of plasmid clones derived from the SPPV genome. It was predicted to encode a protein of 297 amino acids, 38 amino acids longer than the VACV protein. Likewise, it is predicted to be 96, 75, 75, 115, 108 and 104 amino acids longer than the corresponding proteins in the *Capripox*, *Leporipox*, *Suipox*, *Avipox*, *Yatapox* and *Parapox* genera, respectively. In contrast, the MOCV orthologue is predicted to be 147 amino acids longer than the SPPV sequence. Due to the variation in length between the different orthologues an initial alignment of the 17 available sequences, representing the eight different chordopoxvirus genera (and including the SPPV sequence), was performed. This indicated that there was a core of approximately 180 amino acids that were well conserved across all the genera. A phylogenetic tree based on an alignment of these 'core' amino acids was constructed. Bootstrap resampling, based on 100 data sets, was used to examine the statistical significance of the observed clades. Once again the SPPV sequence appeared on a branch of its own in the phylogenetic tree (Fig. 2B), separated from the ORFV sequence (the only parapoxvirus sequence available) with 95 % support from the bootstrapping exercise, and 64 % from the other poxvirus genera. This particular analysis, however, failed to separate the orthopoxviruses from the *Leporipox*, *Suipox*, *Capripox* and *Yatapox* virus genera with any strong bootstrapping support. Therefore, although this phylogenetic tree supports the general observation that SPPV does not readily partition with the parapoxvirus ORFV, the exact relationship between it and the other chordopoxvirus genera is less well defined.

Despite similarities in the base composition, virion morphology and in the pathological symptoms of the disease caused by SPPV when compared to the other parapoxviruses, the phylogenetic analysis presented here provides no support to classify SPPV in the genus

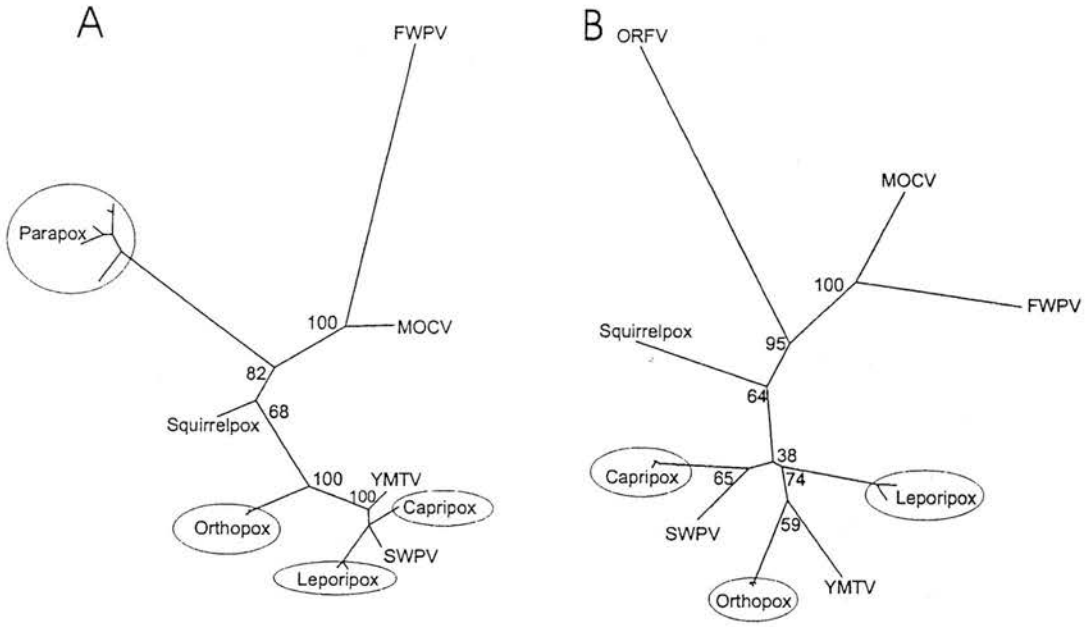

Fig. 2. Phylogenetic analysis was performed on orthologous amino acid sequences aligned using the ClustalW algorithm. Maximum-likelihood trees were generated using the PHYLIP PROML program. The model of amino acid substitution used was that of Jones/Taylor/Thornton (Jones *et al.*, 1992), and a mixed model of rate heterogeneity, with four gamma rates and one invariant rate, was used. The input order of the aligned sequences was jumbled 10 times and the global rearrangement option was selected. The gamma distribution parameter alpha and the fraction of invariable sites were calculated using the TREE-PUZZLE program (Schmidt *et al.*, 2002). The trees were evaluated using 100 bootstrap replicates (Felsenstein, 1985) and a consensus tree produced using the CONSENSE program. Trees were visualized using the graphical software TREEVIEW version 1.6.6 (Page, 1996). Branch lengths are proportionate to genetic distances and numbers indicate the percentage of bootstrap replicates that support each of the internal branches. Where several members of a genus were analysed and grouped together the name of the genus is indicated. When only one member of a genus was used in the analysis the species is indicated. (A) Phylogenetic analysis of 20 orthologues of the VACV major outer envelope protein (encoded by VACV *F13L*). The tree is based on an alignment of amino acids 137 to 313 (numbering with respect to the VACV-COP protein). The accession numbers for each of the sequences used in this analysis are; SPPV (AY312569), ORFV (Q84145), BPSV (Q91UK2), PCPV (Q91UK3), PVNZ (Q91UK1), Sealpox virus (Q8JTI4), VACV (P20638), *Variola virus* (VARV; Q85369), *Cowpox virus* (CPXV; Q8QN05), *Camelpox virus* (CMLV; Q8V2W9), *Ectromelia virus* (ECTV; Q8JLG8), *Swinepox virus* SWPV; Q9IW61), LSDV (Q9QCQ1), *Sheeppox virus* (Q9QCQ2), *Yaba monkey tumour virus* (YMTV; Q9DHT5), MOCV Q98189), *Fowlpox virus* (FWPV; P36316), *Rabbit fibroma virus* [SFV ('Shope fibroma virus'); Q9Q949], *Myxoma virus* MYXV; Q83604) and *Monkeypox virus* (MPXV; Q8V535). (B) Phylogenetic analysis of 17 orthologues of the VACV RNA polymerase 30 kDa subunit (encoded by VACV *E4L*). The tree is based on the alignment of amino acids 23 to 199 numbering with respect to the VACV-COP sequence). The accession numbers for each of the sequences used in this analysis are; SPPV (AY310357), ORFV (AY299390), *Sheeppox virus* (Q84152), SWPV (Q8V3R1), MYXV (Q9Q8R6), VACV (P21082), YMTV (Q9DHS7), LSDV (Q8JU11), *Goatpox virus* (GTPV; Q11319), CMLV (Q8V2W1), MPXV (Q8V527), CTV (AAM92348), CPXV (Q8QMZ7), VARV (Q85373), SFV (Q9Q941), FWPV (Q9J5C0) and MOCV (Q98202).

xvirus. However, a much more extensive study of PV genome and the genes it contains will be d before the virus can be classified with certainty. lassification will be important when considering epidemiological and ecological studies.

preparing this manuscript we noted that the d abbreviation given to the *Squirrelpox virus* is the same as has been given to *Sheeppox virus* egenmortel *et al.*, 2000). We would like to suggest that the alternative abbreviation SQPV be adopted for *Squirrelpox virus*.

ACKNOWLEDGEMENTS

This work was funded by The Sir James Knott Trust, NERC and SEERAD. Thanks go to VLA Lasswade for electron microscopy and to Frank Wright for advice on phylogenetic analysis. We also thank John Gurnell for his role in the red squirrel surveillance programme by which diseased animals were brought to our notice.

EFERENCES

nn, B. Y., Gershon, P. D., Jones, E. V. & Moss, B. (1990). entification of rpo30, a vaccinia virus RNA polymerase gene with ructural similarity to a eucaryotic transcription elongation factor. *ol Cell Biol* **10**, 5433–5441.

echer, P., Konig, M., Muller, G., Siebert, U. & Thiel, H. J. 002). Characterization of sealpox virus, a separate member of e parapoxviruses. *Arch Virol* **147**, 1133–1140.

ane, D., McInnes, C. J., Percival, A. & 7 other authors (2000). Orf us encodes a novel secreted protein inhibitor of granulocyte-crophage colony-stimulating factor and interleukin-2. *J Virol* **74**, 13–1320.

ff, J. P., Scott, A. & Keymer, I. F. (1996). Parapox virus infection of grey squirrel. *Vet Rec* **138**, 527.

wards, F. B. (1962). Red squirrel disease. *Vet Rec* **74**, 739–741.

senstein, J. (1985). Confidence intervals on phylogenies: an roach using the bootstrap. *Evolution* **39**, 783–791.

ming, S. B., McCaughan, C. A., Andrews, A. E., Nash, A. D. & rcer, A. A. (1997). A homolog of interleukin-10 is encoded by the cvirus orf virus. *J Virol* **71**, 4857–4861.

rnell, J. & Pepper, H. (1993). A critical look at conserving the ish red squirrel *Sciurus vulgaris*. *Mammal Rev* **23**, 127–137.

sawi, F. M. T., Roberts, G. M., Gilray, J. A., Pow, I., Reid, H. W., tleton, P. F., Sumption, K. J., Hibma, M. H. & Mercer, A. A. 98). The reactivity of monoclonal antibodies against orf virus other parapoxviruses and the identification of a 39 kDa nunodominant protein. *Arch Virol* **143**, 2289–2303.

shima, Y., Morooka, A. & Sentsui, H. (2000). Detection and nosis of parapoxvirus by the polymerase chain reaction. *J Virol hods* **84**, 201–208.

es, D. T., Taylor, W. R. & Thornton, J. M. (1992). The rapid ration of mutation data matrices from protein sequences. *put Appl Biosci* **8**, 275–282.

ward, R. E. & Holm, J. L. (1989). What future for British red rrels? *Biol J Linn Soc* **38**, 83–89.

acs, G. R. & Moss, B. (1996). The vaccinia virus H5R gene des late gene transcription factor 4: purification, cloning, and expression. *J Virol* **70**, 6796–6802.

d, H. G. (1983). Past and present distribution of red and grey rrels. *Mammal Rev* **13**, 69–80.

e, D. J., Fraser, K. M., Fleming, S. B., Mercer, A. A. & Robinson, . (1994). Homologs of vascular endothelial growth factor are ded by the poxvirus orf virus. *J Virol* **68**, 84–92.

er, A. A., Wise, L. M., Scagliarini, A. & 7 other authors (2002). ular endothelial growth factors encoded by Orf virus show ising sequence variation but have a conserved, functionally int structure. *J Gen Virol* **83**, 2845–2855.

, R. D. (1996). TREEVIEW: an application to display phylogenetic on personal computers. *Comput Appl Biosci* **12**, 357–358.

ton, S. P., Lurz, P. W. W., Gurnell, J. & Fuller, R. (2000). elling the spatial dynamics of a parapoxvirus disease in red and grey squirrels: a possible cause of the decline of the red squirrel in the UK. *J Appl Ecol* **37**, 997–1012.

Rziha, H. J., Bauer, B., Adam, K. H., Rottgen, M., Cottone, R., Henkel, M., Dehio, C. & Buttner, M. (2003). Relatedness and heterogeneity at the near-terminal end of the genome of a parapoxvirus bovis 1 strain (B177) compared with parapoxvirus ovis (*Orf virus*). *J Gen Virol* **84**, 1111–1116.

Sainsbury, A. W. & Gurnell, J. (1995). An investigation into the health and welfare of red squirrels, *Sciurus vulgaris*, involved in reintroduction studies. *Vet Rec* **137**, 367–370.

Sainsbury, A. W., Nettleton, P. & Gurnell, J. (1997). In *The Conservation of Red Squirrels, Sciurus vulgaris* L., pp. 105–108. Edited by J. Gurnell & P. Lurz. London: People's Trust for Endangered Species.

Sainsbury, A. W., Nettleton, P., Gilray, J. & Gurnell, J. (2000). Grey squirrels have a high seroprevalence to a parapoxvirus associated with deaths in red squirrels. *Anim Conserv* **3**, 229–233.

Sands, J. J., Scott, A. C. & Harkness, J. W. (1984). Isolation in cell culture of a poxvirus from the red squirrel (*Sciurus vulgaris*). *Vet Rec* **114**, 117–118.

Savory, L. J., Stacker, S. A., Fleming, S. B., Niven, B. E. & Mercer, A. A. (2000). Viral vascular endothelial growth factor plays a critical role in orf virus infection. *J Virol* **74**, 10699–10706.

Schmidt, H. A., Strimmer, K., Vingron, M. & von Haeseler, A. (2002). TREE-PUZZLE: maximum likelihood phylogenetic analysis using quartets and parallel computing. *Bioinformatics* **18**, 502–504.

Scott, A. C., Keymer, I. F. & Labram, J. (1981). Parapoxvirus infection of the red squirrel (*Sciurus vulgaris*). *Vet Rec* **109**, 202.

Senkevich, T. G., Koonin, E. V., Bugert, J. J., Darai, G. & Moss, B. (1997). The genome of molluscum contagiosum virus: analysis and comparison with other poxviruses. *Virology* **233**, 19–42.

Skelcher, G. (1997). In *The Conservation of Red Squirrels, Sciurus vulgaris* L., pp. 67–78. Edited by J. Gurnell & P. Lurz. London: People's Trust for Endangered Species.

Tompkins, D. M., Sainsbury, A. W., Nettleton, P., Buxton, D. & Gurnell, J. (2002). Parapoxvirus causes a deleterious disease in red squirrels associated with UK population declines. *Proc R Soc Lond B Biol Sci* **269**, 529–533.

Tompkins, D. M., White, A. R. & Boots, M. (2003). Ecological replacement of native red squirrels by invasive greys driven by disease. *Ecol Lett* **6**, 1–8.

Tulman, E. R., Afonso, C. L., Lu, Z., Zsak, L., Kutish, G. F. & Rock, D. L. (2001). Genome of lumpy skin disease virus. *J Virol* **75**, 7122–7130.

Ueda, N., Wise, L. M., Stacker, S. A., Fleming, S. B. & Mercer, A. A. (2003). Pseudocowpox virus encodes a homolog of vascular endothelial growth factor. *Virology* **305**, 298–309.

van Regenmortel, M. H. V., Fauquet, C. M., Bishop, D. H. L. & 8 other editors (2000). *Virus Taxonomy. Seventh Report of the International Committee on Taxonomy of Viruses*, pp. 137–157. San Diego: Academic Press.